Spring 2024

Investigation of Asphaltene Instability Under Gas Injection in Unconventional Reservoirs and its Impact on Oil Recovery Performance

Mukhtar Elturki
Missouri University of Science and Technology

Department: Geosciences and Geological and Petroleum Engineering

INVESTIGATION OF ASPHALTENE INSTABILITY UNDER GAS INJECTION IN UNCONVENTIONAL RESERVOIRS AND ITS IMPACT ON OIL RECOVERY PERFORMANCE

By

MUKHTAR SALEH ELTURKI

A DISSERTATION

Presented to the Graduate Faculty of the

MISSOURI UNIVERSITY OF SCIENCE AND TECHNOLOGY

In Partial Fulfillment of the Requirements for the Degree

DOCTOR OF PHILOSOPHY

in

PETROLEUM ENGINEERING

2023

Approved by:

Shari Dunn-Norman, Advisor
Abdulmohsin Imqam, Co-Advisor
Stephen Gao
Kelly Liu
Ahmed Algarhy

PUBLICATION DISSERTATION OPTION

This dissertation consists of the following six articles, formatted in the style used by the Missouri University of Science and Technology:

Paper I, found on pages 9-46, has been published at the 54th US Rock Mechanics/Geomechanics Symposium held in Golden, Colorado, USA, in June 2020.

Paper II, found on pages 47-86, has been published in SPE Journal, Society of Petroleum Engineers, 2021.

Paper III, found on pages 87-130, has been published in SPE Journal, Society of Petroleum Engineers, 2022.

Paper IV, found on pages 131-176, has been published in SPE Journal, Society of Petroleum Engineers, 2022.

Paper V, found on pages 177-228, has been published in Energy & Fuels Journal, the American Chemical Society, 2022.

Paper VI, found on pages 229-281, has been published in Energy & Fuels Journal, the American Chemical Society, 2023.

ABSTRACT

Unconventional reservoirs, such as shale gas and tight oil formations, have become an important source of energy in recent years. However, these reservoirs often contain high levels of asphaltenes, which can lead to deposition and blockages in production wells and reduce the flow of hydrocarbons during gas enhanced oil recovery (GEOR) techniques. This study aims to experimentally evaluate the impact of miscible and immiscible carbon dioxide (CO_2) and nitrogen (N_2) on asphaltene deposition and its impact on oil recovery performance in unconventional shale reservoirs.

This research began with a comprehensive literature review and data analysis of GEOR methods in unconventional reservoirs. Following this, the minimum miscible pressure of CO_2 and N_2 was determined using the slim tube technique. Two gas injection methods were implemented in this research, including continuous and cyclic (huff-n-puff) modes. In the continuous mode, filter paper membranes which represent shale structure were utilized to demonstrate the severity of asphaltene deposition rate under different scenarios. For the huff-n-puff mode, various Eagle Ford shale cores were used to understand the potential of this mode on asphaltene instability in real shale structures and its influence on oil recovery performance. The plugging impact of asphaltene particles in continuous mode was evaluated using various methods including optical microscopy and scanning electron microscopy (SEM) imaging. Chromatography analysis of crude oil, wettability alteration, and pore size distribution were used to validate and support the findings of this research.

ACKNOWLEDGMENTS

First and foremost, I would like to praise and thank ALLAH “GOD” the ALMIGHTY for his generous help and blessings to accomplish this research.

I would like to express my deepest appreciation to my loving, wonderful, and supportive wife, Marwa Alzoubi, for her tremendous support, care, and patience during my research and rough times. Her encouragement and belief in me kept me going during the most challenging times. Without her continuous encouragement, I would not have been able to complete this research. I would also like to acknowledge this work to my beloved son “Adam” and wish him the same success in the future. Throughout the journey of completing my PhD, your love and presence have been my shining light. I love the little boy you are now and the man you will become.

I would like to express my deepest appreciation, heartfelt gratitude, and love to my parents, Saleh Elturki and Khairia Abu Zayan, for their continuous support during the many challenging times I faced while working on this research. For their love, the sacrifices they made, and the countless ways in which they have supported me throughout my life. I would not be the person I am today without both of you. Special thanks also to my brother and sisters for their support.

I would like to thank my advisor Dr. Shari Dunn-Norman for her support in finishing this research. Also, I am grateful to my co-advisor Dr. Abdulmohsin Imqam for his continuous support, invaluable patience, and feedback through my research. Also, I would like to thank my committee members for their feedback. Finally, I want to thank the Ministry of Education of Libya and Misurata University for awarding me a full scholarship.

TABLE OF CONTENTS

LIST OF ILLUSTRATIONS

LIST OF TABLES

PAPER IV

PAPER V

PAPER VI

1. INTRODUCTION

1.1. STATEMENT AND SIGNIFICANCE OF THE PROBLEM

The substantial growth in oil and gas production in the United States in recent years may be attributed in large part to the discovery of unconventional shale oil resources (Zhou et al., 2018). Gas injection has become a widespread technology to improve oil production in unconventional shale reservoirs in the United States and could be the most reliable method to unlock the remaining oil percentage (Elturki et al., 2020; Tovar et al., 2021). Even though hydraulic fracturing technology in horizontal wells can be used to recover the trapped oil, only 4-6% can be recovered (Tang et al., 2022). Very recently, gas injection methods have been studied and investigated in unconventional shale reservoirs using nitrogen (N_2) and carbon dioxide (CO_2) injection, and the results showed a positive impact on increasing oil recovery (Yu et al., 2015; Elwegaa et al., 2019). In conventional reservoirs, the primary recovery mechanisms are considered the main portion of the recovery. After the primary mechanisms have ended, secondary or tertiary mechanisms are usually implemented to increase the recovery. In an unconventional shale reservoir, gas enhanced oil recovery (EOR) has been proposed to increase the recovery after using hydraulic fracturing as a primary mechanism. The main reason for using CO_2 and N_2 is that these gases are non-hydrocarbon gases that are cheaper and applicable in reservoirs. CO_2 is more viscous than N_2, so its efficiency is higher in the same reservoir conditions. N_2 is soluble than CO_2, so oil swelling of N_2 is poor. In addition, the minimum miscibility pressure (MMP) of CO_2 is lower than N_2, which makes N_2 suitable in high-pressure reservoirs.

One of the major problems during gas injection in unconventional reservoirs is asphaltene deposition and precipitation (Ahmed et al., 2022). Asphaltene precipitation and deposition during miscible gas injection is a prevailing issue in the petroleum industry which results in severe formation damage and permeability reduction. Asphaltene is one of the most complex solid components in the composition of crude oil. Asphaltene can be defined as “the heaviest component of petroleum fluids that is insoluble in light n-alkanes such as n-pentane or n-heptane, but soluble in aromatics such as toluene” (Goual, 2012). The main components of crude oil are saturates, aromatics, resins, and asphaltenes (Elturki and Imqam, 2021). These components are held together with resins which have both polar and nonpolar sites that make them as a perfect connector between all components. As the conditions change, the forces that hold all components become weaker and more severe, causing the asphaltene to precipitate. Common conditions that may change include pressure, temperature, solvent injection such as CO_2, and high oil production flowrate (Bahman et al., 2017). Asphaltene instability can be induced by changing the solubility of heavy components during the gas injection process. Thermodynamic changes including temperature, pressure, and crude oil composition in the reservoir will result in the precipitation of asphaltene on solid surfaces during oil flows from the reservoir to the surface. As a consequence, asphaltene aggregates and nanosized particles can form clusters that may cause crucial issues by blocking wellbore pores and production facilities. Deposition of asphaltene often reduces rock permeability, damages the formation, and plugs the wellbore and well tubing. Overall, these effects reduce the oil well productivity and efficiency (Srivastava and Huang 1997; Srivastava et al., 1999; Sim et al., 2005; Okwen 2006; Bahram et al., 2011; Elturki et al., 2023).

Gas injection for tertiary oil recovery can be conducted in either a continuous or cyclic injection mode. Continuous injection has been widely applied in conventional oil reservoirs, where the gas is injected from the injector well and both oil and separated gas are produced from the producer well (Alagorni et al., 2015). In gas cyclic injection mode, gas is introduced into the oil reservoir during injection, and the injector well is then shut in for period of time to "soak". The injector well is then opened and both separated gas and oil are produced. The gas injection could produce oil by either miscible or immiscible displacement. For gas injection pressures below MMP, immiscible displacement of oil takes place, while if gas injection pressures are above the MMP, miscibility between gas and reservoir oil is achieved. Miscibility is achieved by eliminating the interfacial tension between oil and gas. On a fundamental level, the difference between continuous and cyclic injection is transient and unsteady-state conditions. Thus, the extension of continuous gas injection asphaltene studies to cyclic operation conditions is problematic, particularly given the limited number of studies to date applicable to practical injection conditions. For example, the same well is used for both injection and production in cyclic injection; thus, the changes in oil composition and pressure near the wellbore area are much more complex in cyclic injection. Changes in gas concentration near the wellbore further complicate the asphaltene precipitation during the cyclic injection process. Multiple cyclic injections achieve a higher oil recovery factor, but the effects of pressure, oil composition, and gas injection conditions (composition and time profile) are expected to be varied during injection cycles. In short, the current understanding of asphaltene precipitation mechanisms during continuous injection is not applicable to cyclic injection.

Despite the number of studies on the behavior of asphaltene during continuous gas injection, the interaction of asphaltenes with CO_2 and N_2 during huff-n-puff enhanced oil recovery (EOR) technique under miscible and immiscible conditions remains poorly investigated and understood. This present research aims to investigate the severity of asphaltene damage, especially in nano pore structures, mainly present in unconventional reservoirs. The research then studies asphaltene precipitation and deposition due to CO_2 and N_2 injection in the nanopores and quantifies the asphaltene weight percent in all experiments. Several interactions between the injected gas (CO_2 or N_2) and oil need to be investigated in order to determine the main thermodynamic factors that affect the EOR process in shale reservoirs. By studying the impact of different factors on asphaltene formation damage, asphaltene deposition may be avoided in future applications of N_2 and CO_2 injections.

1.2. EXPECTED IMPACTS AND CONTRIBUTIONS

The ultimate goal of this research is to highlight the severity of asphaltene damage during miscible and immiscible CO_2 and N_2 gas injection, especially in nano pore structures, mainly present in unconventional reservoirs. By undertaking this research, a better understanding of the factors that affect the asphaltene instability during miscible and immiscible injections is achieved. This research will help the industry and academia to address the following questions:

- What are the possible EOR methods which have been applied in unconventional reservoirs? How can we construct a roadmap for the conditions at which different EOR methods are applicable?

- When it comes to asphaltene instability in crude oil stored in unconventional reservoirs, what influence do CO_2 and N_2 play under miscible and immiscible conditions?
- To what extent may asphaltene block nanopores in unconventional reservoirs using continuous gas injection? How does the rate of asphaltene flocculation during gas cyclic injection affect oil recovery?
- How does the profile of cyclic gas injection (including pressure ramping and soak time) influence asphaltene instability?
- How could operating parameters (such as CO_2, N_2, and pressure) be altered to reduce asphaltene deposition rate?

1.3. OBJECTIVES

The primary objective of this research is to provide an intensive and comprehensive laboratory investigation of asphaltene instability in crude oil and determine the factors that impact its stability in crude oil during the gas injection process, in order to help define "when" and "how" to apply CO_2 and N_2 in unconventional shale reservoirs. The following objectives will be met by this research:

- Perform a comprehensive data analysis and review of gas EOR methods in unconventional reservoirs and to understand the most frequently applied techniques and the factors that influence their success in increasing hydrocarbon recovery.
- Provide an extensive EOR study on the main non-hydrocarbon gases (CO_2 and N_2) that are cheaper and more applicable to the reservoirs compared to hydrocarbon gases such as methane (CH_4).

- Determine the MMP of CO_2 and N_2 to investigate the effect of injection pressure above and below the MMP on asphaltene stability in crude oil in order to provide a better understanding of how gas miscibility and immiscibility could affect the recovery and asphaltene instability.
- Perform filtration experiments using nano-composite filter membranes to better understand the effect of pore size on asphaltene deposition and precipitation during continuous and huff-n-puff gas injection modes (using CO_2 and N_2). These experiments will provide a guideline of asphaltene stability and shale pore plugging under gas injection.
- Perform cyclic CO_2 and N_2 injection (i.e., huff-n-puff) experiments in order to investigate the potential of gas enhanced oil recovery to increase oil recovery from shale reservoirs and evaluate the asphaltene deposition on pore plugging and wettability changes to shale structure.

1.4. SCOPE OF WORK

To achieve this study's objectives, this Ph.D. work has been divided into four main tasks as shown in Figure 1.1. Task 1 is a comprehensive review and gas data analysis in unconventional shale reservoirs to provide a better understanding of the structure of such reservoirs and build a strong background on how these reservoirs preserve crude oil. The first task reviews all EOR methods including GEOR which have been applied to unconventional reservoirs, intending to construct a roadmap for the conditions at which different EOR methods are applicable. The systematic review of each method from both laboratory and field tests, if applicable, aims to provide insight into the limitations of each technique. Task 2 is to evaluate asphaltene stability using filtration experiments with various filter paper membranes. A series of evaluation experiments will be conducted during continuous gas injection mode using the filtration vessel, including but not limited to temperature, heterogeneity, and MMP. Task 3 is to evaluate asphaltene instability using the filtration vessel during huff-n-puff mode gas injection. Task 4 is to investigate asphaltene deposition during gas huff-n-puff technique using shale cores (Eagle Ford cores) and to determine the oil recovery performance in all experiments.

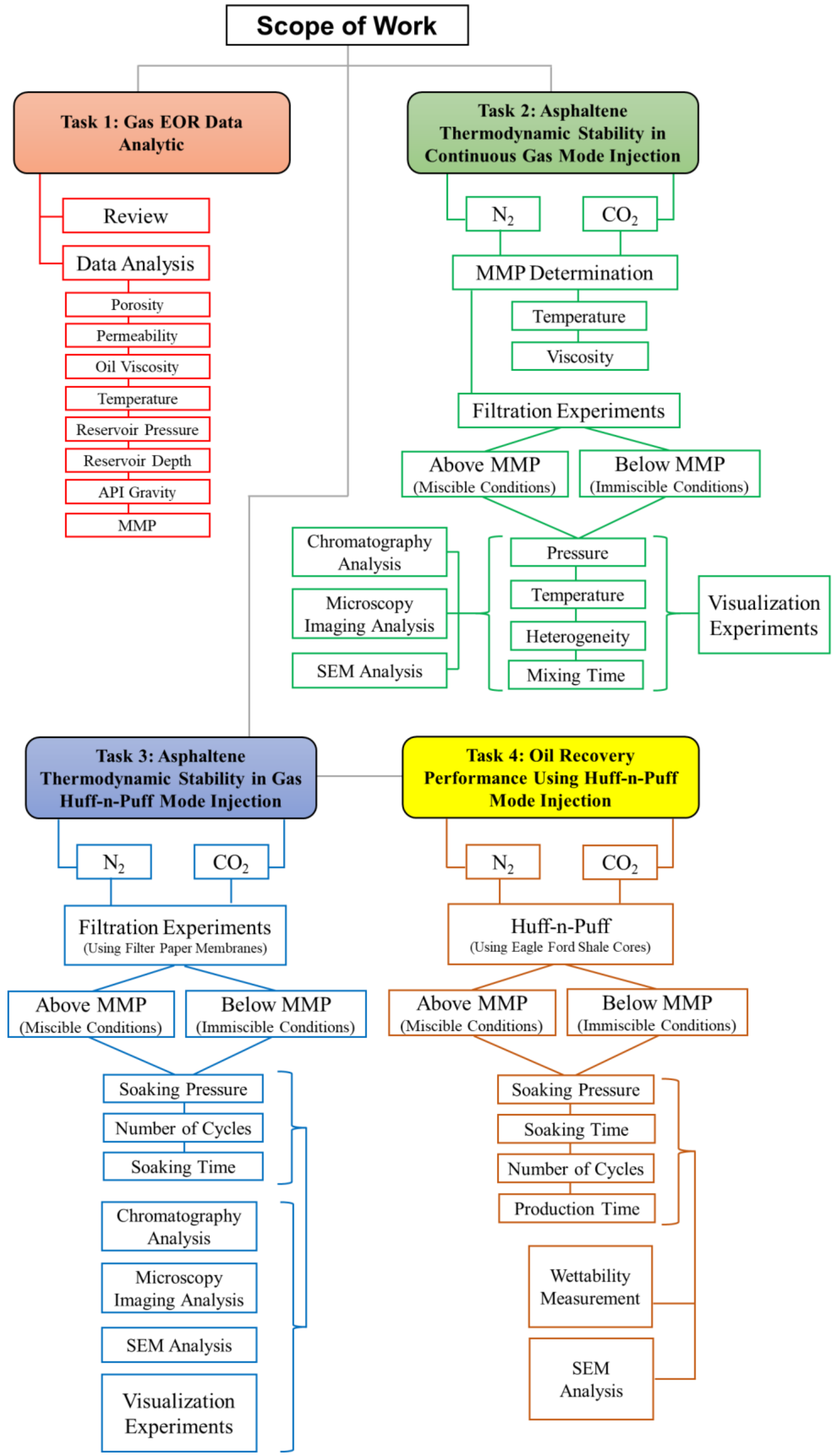

Figure 1.1. Ph.D. scope of work.

PAPER

I. APPLICATION OF ENHANCED OIL RECOVERY METHODS IN UNCONVENTIONAL RESERVOIRS: A REVIEW AND DATA ANALYSIS

Mukhtar Elturki and Abdulmohsin Imqam

Missouri University of Science and Technology

ABSTRACT

Production from unconventional reservoirs using enhanced oil recovery (EOR) has gained much attention in recent years due to its ability to dramatically increase oil recovery. This paper reviews all EOR methods which have been applied in unconventional reservoirs, with the aim of constructing a roadmap for the conditions at which different EOR methods are applicable. The most applicable unconventional techniques that have been reported to enhance oil recovery are Carbon Dioxide (CO_2) gas injection, low salinity water flooding, and surfactant. Various tools are employed to study EOR methods in unconventional reservoirs including simulation, experimental, and field cases. Most of the reviewed studies utilize simulation and experimental tools. Notably, we discovered that gaseous EOR methods, such as huff-n-puff gas injection, were widely used to investigate the applicability of such methods. The most widely used gas that was reportedly used is CO_2. Of the chemical methods, surfactant is the material with the most potential to improve oil recovery due to its ability to change the wettability of the reservoir rocks to water wet.

We present an analysis of the most common fluid and rock properties of unconventional reservoirs.

1. INTRODUCTION

Unconventional reservoirs have significantly changed oil and gas production in recent years. More than 50% of U.S. oil production comes from shale and tight reservoirs (Energy Information Administration (EIA), 2019). Production from tight reservoirs is predicted to increase significantly due to current developments and advancements in the area. The EIA predicted that U.S. tight oil production will increase significantly in the coming decades, as shown in Figure 1. In terms of current production output, more than 4 million barrels of oil were produced daily between 2011 and 2014 in the U.S (Todd et al., 2016). Alvarez et al. (2016) reported that the Bakken formation only delivers about 10% of total U.S. production, with around 1.1 million barrels per day. Primary recovery methods of horizontal wells and hydraulic fracturing have the main impact on increasing oil and gas production from shale plays (Balasubramanian et al., 2018). Understanding the EOR methods in conventional plays is much easier than unconventional ones due to the abundance of information and applications of conventional reservoirs. The applications are dissimilar in unconventional plays due to the ultra-small porosity and permeability of unconventional reservoirs. All unconventional reservoirs share these characteristics: ultra-small permeability and small porosity. The permeability of tight formation is less than 0.1 mD (Jia et al., 2012). Figure 2 shows the types of oil and gas reservoirs according to the permeability cut offs.

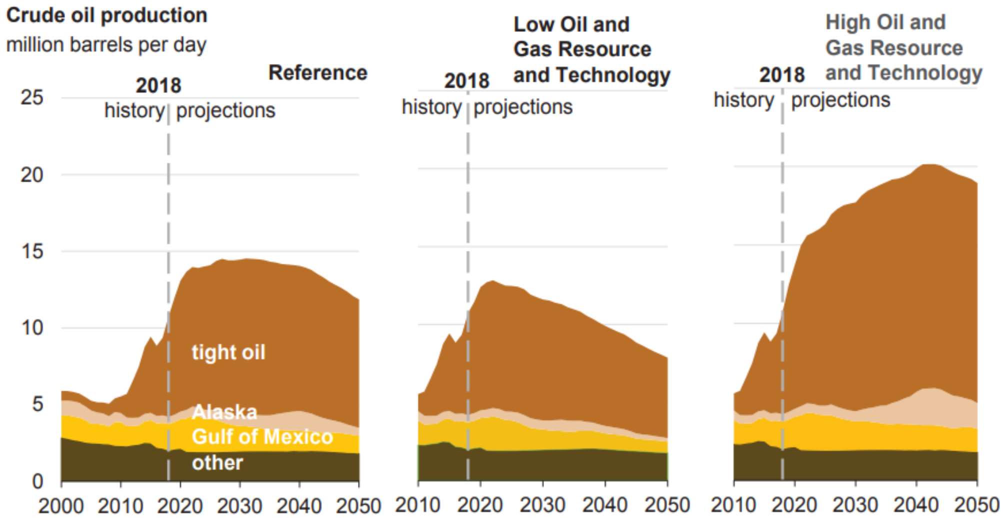

Figure 1. Shale and tight oil production in USA
(U.S. EIA, 2019).

Various studies have reported low oil recovery from these reservoirs due to their ultra-low permeability. Clark (2009) stated that the highest value of oil recovery for an unconventional reservoir is about 7%. We have investigated gas injection, water flooding, and chemical methods using a variety of tools, such as simulation and experimental methods, with the aim of elucidating the applicability of EOR in tight reservoirs. Moreover, we aim to develop technologies to optimize production and yield a large recovery of oil and gas. The ultimate objective of this paper is to summarize the main methods of EOR in unconventional reservoirs. The feasible methods that have been reported based on this study are gas injection, water injection, and chemical methods. There is great heterogeneity in the reporting methods, analysis and conclusions throughout the literature. Our systematic review of each method from both laboratory and field tests, if applicable, aims to provide insight into the limitations of each technique. The following section presents the most commonly used EOR methods in production from unconventional oil resources.

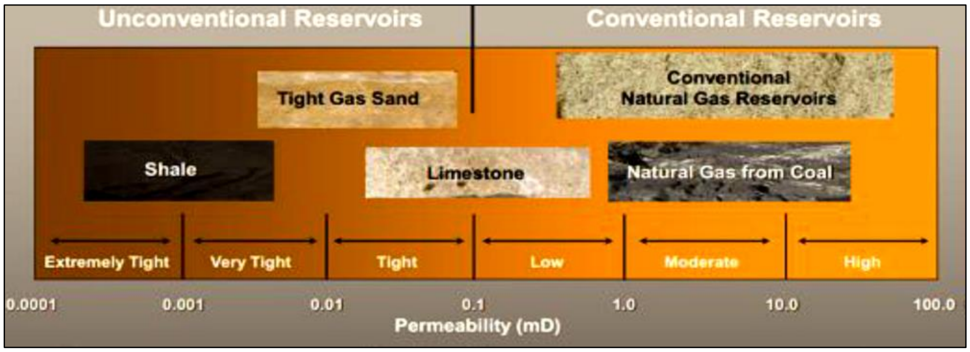

Figure 2. Types of oil and gas reservoirs according to the permeability cut offs (Canadian Society of Unconventional Resources, www.csur.com)

2. EOR METHODS TO PRODUCE UNCONVENTIONAL OIL RESOURCES

2.1. GAS INJECTION TECHNIQUES

2.1.1. Gas Types. Miscible gas injection is one of the most commonly used and widely reported methods implemented in EOR for unconventional reservoirs. Gas can be injected into reservoirs through various modes: huff-n-puff or flooding mode. During the huff-n-puff technique, the fluid is injected to a well. Following this, the in-suit fluids are produced from the same well after period of time. For the flooding mode, a dedicated well is selected to inject the fluid into the reservoir, and oil and gas are produced from another well or wells (Sheng, 2017). Occasionally it is difficult for the injected gas to displace the oil from the injector well to the producer well. This is a result of the ultra-small permeability in the reservoir, the pressure at the producer well decreases, and the pressure at the producer it increases. To combat this issue, the huff-n-puff method was introduced (Wan et al., 2013). Figure 3(a) displays the distribution for various gas injection modes, based on our analyzed data from reported gas injection methods in unconventional reservoirs. It shows that the most common mode used was huff-n-puff mode which was used in more than 60% of the reported studies.

Figure 3(b) illustrates different gases which have been reportedly used in unconventional reservoir studies. Various gases have been injected, including CO_2, nitrogen (N_2), lean gas, and methane. Most of the reported studies were focusing on using CO_2. The use of CO_2 carries many benefits. For example, CO_2 can dissolve easily in shales, decreases the oil viscosity, and swells the oil more effectively compared to other gases. Furthermore, the minimum miscibility pressure (MMP) of CO_2 is lower comparing to other gases such as N_2 (Zhang et al., 2016). However, CO_2 is not without limitations. Sheng (2015) highlighted two disadvantages of CO_2: corrosion of facilities and lack of availability near large fields. Table 1 shows a comparison of some gases used for miscible gas injection method.

Alfarge el al. (2016) stated that the common CO_2 mechanisms for improving oil recovery in unconventional reservoirs are diffusion, reduction in capillary forces, repressurization, extraction, oil swelling, and oil viscosity reduction. Alfarge et al. (2018) and Jin et al. (2016) have both demonstrated that total organic carbon content and exposure time are crucial to the success of CO_2 in unconventional reservoir in laboratory experiments.

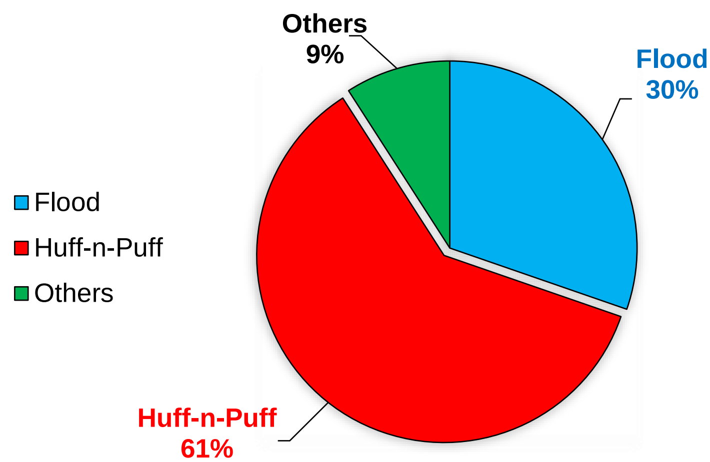

Figure 3-a. Gas injection modes distribution based on the reported gas injection methods.

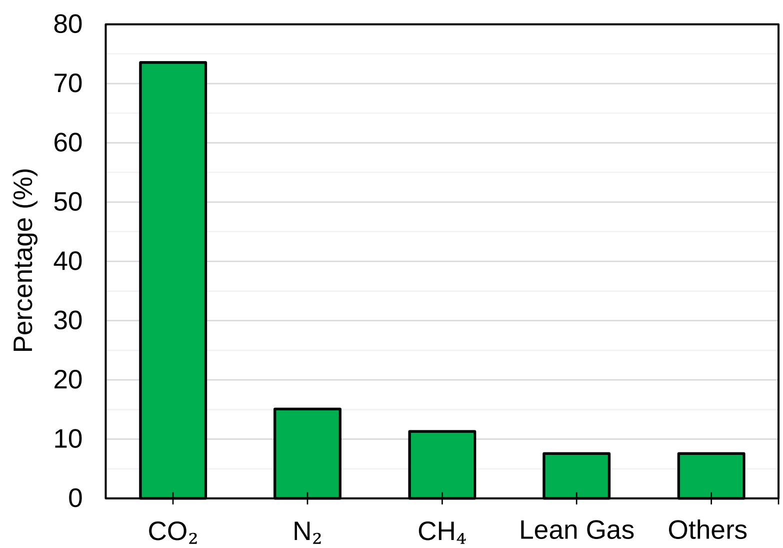

Figure 3-b. Different gases reported in unconventional reservoir studies.

Table 1. Comparison of gases used for miscible gas injection.
(Wang et al., 2017; Alfarge et al., 2018)

Gases	MMP	Sweep Efficiency	Cost	In situ Oil
CO_2	Lowest	Highest	Medium	>25 °API
Natural Gas	Medium	Medium	Highest	>30 °API
N_2	Highest	Lowest	Lowest	>40 °API

2.1.2. Experimental and Modeling Studies. Various laboratory studies investigated the effect of gas injection on oil recovery in tight reservoir cores. Alfarge et al. (2016) concluded that to produce oil from the matrix of shale, long exposure time and large contact area are optimal. Some researchers have varied the gases used in the same cores to better understand each one and their impact on recovery in tight reservoirs. Alharthy et al. (2015) injected different gases such as CO_2, C1-C2 mixtures and N_2 to cores from the middle and lower formation of the Bakken formation. The data indicate that CO_2 recovery is almost the same as C1-C2 mixtures; around 90% from the middle formation and 40% from the lower formation. Yu et al. (2017) conducted a comparative experimental study of N_2 injection in different modes (huff-n-puff and flooding). The authors report that during the same period of operation, the huff-n-puff injection mode was superior to flooding mode, which has a higher recovery in the same shale cores. Additionally, they report that before breakthrough, N_2 flooding revealed the same recovery of N_2 as huff-n-puff. After breakthrough, N_2 huff-n-puff demonstrated better recovery than flooding. Modeling methods have been implemented to investigate the applicability of gas injection in different formations. A compositional model has been used to evaluate the response of cyclic gas injection in naturally and fractured reservoirs (Wan et al., 2014). They concluded that as cyclic CO_2 injection continues, the amount of the dissolved CO_2 in oil increases; thus, the oil viscosity decreases, and oil can move easily to the production well. Zhu et al. (2015) performed a gas model in which the gas can be injected into a fracture along a horizontal well, where the production can be from a near fracture in the same well. They report an improvement in oil recovery by CO_2 injection in the reservoir. Yu et al. (2017) modeled both recovery processes of N_2 gas injection. They performed N_2 huff-n-puff and

N_2 flooding injection using lab-scale simulation. They suggest that the huff-n-puff model could lead to better recovery factor, of around 11%. Numerous simulation studies confirm that gas huff-n-puff is superior to gas injection, as shown in Table 2 (Sheng, 2015).

Table 2. EOR Potentials (Incremental Oil Recovery Factors) From Gas Injection (Sheng, 2015)

10-year primary	5.75%
20-year flooding	2.39%
20-year huff-n-puff	16.69%

2.1.3. Field Studies. Most of the reported field studies are from the Bakken formation (Sheng, 2017). One of the projects of gas flooding was conducted in viewfield Bakken field, Saskatchewan. One central horizontal well, perpendicular to nine horizontal production wells, was used to inject an immiscible gas (lean gas) (Schmidt & Sekar, 2014). Figure 4 shows viewfield Bakken field. This project was initiated in December 2011. After the gas breakthrough, the oil production was decreased to 53bbl/d in 2012. Workover was conducted, after which oil increased to 295 bb/d (Schmidt & Sekar, 2014; Sheng, 2017). Another gas project was reported in the Bakken formation in North Dakota in 2013 (Hoffman & Evans, 2016). This project converted to gas flooding from water flooding because the water flooding was not successful. Five horizontal wells were used in the project: one was an injector, and the others were producers. Produced natural gas was injected for 5 days. This project showed an improvement of oil production over time (Hoffman & Evans, 2016).

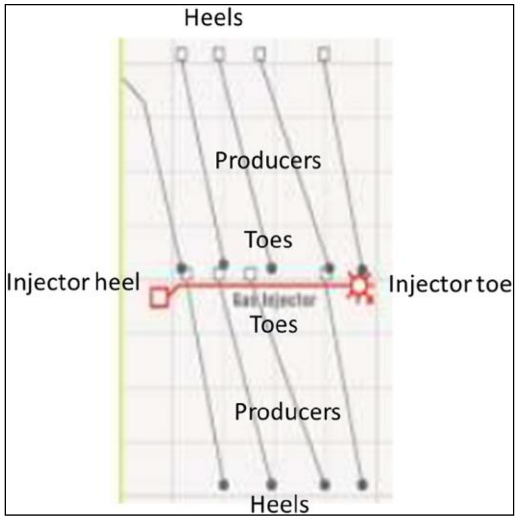

Figure 4. Modified viewfield gas injection pattern.
(Sheng, 2017 based on Schmidt and Sekar, 2014).

Huff-n-puff gas injection projects have been conducted, the Elm Coulee field in the Bakken formation is one of these projects. Hoffman and Evans (2016) conduced this project in 2008 using CO_2 gas, and no injectivity problems were reported. During the 30-day injection, no rate increase was observed (Hoffman & Evans, 2016). Sorensen et al. (2016) reported a project of huff-n-puff CO_2 injection in Parshall Field. In this project, a horizontal well was used with hydraulic fracture treatment. CO_2 breakthrough was observed after 11 days of CO_2 injection. The oil rate was increased after the injection process. To summarize, both modes of gas injected were reported differently. Simulation, experimental and pilots are the tools most commonly used to investigate the applicability of gas injection. Sheng (2017) concluded that the huff-n-puff mode outweighed the flooding mode in shale and tight reservoirs, provided that the huff-n-puff mode is well designed. However, the process of huff-n-puff, such as soaking time, should be optimized for better performance (Sheng, 2017).

2.2. WATER INJECTION TECHNIQUES

2.2.1. Experimental and Modeling Studies. Low salinity water (LSW) flooding for unconventional and tight reservoirs has been studied via various simulation and experimental tools. The main mechanisms of oil increase in this kind of EOR are wettability alteration and interfacial tension (Alfarge, 2016). Balasubramanian et al. (2018) stated that the main influencing mechanisms of LSW are clay swelling and shale cracking, wettability alteration, and water imbibition. Morsy et al. (2013) report experiments which utilized LSW with Eagle Ford formation cores. Both distilled water and KCL solution were used to investigate the recovery factor of each core. They found that the recovery factor of samples in distilled water was higher than from samples in KCL. Morsy and Sheng (2014) tested various cores from different formations (Mancos, Marcellus, Barnett, and Eagle Ford) to evaluate oil recovery. They employed NaCl and KCl brines with different concentrations. As the salinity is lowered to 15%, some of the cores started to convert to small pieces, especially Mancos cores. Barnett cores showed some cracks. No cracks were observed in Eagle Ford cores, but Marcellus showed some minor ones. Simulation studies of water injection concluded that water huff-n-puff injection is superior to water flooding (Sheng, 2015b) as shown in Table 3.

Table 3: EOR Potentials (Incremental Oil Recovery Factors) From Water Injection (Sheng, 2015b)

10-year primary	5.75%
20-year water flooding	2.39%
20-year water huff-n-puff	16.69%

2.2.2. Field Studies. There are only a restricted number of water injection projects in fields that have been reported in the U.S and Canada. The main concern of water injection in tight reservoirs is the injectivity of water. Water is difficult to inject into ultra-small permeability rocks. However, Hoffman and Evans (2016) reported no problem with injectivity in some field projects in the U.S. The findings have been replicated in many projects in China (Sheng, 2017). One of these waterflooding projects was conducted in 2014 in the Bakken formation in Montana. After one year, the producer wells shut in for months, and then, an oil rate increase was observed (Hoffman & Evans, 2016). Huff-n-puff water injection is one of the important reported mechanisms of EOR in tight reservoirs. During this technique water invades the pores of the rock and imbibes slowly into smaller pores to displace the oil (Sheng, 2017). Figure 5 shows the effect of fractures on the imbibition rate. As the fractures increase in the matrix, the water has more ability to penetrate and imbibe into the matrix.

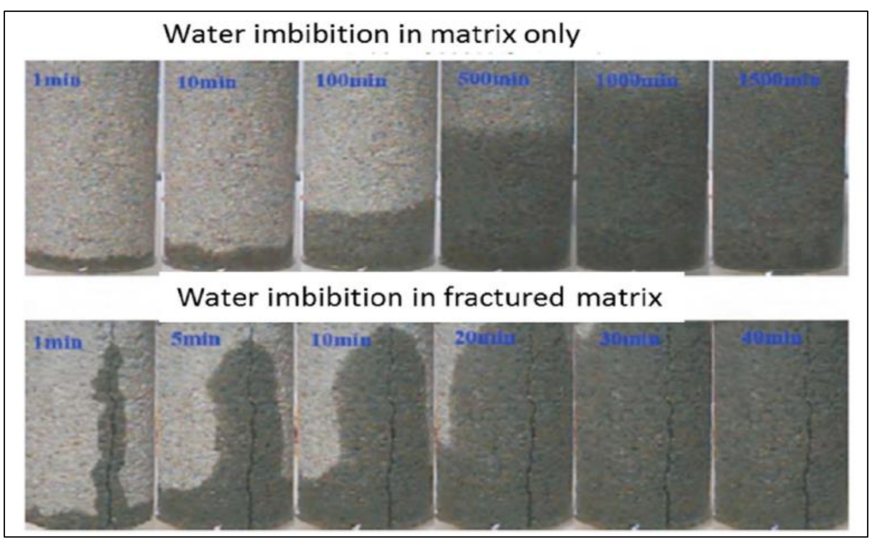

Figure 5. Water imbibition in matrix vs. fractured matrix
(Lin et al., 2016)

Some of the huff-n-puff water projects were conducted in different tight formations. In 2012, huff-n-puff water injection was performed in the Bakken formation in North Dakota. The injection time of this project was one month, with a soaking time of two weeks. There was little or no oil rate increase in this project (Hoffman & Evans, 2016). Sheng (2017) summarized some of the field projects conducted in North America, as shown in Table 4.

Table 4. Different Field Projects of Water Injection Technique (Sheng ,2017)

Field	Performance	Mode	References
Bakken + Lower Shaunavan	Oil rate increase	Waterflooding	Thomas et al., 2014; Wood and Milne, 2011
Bakken in ND	No oil rate increase, low sweep efficiency	Waterflooding	Hoffman and Evans, 2016
Bakken in Montana	Water breakthrough	Waterflooding	Hoffman and Evans, 2016
Bakken, ND	Little or no oil increase, no injectivity issue	Huff-n-puff	Hoffman and Evans, 2016
Parshall Field	No oil increase	Huff-n-puff	Sorensen and Hamling, 2016
Parshall Field	No oil increase	Huff-n-puff	Sorensen and Hamling, 2016

2.3. CHEMICAL TECHNIQUES

The main materials used in chemical methods are surfactant, alkaline, and polymer. Based on the recent EOR reported in tight reservoirs, surfactant is the most commonly studied material. The aim of chemical methods is to change the wettability of the reservoir from oil wet to water wet, which increases the oil recovery. The oil shales that have been reported are most likely oil wet (Phillips et al., 2009; Wang et al., 2011). Changing the wettability to water wet and making the reservoir rocks more imbibition to water are the best ways to increase oil recovery from this kind of tight reservoir. Surfactant is not only used for increasing the oil recovery, but also can be added in fracturing fluids (Sheng, 2017). Many laboratory studies have investigated surfactants, but there is a lack of field studies. A study of the effect of surfactant on the Bakken formation has been reported (Dawson et al., 2015). The experimental study showed about 30-40% of oil recovery that has been obtained from their cores.

Dawson et al. (2015) mainly used the spontaneous imbibition method to conduct this experiment. Wang et al. (2016) conducted an experimental study to investigate the effect of the imbibition rate of the surfactant. In their study, they used simulation methods to upscale their work to the field scale. Also, they studied the effect of penetration depth into the matrix. They stated that the oil recovery would not be much better by using surfactant if it was used only in hydraulically created fractures, because the penetrations of depths were small.

Different types of surfactants, such as non-ionic and anionic, have been investigated in shale reservoir cores (Nguyen et al., 2014). Studies have used cores from the Eagle Ford shale outcrop and Bakken reservoir. It has been reported that the imbibition of surfactant increased the oil recovery from Eagle Ford shale, and the Bakken formation oil recovery would be higher if only brine were used. However, researchers concluded that salinity has an impact on surfactant method; at higher salinity concentration, the ability of surfactant to reduce interfacial tension and wettability would be very low. Finally, alkaline and polymer materials have not been reported in any study. Alfarge et al. (2016) claims that the reason could be the injectivity problems with these materials in unconventional reservoirs. Moreover, pore plugging may occur if the polymer is injected into the reservoir. The compatibility of alkaline and mineral-composition of unconventional reservoirs may be one reason for investigating this kind of material (Alfarge et al., 2016). Finally, no field applications have been reported using surfactant method. The following section presents a data analysis for the significant characteristics of unconventional reservoirs.

3. DATA ANALYSIS

3.1. MOST RECENT EOR METHODS

Recent studies regarding EOR techniques are primarily related to gas injection, low salinity water flooding, and surfactant. The studies employed different methods to investigate the applicability of these techniques, including simulation, experimental, mathematical approaches, and some field tests. Field tests in the U.S. have been performed mainly in the Permian Basin Wolfcamp formation (Balasubramanian et al.,2018). Figure 6 shows different formations that have been reported of EOR in unconventional reservoirs. The majority of these studies originate from the Bakken formation in the U.S and Canada with percent of 58% of total studies. Eagle ford formation has significance in the U.S with 9% of the study reported in unconventional reservoirs. Figure 7 shows the varying tools used to investigate the applicability of EOR methods in North America and China. It is clear that simulation and experimental tools have been used the most due to their simplicity to perform in the laboratory compared to field tests. Tight formations in China have been reported in the Ordos Basin, Zhengger Basin, and Songliao Basin (Sheng, 2017). Figure 8 shows different countries reported different EOR methods including field projects, experimental, and simulation studies of unconventional reservoirs based on our data analysis.

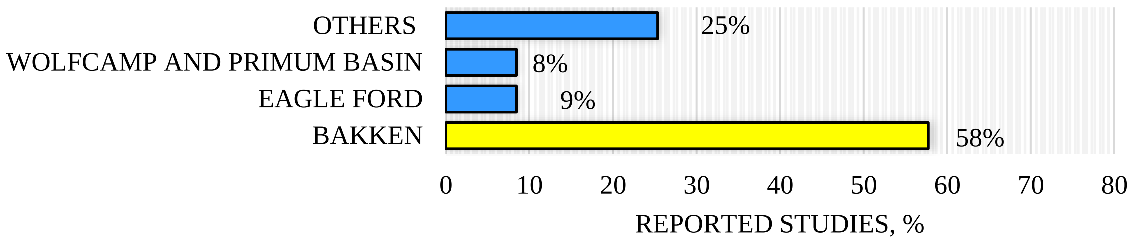

Figure 6. Different formation studies reported for EOR methods in unconventional reservoirs.

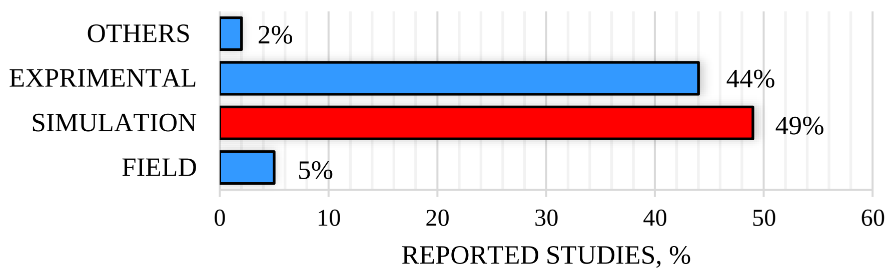

Figure 7. Different tools used to investigate the applicability of EOR methods in unconventional reservoirs.

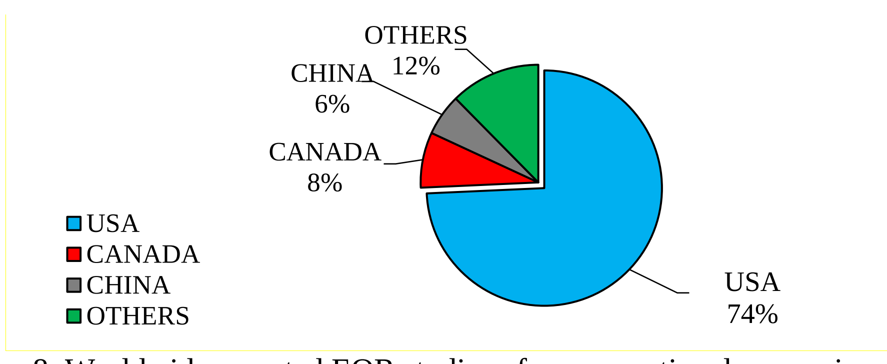

Figure 8. Worldwide reported EOR studies of unconventional reservoirs

3.2. DATA COLLECTION AND PROCESSING METHODS

Collecting information from different publications and then creating a data set was the first step of data quantification and analysis. The data set was created based on 129 reported studies regarding unconventional reservoirs. These studies include field projects, simulation studies, and experimental tests. After processing and analyzing the collected data, two tools were used to present and visualize the data: boxplots and histograms. The following properties have been analyzed in this section: porosity, permeability, viscosity, temperature, minimum miscibility pressure, reservoir pressure, reservoir depth, and API gravity.

3.2.1. Histograms. Also known as frequency plots, used to determine the frequency of specific range of values and how they repeated in the data. The maximum range of values were illustrated in red color of each property. This visualization method allows identification of the most common values used in the reported studies of EOR in unconventional reservoirs. Figure 9 shows an illustration of a typical histogram.

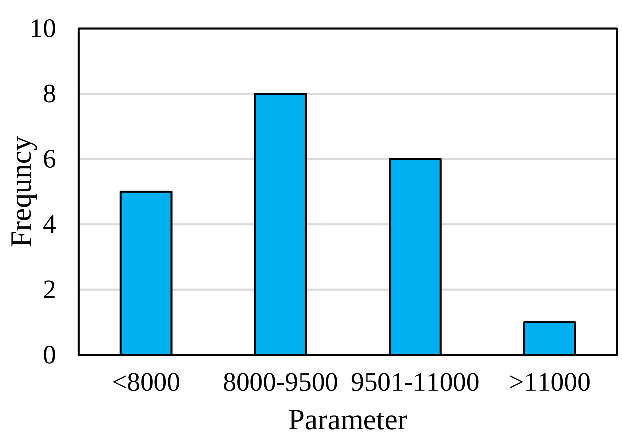

Figure 9- Histogram example

3.2.2. Boxplots. Boxplots used to determine different five sections of the data. The boxplot is divided into five sections as following: the upper bar which presents the maximum value of data, the upper box which represents the third quartile range (75th percentile), the median value which represented by the middle line, the lower box which represents the first quartile range (25th percentile), and the lower bar which represents the lower values of data. Figure 10 shows an example of a boxplot and its sections. Table 5 summarizes all the generated plots and the units used for each factor.

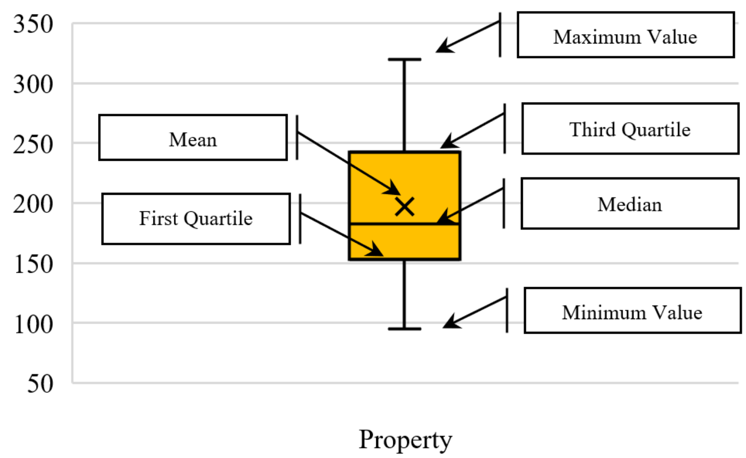

Figure 10. Boxplot example

Table 5- All Generated Plots Summary

Factor	**Unit**	**Histogram**	**Boxplot**
Porosity	Fraction	X	X
Permeability	md	X	X
MMP	psi	X	X
Oil viscosity	cp	X	X
Reservoir pressure	psi	X	X
Oil API gravity	^{o}API	X	X
Reservoir depth	ft	X	X
Reservoir temperature	^{o}F	X	X

3.3. RESULTS AND ANALYSIS

Porosity: The boxplot and histogram of porosity are shown in the following figure. Figure 11 shows that most of the reported porosities in unconventional reservoirs range between 3.1 to 9 %. This range of low porosity confirms the most common quantity reported (Wang et al., 2016; Sorensen et al., 2015; Wang et al., 2012). A maximum of 14% was found and a minimum of 0.6%. The median of data very central, around 6.5%, suggests a normal distribution of the data and no skew. The visualization highlights that the porosity of unconventional reservoirs is low.

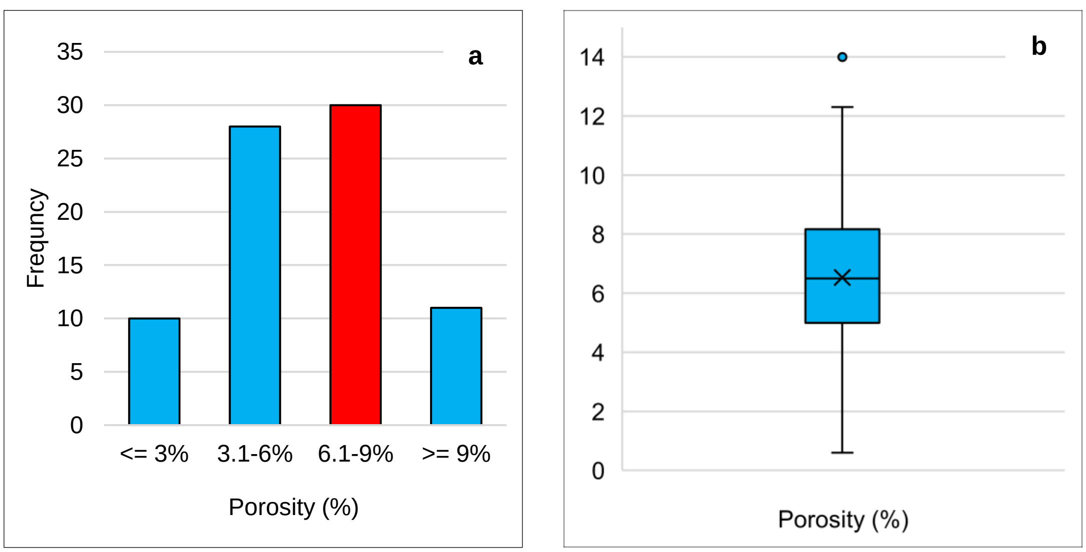

Figure 11. Porosity data distribution.
a) Histogram. b) Boxplot

Permeability: Permeability is the most significant factor which has been discussed and reported in the oil industry with regards to unconventional reservoirs. Hydrocarbons in such permeability are unable to move easily between pore spaces; thus, the oil recovery is very low. Hence, improved technologies of EOR are required. Based on our analysis of data, the permeability data distribution is presented in Figure 12. All tight reservoirs have the same characteristic of ultra-small permeability, and the analysis of the data proved this point. A maximum of 7 millidarcy was reported (Wange et al., 2012) and the median of the data was 0.005 millidarcy. About 61% of the permeability were reported under 0.01 millidarcy and 39% above 0.01 millidarcy. The common quantity is between 0.0001-0.1 md (Kurtoglu et al., 2012).

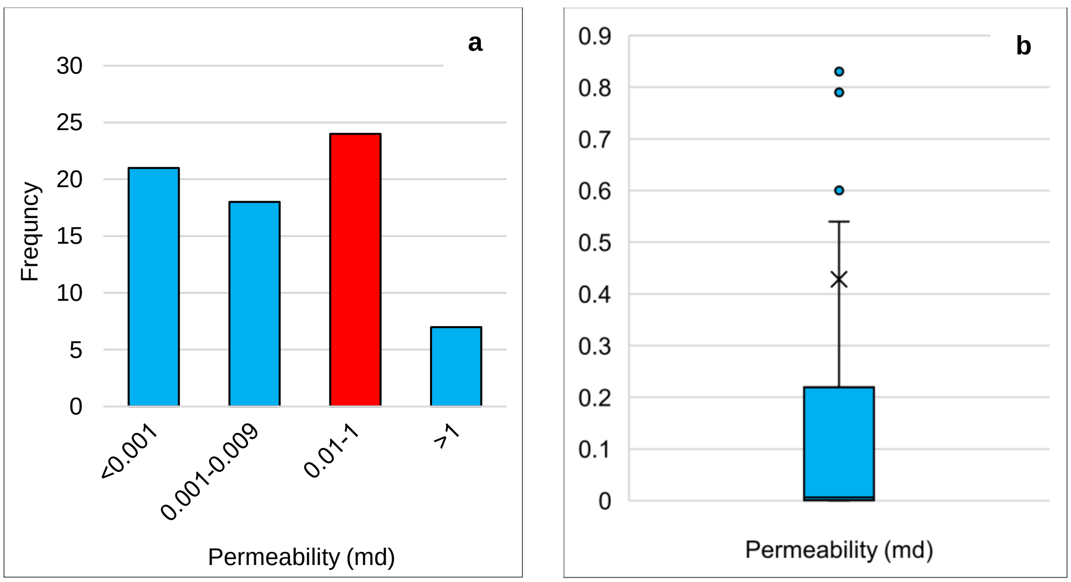

Figure 12. Permeability data distribution.
a) Histogram. b) Boxplot

Minimum Miscibility Pressure (MMP): At a constant temperature and composition, MMP is the lowest pressure at which multiple or first-contact miscibility can be achieved. The value of MMP depends on the gas type. For example, MMP of N_2 is higher than MMP of CO_2. Hence, gas selection is vital in improving the oil recovery during gas injection process. A maximum of 7000 psi of MMP was reported using nitrogen, while the minimum value of MMP was 1500 psi as shown in the boxplot. Most of the reported studies have been used CO_2 to reach MMP. However, most of MMP in tight reservoir studies showed that most of the MMP is below 3000 psi. The common quantity of the MMP of CO_2 is between 2450-2650 psi (Alharthy el al., 2015). Moreover, slim tube packed with sand and rising bubble apparatus were commonly used techniques employed to investigate the MMP in the laboratory. Figure 13 shows the data distribution of MMP.

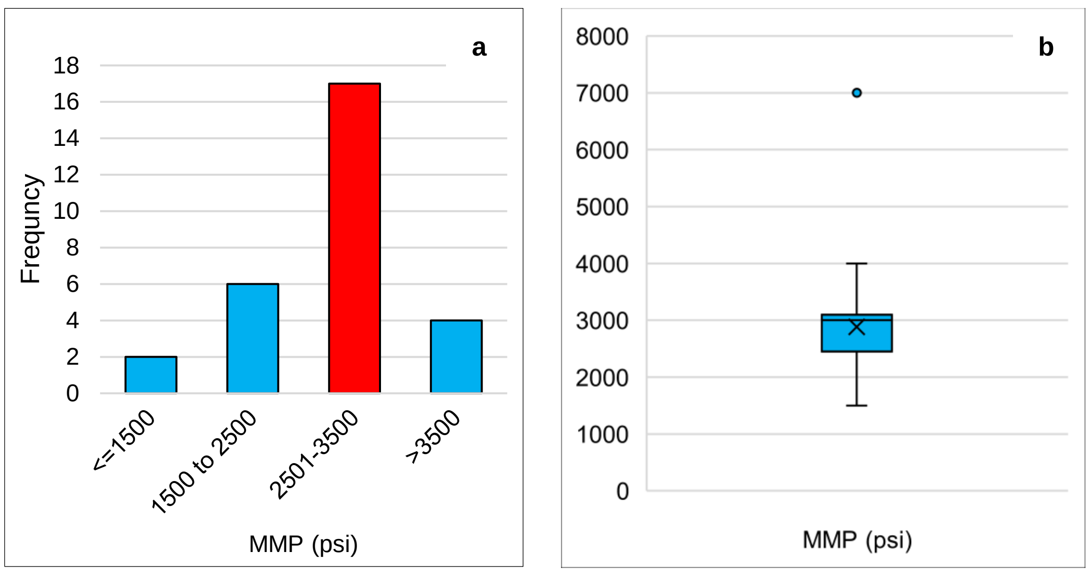

Figure 13. MMP data distribution.
a) Histogram. b) Boxplot

Oil Viscosity: Oil viscosity is a function of oil composition. Many low viscosities were reported in different laboratory studies and some field projects. This analysis found that viscosity range values were between 0.19 to 8.7 cp as shown in the following boxplot. Most of the reported studies showed that the most common viscosity values were less than 4 cp (Wang et al., 2016). The lowest viscosity noted was 0.19 cp of middle Bakken formation under reservoir conditions (Ling et al., 2014) due to high pressure and temperature. The oil viscosity data distribution is presented in Figure 14.

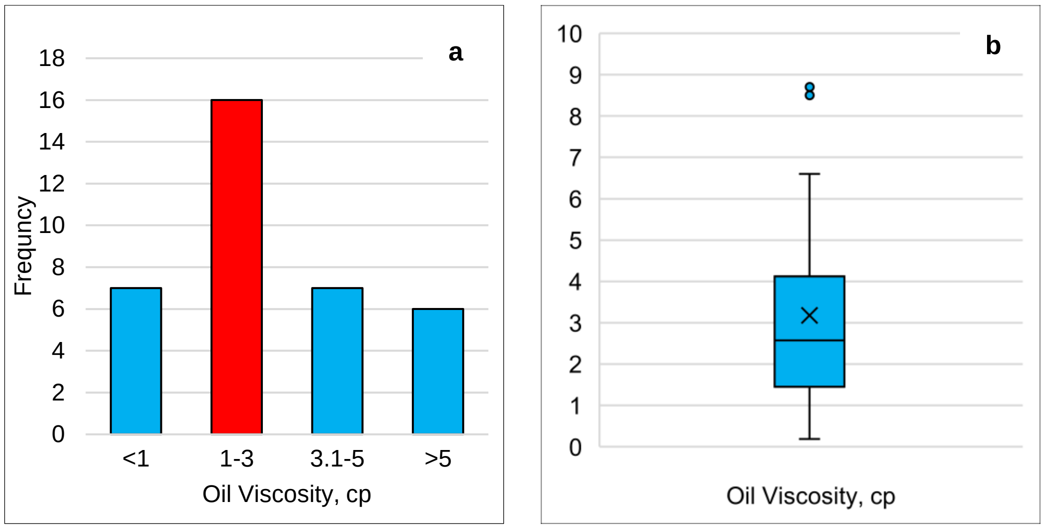

Figure 14. Oil viscosity data distribution
a) Histogram. b) Boxplot

Reservoir Pressure: The reservoir pressure is generally described as the pressure of fluids inside the formation pores. For ultra-low permeable formations, such as shales, the pore fluids cannot always move and support the total overlying rock column. This process generates high pressure in the reservoir. Usually in unconventional reservoirs, the pressure is particularly high. Different studies have been investigating reservoir pressure, including simulation studies, laboratory tests, or field projects. Most of these studies reveal that the common reservoir pressure of tight reservoirs ranges from 2500 to 7000 psi as shown in the following histogram in Figure 15. The maximum value was 9088 psi, and the minimum value is 2200 psi. A median of 6425 psi was obtained.

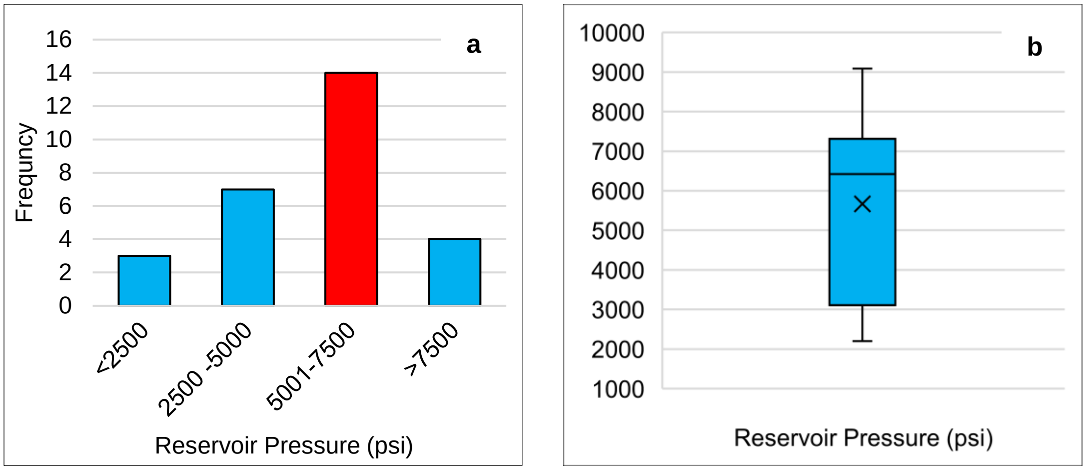

Figure 15. Reservoir pressure data distribution
a) Histogram. b) Boxplot

Oil API Gravity: Oil type based on API is a significant parameter. API measures how oil heavy or light compared to water. As the API increases, the oil becomes lighter. The lower the petroleum liquid density, the higher the API gravity. Based on our analysis, the API ranges from 32 to 52 with a median of 42 as shown in Figure 16. Around 56% of studies showed an API from 40 to 45. The average oil gravity of Bakken crude oil is 42 API (Yu et al., 2014).

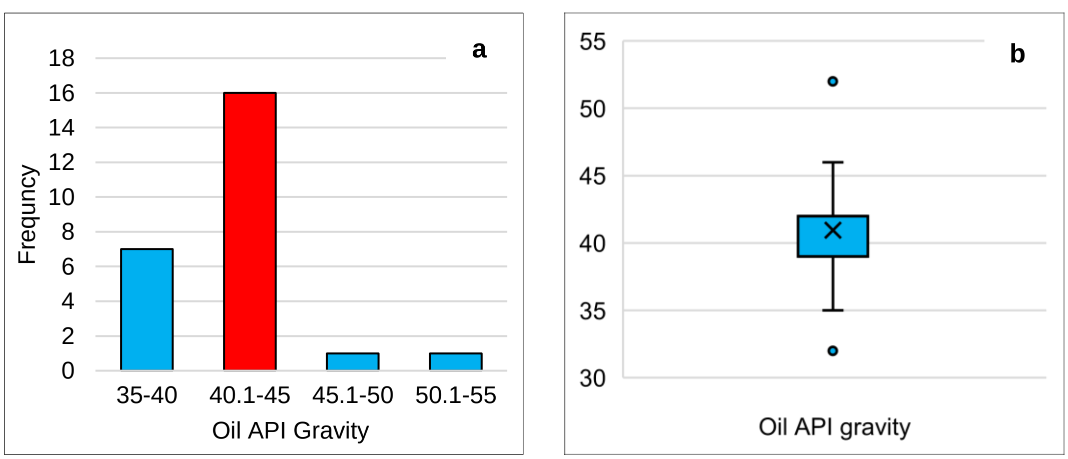

Figure 16. Oil API gravity data distribution
a) Histogram. b) Boxplot

Reservoir Depth: Figure 17 shows the maximum value of the reported studies was 11340 ft and the minimum value was 7389 ft. The mode of reported reservoir depths of tight reservoirs was below 10000 ft.

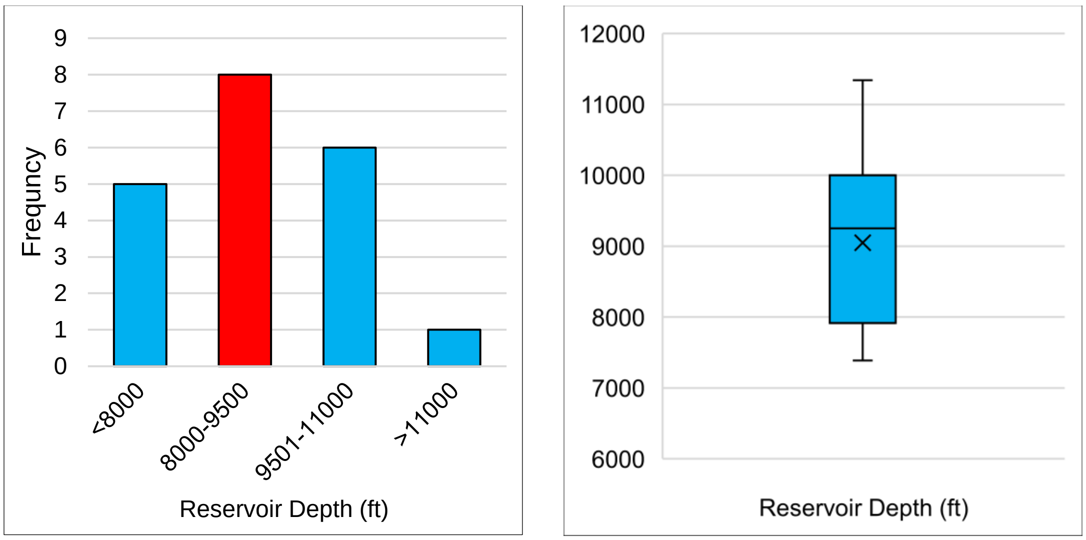

Figure 17. Reservoir depth data distribution
a) Histogram. b) Boxplot

Reservoir Temperature: Reservoir temperature is an important characteristic which affects different properties such as viscosity and MMP. Studying the reservoir temperature gives a better understanding of phase behavior and properties of reservoir fluids. High reservoir temperature also affects the pipeline design and operations. A maximum of 350^{o}F was reported and a minimum of 95^{o}F.

Many studies have reported a temperature between 150-250^{o}F (Zhang, 2016). The following histogram and boxplots in Figure 18 summarize the key values of reservoir temperature. The highest frequency range was observed between 151 - 200^{o}F.

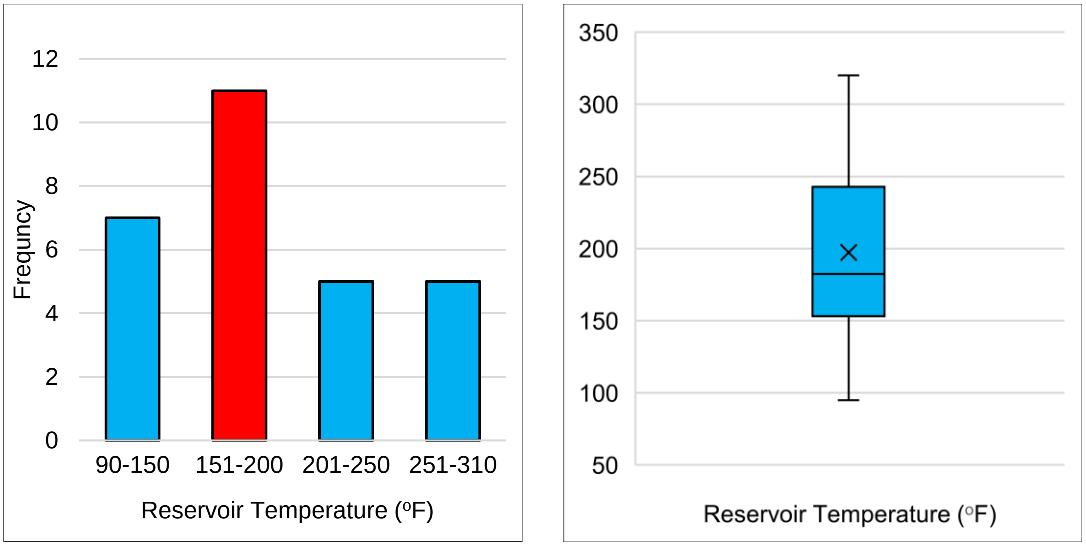

Figure 18. Reservoir temperature data distribution
a) Histogram. b) Boxplot

Table 6 summarizes the most common rock and fluid properties of unconventional reservoirs. The major properties have been characterized from Eagle Ford, Wolfcamp, Bakken, and Barned which has the most productive shale reservoirs.

Table 7 summarizes the criteria values for each property for better understanding the distribution of the reported data of each characteristic. However, various factors that were collected in this research cannot be presented in a histogram or a boxplot due to the lack of data. For example, the commonly reported wettability of the unconventional reservoirs was oil-wet to intermediate-wet before adding the surfactant formulation (Wang et al., 2012). Water saturation was reported for Middle Bakken formation which is between 25% and 50% (Cherian et al., 2012). Moreover, rich total organic content of unconventional reservoirs was reported of 0.1(wt%) to 5(wt%).

Table 6. Most common rock and fluid properties of unconventional reservoirs

Reservoir Property	Unit	Common Quantity	Reference
Porosity	%	4.5-9	Hawthorne et al. (2013) Schmidt et al. (2014)
Permeability	md	0.0001- 0.1	Meng et al. (2017) Alfarge et al. (2018a)
Temperature	ºF	248	Yu et al. (2016b)
Reservoir Depth	ft	6000-11340	Alvarez et al. (2014) Zhang et al. (2016)
Reservoir Pressure	psi	7350	Morsy et al. (2013e)
Wettability	-	Oil wet to intermediate	Alvarez et al. (2016a) Wang et al. (2012)
Oil Saturation	%	50-75	Pu et al. (2016)
Grain Density	g/cc	2.55-2.75	Alvarez et al. (2016b)
Bulk Density	g/cc	2.3-2.5	Alvarez et al. (2016b)
Specific Gravity	-	1.9	Kurtoglu et al. (2014)
Total Organic Content	wt%	0.1 to 11	Alharthy et al. (2015) Alvarez et al. (2016b)
Dominant Grain Size	µm	<62.5	Pu et al. (2016)
Net Thickness	ft	10-40	Jin et al. (2016b)
Clay Content	%	7-30	Alvarez et al. (2016b) Yu et al. (2016c)
Oil Density	API	38-42	Kurtoglu et al. (2013b)
Oil Viscosity	cp	< 8.5	Yu et al. (2017) Schmidt et al. (2014)
Contact Angle	-	81-142	Alvarez et al. (2016b)
MMP for CO_2	psi	1600-2560	Alharthy et al. (2015) Vega et al. (2010)
PH	-	5.7	Kurtoglu et al. (2014)
Total Acid Number	mg KOH/g	0.09	Kurtoglu et al. (2014)
Total Base Number	mg KOH/g	1.16	Kurtoglu et al. (2014)
GOR (Gas Oil Ratio)	SCF/STB	507-1712	Jin et al. (2016b)

Table 7- Summary and Criteria Guide of Data Analysis

Property	Minimum	Maximum	Mean	Median	Standard Deviation
Porosity, %	0.6	14	6.53	6.5	2.73
Permeability, md	0.00004	7	0.36	0.005	0.99
Viscosity, cp	0.19	8.7	3.18	2.57	2.63
MMP, psi	1500	7000	2882.41	3000	1066.92
Reservoir Pressure, psi	2200	9088	5670.93	6425	2045.35
Reservoir Depth, ft	7389	11340	9049.80	9250	1231.44
API Gravity, ^{o}	32	52	40.94	42	3.92
Reservoir Temperature, ^{o}F	95	320	197.29	182.5	61.50

4. FURTHER DISCUSSION

Extensive studies have investigated the applicability of EOR methods in these unconventional reservoirs, whether in the laboratory, as an experimental or simulation, or in field tests. Although some methods are more applicable than others and many factors should be considered when choosing the most applicable method for the target reservoir. The results are complex, but it is clear from this study that CO_2 gas injection, low salinity water injection, and surfactant in chemical methods appear to be the most applicable techniques. This research highlights that these methods may give better results than previously used methods. All methods are subject to some limitations. Table 8 shows the potential mechanisms which may cause the increase in hydrocarbon recovery from unconventional reservoirs.

Table 8. Mechanisms of most potential EOR in unconventional reservoirs

Miscible Gas Injection Method (CO_2, N_2, Natural Gas)
• Extraction • Oil Swelling and pressure maintenance • Reduction of oil viscosity • Displace oil in matrix by high compressibility. • Capillary pressure reduction and gas diffusion • Re-pressurization
Low Salinity Water Method
• Shale cracking and Wettability alteration • Water imbibition and Clay swelling
Chemical Methods
• Wettability alteration and Interfacial tension reduction

5. COMMON EOR PROBLEMS IN UNCONVENTIONAL RESERVOIRS

5.1. INJECTIVITY

Injectivity problems are considered a main obstacle for all EOR in unconventional reservoirs due to their ultra-low permeability. Some studies reported that water injection in flooding mode may result in fractures in the reservoirs (Baker et al., 2016). This suggestion was based on a pilot test conducted in the Bakkan formation in the U.S. The lower the permeability, the better the chance of fractures being created. The other problem associated with gas injection is the type of gas injection mode.

As aforementioned, there are two ways to inject the gas into the reservoir: the huff-n-puff mode and the flooding mode. According to previous studies, the huff-n-puff mode is superior to the flooding process (Sheng, 2017). The huff-n-puff mode gave better recoveries in a variety of laboratory experiments. Alfarge et al. (2016) suggest this is not entirely correct. They propose that the ultra-low permeability is one of the reasons that might prevent the application of the flooding mode.

5.2. IMBIBITION RATE

Another important issue is the imbibition rate. The imbibition of the injection fluid, such as surfactant, was not effective in some cases. The lower the imbibition rate, the lower the recovery from the reservoir. Wang et al. (2016) concluded that the imbibition rate of surfactant cannot proceed more than a few meters in unconventional reservoirs. The natural fractures in the reservoirs will increase the imbibition of the surfactant due to the increase of the contact area between the reservoir and the surfactant. Li et al. (2016) combined low salinity water with surfactant to increase the imbibition rate.

6. OTHER EOR METHODS

Various studies suggest alternative methods which may be considered as a technique to increase the hydrocarbon recovery from unconventional reservoirs. Increasing the reservoir recovery by the thermal technique to high temperature to change the oil viscosity thus increases the oil recovery. This could be true in heavy oil reservoirs, but not unconventional reservoirs; the common property is that their oil is light. This method requires further investigation into its applicability in field scales to be considered as one of the EOR in unconventional.

Sheng (2013b) reported another method which has potential to be used in unconventional reservoirs, the microbial method. Microbial products can be generated by injecting microbial reaction products in reservoir. Usually, this method can be applied to formations that have a low temperature (<98 C) and high permeability (>50 mD) (Sheng ,2013b). The only investigation of this method was conducted in China, where two slugs of microbial solution were injected into the reservoir (Liu et al., 2010). Finally, there have been no investigations of this method in the U.S.

7. CONCLUSIONS

This paper summarizes the main methods of EOR in unconventional reservoirs. Given our results, we suggest the following conclusions:

- Gas injection, low salinity water flooding, and surfactant are the most applicable techniques which have been applied in unconventional reservoirs for increasing hydrocarbon recovery.
- Different tools have been employed to investigate EOR methods in unconventional including simulation, experimental, and field pilots. However, simulation and experimental tools were used more frequently than field tests.
- CO_2, N_2 and methane were the most researched gasses for the unconventional reservoirs. CO_2 was extensively used due to price and availability.
- Huff-n-puff mode was widely used and was superior to flooding mode in gas injection methods.
- Surfactant has the most potential material to improve the oil recovery among the chemical methods due to its ability to change the wettability of the reservoir rocks to water wet. However, alkaline and polymer were not reported for unconventional reservoirs.

- The imbibition rate of surfactant is challenging because it cannot proceed more than few meters in unconventional reservoirs. This can be solved by creating more fractures and mixing the surfactant with low salinity water.
- Of all the countries worldwide, the USA has performed the most research and field tests regarding EOR in unconventional resources.
- There is a major disparity between the laboratory experiments and the applicability of these tests in field scales.
- The rock and fluid properties impact the ability to apply EOR significantly due to the interaction of the EOR-agents with the minerals and the reservoir fluids.
- More field investigations of applicability of all methods need to be done for better understanding of such techniques in field scales.

REFERENCES

Al-Alwani, M. A., Britt, L. K., Dunn-Norman, S., Alkinani, H. H., Al-Hameedi, A. T. T., Al-Attar, A. M., … Al-Bazzaz, W. H. (2019, October 25). From Data Collection to Data Analytics: How to Successfully Extract Useful Information from Big Data in the Oil & Gas Industry? Society of Petroleum Engineers. doi:10.2118/196428-MS

Alfarge, D., Alsaba, M., Wei, M., & Bai, B. (2018a, December 10). Miscible Gases Based EOR in Unconventional Liquids Rich Reservoirs: What We Can Learn. Society of Petroleum Engineers. doi:10.2118/193748-MS

Alfarge, D., Wei, M., & Bai, B. (2017, August 4). Feasibility of CO_2-EOR in Shale-Oil Reservoirs: Numerical Simulation Study and Pilot Tests. Carbon Management Technology Conference. doi:10.7122/485111-MS

Alfarge, D., Wei, M., and Bai, B. (2018). Data Analysis for CO_2-EOR in Shale-Oil Reservoirs Based on a Laboratory Database. Journal of Petroleum Science and Engineering https://doi.org/10.1016/j.petrol.2017.10.087.

Alfarge, D., Wei, M., & Bai, B. (2017, April 23). IOR Methods in Unconventional Reservoirs of North America: Comprehensive Review. Society of Petroleum Engineers. doi:10.2118/185640-MS

Alharthy, N., Teklu, T., Kazemi, H. et al. 2015. Enhanced Oil Recovery in LiquidRich Shale Reservoirs: Laboratory to Field. Society of Petroleum Engineers. DOI: 10.2118/175034-MS.

Alvarez, J.O. and Schechter, D.S. 2016a. Altering Wettability in Bakken Shale by Surfactant Additives and Potential of Improving Oil Recovery During Injection of Completion Fluids. Society of Petroleum Engineers. http:10.2118/SPE-179688-MS.

Alvarez, J. O., Neog, A., Jais, A., & Schechter, D. S. (2014, April 1). Impact of Surfactants for Wettability Alteration in Stimulation Fluids and the Potential for Surfactant EOR in Unconventional Liquid Reservoirs. Society of Petroleum Engineers. doi:10.2118/169001-MS

Alvarez, J. O., & Schechter, D. S. (2016b, August 1). Wettability, Oil and Rock Characterization of the Most Important Unconventional Liquid Reservoirs in the United States and the Impact on Oil Recovery. Unconventional Resources Technology Conference. doi:10.15530/URTEC-2016-2461651

Babadagli, T., 2001. Scaling of concurrent and countercurrent capillary imbibition for surfactant and polymer injection in naturally fractured reservoirs. SPE J. Dec 465–478.

Baker, R., Dieva, R., Jobling, R., Lok, C., 2016. The myths of waterfloods, EOR floods and how to optimize real injection schemes. In: Paper SPE 179536 Presented at the SPE Improved Oil Recovery Symposium Held in Tulsa, Oklahoma, 11–13 April.

Balasubramanian, S., Chen, P., Bose, S., Alzahabi, A., & Thakur, G. C. (2018, April 30). Recent Advances in Enhanced Oil Recovery Technologies for Unconventional Oil Reservoirs. Offshore Technology Conference. doi:10.4043/28973-MS

Behnsen, J., Faulkner, D.R., 2011. Water and argon permeability of phyllosilicate powders under medium to high pressure. J. Geophys Res. 116, B12203.

Canadian Society of Unconventional Resources. http://www.csur.com

Cherian, B. V., Stacey, E. S., Lewis, R., Iwere, F. O., Heim, R. N., & Higgins, S. M. (2012, January 1). Evaluating Horizontal Well Completion Effectiveness in a Field Development Program. Society of Petroleum Engineers. doi:10.2118/152177-MS

Chen, H.L., Lucas, L.R., Nogaret, L.A.D., Yang, H.D., Kenyon, D.E., 2001. Laboratory monitoring of surfactant imbibition with computerized tomography. SPEREE 2,16–25.

Chen, Z., Narayan, S.P., Yang, Z., Rahman, S.S., 2000. An experimental investigation of hydraulic behaviours of fractures and joints in granitic rock. Int. J. Rock Mech. Min. Sci. 37, 1061–1071.

Cheng, J.Y., Wan, Z.J., Zhang, Y.D., 2015. Experimental study on anisotropic strength and deformation behavior of a coal measure shale under room dried and water saturated conditions. Shock Vib. 1–13.

Clark, A. J. (2009, January 1). Determination of Recovery Factor in the Bakken Formation, Mountrail County, ND. Society of Petroleum Engineers. doi:10.2118/133719-STU

Dawson, M., Nguyen, D., Champion, N., & Li, H. (2015). Designing an Optimized Surfactant Flood in the Bakken. Society of Petroleum Engineers. doi:10.2118/175937-MS.

Denoyelle, L.C., Lemonnier, P., 1987. Simulation of CO_2 Huff 'n' Puff Using Relative Permeability Hysteresis. SPE 16710-MS.

Energy Information Administration (EIA), 2016. Initial production rates in tight oil formations continue to rise, 11 February 2016. https://www.eia.gov/todayinenergy/detail.cfm?id¼24932 (Accessed 4 November 2016)

Elwegaa, K., & Emadi, H. (2018). The Effect of Thermal Shocking with Nitrogen Gas on the Porosities, Permeabilities, and Rock Mechanical Properties of Unconventional Reservoirs. Energies, 11(8), 2131. doi:10.3390/en11082131

Elwegaa, K., & Emadi, H. Improving oil recovery from shale oil reservoirs using cyclic cold nitrogen injection – An experimental study,Fuel,Volume 254,2019,115716,ISSN 0016-2361, https://doi.org/10.1016/j.fuel.2019.115716.

Elturki, M., & Imqam, A. (2020, July 20). High Pressure High Temperature Nitrogen Interaction with Crude Oil and Its Impact on Asphaltene Deposition in Nano Shale Pores Structure: An Experimental Study. Unconventional Resources Technology Conference. doi:10.15530/urtec-2020-3241

Faulkner, D., Rutter, E., 2000. Comparisons of water and argon permeability on natural clay-bearing fault gouge under high pressure at 20 C. J. Geophys. Res. 105 (16), 415–416, 426.

Ferno, M.A., Haugen, A., Graue, A., 2012. Surfactant prefloods for integrated EOR in fractured, oil-wet carbonate reservoirs. In: Paper SPE 159213 Presented at the SPE Annual Technical Conference and Exhibition, 8–10 October, San Antonio, Texas, USA.

Hawthorne, S. B., Gorecki, C. D., Sorensen, J. A., Steadman, E. N., Harju, J. A., & Melzer, S. (2013, November 5). Hydrocarbon Mobilization Mechanisms from Upper, Middle, and Lower Bakken Reservoir Rocks Exposed to CO. Society of Petroleum Engineers. doi:10.2118/167200-MS

Hirasaki, G., Zhang, D.L., 2004. Surface chemistry of oil recovery from fractured, oil-wet, carbonate formations. SPE J. (June) 151–162.

Hoffman, B.T., Evans, J.G., 2016. Improved oil recovery IOR pilot projects in the Bakken formation. In: Paper SPE 180270 Presented at the SPE Low Perm Symposium, 5–6 May, Denver, Colorado, USA.

Jansen, T., Zhu, D., Hill, A.D., 2015. Effect of Rock mechanical properties on fracture Conductivity for shale formations. In: Paper SPE 173347-MS Presented at the SPE Hydraulic Fracturing Technology Conference, 3–5 February, The Woodlands, Texas,USA.

Jin, L., Sorensen, J. A., Hawthorne, S. B., Smith, S. A., Bosshart, N. W., Burton-Kelly, M. E., … Harju, J. A. (2016a, February 24). Improving Oil Transportability Using CO_2 in the Bakken System – A Laboratory Investigation. Society of Petroleum Engineers. doi:10.2118/178948-MS

Jin, L., Hawthorne, S., Sorensen, J., Kurz, B., Pekot, L., Smith, S., Harju, J. (2016b, August 1). A Systematic Investigation of Gas-Based Improved Oil Recovery Technologies for the Bakken Tight Oil Formation. Unconventional Resources Technology Conference. doi:10.15530/URTEC-2016-2433692

Jia, C.-Z., Zou, C.-N., Li, J.-Z., Li, D.-H., Zheng, M., 2012. Evaluation criteria, main types, key properties and prospects of the tight oil in China. Acta Pet. Sin. 33 (3), 343–350.

Joslin, K., Ghedan, S.G., Abraham, A.M., Pathak, V., 2017. EOR in tight reservoirs, technical and economical feasibility. In: Paper SPE 185037 Presented at the SPE Unconventional Resources Conference Held in Calgary, Alberta, Canada, 15–16 Feburary.

Kazemi, H., Gilman, J.R., Elsharkawy, A.M., 1992. Analytical and numerical solution of oil recovery from fractured reservoirs with empirical transfer functions. SPERE (May) 219–227.

Kurtoglu, B., Sorensen, J.A., Braunberger, J., Smith, S., Kazemi, H., 2013a. Geologic characterization of a bakken reservoir for potential CO_2 EOR. In: Paper SPE 168915 Presented at the Unconventional Resources Technology Conference, 12–14 August, Denver, Colorado, USA.

Kurtoglu, B., Sorensen, J. A., Braunberger, J., Smith, S., & Kazemi, H. (2013b, August 12). Geologic Characterization of a Bakken Reservoir for Potential CO_2 EOR. Unconventional Resources Technology Conference. doi:10.1190/urtec2013-186

Kurtoglu, B., Kazemi, H., Rosen, R., Mickelson, W., & Kosanke, T. (2014, September 30). A Rock and Fluid Study of Middle Bakken Formation: Key to Enhanced Oil Recovery. Society of Petroleum Engineers. doi:10.2118/171668-MS

Li, K., Horne, R.N., 2006. Generalized scaling approach for spontaneous imbibitions: an analytical model. In: Paper SPE 77544 Presented at the SPE Annual Technical Conference and Exhibition, San Antonio, TX, 29 September – 2 October.

Li, X., Teklu, T. W., Abass, H., & Cui, Q. (2016, August 1). The Impact of Water Salinity/Surfactant on Spontaneous Imbibition through Capillarity and Osmosis for Unconventional IOR. Unconventional Resources Technology Conference. doi:10.15530/URTEC-2016-2461736

Lin, Y.-Y., Wang, P.-P., Li, Q.-D., Han, B.-M., Li, H.-L., Wu, Y.-P., He, W.-S., 2016. Performance analysis of different modes of huff-n-puff water injection in horizontal wells in An-83 Chang-7 tight oil reservoir. Petrochem. Ind. Appl. 35 (6), 94–97.

Ling, K., Shen, Z., Han, G., He, J., & Peng, P. (2014, August 25). A Review of Enhanced Oil Recovery Methods Applied in Williston Basin. Unconventional Resources Technology Conference. doi:10.15530/URTEC-2014-1891560.

Liu, J.-Y., Shen, K., Huang, Z.-W., Huai, H.-N., Chen, F.-L., 2010. A MEOR pilot test in an Ansai low-permeability reservoir. Xinjiang Pet. Geol. 31 (6), 634–636.

Mandal, A., 2015. Chemical flood enhanced oil recovery: a review. Int. J. Oil, Gas Coal Technol. 9 (3), 241–264.

Mattax, C.C., Kyte, J.R., 1962. Imbibition oil recovery from fractured, water-drive reservoir. SPEJ (June) 177–184.

Meng, X., Sheng, J. J., & Yu, Y. (2017, May 1). Experimental and Numerical Study of Enhanced Condensate Recovery by Gas Injection in Shale Gas-Condensate Reservoirs. Society of Petroleum Engineers. doi:10.2118/183645-PA

Mohammed-Singh, L. J., Singhal, A. K., & Sim, S. S.-K. (2006, January 1). Screening Criteria for CO_2 Huff 'n' Puff Operations. Society of Petroleum Engineers. doi:10.2118/100044-MS

Morsy, S and Sheng, J.J., 2014a. Effect of Water Salinity on Shale reservoir Productivity. Advances in Petroleum Exploration and Development 8(1): 9–14. DOI:10.3968/5604

Morsy, S., Gomaa, A., Sheng, J.J., 2014b. Imbibition characteristics of marcellus Shale Formation. In: Paper SPE 169034 Presented at the SPE Improved Oil Recovery Symposium, 12–16 April, Tulsa, Oklahoma, USA.

Morsy, S., Gomaa, A., Sheng, J.J., 2014c. Improvement of eagle ford shale formations water imbibition by mineral dissolution and wettability alteration. In: Paper SPE 168985 Presented at the SPE Unconventional Resources Conference, 1–3 April, The Woodlands, Texas, USA.

Morsy, S., Gomaa, A., Sheng, J.J., Soliman, M.Y., 2013d. Potential of improved waterflooding in acid-hydraulically-fractured shale formations. In: Paper SPE 166403 Presented at the SPE Annual Technical Conference and Exhibition Held in New Orleans, Louisiana, USA. September 30–October 2.

Morsy, S., Sheng, J. J., & Soliman, M. Y. (2013e). Waterflooding in the Eagle Ford Shale Formation: Experimental and Simulation Study. Society of Petroleum Engineers. doi:10.2118/167056-MS

Morsy, S., Sheng, J.J., 2014f. Imbibition characteristics of the barnett Shale Formation. In: Paper SPE 168984 Presented at the SPE Unconventional Resources Conference, 1–3 April, The Woodlands, Texas, USA.

Morsy, S., Sheng, J.J., Soliman, M.Y., 2013g. Improving hydraulic fracturing of shale formations by acidizing. In: Paper SPE 165688 Presented at the SPE Eastern Regional Meeting Held in Pittsburgh, Pennsylvania, USA. August 20–22.

Nguyen, D., Wang, D., Oladapo, A., Zhang, J., Sickorez, J., Butler, R., Mueller, B., 2014. Evaluation of surfactants for oil recovery potential in shale reservoirs. Paper SPE 169085. Presented at the SPE Improved Oil Recovery Symposium. Tulsa, Oklahoma. April 12–16.

Olson, D.K., Hicks, M.D., Hurd, B.G., Sinnokrot, A.A., Sweigart, C.N., 1990. Design of a novel flooding system for an oil-wet Central Texas carbonate reservoir. In: Paper SPE 20224 Presented at the SPE/DOE Enhanced Oil Recovery Symposium, 22–25 April, Tulsa, Oklahoma, USA.

Pedlow, J., Sharma, M., 2014. Changes in shale fracture conductivity due to interactions with water-based fluids. In: Paper SPE 168586 Presented at the SPE Hydraulic Fracturing Technology Conference, Woodlands, TX, 4–6 Feb.

Phillips, Z.D., Halverson, R.J., Strauss, S.R., Layman II, J.M., Green, T.W., 2009. Paper SPE 108045 presented the rocky mountain oil & gas technology symposium, 16–18 April, Denver, Colorado, U.S.A.

Potapenko, D.I., Tinkham, S.K., Lecerf, B., Fredd, C.N., Samuelson, M.L., Gillard, M.R., Le Calvez, J.H., Daniels, J.L., 2009. Barnett shale refracture stimulations using a novel diversion technique. In: Paper SPE 119636 Presented at the SPE Hydraulic Fracturing Technology Conference, 19–21 January, The Woodlands, Texas.

Pu, H., & Li, Y. (2016, April 11). Novel Capillarity Quantification Method in IOR Process in Bakken Shale Oil Reservoirs. Society of Petroleum Engineers. doi:10.2118/179533-MS

Rai, S.K., Bera, A., Mandal, A., 2015. Modeling of surfactant and surfactant–polymer flooding for enhanced oil recovery using STARS (CMG) software. J. Petroleum Explor. Prod. Technol. 5 (1), 1–11.

Samanta, A., Bera, A., Ojha, K., Mandal, A., 2012. Comparative studies on enhanced oil recovery by alkali–surfactant and polymer flooding. J. Petroleum Explor. Prod. Technol. 2 (2), 67–74.

Schmidt, M., Sekar, B.K., 2014. Innovative Unconventional2 EOR-a light EOR an unconventional tertiary recovery approach to an unconventional bakken reservoir in southeast saskatchewan. In: Paper WPC-21–1921 Presented at the 21st World Petroleum Congress, 15-19 June, Moscow, Russia.

Sheng, J.J. 2015. Enhanced oil recovery in shale reservoirs by gas injection, Journal of Natural Gas Science and Engineering, 22: 252–259.

Sheng, J.J., 2013. Introduction to MEOR and field applications in China. In: Sheng, J.J.(Ed.), Chapter 19 in EOR Field Case Studies. Elsevier, pp. 543–560.

Sheng, J.J., Critical review of field EOR projects in shale and tight reservoirs, Journal of Petroleum Science and Engineering, Volume 159, 2017, Pages 654-665

Shuler, P., Tang, H., Zayne, Lu., Tang, Y., 2001. Chemical processes for improved oil recovery from Bakken shale Paper SPE 147531. Presented at the Canadian Unc. Res. Conf. Calgary, Alberta. November 15–17.

Sorensen, J.A., Hamling, J.A., 2016. Historical bakken test data provide critical insights on EOR in tight oil plays. http://www.aogr.com/magazine/cover-story/historicalbakken-test-data-provide-critical-insights-on-eor-in-tight-oil-p accessed 12 Nov 2016.

Sorensen, J. A., Braunberger, J. R., Liu, G., Smith, S. A., Hawthorne, S. A., Steadman, E. N., & Harju, J. A. (2015). Characterization and Evaluation of the Bakken Petroleum System for CO Enhanced Oil Recovery.Society of Petroleum Engineers. doi:10.2118/178659-MS

Thomas, A., Kumar, A., Rodrigues, K., Sinclair, R.I., Lackie, C., Galipeault, A., Blair, M., 2014. Understanding water flood response in tight oil formations: a case study of the lower Shaunavon. In: Paper SPE 171671 Presented at the SPE/CSUR Unconventional Resources Conference – Canada, 30 September–2 October, Calgary, Alberta, Canada.

Todd, H. B., & Evans, J. G. (2016, May 5). Improved Oil Recovery IOR Pilot Projects in the Bakken Formation. Society of Petroleum Engineers. doi:10.2118/180270-MS

Wan, T., Meng, X., Sheng, J.J., Watson, M., 2014a. Compositional modeling of EOR process in stimulated shale oil reservoirs by cyclic gas injection. In: Paper SPE 169069 Presented at the SPE Improved Oil Recovery Symposium, 12–16 April, Tulsa, Oklahoma, USA.

Wan, T., Sheng, J.J., Soliman, M.Y., 2013. Evaluation of the EOR potential in shale oil reservoirs by cyclic gas injection. In: Paper SPWLA-D-12-00119 Presented at the SPWLA 54th Annual Logging Symposium Held in New Orleans, Louisiana, 22-26 June.

Wang, D., Butler, R., Zhang, J., & Seright, R. (2012, December 1). Wettability Survey in Bakken Shale With Surfactant-Formulation Imbibition. Society of Petroleum Engineers. doi:10.2118/153853-PA

Wang, D., Butler, R., Liu, H., Ahmed, S., 2011. Flow-rate behavior and imbibition in shale. SPEREE 14 (4), 485–492.

Wang, D., Zhang, J., Butler, R., & Olatunji, K. (2016, July 1). Scaling Laboratory-Data Surfactant-Imbibition Rates to the Field in Fractured-Shale Formations. Society of Petroleum Engineers. doi:10.2118/178489-PA

Wang, X., Luo, P., Er, V., & Huang, S.-S. S. (2010). Assessment of CO_2 Flooding Potential for Bakken Formation, Saskatchewan. Society of Petroleum Engineers. doi: 10.2118/137728-MS.

Xie, X., Weiss, W.W., Tong, Z., Morrow, N.R., 2005. Improved oil recovery from carbonate reservoirs by chemical stimulation. SPE J. 276–285.

Yu, Y., Li, L. and Sheng J., (2016a). Further Discuss the Roles of Soaking Time and Pressure Depletion Rate in Gas Huffn-Puff Process in Fractured Liquid-Rich Shale Reservoirs. SPE-181471-MS paper presented in at the SPE Annual Technical Conference and Exhibition held in Dubai, UAE, 26-28 September 2016.

Yu, Y., Li, L., Sheng, J.J., 2017. A comparative experimental study of gas injection in shale plugs by flooding and huff-N-puff processes. J. Nat. Gas Sci. Eng. 38, 195–202.

Yu, W., Lashgari, H., & Sepehrnoori, K. (2014). Simulation Study of CO_2 Huff-n-Puff Process in Bakken Tight Oil Reservoirs. Society of Petroleum Engineers. doi:10.2118/169575-MS.

Yu, Y., & Sheng, J. J. (2016b, April 11). Experimental Evaluation of Shale Oil Recovery from Eagle Ford Core Samples by Nitrogen Gas Flooding. Society of Petroleum Engineers. doi:10.2118/179547-MS

Yu, Y., & Sheng, J. J. (2016c, May 23). Experimental Investigation of Light Oil Recovery from Fractured Shale Reservoirs by Cyclic Water Injection. Society of Petroleum Engineers. doi:10.2118/180378-MS

Zhang, K., 2016. Experimental and Numerical Investigation of Oil Recovery from Bakken Formation by Miscible CO_2 Injection. Paper SPE 184486 presented at the SPE international Student Paper Contest at the SPE Annual Technical Conference and Exhibition held in Dubai, UAE, 26-28 September 2016.

Zhu, P., Balhoff, M. T., & Mohanty, K. K. (2015). Simulation of Fracture-to-Fracture Gas Injection in an Oil-Rich Shale. Society of Petroleum Engineers. doi:10.2118/175131-MSSPE-180270-MS17.

Zubari, H. K., & Sivakumar, V. C. B. (2003, January 1). Single Well Tests to determine the Efficiency of Alkaline-Surfactant Injection in a highly Oil-Wet Limestone Reservoir. Society of Petroleum Engineers. doi:10.2118/81464-MS

II. ASPHALTENE THERMODYNAMIC FLOCCULATION DURING IMMISCIBLE NITROGEN GAS INJECTION

Mukhtar Elturki and Abdulmohsin Imqam

Missouri University of Science and Technology

ABSTRACT

Gas enhanced oil recovery (GEOR) is one of the most advantageous enhanced oil recovery methods. Nitrogen (N_2) is one of the most investigated gases due to its beneficial properties. However, during its interaction with crude oil, N_2 can induce asphaltene deposition, which may result in severe formation damage and pore plugging. Few works have investigated the impact of N_2 on asphaltene instability. This research studied the immiscibility conditions for N_2 in nanopores and the impact of N_2 on asphaltene precipitations, which could lead to plugging pores and oil recovery reduction. A slim tube was used to determine the minimum miscibility pressure (MMP) of N_2 to ensure that all the experiments would be carried out below the MMP. Then, filtration experiments were conducted using nano-filter membranes to highlight the impact of the asphaltene particles on the pores of the membranes. A special filtration vessel was designed and employed to accommodate the filter paper membranes. Various factors were investigated, including N_2 injection pressure, temperature, N_2 mixing time, and pore size heterogeneity. Supercritical phase N_2 was used during all filtration experiments. Visualization tests were implemented to observe the asphaltene precipitation and deposition mechanism over time. Increasing the N_2 injection pressure resulted in an increase in the asphaltene weight percent in all

experiments. Decreasing the pore size of the filter membranes resulted in an increase in the asphaltene wight percent. Greater asphaltene weight percents were observed with a longer N_2 mixing time. Visualization tests revealed that asphaltene clusters started to form after 1h and fully deposited after 12 h in the bottom of the test tubes. Chromatography analysis of the produced oil confirmed that there was a reduction in the heavy components and asphaltene weight percent. Microscopy and scanning electron microscopy (SEM) imaging of the filter paper membranes found that significant pore plugging resulted from asphaltene deposition and precipitation. This research investigated asphaltene precipitation and deposition during immiscible N_2 injection to understand the main factors that impact the success of using such a technique in unconventional shale reservoirs.

1. INTRODUCTION

Gas injection enhanced oil recovery (EOR) methods have been investigated in unconventional reservoirs, with the results showing an increase in oil recovery. Experimental studies have indicated a positive result in increasing oil recovery from shale cores using cyclic N_2 and carbon dioxide (CO_2) injection (Gamadi et al., 2013; Yu et al, 2015). Injection of CO_2 and N_2 mixtures has been studied for storing CO_2 and increasing hydrocarbon production from unconventional resources (Hassanpouryouzband et al, 2018; 2019). They investigated the CO_2 capture efficiency at various injection pressure and the results demonstrated that the efficiency of CO_2 capture depends on the reservoir conditions such as pressure and temperature. The results also showed that there is an optimal reservoir pressure for a given reservoir temperature at which the maximum volume of CO_2 can be extracted from the injected flue gas or CO_2-N_2 mixtures. However, injection of a gas changes the equilibrium conditions and fluid properties of the oil in the reservoir. Changing the equilibrium may lead to instability in the colloidal suspension, manifested by asphaltene precipitation and flocculation. CO_2 and N_2 could cause a different degree of asphaltene flocculation into the reservoir. CO_2 has good solubility in crude oil and can easily attain a supercritical condition in reservoir conditions (Wang et al., 2018). Thus, the mass transfer ability of supercritical CO_2 is strong. In CO_2 injection process, the CO_2-crude oil system could easily reach a miscible or near-miscible state that enhances extracts the light hydrocarbon components from crude oil into the gas phase. At similar thermodynamic conditions, N_2 has weaker solubility in crude oil than CO_2. N_2 has a weak mass transfer capacity which could lead to the poor extraction of light hydrocarbons and probably less asphaltene flocculation compared to CO_2 (Chung, 1992; Wang et al., 2018). Asphaltene is the heaviest component that occurs in petroleum fluids and that is insoluble in light n-alkanes, such as n-pentane or n-heptane. However, asphaltene is soluble in aromatics, such as toluene or benzene (Goual et al., 2012). Asphaltene, a solid component of crude oil, has an extremely high molecular weight (Mozaffari et al., 2015). Under reservoir temperature and pressure conditions, asphaltene can be in solution or in a colloidal suspension (Jamaluddin et al., 2002). Asphaltene instability can be induced when the injection of CO_2, N_2 and hydrocarbon gases changes the solubility of the reservoir fluids (Yang et al., 1999; Dehghani et al., 2008; Moradi et al., 2012a; Shen et al., 2016). When the solid phase is formed after the liquid phase, precipitation occurs. The deposition is the adherence of the solid phase to the reservoir rocks (Zendehboudi et al., 2014). This is the fundamental cause of problems related to asphaltene deposition and precipitation, in which asphaltene becomes denser in the reservoir, production facilities, and transportation pipelines.

Understanding the behavior and the factors that affect asphaltene deposition and precipitation is crucial due to the additional economic costs that must be incurred to solve the aforementioned asphaltene deposition issues.

Recently, the effects of asphaltene deposition on enhanced oil recovery have gained more attention due to its impact on production processes and its deposition resulting in lower oil recovery. Many studies have investigated asphaltene deposition and have aimed to improve shale recoveries during CO_2 injection (Alta'ee et al., 2012; Ren et al., 2011). However, there is a lack of N_2 immiscible injection research in the oil industry (Necmettin, 2003; Jamaluddin et al., 2002; Moradi et al., 2012a; Zadeh et al., 2011; Elwegaa et al., 2019; Mansoori et al., 2010; Hajizadeh et al., 2009; Khalaf and Mansoori, 2019; Elturki et al., 2020a, 2021). Elwegaa et al. (2019) conducted an experiment using cold N_2 via cyclic gas injection in shale cores. The results demonstrated a higher recovery factor when the pressure increased using the cold N_2 injection. Jamaluddin et al. (2002) stated that asphaltene instability was aggravated by N_2 injection, and the bulk precipitation amount was increased by elevating the concentration of N_2 in the reservoir fluids. Zadeh et al. (2011) examined the effect of N_2 on asphaltene instability by combining 10 mole percent of N_2 with the target oil at a reservoir temperature of 240^{o}F. Due to the low asphaltene content of the target oil, the asphaltene precipitation was not clearly detected, and the N_2 mole percentage was increased in the second sample. Zadeh et al. (2011) also investigated the effect of a lower temperature than 240^{o}F, finding that asphaltene became more unstable as the temperature increased when the pressure was above the bubble point. Moradi et al. (2012a) studied asphaltene particle precipitation, aggregation, and breakup using natural depletion and miscible N_2 injection processes. Using high-pressure filtration, it was observed that N_2 injection stabilized asphaltenes. Moreover, the study highlighted that the problems were more severe in heavier crude oil.

The negative effects of asphaltene deposition and precipitation on plugging pores are much more prevalent in unconventional reservoirs. Shale pores and throat sizes are usually much smaller than those in conventional reservoirs (Elturki et al., 2020b). Maroudas (1996) concluded that particles that have a size greater than 1/3 of pores sizes would block the pores and throats. When asphaltene particles are destabilized in solution, asphaltene flocculation occurs and can cause severe problems. Moradi et al. (2012b) conducted an experiment using N_2 and methane with a 0.2-µm pore size filter membrane and reported that asphaltene deposition was much higher in methane than in N_2. However, very few studies have been conducted to investigate asphaltene instability in crude oil during N_2 injection in nanopore-sized features, such as unconventional shale reservoirs. The ultimate goal of this research is to highlight the severity of asphaltene damage during N_2 gas injection, especially in nanopore structures, which are mainly present in unconventional reservoirs. By studying the impact of different factors on asphaltene formation damage, asphaltene deposition may be mitigated in future applications of N_2 injection.

2. ASPHALTENE DEPOSITION AND PRECIPITATION

Multiple compounds can be found in crude oil, depending on its composition. These compounds can be found in three phases: gases, liquids, and solids. The liquid phase consists of saturates, aromatics, and resins. Asphaltenes are the most common solids that exist in crude oil. Asphaltenes are the main polar components of crude oil, and they contain heteroatoms, such as N_2, sulfur, or oxygen, which can be soluble in aromatic solvents but insoluble in paraffinic liquids (Goual et al., 2002; Speight, 2014; Rashed et al., 2019; Nguyen et al., 2020). However, saturates and aromatics are nonpolar compounds. Resins can be a good bridging agent to hold the polar and nonpolar components because resins have both polar and nonpolar sites. Figure 1 shows the main components of crude oil and asphaltenes. Plugging reservoir pores and changing the formation wettability are common issues (Shen et al., 2016). Figure 2 presents formation wettability alterations due to asphaltene precipitation.

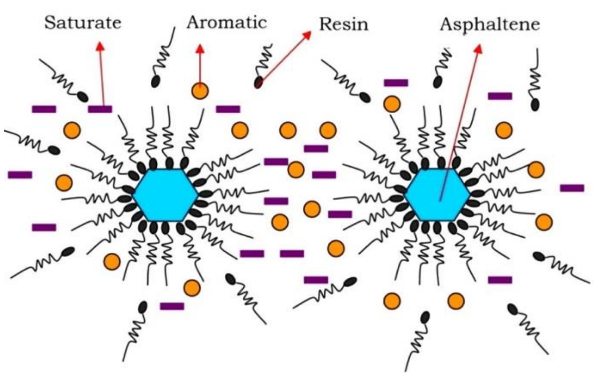

Figure 1. Main components of crude oil with asphaltene
(Ashoori et al., 2017).

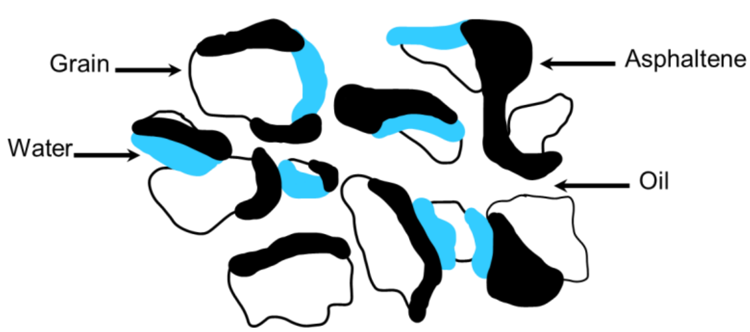

Figure 2. Formation wettability alterations due to asphaltene precipitation.

3. EXPERIMENTAL TEST MATRIX

Three sets of experiments were conducted: MMP experiments, filtration experiments, and asphaltene visualization experiments, with Figure 3 displaying an experimental flow chart. Table 1 presents a description of all of the experiments conducted in this research along with the significant factors they investigated.

Table 1. Summary of all experiments conducted in this research.

No.	**Experiment/analysis type**	**Factor**				
		N_2 injection pressure (psi)	**Filter membrane pore size (nm)**	**Filter membrane distribution**	**Mixing time**	**Temperature (ºC)**
1	MMP	500 to 2000	-	-	-	32ºC
2	MMP	500 to 2000	-	-	-	70ºC
3	Filtration	1000	450, 100, 50	Heterogenous	2 h	32ºC
4	Filtration	1250	450, 100, 50	Heterogenous	2 h	32ºC
5	Filtration	1500	450, 100, 50	Heterogenous	2 h	32ºC
6	Filtration	1000	100, 100, 100	Uniform	2 h	32ºC
7	Filtration	1000	450, 100, 50	Heterogenous	1 h	32ºC
8	Filtration	1000	450, 100, 50	Heterogenous	10 min	32ºC
9	Filtration	1000	450, 100, 50	Heterogenous	2 h	70ºC
10	Visualization	1000	450, 100, 50	Heterogenous	2 h, 1 h	32ºC
11	Visualization	1000	450, 100, 50	Heterogenous	10 min	32ºC
12	Visualization	1250	450, 100, 50	Heterogenous	2 h	32ºC
13	Visualization	1500	450, 100, 50	Heterogenous	2 h	32ºC
14	Microscope Imaging	1000, 1250, 1500	450, 100, 50	Heterogenous	2 h	32ºC
15	Gas Chromatography	1000, 1500	-	Heterogenous	-	-
16	SEM Analysis	1000, 1500	450, 100, 50	Heterogenous	2 h	32ºC
17	Pore Size Distribution	1000, 1500	450, 100, 50	Heterogenous	2 h	32ºC

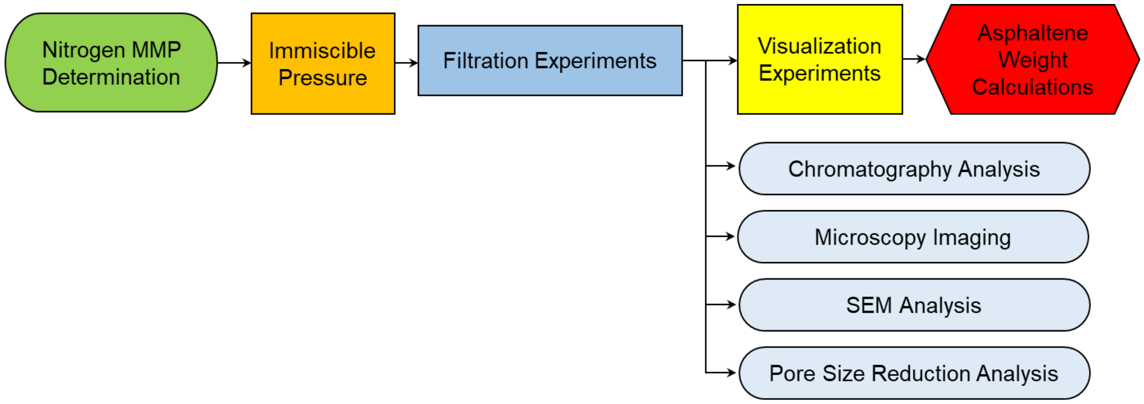

Figure 3. Experimental design flow chart.

3.1. EXPERIMENTS MATERIALS

The experimental materials used in this research included the following:

- Crude oil: The crude oil had a viscosity of 19 cp, density of 0.864 gm/cc, and °API of 32. The viscosity was measured using a rheometer. Gas chromatography-mass spectrometry was used to determine the composition of the crude oil, as shown in Table 2.

- Nitrogen: An N_2 gas cylinder with 99.9% purity was connected to the filtration vessel and used for N_2 injection, with a pressure regulator controlling the N_2 cylinder pressure.

- Filter membranes: Various filter membranes (i.e., 50, 100, and 450 nm) were used to investigate the effect of different pore sizes. The membranes were cut to the desired shape based on the 45-mm diameter of the filtration vessel.

- Specially designed HPHT filtration vessel: A high-pressure, high-temperature (HPHT) filtration vessel was specially designed in the lab to accommodate the filter paper membranes.

- Oven: An oven that accommodated the filtration vessel was used to investigate the effect of various temperatures on asphaltene precipitation and deposition during N_2 injection.

- N-heptane: A solvent was used to dissolve the oil samples in tubes to quantify the asphaltene weight percent after each experiment.

- Slim tube: A stainless steel slim tube packed with sand was used to determine the minimum miscibility pressure of N_2.

Table 2. Crude oil composition

Component	**Weight percentage (%)**
C_8 -C_{14}	65.14
C_{15}-C_{19}	6.06
C_{20}-C_{24}	9.16
C_{25}-C_{29}	14.48
C_{30+}	5.17
Total	100.00

3.2. MMP EXPERIMENT

3.2.1. MMP Experiment Procedure. The MMP experiment was conducted to ensure that all subsequent filtration experiments were carried out below the MMP. The MMP can be defined as the lowest pressure at which a gas can create miscibility with the reservoir oil at the reservoir temperature. In other words, the MMP is the lowest pressure at which miscibility between the injected gas and reservoir oil is achieved when the interfacial tension between the oil and gas vanishes after multiple contacts. Figure 4 shows a schematic diagram of the slim tube experimental setup. The main components of the slim tube test were a syringe pump, three accumulators, gas cylinders, a stainless-steel slim tube packed with sand, and a back pressure regulator. The slim tube tests were divided into several steps, starting with the pretest to calculate the pore volume. The second step was to fill the slim tube with the crude oil at a low rate of 0.5 PV to ensure that the slim tube was 100% saturated at the end of the pumping. The final step involved experimental manipulation, whereby the temperature was adjusted to a predefined level, the gas cylinder was filled with N_2, and gas was injected at a rate of 1.2 PV. A back pressure regulator was installed at the outlet of the slim tube and used to adjust the pressure with another water pump as a back pressure reservoir.

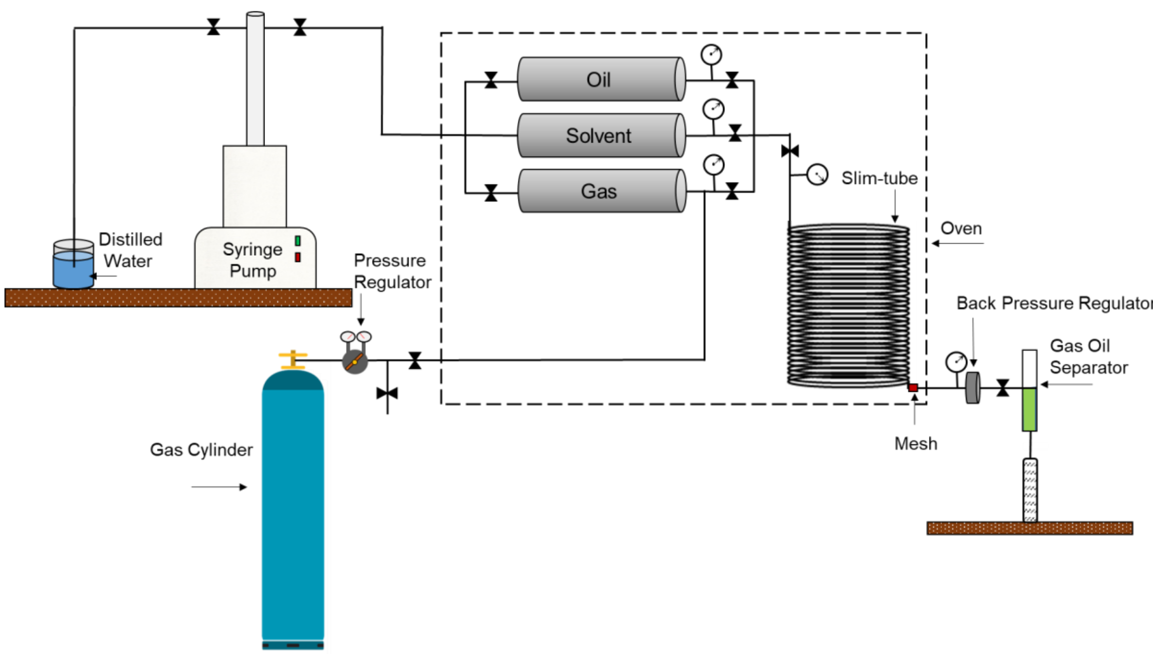

Figure 4. Slim tube experimental setup.

Starting with the slim tube which was fully saturated with distilled water. Following the oil was then injected into the slim tube unit fully saturated. This can be observed at the outlet of the slim tube when the produced liquids are only oil and thus ensure the slim tube is fully saturated. During all the experiments, the back pressure regulator was placed at the outlet with the desired pressure. The gas accumulator was filled with N_2. Then, N_2 was injected at a rate of 0.25 ml/min. Each experiment was stopped when 1.2 PV of gas injected or when the gas broke through. The effluent was used to collect the produced oil. The MMP can be determined by plotting N_2 injection pressures versus cumulative oil recoveries. Finally, the solvent of Xylene was used after each experiment to clean the slim tube setup and to make sure there is no oil left in the slim tube that may affect the next experiment.

3.3. FILTRATION EXPERIMENTS

3.3.1. Filtration Experimental Procedure. Figure 5 illustrates all the components of the experimental setup. The main components included a high purity N_2 cylinder with a pressure regulator to control the pressure from the cylinder. The filtration vessel was designed to accommodate three mesh screens to support the filter membranes and prevent them from folding under high pressures. The mesh screens were created with small holes that allowed the oil to pass through easily.

Spacers between each mesh screen supported the screens in place; rubber O-rings were used above and below each spacer to prevent any leakage and to ensure that the oil and gas would pass through the filter paper membranes. A back pressure regulator was installed at the outlet of the filtration vessel and used to adjust the pressure via a syringe pump. The produced oil was collected using an effluent below the filtration vessel. An oven controlled the temperature of the filtration vessel to study the effect of different temperatures. Finally, two transducers were installed at the inlet and outlet of the filtration vessel and were connected to a computer to monitor and record the pressure difference.

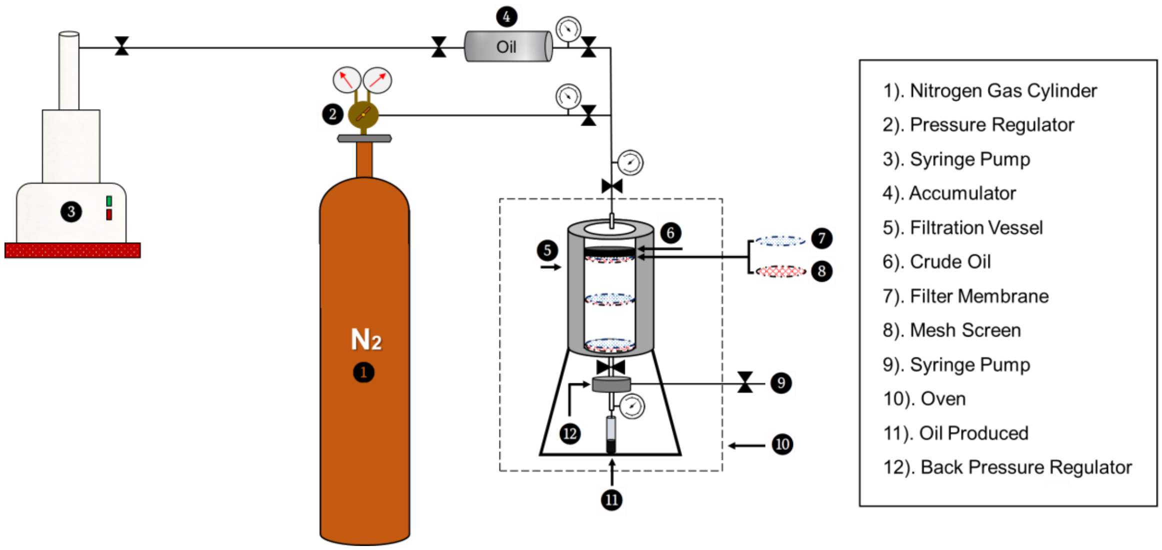

Figure 5. Filtration experimental setup.

These steps were followed to conduct the filtration experiments:

1. The first set of mech screens, filter membrane papers, rubber O-rings, and spacers were placed inside the filtration vessel. This step was repeated for the next two sets.
2. The vessel was closed tightly using a specially designed cap to ensure that all of the sets remained tightly bound together and to prevent any leakage during the experiment.
3. Crude oil (30 ml) was poured into the accumulator, with a syringe pump to inject the oil into the vessel.
4. N_2 was injected into the cylinder to reach the desired level. The crude oil was then exposed to the gas for a predetermined mixing time.
5. After mixing, the syringe pump at the outlet was employed at constant pressure. It was adjusted to the required back pressure for each experiment to let the crude oil pass through the membranes.

6. N_2 was injected into the vessel, and the produced oil was collected. The experiment was stopped when no further oil production was observed.
7. The inlet and outlet pressures were observed and recorded using transducers that connected to a computer. The difference between the two pressures did not exceed 50 psi.
8. After the gas injection was complete, the vessel was opened, and the remaining crude oil was collected from each filter membrane for asphaltene analysis.

3.4. ASPHALTENE DETECTION TEST AND VISUALIZATION EXPERIMENTS

Asphaltene weight percent can be calculated by weighting the filter paper before and after filtration. The difference between the weights determined the asphaltene percent weight, using the following equation:

$$\text{Asphaltene wt\%} = \frac{\text{wt}_{\text{asphaltene}}}{\text{wt}_{\text{oil}}} * 100 \tag{1}$$

Where asphaltene wt% is the asphaltene weight percent, $\text{wt}_{\text{asphaltene}}$ is the asphaltene weight on the filter paper, and wt_{oil} is the oil sample weight. The asphaltene quantification test procedure can be summarized in the flowchart shown in Figure 6. Photos were taken of the asphaltene precipitation in the test tubes at specific time points (i.e., 0, 2, 4, and 12 h) to observe the change in asphaltene settling over time.

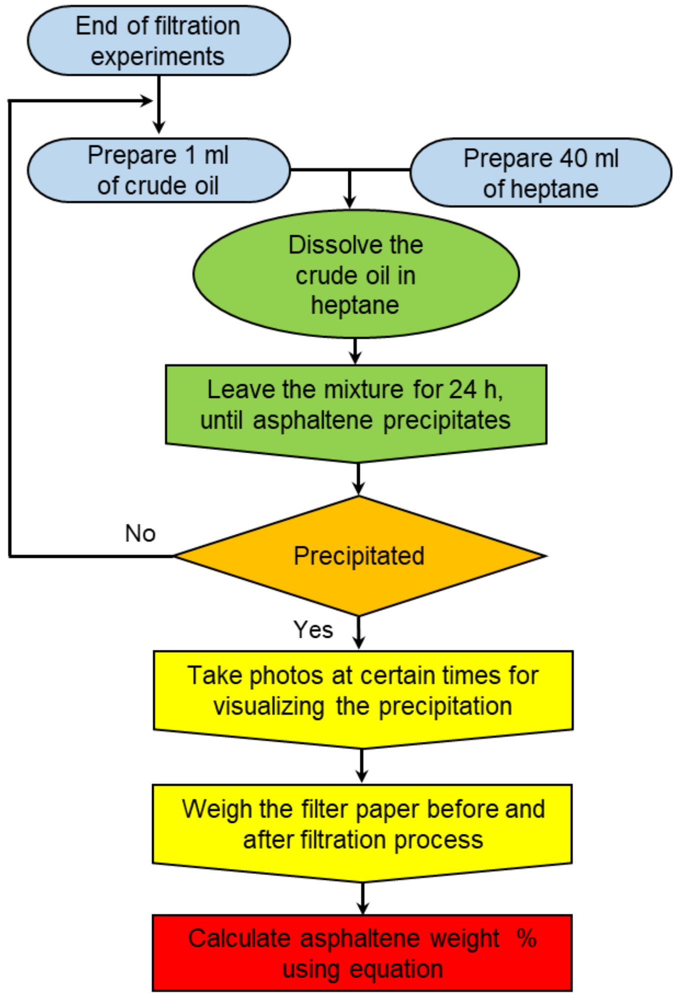

Figure 6. Flowchart highlighting the main steps of asphaltene quantification.

4. RESULTS AND DISCUSSION

4.1. MMP EXPERIMENTS RESULTS

N_2 can achieve miscibility using the same mechanism as CO_2: the vaporizing mechanism. The N_2 MMP experiments sought to ensure that the filtration experiments would be conducted under immiscible injection pressure. The effect of temperature on the N_2 MMP was investigated to ensure that at higher temperatures, the filtration experiments would be less than the MMP. Oil recoveries were recorded at gas breakthrough or at 1.2

PV of the gas injected and were plotted with the tested injection pressures. The MMP can be estimated when the cumulative oil recovery is greater than or equal to 90% of the original oil in place (OOIP). The solid lines in Figure 7 were used to determine the sudden slope change point in the measured oil recovery versus injection pressure. The intersection point can be used to determine the MMP. The MMP of N_2 at 32ºC was 1600 psi. Hence, 1000, 1250, and 1500 psi along with a temperature of 32ºC were selected for investigating asphaltene precipitation under immiscible gas injection conditions.

The results also showed that the MMP of N_2 at 70ºC was 1350 psi. The temperature is inversely proportional to the N_2 MMP due to the N_2 remaining in the gaseous phase at the same conditions (Belhaj et al., 2013; Vahidi et al., 2007; Sebastian et al., 1992). Thus, the effect of temperature can be investigated because of the immiscible pressure conditions at higher temperatures.

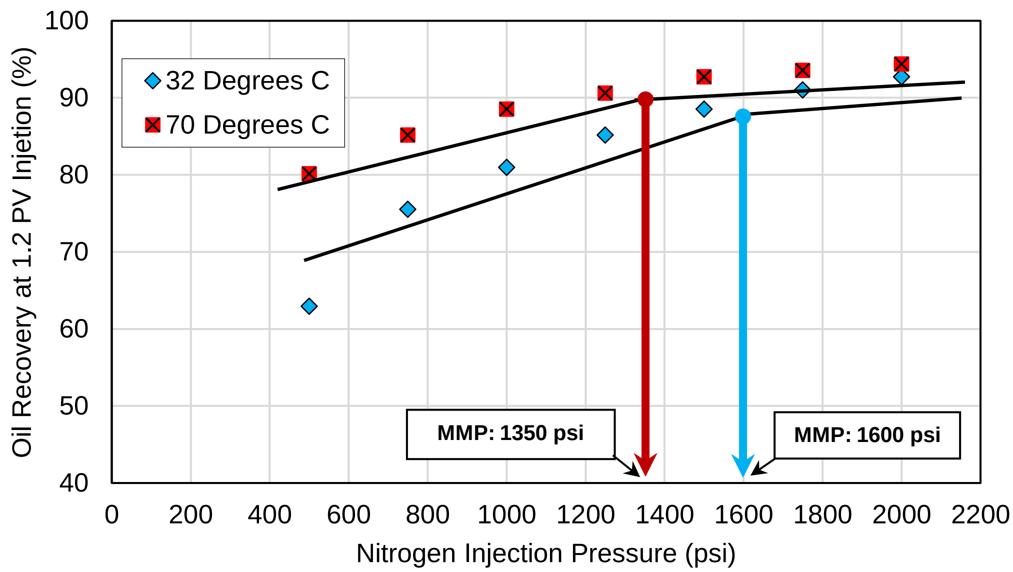

Figure 7. N_2 MMP determination using an oil viscosity of 19 cp at 32ºC and 70ºC.

4.2. FILTRATION AND VISUALIZATION RESULTS

4.2.1. Effect of Immiscible Conditions of Pressure Using Uniform Membrane Distribution. Uniform membrane distribution means that the same pore size of the filter membrane was used in all of the filtration experiments. Figure 8 shows the paper membrane distribution inside the vessel, where the entire membrane had a pore size of 100 nm. The selection of filter membrane pore sizes was based on the pore size distribution of shale reservoirs, specifically Eagle Ford (Shen et al., 2017).

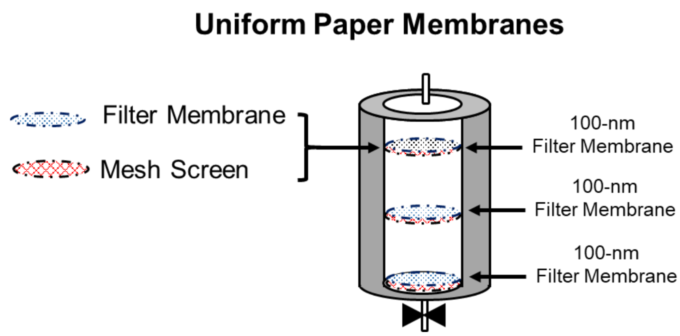

Figure 8. Uniform paper membrane distributions inside the vessel.

Figure 9 displays the effect of using a uniform pore size filter paper membrane on the asphaltene deposition during the filtration test. Three 100-nm filter membranes were placed inside the vessel in each mesh screen to investigate the effect of using the same pore size, and the results were compared with a heterogeneous distribution. An N_2 pressure of 1000, 1250, and 1500 psi and temperature of 32ºC were used throughout this experiment.

The results revealed that the asphaltene deposition was almost equal across all the paper membranes. For instance, the asphaltene weight percent ranged from 5.26% in the upper part of the 100-nm paper membrane to 5.62% in the lower part of the 100-nm paper membrane during the 1000 psi gas injection. A slightly higher asphaltene weight percent was observed on the upper part of the filter membrane, which could have occurred because some asphaltene particles plugged some pores, thereby preventing effective oil passage. The asphaltene particles with a size greater than 100 nm precipitated on the upper section of the filter membrane, while the particles with a size less than 100 nm passed through to where the produced oil was collected. For example, a pressure of 1500 psi produced many more asphaltene clusters than did 1000 psi and also led to more asphaltene being deposited on the filter membranes. The higher pressure resulted in more clusters sized 100 nm or more. Thus, more asphaltenes were quantified at higher pressure levels in all filter membranes. Some of the particles plugged some pores on the middle and lower parts of the filter membrane, as can be observed in the results as a slight fluctuation in the asphaltene weight percent. However, these plugged pores resulted in a decrease in the asphaltene weight percent in the produced oil. It can be concluded that the asphaltene was mobilized and forced into the filter membranes with almost the same concentration due to the uniform pore sizes.

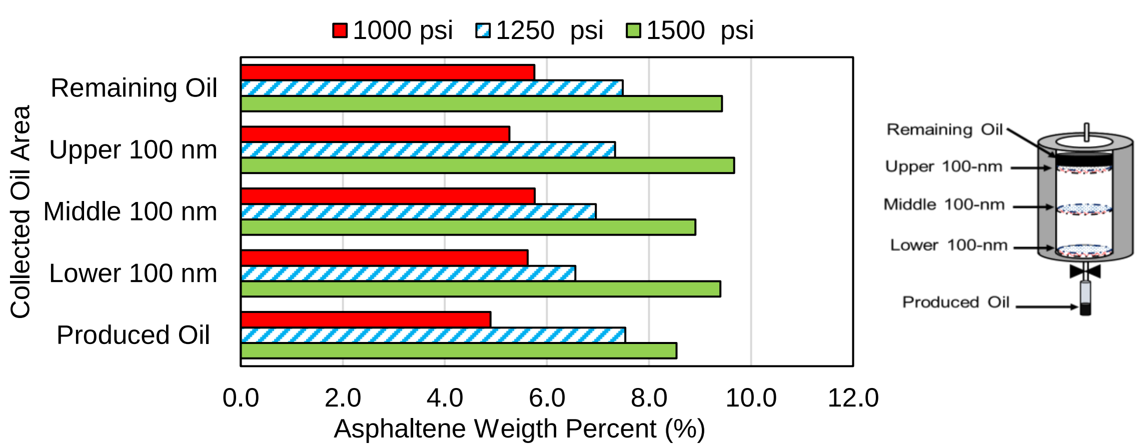

Figure 9. Asphaltene weight percent using a uniform paper membrane distribution when injecting nitrogen at 1000, 1250, and 1500 psi.

A 1000 psi N_2 injection pressure was selected for further investigation of the asphaltene precipitation over time. The remaining oil was collected after each experiment and dissolved in n-heptane at a ratio of 1:40. Various times were selected (i.e., 1, 4, and 12 h) to investigate and visualize the asphaltene deposition process. Figure 10 presents the uniform asphaltene visualization tests at 1000 psi with 100-nm pore size membranes at 32ºC. The results showed an almost equal deposition process in all 100-nm membranes. At zero elapsed time, no asphaltene was observed, and the crude oil sample was entirely dissolved in n-heptane. After 1 h, the asphaltene started to precipitate and form deposits such that asphaltene particles accumulated at the bottom of the tube. Over time, the solution color lightened at the top of the lab tubes with the presence of some suspended asphaltene particles. Finally, after 12 h, almost all asphaltene particles were deposited, and the overall solution color was much lighter compared to the solution observed at zero time. The results confirmed that the asphaltene particles that passed through all of the filter membranes had almost the same percent.

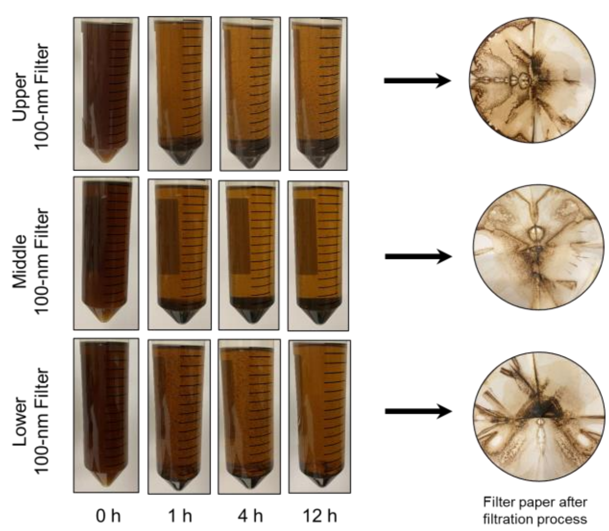

Figure 10. Visualization of asphaltene precipitation and deposition at 1000 psi using a uniform membrane size distribution.

4.2.2. Effect of Pore Size Heterogeneity. Varying the filter membrane's pore size inside the vessel created heterogeneity in the pore size distribution among membranes. Figure 11 presents a heterogeneous paper membrane vessel consisting of (1) a filter membrane size of 450 nm located at the top of the vessel, (2) 100 nm in the middle, and (3) 50 nm at the lower part of the vessel. Experiments were conducted with N_2 injection pressures of 1000, 1250, and 1500 psi at 32ºC.

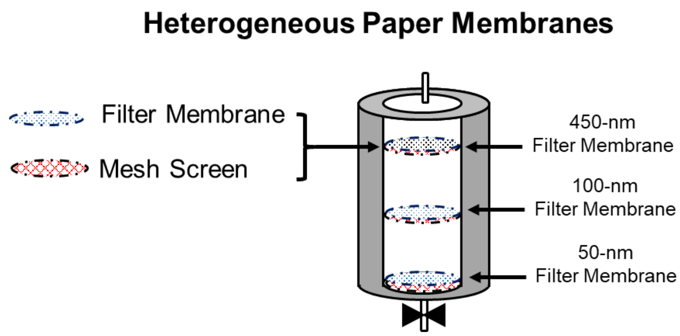

Figure 11. Illustration of the heterogeneous paper membrane distributions inside the vessel.

Figure 12 illustrates that as the filter membrane's pore size decreased, the asphaltene deposition increased. Furthermore, the asphaltene weight percent increased for all injection pressures. The asphaltene weight percent increased from 2.50% in 450-nm paper to 8.14% in 50-nm paper at 1000 psi. Higher asphaltene weight percent were observed using 1250 psi, where the percent were 3.16% and 9.8% in 450-nm and 50-nm papers, respectively. About 11% asphaltene weight percent was observed in a 50-nm paper membrane using 1500 psi. These data indicate that larger pore sizes allowed the asphaltene particles to pass through and resulted in less asphaltene precipitation. However, as the pore size of the filter membrane decreased, asphaltene particle passage was disrupted, leading to more asphaltene deposition. For instance, asphaltene particles with a size larger than 450 nm were incapable of passing through the 450-nm filter membrane. The asphaltene particle sizes that were more than 50 nm and less than 100 nm precipitated on the 50-nm filter membrane. Asphaltene particles that were less than 50 nm could pass through the membrane and collect in the produced oil. Thus, the asphaltene that precipitated on the 450-nm, 100-nm, and 50-nm filter membranes was greater than 450 nm, between 450 and 100 nm, and between 100 nm and 50 nm, respectively. As a result of Brownian motion, the asphaltene aggregates continued to interact with one another, forming larger particles. Because of the large radial diffusivity of the particles, smaller aggregates have a higher tendency to deposit (Hassanpouryouzband et al., 2017). In all experiments, the asphaltene weight percent in the produced oil was the lowest, as the asphaltene particles precipitated and plugged the nanopaper membranes gradually, which then led to reduced amounts of asphaltene in the oil outlet. Due to asphaltene deposition, the plugging pore size appears to be critical when increasing the N_2 injection pressure. This could result in pore plugging and cause severe problems during production operations, thus decreasing oil recovery.

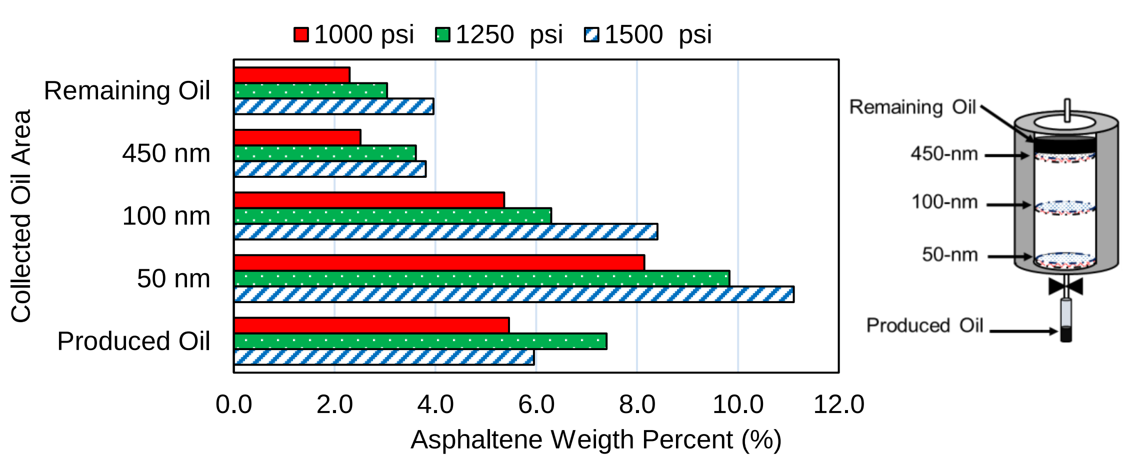

Figure 12. Asphaltene weight percent using a heterogenous paper membrane distribution at various nitrogen injection pressures.

A 1000 psi N_2 injection pressure was also selected for further investigation of the asphaltene precipitation over time (Figure 13) in a heterogeneous membrane pore size distribution. Initially, no clear asphaltene could be observed. At zero elapsed time, the solution was dark colored for all the filter membranes. For the 450-nm filter membrane, some asphaltene deposition was seen after 1 h, and a lighter solution color was reached after 12 h. This could be due to the large pore size of 450 nm allowing less asphaltene particle precipitation in the filter membrane. For the 100-nm filter membrane, asphaltene deposition was observed after 1 h and was very similar to that of the 450-nm condition. Although the observation was almost the same at this time, the final observation of the 50-nm filter after 12 h was higher in asphaltene deposition compared to the 100-nm and 450-nm membranes. This indicates that smaller membrane pore sizes prevented the passage of all asphaltene particles through the membrane. It is plausible that as the filter membrane pore size decreases, some asphaltene particles cannot flow through. This is likely due to asphaltene particle sizes, which were the same or larger than the filter membrane pore size. This can be observed clearly in the 50-nm filter membrane, where after 1 h, a darker color was observed compared to the 450- and 100-nm filter. As time progressed, some asphaltene particles were suspended in the n-heptane, and most of the asphaltene was deposited after 4 h. Finally, greater asphaltene deposition was observed at the bottom of the test tube, signifying an elevated asphaltene deposition. In Figure 10, the asphaltene deposition and precipitation process was similar compared to the process in the uniform tests shown in Figure 13. In heterogenous tests, the asphaltene weight percent using the 100-nm filter membrane was 5.36% compared to 5.26% in the upper part of the 100-nm filter membrane in the uniform test. This confirms that the same pore size will be impacted by asphaltene clusters in the same way under the same conditions, as it is here with the same pressure of 1000 psi.

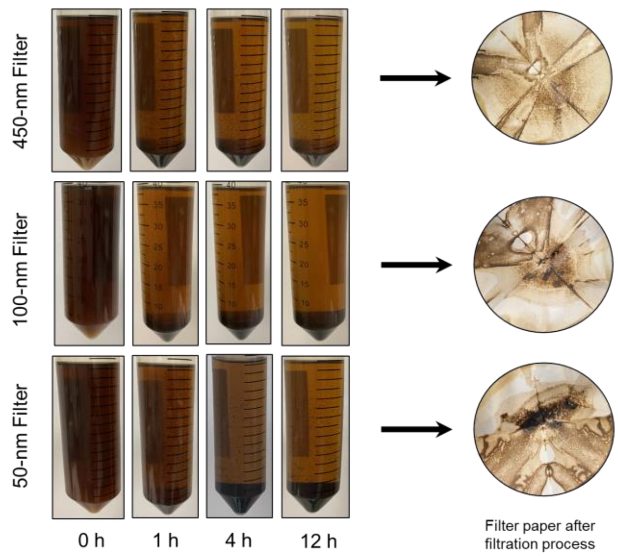

Figure 13. Visualization of asphaltene precipitation and deposition at 1000 psi using a heterogeneous distribution.

Further visualization analysis of asphaltene was obtained at 1000, 1250, and 1500 psi using asphaltene collected from the remaining oil. Figure 14 shows the asphaltene visualization experiments with different pressures at 32^{o}C with a 2-h mixing time. With 0 h elapsed, all of the tubes showed almost the same results at all pressures: asphaltene was entirely dissolved in n-heptane and no clear asphaltene depositions or precipitations were observed. After 1 h, the asphaltene started to flocculate in the tubes, especially at 1250 and 1500 psi, as displayed in the representative images. Interestingly, for 1000 psi, no clear asphaltene deposition was observed, and the particles appeared to remain stable due to exposure to a lower N_2 injection pressure. After 4 h, the flocculation had begun to settle, and deposits were observed at the bottom of the tube, with more deposits at the highest pressure (i.e., 1500 psi). This indicates that higher pressure affected the instability of asphaltene faster than did the lower pressure. As time progressed, more asphaltene deposition was observed under all conditions. The lighter the color of the mixture, the higher the asphaltene deposition at the bottom of the tubes. The visualization experiments showed that the asphaltene flocculation requires time to complete, making time a crucial factor in the asphaltene precipitation process. Detecting and understanding asphaltene deposition over time can facilitate mitigating the expected formation damage.

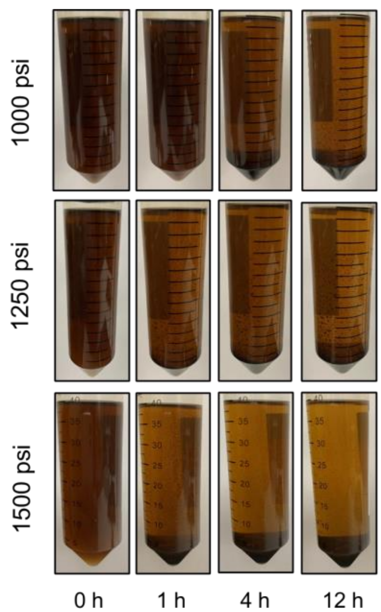

Figure 14. Asphaltene precipitation and deposition visualization of the remaining oil using different pressures at 32ºC with a 2-h mixing time.

4.2.3. Effect of Mixing Time. Mixing time is defined as the total time the oil was exposed to the desired N_2 pressure inside the filtration cell and left at 32ºC to let the N_2 mix well with the crude oil. Times of 10, 60, and 120 min were selected to investigate the effect of the mixing time on the asphaltene precipitation and deposition during 1000 psi N_2

injection at a temperature of 32ºC. Figure 15 highlights that increasing the mixing time resulted in a slight increase in the asphaltene weight percent. For 450-nm paper, the asphaltene weight percent ranged from 3.7% to 5.17% for the mixing times of 10 min and 2 h, respectively. It was observed that decreasing the filter membrane size led to an increase in asphaltene weight percent. This is due to the pore plugging from asphaltene clusters. For the 50-nm paper membrane, there were notable increases in the asphaltene weight percent, especially for 60- and 120-min mixing times. However, there were no significant differences between the asphaltene weight percentages in each filter membrane for these two mixing times. These data indicate that the mixing time did not have an intrinsic effect on the asphaltene deposition within 120 min but might cause a slight effect over longer times. Increased mixing times that expose the crude oil to N_2 will increase the asphaltene weight percent, thus increasing the precipitation and deposition of asphaltene, especially in smaller pores.

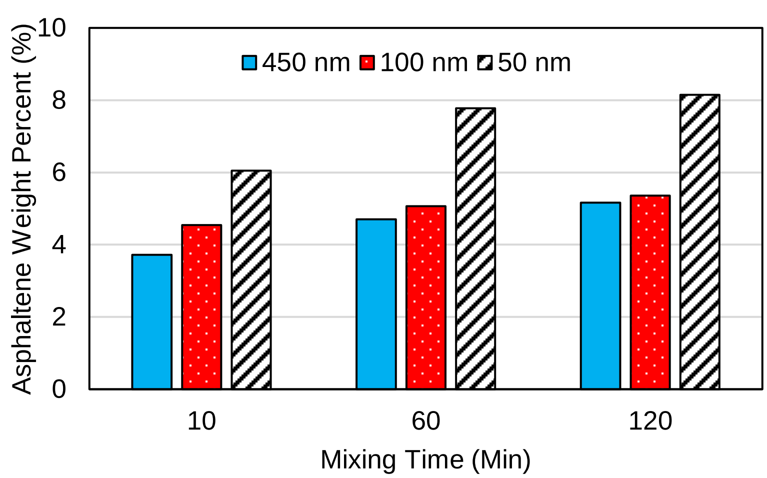

Figure 15. Asphaltene weight percent at 10, 60, and 120 min of mixing time using 450-, 100-, and 50-nm filter membranes.

Figure 16 shows the asphaltene precipitation process of N_2 injections at 1000 psi for 10-, 60- and 120-min mixing times at 32ºC. As mentioned above, the results of the visualization experiments indicated that increased mixing time also increased the asphaltene deposition and precipitation process. For a 10-min mixing time, the asphaltene deposition process was relatively slow, and the asphaltene settled after 12 h. The solution at the top of the tube after 1 h was still dark brown in color, which suggests less settling at this time interval. However, after 120 min of mixing time, the bottommost section of the tube was dark after 1 h of settling, while a lighter color was observed at the top of the tube. The asphaltene continued to settle, and sediment at the bottom of the tube was substantially darker after 4 h. After 12 h of settling, there were no significant observable changes in the asphaltene deposition process for all initial mixing times. Given these observations, it is necessary to analyze asphaltene instability and the effect of the mixing time to avoid any asphaltene-related problems. After the filtration process, the filter membranes exhibited a higher asphaltene percent after 120 min of mixing time compared to 10 min.

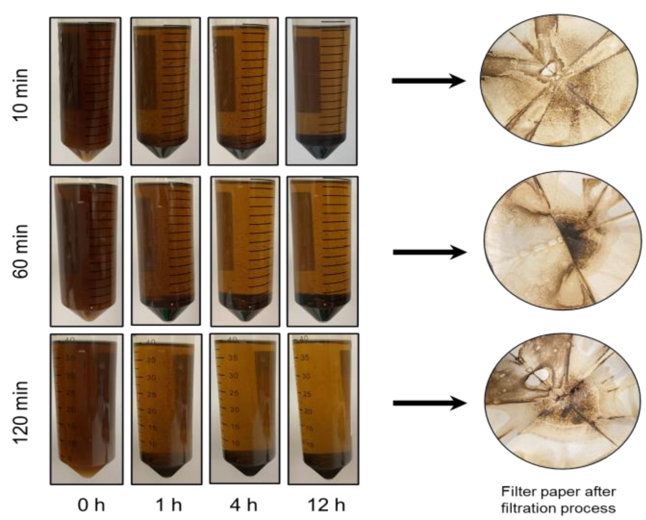

Figure 16. Visualization of asphaltene precipitation and deposition at different mixing times.

4.2.4. Effect of Temperature on Asphaltene Deposition. All of the above experiments were conducted at 32ºC, but the effect of a higher temperature will be discussed in this section. Temperature can strongly impact asphaltene deposition and precipitation in crude oil. Two experiments were conducted at two temperatures (i.e., 32ºC and 70ºC) to investigate the effect of a high temperature on the asphaltene stability. The 32ºC represents room temperature, and 70ºC represents the average temperature of shale basins. In both experiments, the entire filtration vessel was placed inside an oven to ensure the stability of the required temperature.

A pressure of 1000 psi for the N_2 injection and a 2-h mixing time were used in both experiments. Figure 17 shows that increasing the temperature resulted in a decrease in the asphaltene weight percent. The higher asphaltene weight percent was observed in the 50-nm filter membrane: 5.11% and 3.12% for 32ºC and 70ºC, respectively. This is likely due to the bonds between asphaltene and resins in the crude oil structure being weakened by the increased temperature, which increased the rate of asphaltene precipitation. The higher the temperature, the higher the asphaltene solubility rate and the lower the asphaltene concentrations. In stable oils, the suspension colloidal particles of asphaltene are covered by resins that are strongly connected to the asphaltene. This connection between asphaltene and resins becomes stronger at higher temperatures, which keeps the asphaltene dissolved in oil (Hoepfner et al., 2013).

At higher temperatures, a smaller amount of asphaltene colloidal will form, and it will tend not to create strong associations due to the colloids being dispersed effectively by the resins (Branco et al., 2001). The precipitated asphaltenes that develop from the colloidal suspension particles at higher temperatures tend to dissolve in the oil; thus, more asphaltenes will form in soluble conditions but fewer in colloidal conditions (Chandio et al., 2015).

The resins can have a tendency to self-associate, and that tendency is much stronger at lower temperatures. Therefore, the bond between asphaltene and resins weaken (Pereira et al., 2007). Consequently, greater asphaltene precipitation can form due to the molecules of asphaltene becoming stronger in terms of their polarity, resulting in more aggregation at lower temperatures. Also, membrane pore size had the same effect at both temperatures: as the filter paper membrane pore size decreased, the asphaltene weight percent increased. This is because the asphaltene particle size plugged the pores much more in the 50-nm filter membrane; thus, more asphaltene was observed.

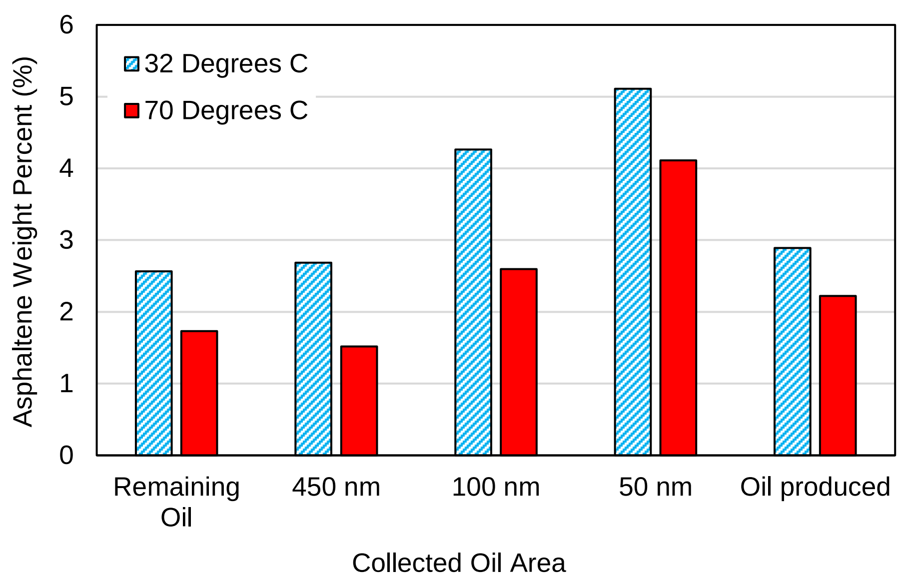

Figure 17. Asphaltene weight percent at different temperatures using 1000 psi.

5. FURTHER ANALYSIS AND DISCUSSION

5.1. CHROMATOGRAPHY ANALYSIS

Gas chromatography-mass spectrometry (GC6890-MS5973) was used to detect the main chemical components and their presence in the produced oil, including asphaltene, to confirm the results mentioned above concerning asphaltene aggregation. Table 3 presents the gas chromatography analysis before and after the N_2 gas injection experiments at 1000 and 1500 psi. First, the original crude oil with 19 cp was analyzed to compare its components to the oil after the experiments. The oil produced from the N_2 injection pressures at 1000 and 1500 psi was selected to highlight the asphaltene changes. The asphaltene components are included in the heavy components of C_{30+}. The analysis showed that when increasing the pressure, the heavy components also increased.

The heavy compounds, including asphaltene, decreased from 5.17% to 1.96% with a 1000 psi gas injection, which confirmed that the filter membranes inside the filtration vessel had a significant effect on the heavy components, including the asphaltene. The asphaltene molecules plugged the filter membrane's pores gradually, thus reducing the asphaltene content at the outlet that produced the oil. However, the analysis showed that a higher-pressure of 1500 psi produced fewer asphaltene components (2.50%) compared to the original oil (5.17%) but higher than the compounds compared to 1000 psi (i.e., 1.96%). This results from the higher injection pressure causing the resins around the asphaltene molecules to weaken, thus providing a higher asphaltene content.

Table 3. Gas chromatography analysis before and after the experiments with 1000 and 1500 psi nitrogen gas injection

Component	**Before Experiment [Original oil]**	**After Experiment [1000 psi]**	**After Experiment [1500 psi]**
	Weight percentage (%)		
C_8 -C_{14}	65.14	87.43	92.43
C_{15}-C_{19}	6.06	3.59	2.20
C_{20}-C_{24}	9.16	2.27	1.25
C_{25}-C_{29}	14.48	4.76	1.62
C_{30+} (Including asphaltene)	5.17	1.96	2.50
Total	100.00	100.00	100.00

5.2. MICROSCOPY IMAGING ANALYSIS

The asphaltene particles were induced by gas injection, where large asphaltene clusters can form, leading to asphaltene holdup in a reservoir. Asphaltene can plug the pores and cause severe problems, including a reduction in oil relative permeability, alteration of the wettability of the rock, and an overall reduction in oil production. The filter paper membranes of 450 and 50 nm with 1500 psi gas injection were cleaned by the solvent n-heptane to highlight the pore plugging in the filter paper. Figure 18 illustrates the filter membrane before and after conducting the filtration experiment as well as after cleaning the crude oil from the filter membrane. The photo shows the asphaltene deposited in the filter membrane pores and the plugged path through which the crude oil had to move, especially in the 50-nm filter membrane, due to its smaller pore size.

For a better understanding of the effect of asphaltene on pore plugging, a HIROX digital microscope was utilized to identify the plugging pores in the filter membranes. Showing the filter membranes' microstructure will highlight the severity of the asphaltene aggregation on different pore size structures.

Figure 19 displays the microscopic images (20 μm) of the filter membrane's pore structure of 450-, 100-, and 50-nm filters using an N_2 injection pressure of 1000, 1250, and 1500 psi at 32ºC. The images were captured after cleaning and exposing the filter membranes to an n-heptane solvent for 24 h. Obvious differences occurred in the aggregation of the precipitated asphaltene molecules in the filter membrane images: the higher pressure coupled with a filter membrane having a smaller pore size resulted in more deposition of asphaltene and increased amounts of pore plugging, which is evident in the darker color of the images.

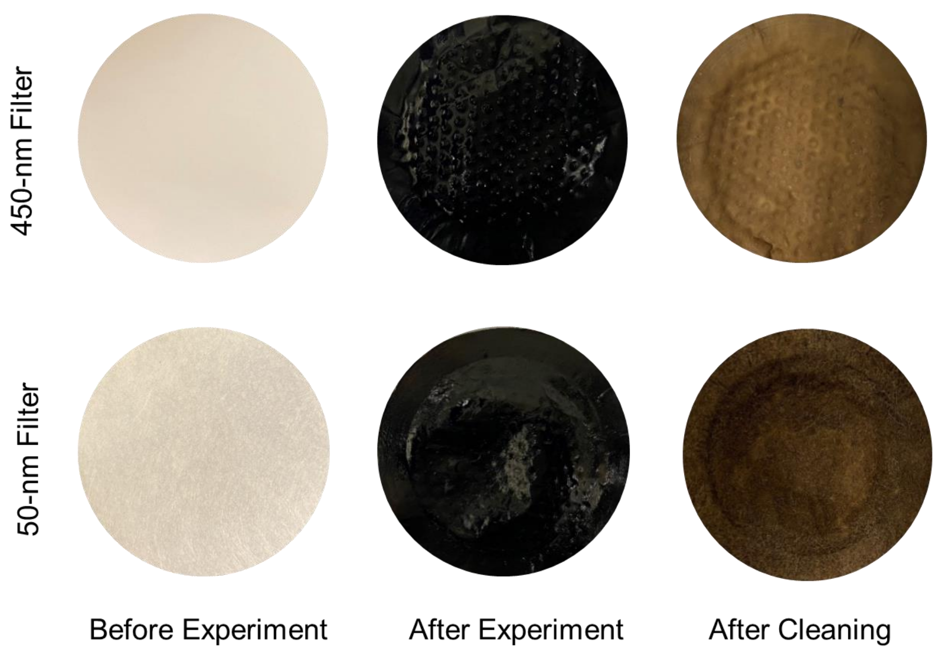

Figure 18. Illustration of the filter membranes (450- and 50-nm) at 1500 psi before and after the experiment, and after cleaning.

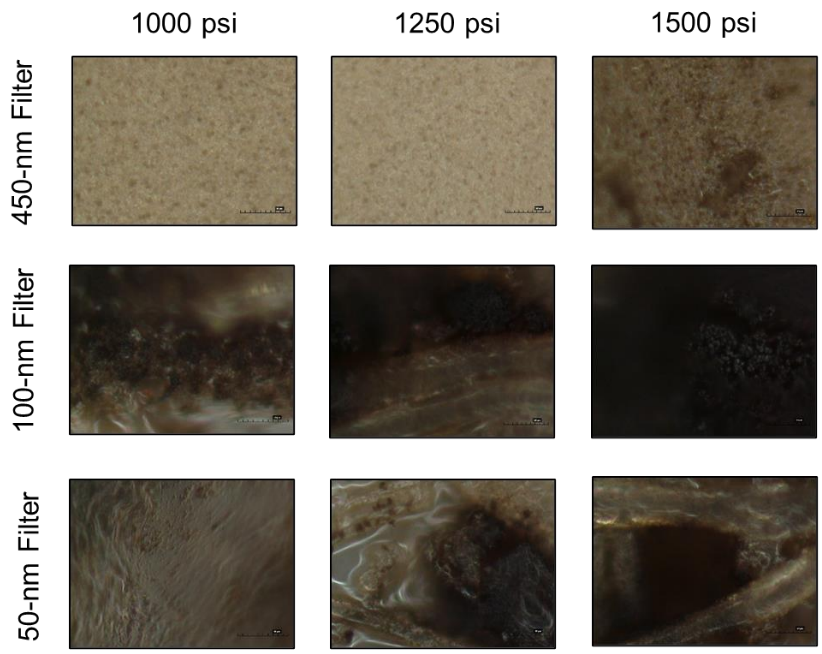

Figure 19. Digital microscopic images (20 µm) of 450-, 100-, and 50-nm filter membranes using various nitrogen injection pressures.

5.3. SEM ANALYSIS

Scanning electron microscopy (SEM) is an advanced imaging analysis that can determine pore structure, particularly in unconventional shale structures that are known for their small pore sizes. SEM was utilized to highlight the impact of pressure and asphaltene particles on pore size plugging. To illustrate this, a collection of SEM images was taken for all heterogenous filter membranes (i.e., 450-, 100-, and 50-nm) during nitrogen injection at 1000 and 1500 psi. Figure 20 provides SEM images (5 µm) of the filter membranes' pore structure of the 450-, 100-, and 50-nm filter paper using an N_2 injection pressure of 1000 and 1500 psi at 32ºC.

For the 450-nm filter paper, the images depict asphaltenes accumulated inside the structure, which were black in color at injection pressures of 1000 and 1500 psi. The filter paper pore plugging was more severe in the 450-nm filter membrane using 1500 psi. The structure of the 450-nm filter membranes was captured clearly due to the larger pore size compared to the 100- and 50-nm filters. As the pore size of the filter membrane decreased, dark colors were observed for the 100-nm filter membrane. Most of the area of the 100-nm filter papers was affected by asphaltene depositions, with the darkest color occurring at an injection pressure of 1500 psi. This confirms that the asphaltenes had more impact on the smallest pore structure compared to the largest (450 nm). Due to their smaller pore sizes, most of the photo areas of the 50-nm filter membranes were obstructed by asphaltenes.

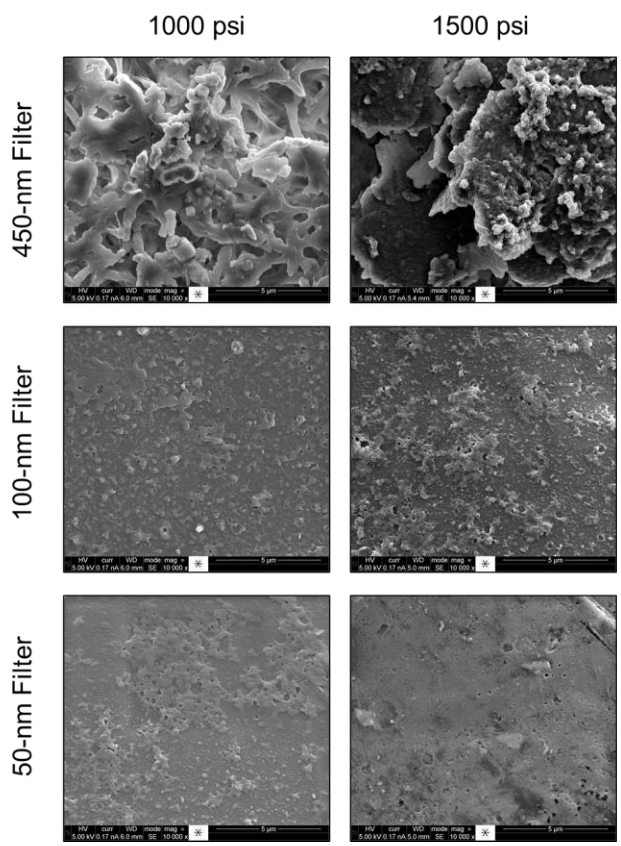

Figure 20. Scanning electron microscope (SEM) images (5 μm) of 450-, 100-, and 50-nm filter membranes at 1000 and 1500 psi injection pressure.

5.4. PORE SIZE REDUCTION DUE TO ASPHALTENE DEPOSITION

To identify the effect of asphaltene on the pore plugging of the filter paper membranes, SEM images were processed using computer software to analyze the pore size of each filter membrane. Figure 21 compares the pore size distribution in the 450-nm filter membrane after N_2 injections at 1000 and 1500 psi. The estimated pore size distribution of the 450-nm filter paper ranged from 40 nm to 400 nm at 1000 psi, but 50 nm to 200 nm at 1500 psi. The results showed that higher pressure (1500 psi) had a greater impact on pore plugging compared to the lower pressure (1000 psi) because the higher pressure created more asphaltene particles and resulted in higher asphaltene precipitation and deposition, which reduced the pore sizes. The oil path in the filter membranes became smaller due to the asphaltene deposition. The same observations were found in 100-nm and 50-nm filter membranes. For the 100-nm filter membrane, the pore size distribution ranged from 10 and 50 nm for the lower pressure (1000 psi) and from 15 nm to 35 nm for the higher pressure (1500 psi), as shown in Figure 22. A smaller pore size distribution was observed in the 50-nm filter membrane due to the smaller size of the pores. Figure 23 presents the results of the pore size distribution in the 50-nm filter membrane. The asphaltene particles accumulated at higher percentages in the smaller pore sizes of the filter membranes and then plugged most of the pores. Smaller pore size leads to more asphaltene concentration which lead to more pore plugging. Su et al (2021) developed an integrated simulation approach to predict permeability reduction under asphaltene particle aggregation and deposition. They concluded that longer aggregation time, higher flow velocity, and bigger precipitation concentrations will lead to a faster reduction in permeability. These results in this study revealed that asphaltenes in crude oil can be induced by N_2 injection and cause severe issues in pore plugging, especially in unconventional resources with a small pore size.

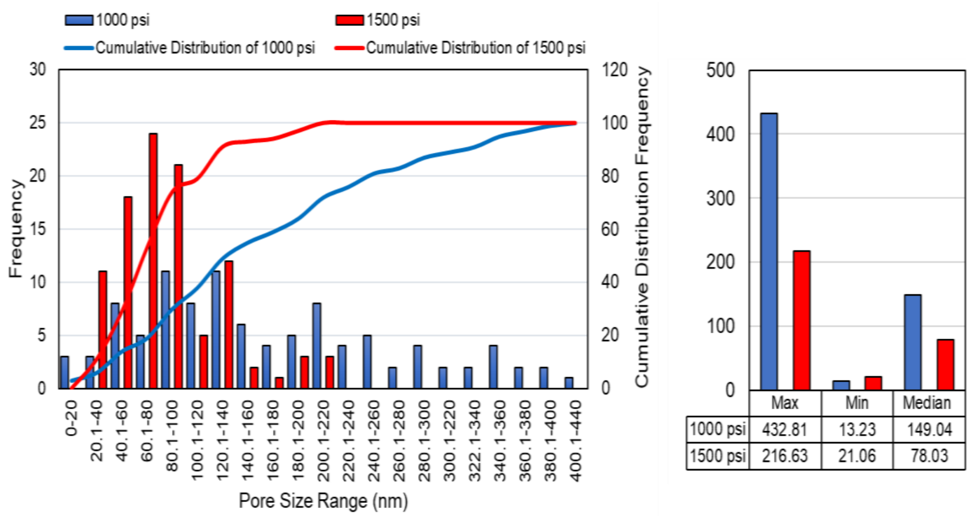

Figure 21. Comparison of the pore size distribution in a 450-nm filter membrane after 1000 and 1500 psi N_2 injections.

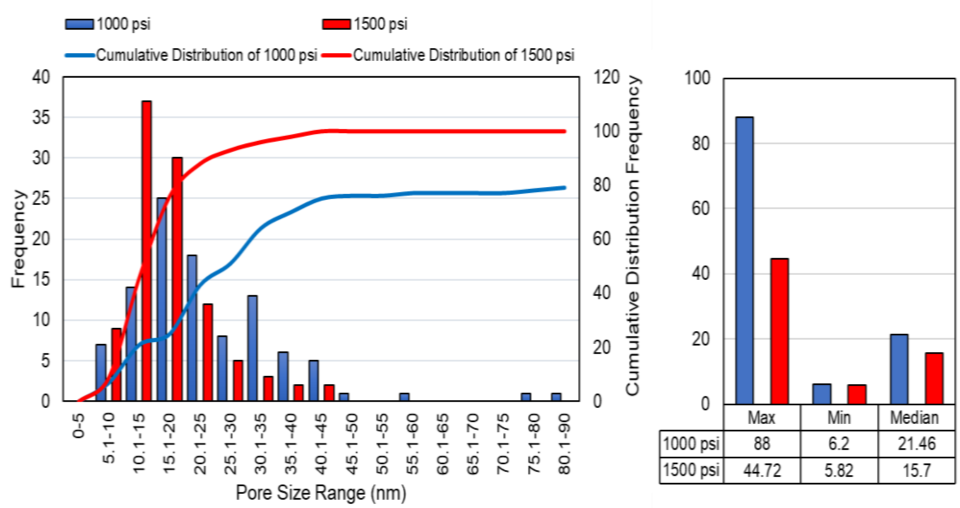

Figure 22. Comparison of the pore size distribution in a 100-nm filter membrane after 1000 and 1500 psi N_2 injections.

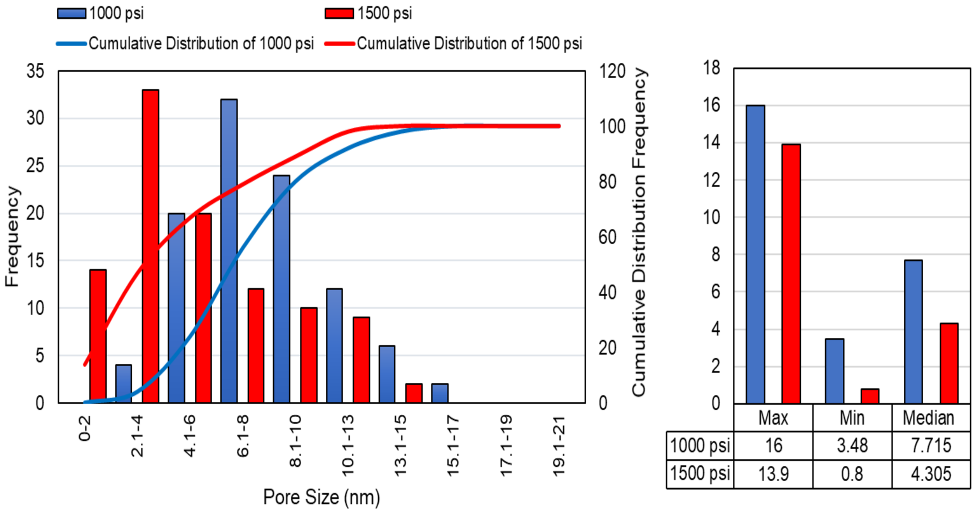

Figure 23. Comparison of the pore size distribution in a 50-nm filter membrane after 1000 and 1500 psi N_2 injections.

6. CONCLUSIONS

Three sets of experiments investigated N_2 immiscible pressure, filtration, and visualization of asphaltene. The asphaltene stability in crude oil was observed and investigated during N_2 injection. Various factors, including injection pressure, temperature, mixing time, filter membrane distribution, and pore size were investigated. The results support the following conclusions:

- As the N_2 injection pressure rose, the asphaltene weight percent also rose. Increasing the injection pressure resulted in a slight increase in the asphaltene deposition time.
- As the pore size decreased in the heterogeneous pore size distribution, asphaltene clusters were unable to pass through easily. Subsequently, asphaltene precipitation and deposition increased.

- Utilizing a uniform pore size distribution inside a vessel with a 100-nm filter gave almost the same asphaltene weight percent for all of the filter paper membranes because the same asphaltene particles passed through all of the same pore-sized membranes.
- Increasing the temperature resulted in a decrease in the asphaltene weight percent. The higher the temperature, the higher the asphaltene solubility rate, and the lower the asphaltene concentrations.
- The results demonstrated that increasing the mixing time, which exposed the crude oil to the N_2 for a longer time, increased the asphaltene instability, leading to increases in asphaltene precipitation and deposition.
- The chromatography results demonstrated that the weight percent of the heavy components, including asphaltene, was higher when using 1500 psi than 1000 psi.
- The microscopy imaging demonstrated the severity of the asphaltene deposition on the pore plugging. The results showed an increase in pore plugging when the pressure rose combined with a decrease in the pore size of the filter membranes.
- SEM observation confirmed that at a higher pressure and with a smaller pore size, the asphaltene particles created more severe pore plugging. Pore size distribution analysis indicated that the pore size decreased significantly in all filter paper membranes due to asphaltene plugging.

REFERENCES

Alta'ee, A. F., Hun, O. S., Alian, S. S., & Saaid, I. M. (2012). Experimental Investigation on the Effect of CO_2 and WAG Injection on Permeability Reduction Induced by Asphaltene Precipitation in Light Oil. International Journal of Materials and Metallurgical Engineering, 6(12), 1203-1208.

Ashoori, S., Sharifi, M., Masoumi, M., & Salehi, M. M. (2017). The relationship between SARA fractions and crude oil stability. Egyptian Journal of Petroleum, 26(1), 209-213.

Belhaj, H., Abu Khalifeh, H. A., & Javid, K. (2013, April 15). Potential of Nitrogen Gas Miscible Injection in South East Assets, Abu Dhabi. Society of Petroleum Engineers. doi:10.2118/164774-MS

Branco, V. A. M., Mansoori, G. A., Xavier, L. C. D. A., Park, S. J., & Manafi, H. (2001). Asphaltene flocculation and collapse from petroleum fluids. Journal of Petroleum Science and Engineering, 32(2-4), 217-230.

Chandio, Z. A., Ramasamy, M., & Mukhtar, H. B. (2015). Temperature effects on solubility of asphaltenes in crude oils. Chemical Engineering Research and Design, 94, 573-583.

Chung, T. H. (1992, January). Thermodynamic modeling for organic solid precipitation. In SPE Annual Technical Conference and Exhibition. Society of Petroleum Engineers.

Dehghani, A.K., Gholami, V., Moghadasi, J. and Abdi, R., Formation Damage through Asphaltene Precipitation Resulting From CO_2 Gas Injection Iranian Carbonate Reservoir, SPE Production & Operations, May: 210-214 (2008).

Elturki, M., Imqam, A. High Pressure-High Temperature Nitrogen Interaction with Crude Oil and Its Impact on Asphaltene Deposition in Nano Shale Pore Structure: An Experimental Study. Paper presented at the SPE/AAPG/SEG Unconventional Resources Technology Conference, Virtual, July 2020a. doi: https://doi.org/10.15530/urtec-2020-3241

Elturki, M., Imqam, A. (2020b, June 28). Application of Enhanced Oil Recovery Methods in Unconventional Reservoirs: A Review and Data Analysis. American Rock Mechanics Association.

Elturki, M., & Imqam, M. (2021, June 28). Analysis of Nitrogen Minimum Miscibility Pressure (MMP) and Its Impact on Instability of Asphaltene Aggregates - An Experimental Study. Society of Petroleum Engineers. doi:10.2118/200900-MS

Elwegaa, K., & Emadi, H. (2019). Improving oil recovery from shale oil reservoirs using cyclic cold nitrogen injection–An experimental study. Fuel, 254, 115716.

Gamadi, T. D., Sheng, J. J., & Soliman, M. Y. (2013, September). An experimental study of cyclic gas injection to improve shale oil recovery. In SPE annual technical conference and exhibition. Society of Petroleum Engineers.

Goual, L., & Firoozabadi, A. (2002). Measuring asphaltenes and resins, and dipole moment in petroleum fluids. AIChE Journal, 48(11), 2646-2663.

Hajizadeh, A., Ravari, R. R., & Amani, M. (2009, October). The Comparison of Effects of Injection of Natural/Nitrogen Gases on Asphaltene Precipitation Process. In SPE/EAGE Reservoir Characterization & Simulation Conference (pp. cp-170). European Association of Geoscientists & Engineers.

Hassanpouryouzband, A., Joonaki, E., Taghikhani, V., Bozorgmehry Boozarjomehry, R., Chapoy, A., & Tohidi, B. (2017). New two-dimensional particle-scale model to simulate asphaltene deposition in wellbores and pipelines. Energy & Fuels, 32(3), 2661-2672.

Hassanpouryouzband, A., Yang, J., Tohidi, B., Chuvilin, E., Istomin, V., Bukhanov, B., & Cheremisin, A. (2018). CO_2 capture by injection of flue gas or CO_2–N_2 mixtures into hydrate reservoirs: Dependence of CO_2 capture efficiency on gas hydrate reservoir conditions. Environmental science & technology, 52(7), 4324-4330.

Hassanpouryouzband, A., Yang, J., Tohidi, B., Chuvilin, E., Istomin, V., & Bukhanov, B. (2019). Geological CO_2 capture and storage with flue gas hydrate formation in frozen and unfrozen sediments: method development, real time-scale kinetic characteristics, efficiency, and clathrate structural transition. ACS Sustainable Chemistry & Engineering, 7(5), 5338-5345.

Hoepfner, M. P., Limsakoune, V., Chuenmeechao, V., Maqbool, T., & Fogler, H. S. (2013). A fundamental study of asphaltene deposition. Energy & fuels, 27(2), 725-735.

Jamaluddin, A. K. M., Joshi, N., Iwere, F., & Gurpinar, O. (2002, January). An investigation of asphaltene instability under nitrogen injection. In SPE International Petroleum Conference and Exhibition in Mexico. Society of Petroleum Engineers.

Khalaf, M. H., & Mansoori, G. A. (2019). Asphaltenes aggregation during petroleum reservoir air and nitrogen flooding. Journal of Petroleum Science and Engineering, 173, 1121-1129.

Maroudas, A.: "Particles Deposition in Granular Filter Media-2," Filtration and separation, v. 3, No. 2, Mar/Apr. 1996, pp. 115-121.

Mansoori, G. A., & Elmi, A. (2010). Remediation of asphaltene and other heavy organic deposits in oil wells and in pipelines. Socar proceedings, 4, 12-23.

Moradi, S., Dabir, B., Rashtchian, D., & Mahmoudi, B. (2012a). Effect of miscible nitrogen injection on instability, particle size distribution, and fractal structure of asphaltene aggregates. Journal of dispersion science and technology, 33(5), 763-770.

Moradi, S., Dabiri, M., Dabir, B., Rashtchian, D., & Emadi, M. A. (2012b). Investigation of asphaltene precipitation in miscible gas injection processes: experimental study and modeling. Brazilian Journal of Chemical Engineering, 29(3), 665-676.

Mozaffari, S., Tchoukov, P., Atias, J., Czarnecki, J., & Nazemifard, N. (2015). Effect of asphaltene aggregation on rheological properties of diluted athabasca bitumen. Energy & Fuels, 29(9), 5595-5599.

Mullins O.C. (2010) The modified yen model. Energy Fuels 24(4), 2179–2207

Necmettin, M. (2003, January). High pressure nitrogen injection for miscible/immiscible enhanced oil recovery. In SPE Latin American and Caribbean Petroleum Engineering Conference. Society of Petroleum Engineers.

Nguyen, M. T., Nguyen, D. L. T., Xia, C., Nguyen, T. B., Shokouhimehr, M., Sana, S. S., ... & Van Le, Q. (2020). Recent advances in asphaltene transformation in heavy oil hydroprocessing: Progress, challenges, and future perspectives. Fuel Processing Technology, 106681.

Pereira, J. C., López, I., Salas, R., Silva, F., Fernández, C., Urbina, C., & López, J. C. (2007). Resins: The molecules responsible for the stability/instability phenomena of asphaltenes. Energy & fuels, 21(3), 1317-1321.

Rashid, Z., Wilfred, C. D., Gnanasundaram, N., Arunagiri, A., & Murugesan, T. (2019). A comprehensive review on the recent advances on the petroleum asphaltene aggregation. Journal of Petroleum Science and Engineering, 176, 249-268.

Ren, B., Xu, Y., Ren, S., Li, X., Guo, P., & Song, X. (2011, January). Laboratory assessment and field pilot of near miscible CO_2 injection for IOR and storage in a tight oil reservoir of Shengli Oilfield China. In SPE Enhanced Oil Recovery Conference. Society of Petroleum Engineers.

Roshanaei Zadeh, G. A., Moradi, S., Dabir, B., Ali Emadi, M., & Rashtchian, D. (2011, January). Comprehensive study of asphaltene precipitation due to gas injection: experimental investigation and modeling. In SPE Enhanced Oil Recovery Conference. Society of Petroleum Engineers.

Sebastian, H. M., & Lawrence, D. D. (1992, January). Nitrogen minimum miscibility pressures. In SPE/DOE enhanced oil recovery symposium. Society of Petroleum Engineers.

Shen, Z., & Sheng, J. J. (2016, April). Experimental study of asphaltene aggregation during CO_2 and CH_4 injection in shale oil reservoirs. In SPE improved oil recovery conference. Society of Petroleum Engineers.

Shen, Z., & Sheng, J. J. (2017). Experimental study of permeability reduction and pore size distribution change due to asphaltene deposition during CO_2 huff and puff injection in Eagle Ford shale. Asia-Pacific Journal of Chemical Engineering, 12(3), 381-390. https://doi.org/10.1002/apj.2080

Speight, J. G. (2014). The chemistry and technology of petroleum. CRC press.

Vahidi, A., & Zargar, G. (2007, January). Sensitivity analysis of important parameters affecting minimum miscibility pressure (MMP) of nitrogen injection into conventional oil reservoirs. In SPE/EAGE reservoir characterization and simulation conference. Society of Petroleum Engineers.

Yang, Z., Ma, C.F., Lin, X.S., Yang, J.T. and Guo, T.M., Experimental and Modeling Studies on the Asphaltene Precipitation in Degassed and Gas-Injected Reservoir Oils, Fluid Phase Equilibria 157: 143–158 (1999).

Yu, Y., & Sheng, J. J. (2015, July). An experimental investigation of the effect of pressure depletion rate on oil recovery from shale cores by cyclic N_2 injection. In Unconventional Resources Technology Conference, San Antonio, Texas, 20-22 July 2015 (pp. 548-557).

Zendehboudi, S., Shafiei, A., Bahadori, A., James, L. A., Elkamel, A., & Lohi, A. (2014). Asphaltene precipitation and deposition in oil reservoirs–Technical aspects, experimental and hybrid neural network predictive tools. Chemical engineering research and design, 92(5), 857-875.

III. ASPHALTENE THERMODYNAMIC PRECIPITATION DURING MISCIBLE NITROGEN GAS INJECTION

Mukhtar Elturki and Abdulmohsin Imqam

Missouri University of Science and Technology

ABSTRACT

For many years, miscible gas injection has been the most beneficial enhanced oil recovery (EOR) method in the oil and gas industry. However, injecting a miscible gas to displace oil often causes the flocculation and deposition of asphaltenes, which subsequently leads to a number of production problems. Nitrogen (N_2) injection has been employed to enhance oil recovery in some oilfields, seeking to improve oil recovery. However, few works have been implemented N_2 injection and investigated its effect on asphaltene precipitation and deposition. This research investigated the N_2 miscible flow mechanism in nanopores and its impact on asphaltene precipitations, which can plug pores and reduce oil recovery. First, a slim tube was used to determine the minimum miscibility pressure (MMP) of N_2 to ensure that all of the experiments would be conducted at levels above the MMP. Second, filtration experiments were conducted using nanocomposite filter membranes to study asphaltene deposition on the membranes. A filtration apparatus was specially designed and built to accommodate the filter membranes. The factors studied include N_2 injection pressure, temperature, N_2 mixing time, and pore size heterogeneity. Visualization tests were conducted to highlight the asphaltene precipitation process over time. Increasing the N_2 injection pressure resulted in an increase in the asphaltene weight

percent in all experiments. Decreasing the pore size of the filter membranes increased the asphaltene weight percent. More N_2 mixing time also resulted in an increase in asphaltene weight percent, especially early in the process. Visualization tests revealed that after 1 h, the asphaltene particles were conspicuous, and more asphaltene clusters were found in the test tubes of the oil samples from the filter with the smallest pore size. Chromatography analysis of the produced oil confirmed the reduction in the asphaltene weight percent. Microscopy and scanning electron microscopy (SEM) imaging of the filter membranes indicated significant pore plugging from the asphaltenes, especially for the smaller pore sizes. This research highlights the severity of asphaltene deposition during miscible N_2 injection in nanopore structures so as to understand the main factors that may affect the success of miscible N_2 injection in unconventional reservoirs.

1. INTRODUCTION

The gas injection method has become a widespread technology to improve oil production in unconventional shale reservoirs in the United States. Although hydraulic fracturing technology in horizontal wells can be employed to retrieve trapped oil, only 4 to 6% can be recovered (Elturki et al., 2021). Very recently, gas injection methods have been studied in unconventional shale reservoirs using N_2 and carbon dioxide (CO_2) injection, and the results have demonstrated a positive impact on increasing oil recovery (Elwegaa and Emadi., 2019; Altawati et al., 2020). Multiphase flow production has the potential to cause many issues in the oil industry which the multiphase fluids (i.e., gas, oil, condensate, and water) together with scales can cause some problems including wax and asphaltene deposition, formation of hydrates, slugging, and emulsions (Shi et al., 2021). Deposition of organic hydrocarbon solids in oil and gas reservoirs could cause many flow assurance problems during the oil and gas production process. These materials could increase the flow resistance and production disrupt or even plug the pipelines (Hassanpouryouzband et al., 2020; Ali et al., 2021). One of the major problems during gas injection in unconventional reservoirs could be asphaltene deposition and precipitation. Asphaltene, a solid component of crude oil, has an extremely high molecular weight (Mozaffari et al., 2015; Rashid et al., 2019). Asphaltene can be found in colloidal suspensions or in solution under reservoir pressure and temperature conditions (Jamaluddin et al., 2002). Asphaltene instability can be induced when the solubility of heavy components changes during the gas injection process. Changes in temperature, pressure, and crude oil composition in a reservoir will result in the precipitation of asphaltene on solid surfaces during oil flows from the reservoir to the surface (Kar et al., 2020). As a consequence, asphaltene aggregates, and nanosized particles can form clusters that may cause critical issues by blocking wellbore pores and production facilities (Alves et al., 2019). CO_2 and N_2 could cause a different degree of asphaltene flocculation into the reservoir. CO_2 has good solubility in crude oil and can easily attain a supercritical condition in reservoir conditions (Wang et al., 2018). For dead oils, CO_2 solubility ranges from 0.100 to 0.800 (mole fraction) for low and high temperatures, respectively (Nguyen et al., 1998; Mahdaviara et al., 2021). On the other hand, the CO_2 solubility of live oils ranges from 0.062 to 0.966 (mole fraction) for low and high temperatures, respectively (Rostami et al., 2017). Thus, the mass transfer ability of supercritical CO_2 is strong. In CO_2 injection process, the CO_2-crude oil system could easily reach a miscible or near-miscible state that enhances extracts the light hydrocarbon components from crude oil into the gas phase. At similar thermodynamic conditions, N_2 has weaker solubility in crude oil than CO_2. N_2 has a weak mass transfer capacity which could lead to the poor extraction of light hydrocarbons and probably less asphaltene flocculation compared to CO_2 (Chung, 1992; Wang et al., 2018).

Recently, many experimental studies have examined the effect of gas injection, including CO_2 and N_2, on the stability of asphaltene in a crude oil system (Jamaluddin et al., 2002; Moradi et al., 2012a; Soroush et al., 2014; Alimohammadi et al., 2017; Alves et al., 2019; Afra et al., 2020; Kar et al., 2020; Elturki and Imqam, 2020a, 2021a). Jamaluddin et al. (2002) combined various molar concentrations of N_2 with the reservoir fluid to investigate the instability of asphaltene. Their results showed that raising the concentration of N_2 increased the instability of asphaltene and also expanded the bulk precipitated amount. Moradi et al. (2012a) used natural depletion and N_2 injection processes to study the instability of asphaltene aggregates. N_2 produced an extreme negative alteration in the asphaltene instability, especially for heavier crudes. They also stated that the evaporation of N_2 improved the capability of oil to overcome the association of the flocs and break down the complex clusters. Soroush et al. (2014) investigated the effect of miscible and immiscible CO_2 flooding on the damage to porous media. They concluded that (1) above the MMP of CO_2, the trapped gas in porous structures could reduce the permeability, and (2) the pore plugging was much more severe compared to conditions below the MMP. On the other hand, asphaltene deposition was the principal factor in reducing the permeability during miscible injection pressure. Alves et al. (2019) researched the effect of temperature on asphaltene precipitation and concluded that when the temperature rose, the asphaltene precipitation decreased. Afra et al. (2020) studied the effect of CO_2 injection on the structure and stability of asphaltene using four crude oil samples. Their work using infrared spectroscopy and acid/base identification demonstrated that asphaltene stability was disturbed when the amine group of one of the tested asphaltene samples could form an amide functional group by reacting with CO_2. They also stated that as the oil viscosity increased, the asphaltene concentration also rose. Kar et al. (2020) performed static vial tests and dynamic flow tests using six nonionic, weakly ionic, and ionic surfactants to study the effect of various surfactants on removing the deposited asphaltene on the surface of flowlines. Their results demonstrated that all surfactants removed the deposited asphaltene with less severe asphaltene aggregation. Additionally, ionic surfactants were found to be the most effective chemical in asphaltene deposition removal. Injection of CO_2 and N_2 mixtures has been studied for storing CO_2 and increasing hydrocarbon production from unconventional resources (Hassanpouryouzband et al, 2018; 2019). They investigated the CO_2 capture efficiency at various injection pressure and the results demonstrated that the efficiency of CO_2 capture depends on the reservoir conditions such as pressure and temperature. The results also showed that there is an optimal reservoir pressure for a given reservoir temperature at which the maximum volume of CO_2 can be extracted from the injected flue gas or CO_2-N_2 mixtures.

Few studies have investigated the negative effects of asphaltene deposition and precipitation on pore plugging in unconventional reservoirs. Moradi et al. (2012b) conducted an experiment using N_2 and methane, with a 0.2-µm pore size filter membrane and reported that the asphaltene deposition was much higher when using methane than with N_2. Shen and Sheng (2018) studied the asphaltene aggregates precipitated during CO_2 and methane injection in shale oil samples. They used different filter membranes (i.e., 200, 100, and 30 nm) to investigate asphaltene deposition. Their study of core flooding concluded that the oil recovery decreased due to the increase in asphaltene precipitation and deposition. Elturki and Imqam (2020b) conducted experiments during immiscible N_2 injection into nano shale pore structures to investigate the instability of asphaltene. Various parameters were selected and examined, including temperature, pressure, and mixing time. They concluded that higher pressure resulted in a higher asphaltene weight percent, especially in smaller pore size structures, but the temperature had the opposite effect. However, a literature review found limited investigations of the factors impacting asphaltene deposition during N_2 injection, especially in nanopore reservoirs.

Even though there are many studies on the thermodynamic behavior of asphaltene precipitation during CO_2 injection, the structure and chemistry of the asphaltene reaction with N_2 remains poorly investigated and understood, especially in unconventional shale reservoirs. This research extends the previous work conducted by Elturki and Imqam (2021b) which investigated the impact of immiscible N_2 injection on asphaltene precipitation. The present research aimed to investigate the severity of asphaltene damage, especially in nanopore structures present in unconventional reservoirs. By studying the impact of various factors on asphaltene formation damage, asphaltene deposition may be mitigated in future applications of N_2 injections.

2. ASPHALTENE DEFINITION AND PRECIPITATION MECHANISM

Asphaltene is one of the most complex solid components comprising crude oil. Asphaltene can be defined as “the heaviest component of petroleum fluids that is insoluble in light n-alkanes such as n-pentane or n-heptane, but soluble in aromatics such as toluene" (Goual, 2012). The main components of crude oil are saturates, aromatics, resins, and asphaltenes. All of these components are held together with resins that have both polar and nonpolar sites, making resins a perfect connector between all of the components. As conditions change, the forces that bind all of the components become weaker and more severe; thus, the asphaltene starts to precipitate. The common conditions that may change include pressure; temperature; solvent injection, such as CO_2; and a high oil production flowrate (Bahman et al., 2017). High density asphaltene flocculation starts to form after the precipitation, if conditions are suitable. This flocculation will start to be deposited in the pores of the reservoirs (Srivastava et al., 1997), with buildups forming if an excessive deposition occurs, causing pore plugging. Figure 1 shows the main alterations that can occur because of asphaltene deposition, including pore plugging and adsorption of the asphaltene to the rock grains both result in wettability changes (Al-Hosani, 2020).

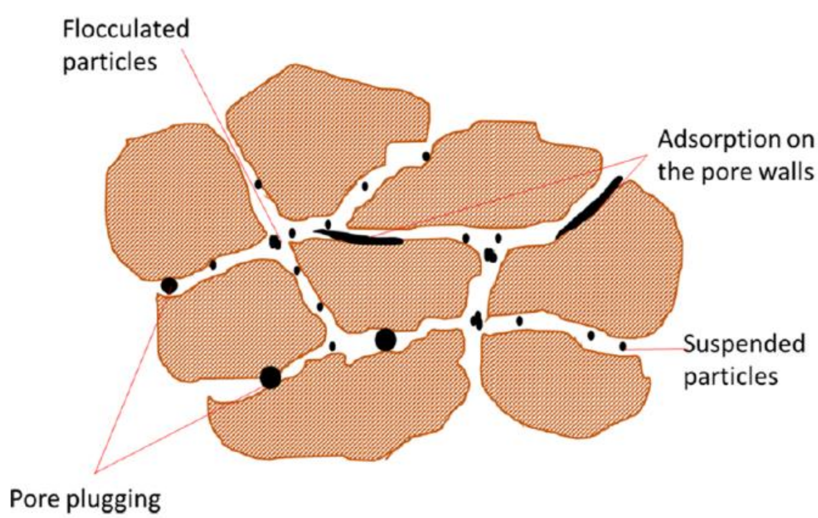

Figure 1. Asphaltene impacts oil recovery.
(Al-Hosani, 2020)

3. EXPERIMENTAL DESIGN

Figure 2 shows the experimental flowchart for the three types of experiments that were conducted: (1) MMP determination, (2) filtration, and (3) asphaltene visualization. First, the MMP of N_2 was determined to ensure the pressure in the filtration experiments fell within miscible conditions. Then, the visualization experiments were conducted, after which the asphaltene weight percentages were calculated. Chromatography analysis of crude oil confirmed the change in the asphaltene weight percent after the filtration experiments compared to the original crude oil. Microscopy imaging was used to highlight the effect of the asphaltene deposition into the pores of the filter membranes.

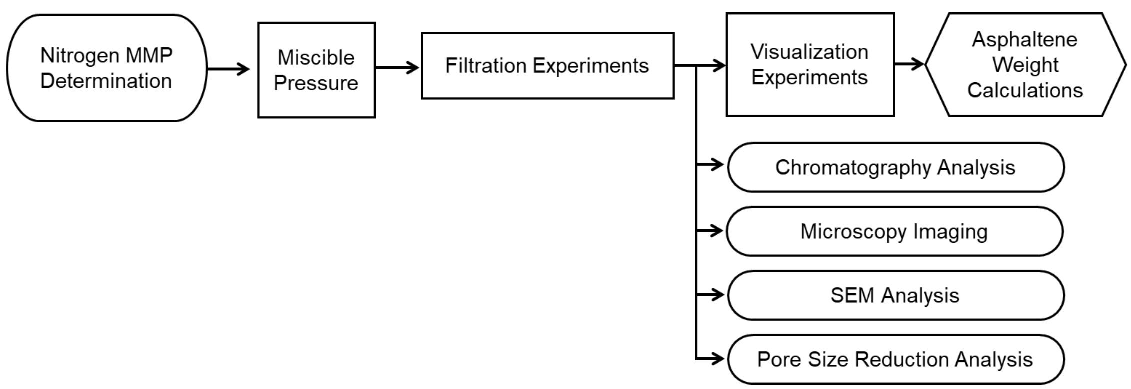

Figure 2. Experimental design flowchart.

3.1. EXPERIMENTAL MATERIAL AND DESCRIPTION

The experimental materials included the following:

- Crude oil: Crude oil with a viscosity of 19 cp, density of 0.864 gm/cc, and °API of 32 was used. The viscosity was measured using a rheometer. Gas chromatography-mass spectrometry determined the composition of the crude oil, as shown in Table 1.

- Filter membranes**:** Various sizes of filter membranes (i.e., 50, 100, and 450 nm) were used to investigate the effect of different pore sizes. The selection of filter membrane pore sizes was based on the pore size distribution of shale reservoirs, specifically Eagle Ford (Shen et al., 2017). The membranes were cut to the desired shape based on the 45-mm diameter of the filtration vessel.

- Specially designed HPHT filtration vessel: A high-pressure high-temperature (HPHT) filtration vessel was designed specifically to accommodate filter paper membranes for oil filtration experiments. The filtration vessel had a length of 15.24 centimeters with inside and outside diameters of 5 and 7.62 centimeters, respectively.

- Nitrogen: An N_2 gas cylinder with 99.9% purity was connected to the filtration vessel and used for the N_2 injection. A pressure regulator controlled the N_2 cylinder pressure.

- Oven: An oven with enough space to accommodate the filtration vessel was used to investigate the effect of various temperatures on asphaltene precipitation and deposition during N_2 injection. The oven manufactured by Despatch, Model: LBB2-27-2, Chamber dimensions: 94(width) x 94(depth) x 89(height) centimeters.

- N-heptane: This solvent was used to dissolve the oil samples in the tubes to quantify the asphaltene weight percent after each experiment.

- Slim tube: A stainless steel slim tube packed with sand was used to determine the minimum miscibility pressure of N_2. The slim tube had a wight of 2211 gram with a length of 13.1 meter (inside and outside diameters were 0.21 and 0.41 centimeters, respectively).

Table 1. Crude oil composition

Component	Weight percentage (%)
C_8	64.55
C_9	0.28
C_{14}	0.31
C_{15}	0.35
C_{16}	0.43
C_{17}	3.92
C_{18}	0.20
C_{19}	1.17
C_{20}	3.60
C_{21}	0.93
C_{22}	2.66
C_{24}	1.97
C_{27}	5.94
C_{28}	7.22
C_{29}	1.32
C_{30+} (including asphaltene)	5.17
Total	100

A summary describing all of the experiments conducted in this research and the significant factors that were investigated are presented in Table 2.

Table 2. Summary of all experiments conducted in this research.

No.	Experiment/ Analysis	Factor Studied	Factor Value	Pressure
1	MMP	Temperature	32ºC, 70ºC	-
2	Filtration	Temperature	32ºC, 70ºC, 90ºC	1750 psi
3		Mixing time	10, 60, and 120 min	1750 psi
4		Injection pressure /Heterogeneity	450, 100, and 50 nm	1750, 2000, and 2250 psi
5			100, 100, and 100 nm*	1750, 2000, and 2250 psi
6	Visualization	Mixing time	10, 60, and 120 min	1750 psi
7		Injection pressure /Heterogeneity	450, 100, and 50 nm	1750, and 2250 psi
8			100, 100, and 100 nm*	2000 psi
9	Microscope imaging	Pore size plugging	450, 100, and 50 nm	1750, 2000, and 2250 psi
10	SEM analysis	Pore size plugging	450, 100, and 50 nm	1750 and 2250 psi
11	Gas chromatography	Chemical structure	1750 and 2250 psi	1750 and 2250 psi
12	Pore plugging	Pore size distribution	450, 100, and 50 nm	1750 and 2250 psi
*Uniform pore size distribution				

3.2. MMP EXPERIMENT

To ensure that all of the filtration experiments would occur above the MMP, experiments were initially conducted to determine the MMP. The MMP can be defined as the lowest pressure at which a gas can create miscibility with the reservoir oil at the reservoir temperature. In other words, the MMP is the lowest pressure at which miscibility between the injected gas and reservoir oil is achieved when the interfacial tension between the oil and gas disappears after multiple contacts. Figure 3 shows a schematic diagram of the slim tube experimental setup. The main components of the MMP experiment included a syringe pump, three accumulators, gas cylinders, a stainless-steel slim tube packed with sand, and a back pressure regulator. The first step was a pretest to calculate the pore volume. In the second step, the slim tube was filled with the crude oil at a low rate of 0.5 PV to ensure that the slim tube was 100% saturated at the end of pumping. The final step involved experimental manipulation, whereby the temperature was adjusted to a predefined level, the gas cylinder was filled with N_2, and gas was pumped at a rate of 1.2 PV of gas injected. A back pressure regulator was installed at the outlet of the slim tube and used to adjust the pressure by using another water pump as a back pressure reservoir.

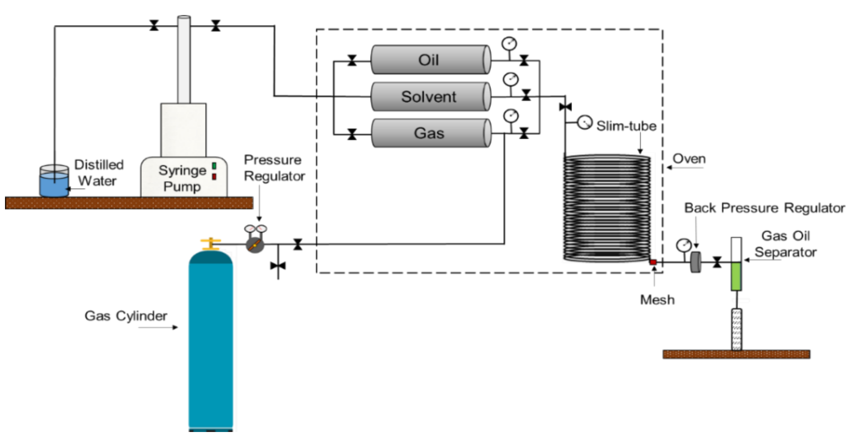

Figure 3. Main components of the slim tube experimental setup

3.2.1. MMP Experiment Procedure. Starting with the slim tube which was fully saturated with distilled water. Following the oil was then injected into the slim tube unit fully saturated. This can be observed at the outlet of the slim tube when the produced liquids are only oil and thus ensure the slim tube is fully saturated. During all the experiments, the back pressure regulator was placed at the outlet with the desired pressure. The gas accumulator was filled with N_2. Then, N_2 was injected at a rate of 0.25 ml/min. Each experiment was stopped when 1.2 PV of gas injected or when the gas broke through. The effluent was used to collect the produced oil. The MMP can be determined by plotting N_2 injection pressures versus cumulative oil recoveries. Finally, the solvent of Xylene was used after each experiment to clean the slim tube setup and to make sure there is no oil left in the slim tube that may affect the next experiment.

3.3. FILTRATION EXPERIMENTS

The components of the filtration setup are shown in Figure 4. The main components included a high-purity N_2 with a pressure regulator to control the pressure from the cylinder. The HPHT filtration vessel was designed to accommodate three mesh screens to support the filter membranes and prevent them from folding under high pressure. The mesh screens were designed with small holes that allowed the oil to pass through easily. Spacers between each mesh screen were added to support each mesh screen in its place, and rubber O-rings were used above and below each spacer to prevent leakage and to ensure that the oil and gas would pass through the filter paper membranes. A back pressure regulator was installed at the outlet of the filtration vessel and used to adjust the pressure in the syringe pump. The produced oil was collected using an effluent below the filtration vessel for further analysis.

An oven controlled the temperature of the filtration vessel to study the effect of different temperatures. Finally, two transducers were installed at the inlet and outlet of the filtration vessel and were connected to a computer to monitor and record the pressure differences.

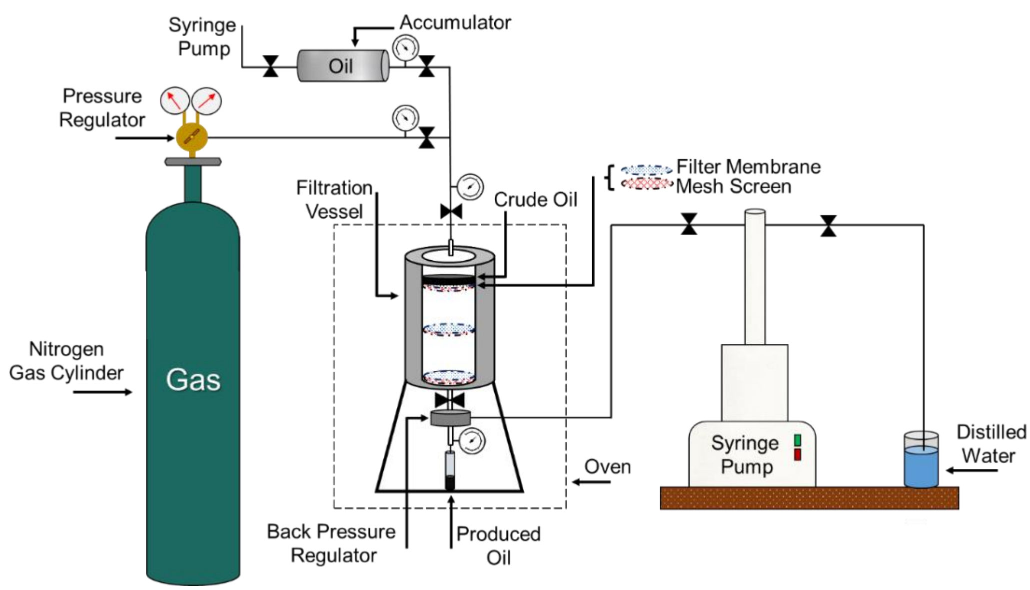

Figure 4. Filtration experimental setup.

3.3.1. Filtration Experimental Procedure. The first set of mesh screens along with a filter membrane paper, rubber O-ring, and spacer were placed inside the filtration vessel, in that order. This step was repeated with the next two sets, after which the vessel was closed using a specially designed cap that ensured a tight connection between all of the sets and prevented leakage during the experiment. An oil accumulator injected 30 ml of crude oil into the vessel using a syringe pump. Next, the N_2 cylinder injected gas into the vessel to the desired level and exposed the crude oil to the gas for a specific mixing time. Then, the syringe pump at the outlet was turned to constant pressure but was adjusted to the required back pressure for each experiment to let the crude oil pass through the membranes. N_2 was injected continuously into the vessel, and the produced oil was collected for further analysis (e.g., chromatography analysis). The experiment was stopped when no further oil production was observed. During the experiment, the inlet and outlet pressures were recorded using transducers connected to a computer. The difference between the two pressures did not exceed 50 psi. After the experiment, the vessel was opened, and the remaining crude oil was collected from each filter membrane for analysis. Finally, the solvent n-heptane was used to clean the vessel, mesh screens, and spacers from oil in preparation for the next experiment.

3.4. VISUALIZATION EXPERIMENTS

3.4.1. Asphaltene Visualization Experiments Procedure. Asphaltene visualization experiments provide evidence of how asphaltene behaves in terms of precipitation and deposition at various conditions. These experiments were conducted to visualize the asphaltene precipitation and deposition using the following procedure:

1. Place in a test tube 1 ml of crude oil collected from all filter membranes, the produced oil, and the remaining oil from the filtration experiments. The oil was collected using a pipette to ensure the accuracy of all samples.
2. Add 40 ml of n-heptane to each test tube. Tubes were closed tightly to prevent n-heptane evaporation.
3. Each test tube was shaken well to ensure that the n-heptane was well dispersed within the crude oil.
4. A special laboratory stand was used to handle all of the test tubes. The asphaltene then started to settle slowly.

5. Photos were taken at specific time points (i.e., 0, 2, 4, and 12 h) to observe the change in asphaltene settling over time.

Asphaltene weight percent can be calculated by weighing the filter paper before and after the filtration process. The difference between these weights determines the asphaltene weight percent using the following equation:

$$\text{Asphaltene wt\%} = \frac{\text{wt}_{\text{asphaltene}}}{\text{wt}_{\text{oil}}} * 100 \tag{1}$$

Where asphaltene wt% is the asphaltene weight percent, $\text{wt}_{\text{asphaltene}}$ is the asphaltene weight on the filter paper, and wt_{oil} is the oil sample weight. The asphaltene quantification test procedure is summarized in a flowchart in Figure 5.

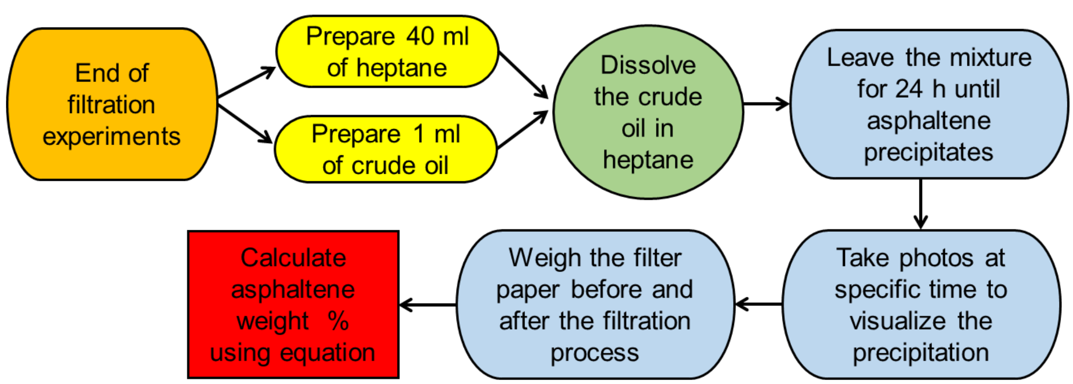

Figure 5. Flowchart highlighting the main steps of asphaltene quantification.

4. RESULTS AND DISCUSSION

4.1. MMP EXPERIMENTAL RESULTS

The MMP experiments were conducted to ensure that all of the filtration experiments would occur above miscible gas injection conditions. Crude oil with a viscosity of 19 cp, density of 0.864 gm/cc, and ºAPI of 32 was used. The effect of temperature was studied on the MMP of N_2 to ensure that the miscible injection pressure was still achievable during the high pressure of the filtration experiments.

To determine the MMP, the tested N_2 injection pressures were plotted versus oil recoveries at 1.2 PV of gas injected or at gas breakthrough. The MMP can be estimated when the cumulative oil recovery is greater than or equal to 90% of the original oil in place (OOIP). The solid lines in Fig. 6 were used to determine the sudden slope change point in the measured oil recovery versus injection pressure. The intersection point can be used to determine the MMP. The results demonstrated that with increasing temperature, the MMP decreased. This is the opposite of what occurs with a CO_2 MMP. The MMP of N_2 at 32ºC was 1600 psi, while at a higher temperature of 70ºC, the MMP of N_2 was 1350 psi, as shown in Figure 6.

Various studies stated that the MMP can increase or decrease depending on the oil composition (Belhaj et al., 2013; Vahidi et al., 2007; Sebastian et al., 1992). Therefore, the results of this research can be explained by the fact that the temperature is inversely proportional to the N_2 MMP due to the N_2 remaining in the gaseous phase at the same conditions. Consequently, the effect of temperatures higher than 32ºC were investigated in this research because miscibility can be achieved at higher temperatures.

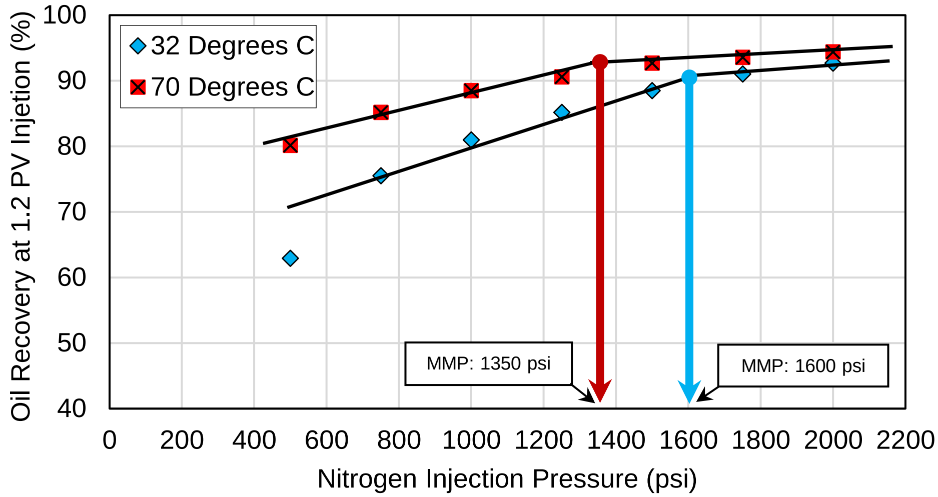

Figure 6. N_2 MMP determination using an oil viscosity of 19 cp at 32ºC and 70ºC.

4.2. FILTRATION AND VISUALIZATION RESULTS

4.2.1. Effect Of Miscible Pressure Using Uniform Membrane Distribution.

Three 100-nm filter membranes were placed in the filtration vessel to investigate the effect of using the same pore size structure and to compare the results to those using a heterogeneous distribution. A uniform distribution means that filter membranes of the same pore size were used. Figure 7 illustrates the paper membrane distribution inside the vessel. An N_2 pressure of 1750, 2000, and 2250 psi and a temperature of 32ºC were used throughout these experiments.

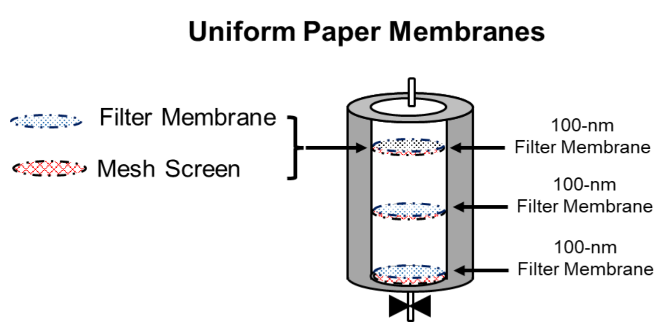

Figure 7. Illustration of the uniform paper membrane distribution inside the vessel.

Figure 8 shows the asphaltene weight percent versus N_2 injection pressure when using a uniform distribution. The results showed that the asphaltene weight percent was almost equal for most of the filter membranes used. At 1750 psi injection pressure, the weight percent of asphaltene decreased slightly from 12.68% in the upper part of the 100-nm filter membrane to 12.07% in the lower part due to the asphaltene clusters having plugged the pores in the upper and middle areas of the 100-nm filter membrane. This prevented some oil from passing through and thus reduced the asphaltene percent in the lower part of the filter membrane. However, this did not occur when using 2000 psi injection pressure, at which the asphaltene weight percent increased slightly from 13.69% to 13.80% in the upper and lower parts of the 100-nm filter, respectively. These observations demonstrated that the asphaltene clusters passed through all the filter membranes with approximately the same behavior at all the injection pressures studied. The asphaltene particles greater than 100 nm precipitated on the upper portion of the filter membrane, while the smaller particles passed through all the filters and reached the outlet with the produced oil. The slight fluctuation in the asphaltene weight percent occurred because some of the asphaltene clusters plugged some pores in the middle or lower filter membranes. The flow of oil inside the vessel was not smooth in all of the filter membranes because the pore plugging could not be controlled. The lowest amount of asphaltene was also found in the produced oil due to the pore plugging that resulted from the asphaltene clusters present throughout all the filter membranes.

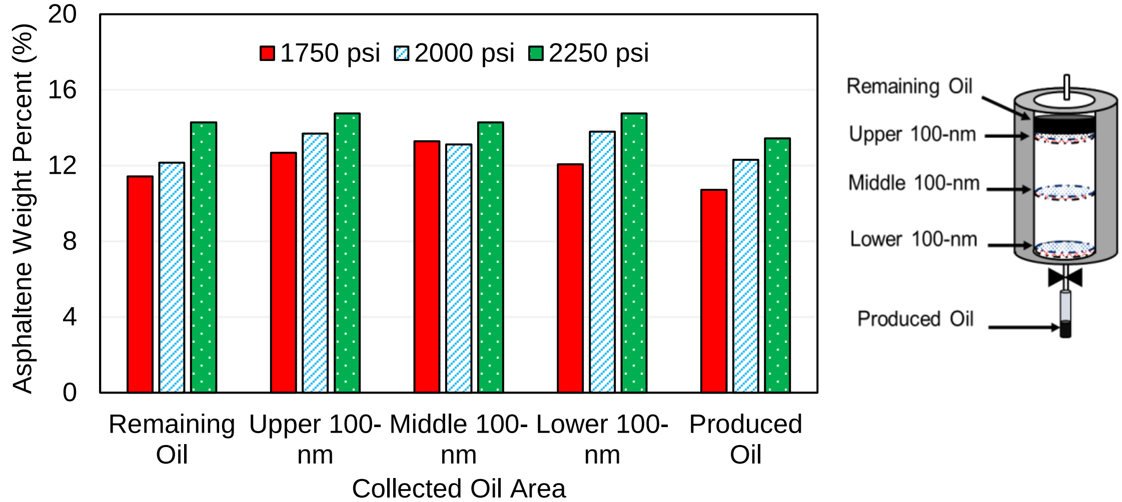

Figure 8. Asphaltene weight percent distribution using uniform paper membranes with N_2 injections at 1750, 2000, and 2250 psi.

A 2000 psi N_2 injection pressure was selected to investigate the asphaltene precipitation over time. Figure 9 shows the asphaltene visualization process along a uniform membrane pore size distribution. At zero elapsed time, no asphaltene was observed, and the crude oil sample was entirely dissolved in n-heptane. After 1 h, asphaltene started to form and precipitate, and suspended particles could be seen in the uppermost section of the test tubes. The lower portion of the 100-nm filter exhibited slightly more suspended particles due to asphaltene plugging more pores in the upper and middle parts of the filter membranes. Over time, more asphaltene was deposited on the bottommost section of the test tubes. The visualization tests showed that most of the asphaltene particles formed and were deposited over 1-4 h. Finally, after 12 h, most of the asphaltenes were deposited and few particles could be found in the supernatant. These results indicate that the asphaltene amount in all the filter membranes using the uniform distribution was almost equal in all 100-nm filters used. This confirms the results of the filtration experiment, which showed the same trend.

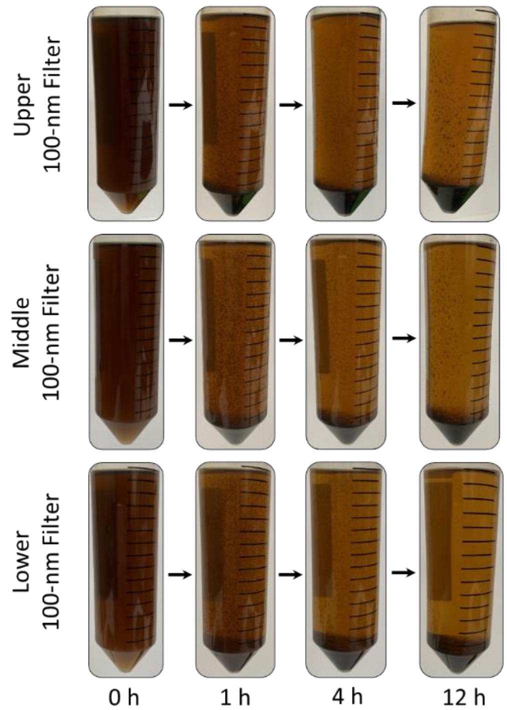

Figure 9. Asphaltene precipitation and deposition visualization process using 2000 psi injection pressure and a uniform distribution at 32ºC with a 2-h mixing time.

4.2.2. Effect of Pore Size Heterogeneity. Three miscible N_2 pressures were investigated (i.e., 1750, 2000, 2250 psi) at 32ºC with a 2-h mixing time. The mixing time effect will be presented in the following sections. A heterogeneous condition of the filter membranes was examined, starting with a 450-nm filter in the upper mesh screen, 100-nm filter in the middle, and 50-nm filter in the lower mesh screen, as shown in Figure 10. Increasing the pressure resulted in an increase in the asphaltene weight percent because the asphaltene resins connect all the solid components in crude oil that break down; thus, asphaltene levels will increase.

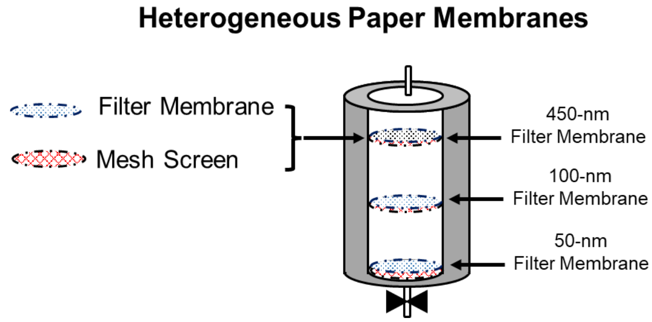

Figure 10. Illustration of the heterogeneous paper membrane distribution inside the vessel.

Figure 11 presents the asphaltene weight percent using a heterogeneous paper membrane distribution during various N_2 injection pressures. When using 1750 psi gas injection, the asphaltene weight percent increased significantly, from 11.67% to 17.33% in the 450-nm and 50-nm filters, respectively. This indicated that the asphaltene particles and clusters were affected by the injected pressure, which resulted in asphaltene deposition depending on the asphaltene particle size. This led to plugged pores in the filter membranes, especially in the 50-nm filter. The ability of asphaltene particles to pass through the filter membranes was affected by the size of their pores. As a result of Brownian motion, the asphaltene aggregates continued to interact with one another, forming larger particles. Because of the large radial diffusivity of the particles, smaller aggregates have a higher tendency to deposit (Hassanpouryouzband et al., 2017). These observations strongly indicated that the asphaltene had altered the ability of the oil to pass through, which can occur in real reservoirs, causing severe problems. The produced oil had a lower asphaltene weight percent due to the asphaltene clusters having plugged the pores in all the filter membranes. Also significant is that when the filtration vessel was opened to collect the crude oil, the volume of the oil had increased, and bubbles could be seen in the oil. This can be explained by the pressure increase, which made the N_2 more soluble in the oil; thus, the oil swelled. This phenomenon resulted in a slight decrease in the N_2 pressure inside the vessel. The N_2 started to be liberated from the oil after the pressure was relieved. Finally, the oil returned to its original volume. Figure 12 shows the bubbles that formed in the oil when it was collected from the filtration vessel.

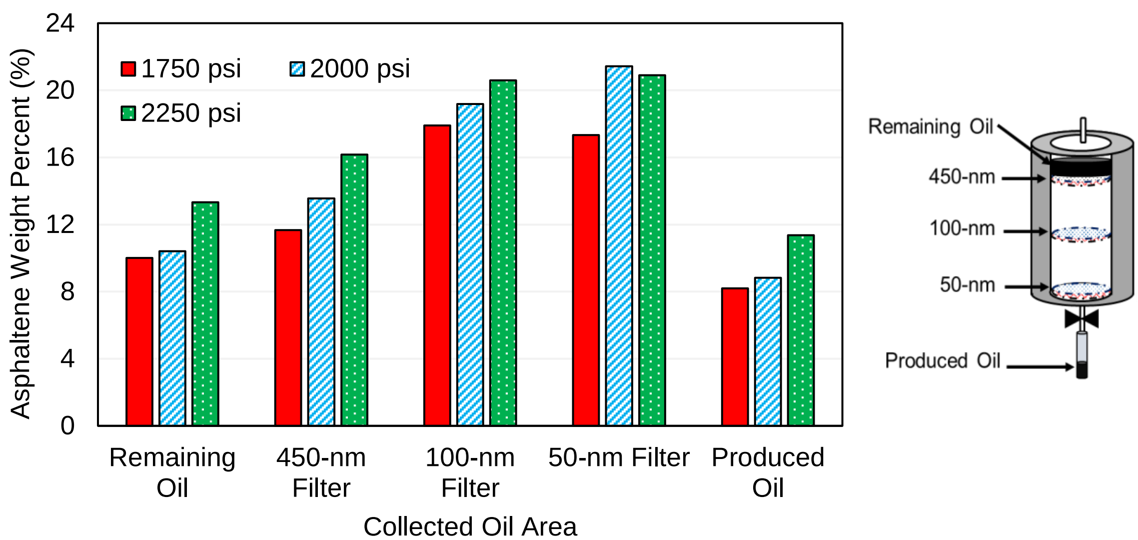

Figure 11. Asphaltene weight percent using a heterogeneous distribution at 1750, 2000, and 2250 psi N_2 injection.

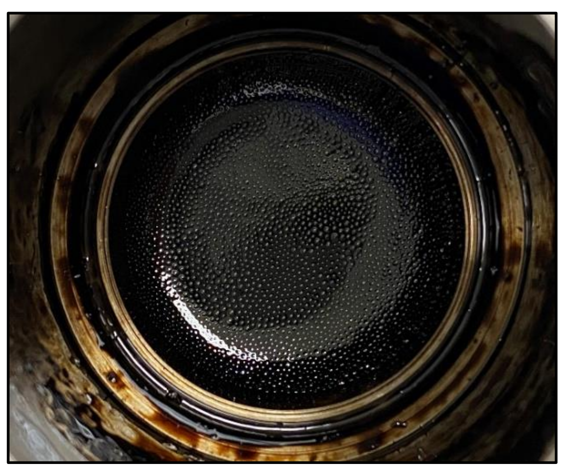

Figure 12. N_2 dissolved in the crude oil being liberated at an injection pressure of 1750 psi.

The visualization of the asphaltene deposition process over time was implemented by analyzing the collected oil after concluding each experiment. The oil collected from 450-, 100-, and 50-nm filter membranes was analyzed under 1750, 2000, and 2250 psi N_2 injection pressures. Test tubes were used to mix the oil samples with the solvent n-heptane at a ratio of 1:40. Four times were selected (i.e., 0, 1, 4, and 12 h) to investigate and visualize the asphaltene deposition process. The photos illustrate that at 0 h, all the test tubes held oil that was fully dissolved in n-heptane, and no asphaltene was observed during all the selected injection pressures using any of the filter membranes. After 1 h, it was observed that asphaltenes started to form because the bonds between the asphaltene and resins were weakened by pressure. Interestingly, the image of the 50-nm filter showed a slightly higher amount of suspended asphaltenes during the 1750 psi gas injection because the smaller pore size trapped more particles of asphaltene, as shown in Figure 13. This observation also occurred during the 2000 psi gas injection, but not at 2250 psi.

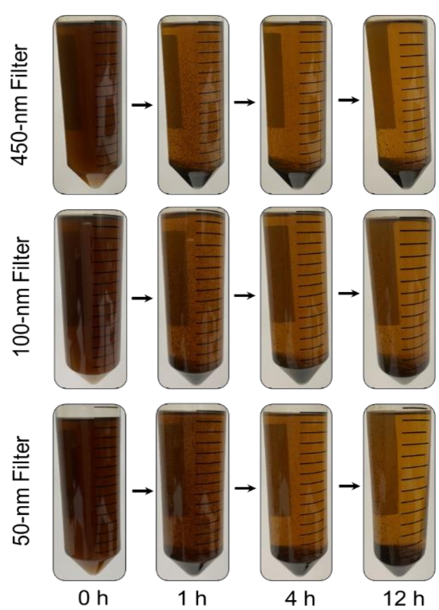

Figure 13. Visualization of the asphaltene precipitation and deposition process at 1750 psi using a heterogeneous distribution at 32ºC.

During the highest pressure (2250 psi), the asphaltene precipitated slightly faster than at the lower pressures, as shown in Figure 14. Moreover, the asphaltene deposition and precipitation started after 1 h, which can be observed at the bottommost section of the test tubes, as they became dark in color due to the high asphaltene concentration. After 4 h, more asphaltene settled, and less asphaltene suspension was found in the supernatant. This observation was more obvious at the highest-pressure condition of 2250 psi. As time progressed, more asphaltene deposition was observed in all captured photos of all test tubes. After 12 h of precipitation, the supernatant became lighter in color, but a darker color was still found in the bottom of all test tubes, representing asphaltenes. These results demonstrated that pressure has a significant effect on asphaltene instability. It is therefore important to analyze the pressure effect on the asphaltene stability to anticipate and avoid any related issues.

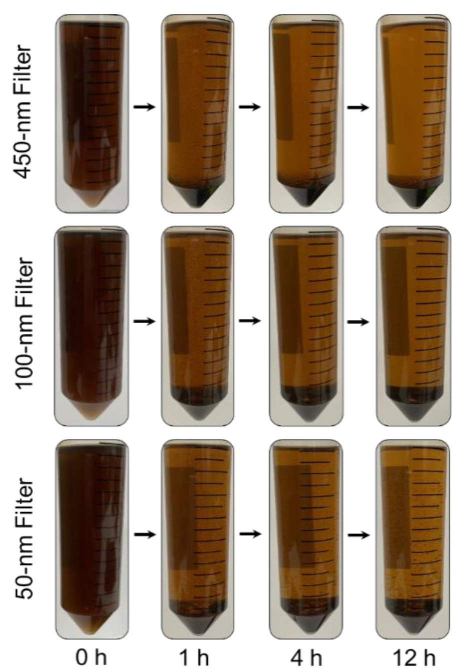

Figure 14. Visualization of the asphaltene precipitation and deposition process at 2250 psi using a heterogeneous distribution at 32ºC.

4.2.3. Effect of Mixing Time. The mixing time is the total time the oil was exposed to the desired N_2 pressure inside the reservoir cylinder and left at 32ºC to allow the N_2 to mix well with the crude oil. Three different experiments with times of 10, 60, and 120 min were selected to investigate the effect of the mixing time on the asphaltene precipitation and deposition during 1750 psi N_2 injection at a temperature of 32ºC. Figure 15 shows the asphaltene weight percent in all filter membranes during various mixing times. The results highlight that increasing the mixing time resulted in an increase in the asphaltene weight percent. For a 450-nm filter, the asphaltene weight percent increase ranged from 8.95% to 11.67% for 10 and 120 min, respectively. Decreasing the filter membrane size led to an increase in the asphaltene weight percent because of pore plugging from asphaltene clusters. A 10-min mixing time had a lower effect on the asphaltene clusters due to the limited time for the gas to weaken the bonds between the asphaltene and resins. Given these observations, the mixing time has an effect on the instability of asphaltene aggregation. These data highlight that the mixing time has a crucial effect on the asphaltene deposition within 120 min, although this deposition may increase slightly over longer times, especially in smaller pores.

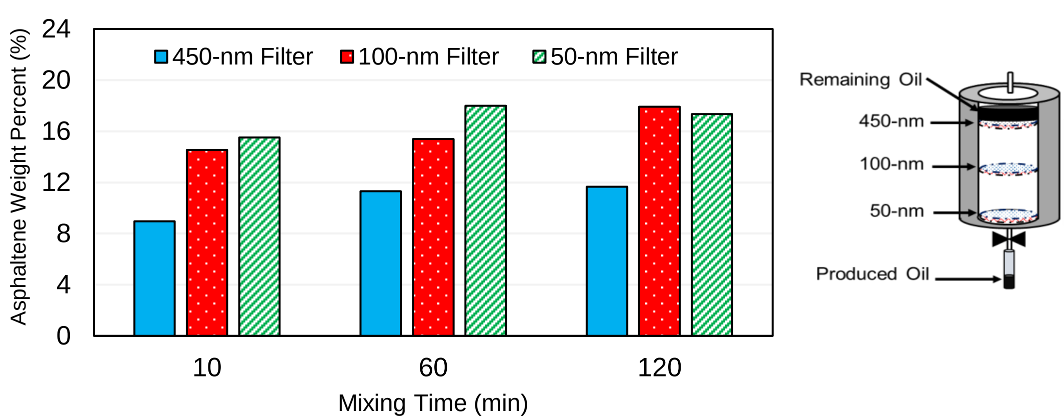

Figure 15. Asphaltene weight percent at mixing times of 10-, 60-, and 120-min using 450-, 100-, and 50-nm filter membranes.

The remaining oil was collected from all of the filtration experiments and all mixing times. Every experiment was conducted at 1750 psi and 32ºC. Figure 16 shows the effect of a 1750 psi N_2 injection on the remaining oil, using mixing times of 120, 60, and 10 min. Increasing the mixing time also increased the asphaltene precipitation process time. For 10 min of mixing time, the asphaltene deposition process was slower than for 60 and 120 min. This could result from the short time (10 min), during which the N_2 could impact the asphaltene instability; thus, there were fewer suspended asphaltene particles in the test tube, especially after 1 h. After 4 h, the bottommost section of the test tubes for the 120-min mixing time became darker than during the 10-min mixing time. This indicates that the asphaltene particles significantly aggregated during longer mixing times.

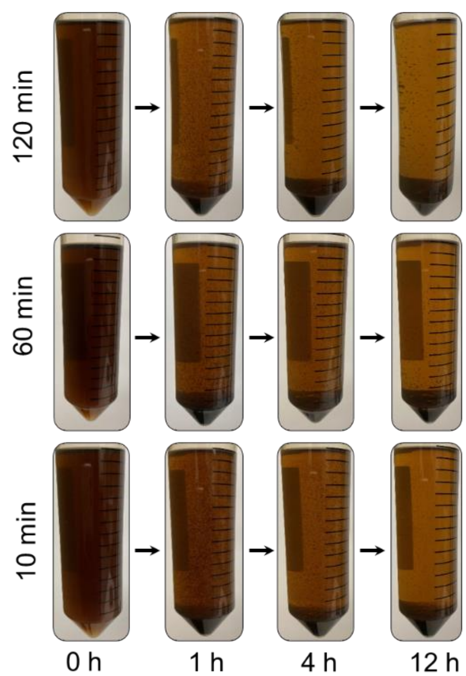

Figure 16. Visualization of the asphaltene precipitation and deposition process at different mixing times.

For all mixing times, after 12 h from the beginning of the experiment, most of the asphaltene particles had settled, although there were some suspended particles in the supernatant of the 60- and 120-min mixing times. The prolonged interaction of the N_2 with the oil resulted in more asphaltene instability; thus, severe problems could occur in actual unconventional reservoirs.

4.2.4. Effect of Temperature on Asphaltene Deposition. Since the MMP of N_2 decreases as the temperature increases, the investigation of higher temperatures is achievable because miscibility will always occur with higher pressures when the temperature is high. Experiments were conducted at two temperatures (i.e., 70ºC and 90ºC) to investigate the effect of a higher temperature on the asphaltene stability and to compare that with the experiment discussed earlier at 32ºC. The 32ºC represents room temperature, and 70ºC represents the average temperature of shale basins. To ensure the stability of the required temperature, a specially designed vessel was placed inside the oven in both experiments. Both experiments used a pressure of 1750 psi for N_2 injection, a heterogeneous filter membrane distribution, and a 2-h mixing time. Increasing the temperature increased the asphaltene weight percent, as shown in Figure 17.

The results demonstrated that the highest asphaltene weight percent occurred on the 50-nm filter membranes due to their smaller-sized pores. The asphaltene weight percent decreased in the 50-nm filter from 14.28% to 11.59% for 70ºC and 90ºC, respectively, compared to 17.33% for 32ºC. In stable oils, the suspension colloidal particles of asphaltene were covered by resins that bind strongly with asphaltene. This connection between asphaltene and resins becomes stronger at higher temperatures, which keeps the asphaltene dissolved in oil (Hoepfner et al., 2013). At higher temperatures, a smaller amount of asphaltene colloidal will be produced, but it will tend not to form strong associations because the colloids are dispersed effectively by resins (Branco et al., 2001). The precipitated asphaltenes that form from the colloidal suspension particles at higher temperatures tend to dissolve in the oil; thus, more asphaltenes will be produced in a soluble condition but fewer in colloidal conditions (Chandio et al., 2015).

The resins have a tendency to self-associate, and that tendency is much stronger at lower temperatures. Therefore, the bond between the asphaltenes and resins becomes weaker (Pereira et al., 2007). Consequently, a higher amount of asphaltene precipitation can form because the molecules of asphaltene become stronger in terms of polarity, resulting in more aggregation at lower temperatures.

Note that the membrane pore size had the same effect at both temperatures: as the filter paper membrane pore size decreased, the asphaltene weight percent increased. This is due to the asphaltene particle size plugging the pores much more in the 50-nm filter membrane, such that more asphaltene was observed.

In all experiments, the asphaltene weight percent in the produced oil was the lowest as the asphaltene particles precipitated and plugged the nano-paper membranes gradually, which then reduced the amount of asphaltene in the oil outlet.

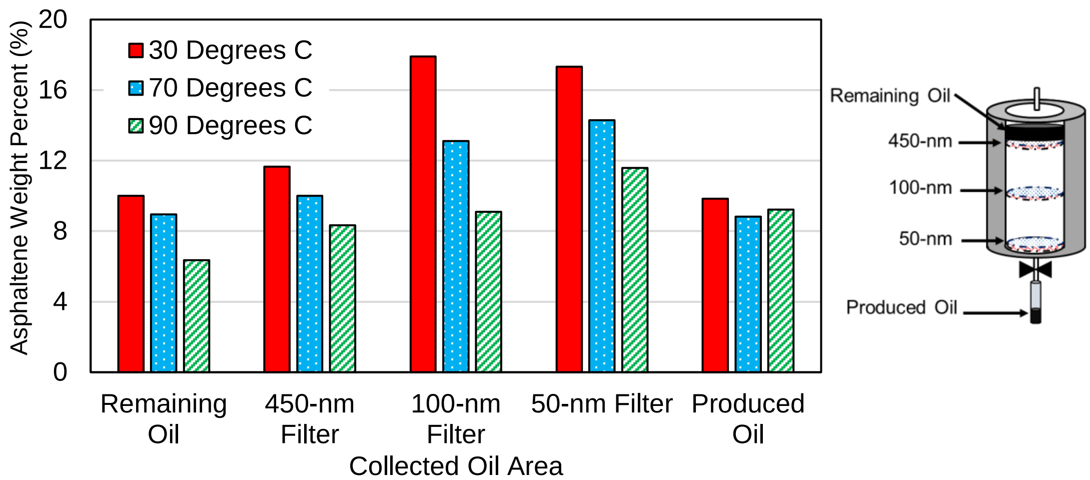

Figure 17. Asphaltene weight percent using a heterogeneous distribution during a N_2 injection at 1750 psi at different temperatures.

5. FURTHER ANALYSIS AND DISCUSSION

5.1. CHROMATOGRAPHY ANALYSIS

The produced oil was collected from the gas injection filtration experiments. Then, gas chromatography-mass spectrometry (GC6890-MS5973) was used to identify the main chemical components and their presence, including asphaltenes. First, the original oil with 19 cp viscosity that was used in all experiments was analyzed and its components were compared to the oil analysis after the experiments. Two pressures (i.e., 1750 and 2250 psi) were selected to investigate the chemical changes in the oil after the experiments, especially the heavy components of asphaltene. Figure 18 shows the distribution of oil components before and after N_2 gas injection filtration experiments at 1750 and 2250 psi. The results revealed that the asphaltene components decreased from 5.17% to 3.14% using 1750 psi N_2 gas injection. This indicates that the filer paper membranes inside the filtration vessel reduced the ability of the asphaltene clusters to pass through, thus the pores were plugged. This resulted in a decrease in the heavy components in the produced oil. Increasing the pressure to 2250 psi resulted in more asphaltene components, with the analysis showing an increase from 3.14% to 3.91% when using 1750 and 2250 psi, respectively. This was because higher pressure will force more asphaltene clusters to pass through, thereby causing there to be a higher percentage of asphaltene in the produced oil. Table 3 presents the chromatography analysis of the original oil and the produced oil during 1750 and 2250 psi.

Table 3. Gas chromatography analysis before and after N_2 gas injection filtration experiments at 1750 and 2250 psi

Component Group	**Weight percentage (%)**		
	Before Experiment [Original oil]	**After Experiment [1750 psi]**	**After Experiment [2250 psi]**
C_1 -C_7	0.00	0.00	0.00
C_8 -C_{14}	65.14	37.58	59.44
C_{15}-C_{19}	6.06	11.08	11.76
C_{20}-C_{24}	9.16	21.83	7.68
C_{25}-C_{29}	14.48	26.37	17.21
C_{30+} (Including asphaltene)	5.17	3.14	3.91
Total	100.00	100.00	100.00

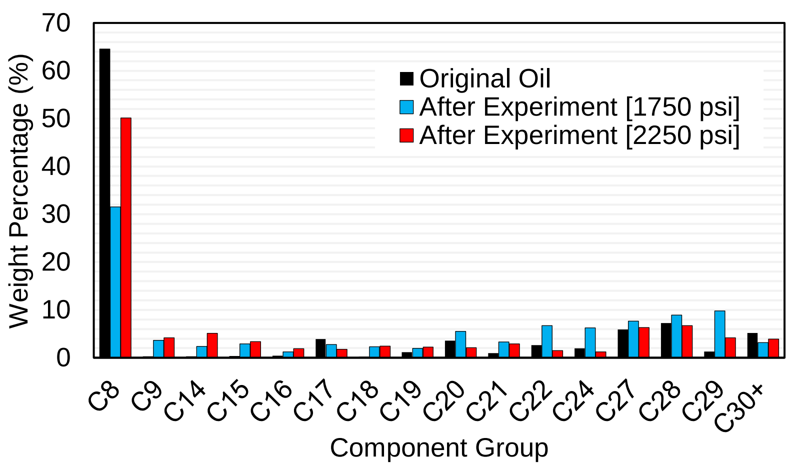

Figure 18. Distribution of oil components before and after N_2 gas injection filtration experiments at 1750 and 2250 psi.

5.2. MICROSCOPY IMAGING ANALYSIS

Asphaltene particles are induced by gas injection, and large asphaltene clusters can be formed, leading to asphaltene holdup in a reservoir. Asphaltene can plug the pores and cause severe problems, including a reduction in oil relative permeability, altering the wettability of the rock, and an overall reduction in oil production. The 450- and 50-nm filter paper membranes with a 2000 psi gas injection were cleaned by the solvent n-heptane to highlight the pore plugging in the filter paper. Figure 19 shows the filter membrane before conducting the experiments, after conducting the filtration experiments, and after cleaning the crude oil from the filter membranes. The photo shows the asphaltene deposited in the filter membrane pores and the plugged path for the crude oil to move, especially in the 50-nm filter membrane, which had the smallest pore size.

A HIROX digital microscope was used to identify the plugged pores in the filter membranes. Showing the filter membranes' microstructure can highlight the severity of the asphaltene aggregation on different pore size structures. Figure 20 shows the microscopic images (20 µm) of the filter membranes' pore structure of the 450-, 100-, and 50-nm filters using a miscible N_2 injection pressure of 1750, 2000, and 2250 psi at 32ºC. The images were captured after cleaning and also after exposure to the filter membranes in an n-heptane solvent for 24 h. Noticeable differences occurred in the aggregation of the precipitated asphaltene molecules in the filter membrane images. Higher pressure combined with filter membranes having smaller pore sizes resulted in more asphaltene deposition and pore plugging, as indicated by the darker color in the images. The 50-nm filter paper membrane exhibited darker colors compared to the 450- and 100-nm filters due to the small size of the pores, which led to greater asphaltene deposition.

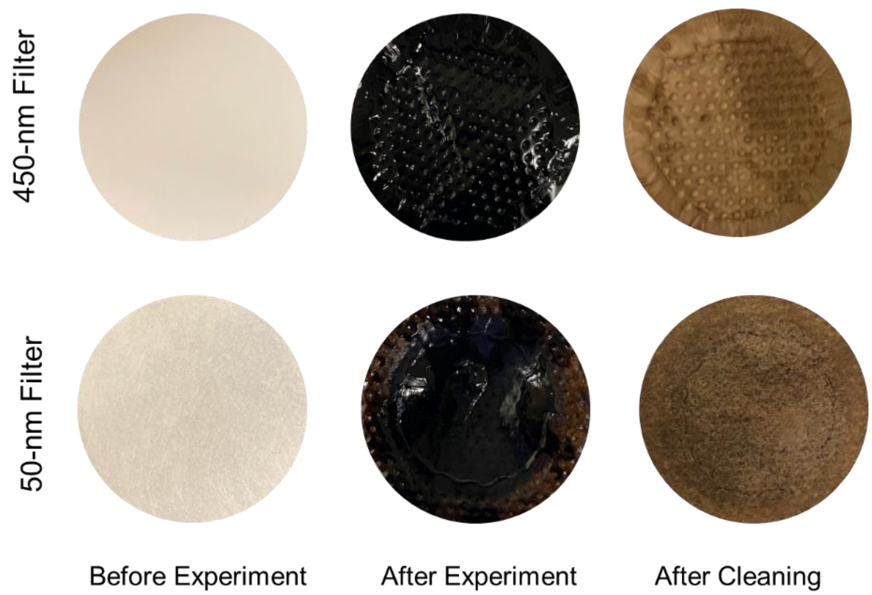

Figure 19. Illustration of the filter membrane (450- and 50-nm) at 2000 psi before and after the experiment, and after cleaning.

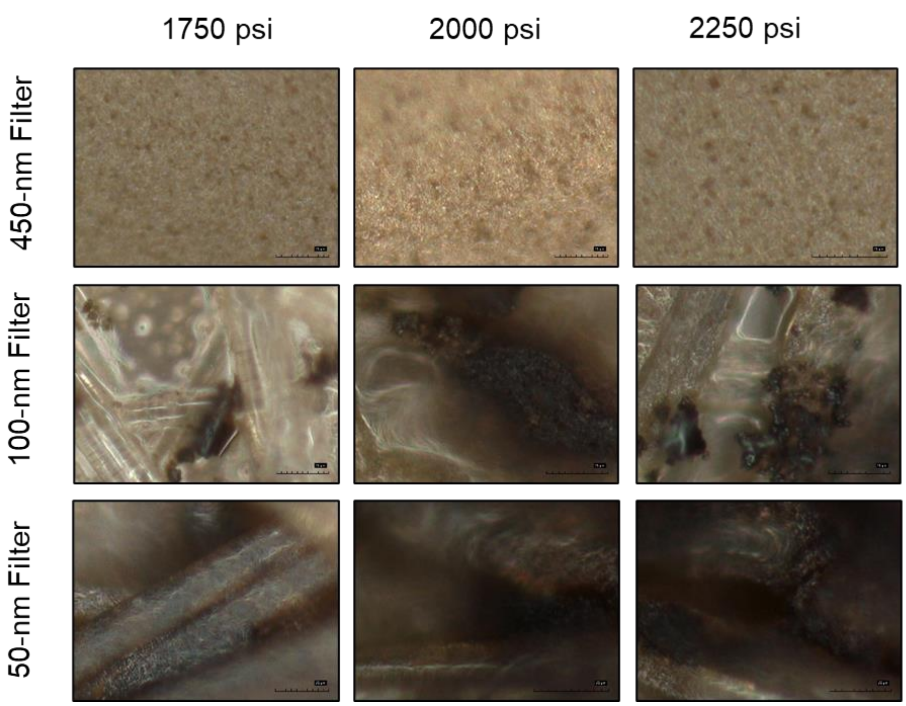

Figure 20. Digital microscopic images (20 µm) of 450-, 100-, and 50-nm filter membranes using various miscible N_2 injection pressures.

5.3. SEM ANALYSIS

Scanning electron microscopy (SEM) provides advanced imaging analysis that can determine the pore structure, particularly in unconventional shale formations, which are known for their small pore sizes. SEM was utilized to highlight the impact of pressure and asphaltene particles on pore plugging. To illustrate this, a collection of SEM images was taken for all heterogenous filter membranes (450, 100, and 50 nm) during 1750 and 2250 psi N_2 injection. Figure 21 shows SEM images (5 μm) of the filter membrane's pore structure for 450-, 100-, and 50-nm filters using N_2 injection pressures of 1750 and 2250 psi at 32ºC. For 450-nm filter paper, the images show asphaltenes accumulated inside the structure, which is colored black, during 1750 and 2250 psi injection pressure. The filter paper pore plugging was the most severe in the 50-nm filter membrane using 2250 psi. Because of 450-nm filter has larger pore size, the imaging clearly captured the structure of the 450-nm filter membranes, but not those of the smaller filters. As the pore size of the filter membrane decreased, dark colors were observed for the 100-nm filter membrane. Most of the area of 100-nm filter papers was affected by asphaltene depositions, with the darker color observed at 1750 psi injection pressure. This confirms that the asphaltenes had a greater impact on the smaller pore structure compared to the 450-nm filter. For the 50-nm filter membranes, most of the photo areas were impacted by asphaltenes due to the smaller pores.

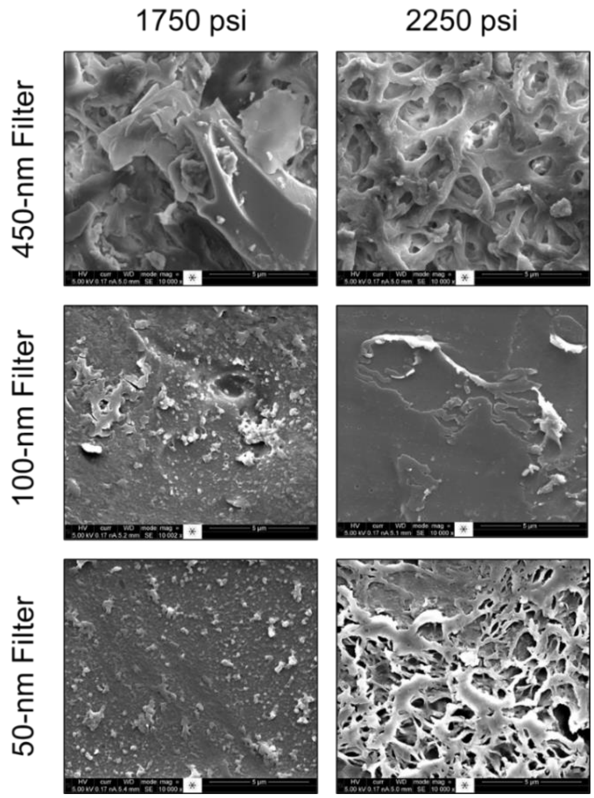

Figure 21. Scanning electron microscope (SEM) images (5 µm) of 450-, 100-, and 50-nm filter membranes at 1750 and 2250 psi injection pressures.

5.4. PORE SIZE REDUCTION DUE TO ASPHALTENE DEPOSITION

To identify the effect of asphaltene on the pore plugging of the filter paper membranes, the SEM images were processed using computer software to analyze the pore size of each filter membrane. Figure 22 compares the pore size distribution in a 450-nm filter membrane after N_2 injections of 1750 and 2250 psi. The estimated pore size distribution in a 450-nm filter paper ranged from 40 nm to 250 nm using 1750 psi, and 50 nm to 180 nm using 2250 psi. The results showed that the higher pressure (2250 psi) had a greater impact on pore plugging compared to the lower pressure (1750 psi). This occurred because the higher pressure had a greater effect on the asphaltene particles and resulted in more asphaltene precipitation and deposition, thus reducing the pore sizes. The oil path in the filter membranes became smaller due to asphaltene deposition and resulted in reductions in the pore sizes in the filter membrane. The same observations were also found in the 100-nm and 50-nm filter membranes. For the 100-nm filter membrane, the pore size distribution ranged between 10 nm and 40 nm for the lower pressure (1750 psi) and 15 nm to 35 nm for the higher pressure (2250 psi), as shown in Figure 23. Smaller pore size distributions were observed in the 50-nm filter membrane due to the smaller size of the pores. The results of the pore size distribution in the 50-nm filter membrane are shown in Figure 24. The asphaltene particles accumulated at higher percentages in the smaller pores of the filter membranes and then plugged most of the pores. Smaller pore size leads to more asphaltene concentration which lead to more pore plugging. Su et al (2021) developed an integrated simulation approach to predict permeability reduction under asphaltene particle aggregation and deposition. They concluded that longer aggregation time, higher flow velocity, and bigger precipitation concentrations will lead to a faster reduction in permeability. These results revealed that asphaltenes in crude oil can be induced by N_2 injection and can cause severe pore plugging, especially in reservoirs that have the small pores that are present in unconventional reservoirs.

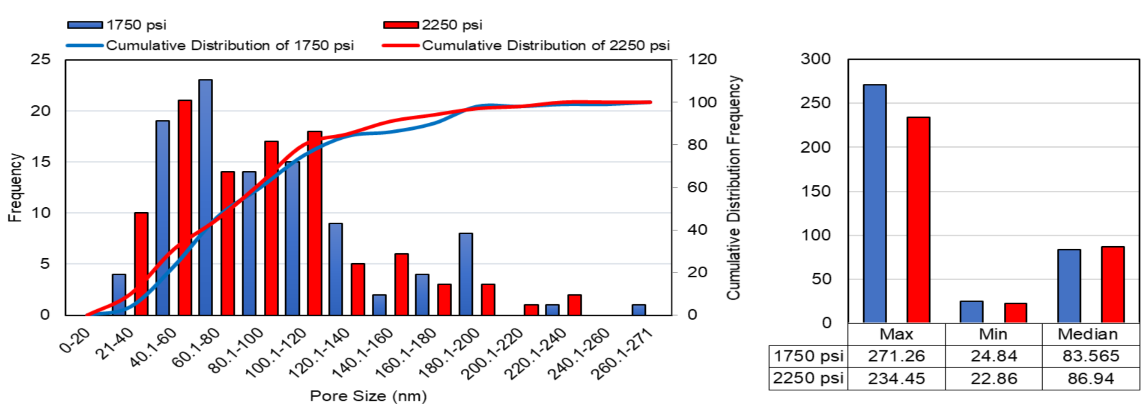

	Max	Min	Median
1750 psi	271.26	24.84	83.565
2250 psi	234.45	22.86	86.94

Figure 22. Comparison of the estimated pore size distribution in a 450-nm filter membrane after N_2 injections of 1750 and 2250 psi.

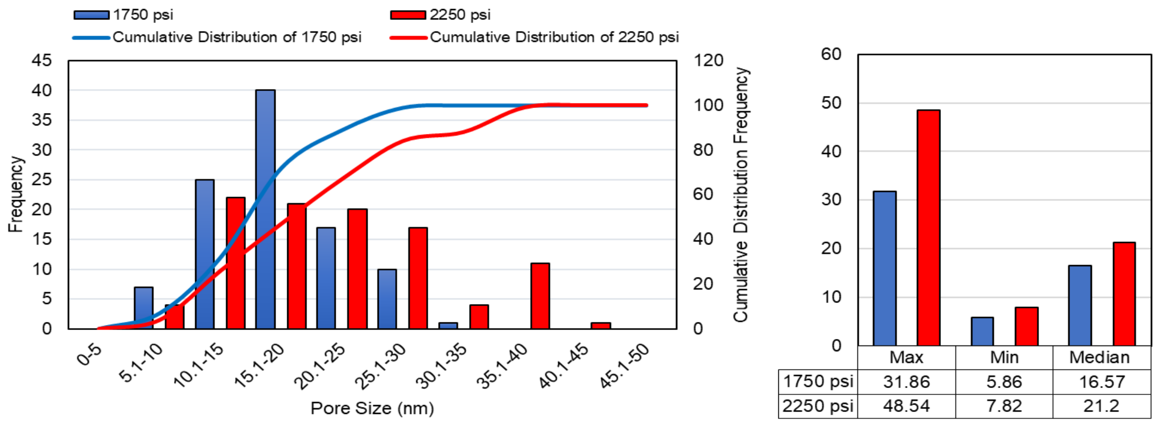

Figure 23. Comparison of the estimated pore size distribution in a 100-nm filter membrane after N_2 injections. of 1750 and 2250 psi.

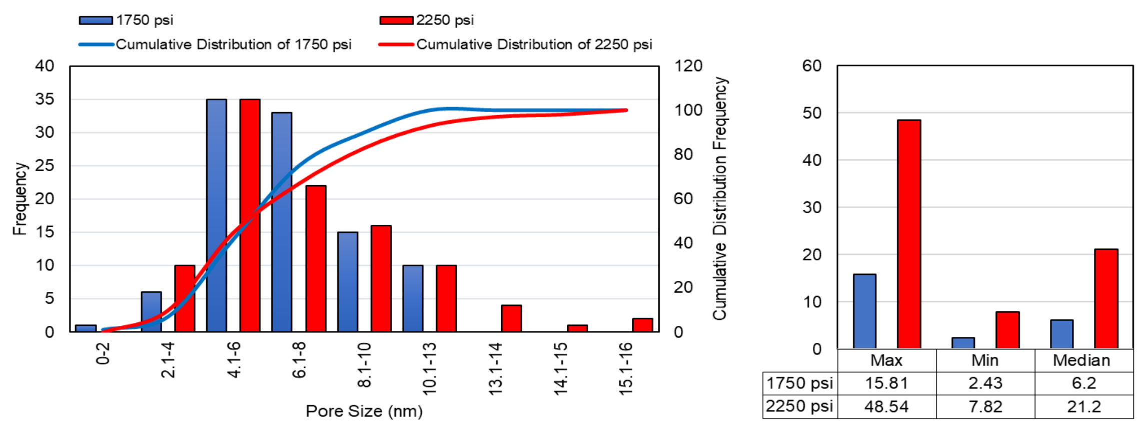

Figure 24. Comparison of the estimated pore size distribution in a 50-nm filter membrane after N_2 injections of 1750 and 2250 psi.

5.5. MISCIBLE VS. IMMISCIBLE DISCUSSION

Asphaltene deposition and precipitation during N_2 gas injection is a major problem in EOR projects. Investigating of asphaltene instability in crude oil during miscible and immiscible N_2 gas injection is very important to avoid any future problems such as pore plugging and permeability reduction. In this research, the miscible N_2 gas injection impacted the stability of the asphaltene clusters in the crude oil. To provide a whole picture of the impact of miscible and immiscible N_2 gas injection on asphaltene clusters, the essential results of immiscible N_2 condition from the previous work will be discussed (Elturki and Imqam, 2021b). Figure 25 shows a comparison of asphaltene wight percent in immiscible (i.e., 1000, 1250, and 1500 psi) and miscible (1750, 2000, and 2250 psi) N_2 injection in 450, 100, and 50-nm filter paper membranes. Table 4 presents the estimated asphaltene weight percentages from different collected areas during immiscible and miscible conditions. The results demonstrated that the asphaltene clusters in the crude oil were induced due to N_2 gas injection in all experiments. When the pressure is lower than the N_2 MMP, a lower average of asphaltene wight percent was observed comparted to miscible conditions. Once the pressure exceeds the MMP, the asphaltene weight percent increased significantly in all filter membranes, especially in smaller pore size structure (i.e., 50-nm). More oil produced during higher pressures and thus a higher asphaltene weight percent was determined. Smaller pore size structure led to higher asphaltene percentages. These observations confirm that during miscible gas injection of N_2, higher oil recovery is expected with more asphaltene issues during production processes. The N_2 evaporation during pressures less than MMP improves the crude oil capability to overcome the asphaltene clusters' breaks down. During miscible conditions, the connection between asphaltenes and resins in the crude oil becomes much weaker and leads to higher rate of asphaltene deposition and fluctuations. As a result, asphaltene aggregation and fluctuation during immiscible N_2 injection would not be challenging in EOR process as miscible N_2 injection.

Table 4. Estimated asphaltene weight percentages from different collected areas during immiscible and miscible conditions.

Collected Oil Area	Immiscible pressure (psi)			Miscible pressure (psi)		
	1000	**1250**	**1500**	**1750**	**2000**	**2250**
	Asphaltene weight (%)			**Asphaltene weight (%)**		
Remaining Oil	2.30 %	3.04 %	3.96 %	10.00 %	10.42 %	13.33 %
450-nm Filter	2.52 %	3.61 %	3.81 %	11.67 %	13.56 %	16.18 %
100-nm Filter	5.36 %	6.30 %	8.40 %	17.91 %	19.18 %	20.59 %
50-nm Filter	8.14 %	9.83 %	11.11 %	17.33 %	21.43 %	20.90 %
Produced Oil	5.46 %	7.39 %	5.95 %	8.20 %	8.82 %	11.36 %

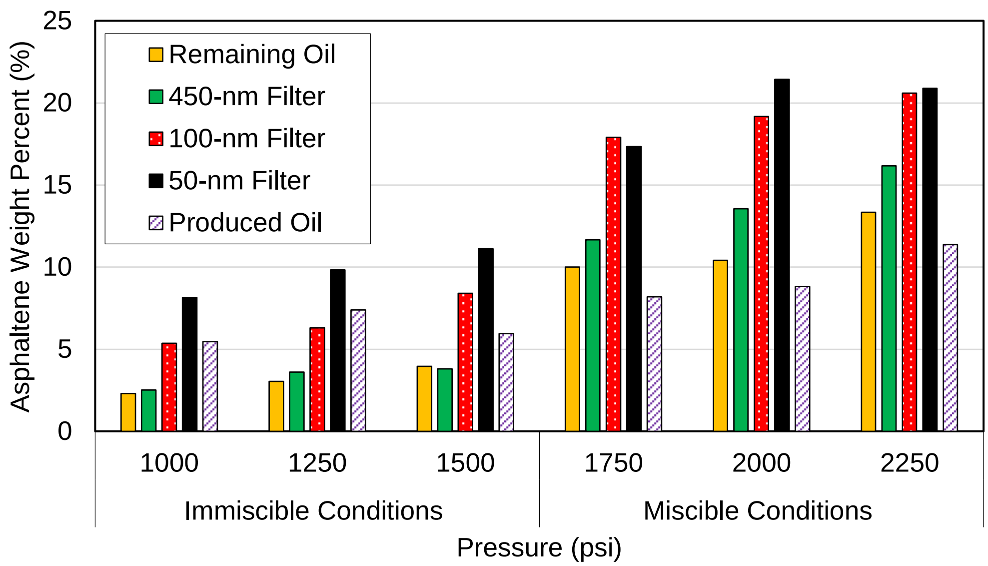

Figure 25. Comparison of asphaltene weight percentages during miscible and immiscible N_2 injection

6. CONCLUSIONS

This research implemented three sets of experiments to investigate asphaltene stability under miscible N_2 injection pressure. First, the MMP of N_2 was determined using a slim tube. Then, filtration and visualization asphaltene experiments were conducted. The following factors were investigated: injection pressure, temperature, mixing time, filter membrane heterogeneity, and different pore sizes. Based on the results, we suggest the following conclusions:

- The asphaltene weight percent increased as the N_2 injection pressure increased in all the filtration experiments because the higher pressure weakened the bonds between the resins and asphaltenes, which led to asphaltene deposition.
- At higher temperatures, the precipitated asphaltenes that formed from the colloidal suspension particles tended to dissolve in the oil; thus, more asphaltenes will form in a soluble condition but fewer will form under colloidal conditions.
- When using a heterogeneous distribution of filter sizes (i.e., 450, 100, and 50 nm) and as the pore size decreased, the asphaltene weight percent increased because the asphaltene clusters were unable to pass easily through the smaller pores of the filter membranes.
- Using a uniform pore size distribution inside the vessel (100 nm) resulted in almost the same asphaltene weight percent as the heterogeneous distribution because of the size of the asphaltene particles that passed through all of the same pore size filter membranes. Additionally, increasing the mixing time produced a higher asphaltene weight percent.
- The chromatography results demonstrated that the weight percent of the heavy components, including asphaltene, was higher when using 1750 psi than 2250 psi.
- The microscopy imaging illustrated the severity of the asphaltene deposition on pore plugging. The results showed an increase in pore plugging when the pressure increased coupled with a decrease in the pore size.

- SEM showed how the asphaltene particles affected the pore plugging: at a higher pressure and with a smaller pore size, the asphaltene particles caused more severe pore plugging.
- Pore size distribution analysis showed that the pore size decreased significantly in all the filter paper membranes due to asphaltene plugging.

REFERENCES

Afra, S., Samouei, H., Golshahi, N., & Nasr-El-Din, H. (2020). Alterations of asphaltenes chemical structure due to carbon dioxide injection. Fuel, 272, 117708. https://doi.org/10.1016/j.fuel.2020.117708

Al-Hosani, A., Ravichandran, S., & Daraboina, N. (2020). Review of Asphaltene Deposition Modeling in Oil and Gas Production. Energy & Fuels.

Altawati, F., Sheng, J., & Emadi, H. (2020, June). Investigating Effects of Water on Shale Oil Formation by Using Cyclic Gas Injection Technique-An Experimental Study. In 54th US Rock Mechanics/Geomechanics Symposium.

Ali, S. I., Lalji, S. M., Haneef, J., Ahsan, U., Tariq, S. M., Tirmizi, S. T., & Shamim, R. (2021). Critical analysis of different techniques used to screen asphaltene stability in crude oils. Fuel, 299, 120874. https://doi.org/10.1016/j.fuel.2021.120874

Alimohammadi, S., Sayyad Amin, J. & Nikooee, E. Estimation of asphaltene precipitation in light, medium and heavy oils: experimental study and neural network modeling. Neural Comput & Applic 28, 679–694 (2017). https://doi.org/10.1007/s00521-015-2097-3

Alves, C. A., Romero Yanes, J. F., Feitosa, F. X., & de Sant’Ana, H. B. (2019). Effect of Temperature on Asphaltenes Precipitation: Direct and Indirect Analyses and Phase Equilibrium Study. Energy & Fuels, 33(8), 6921-6928. https://doi.org/10.1021/acs.energyfuels.9b00408

Belhaj, H., Abu Khalifeh, H. A., & Javid, K. (2013, April 15). Potential of Nitrogen Gas Miscible Injection in South East Assets, Abu Dhabi. Society of Petroleum Engineers. https://doi.org/10.2118/164774-MS

Bahman, J., Nasiri, M., Sabeti, M., & Mohammadi, A. H. (2017). An Introduction to Asphaltenes Chemistry. Heavy Oil: Characteristics, Production and Emerging Technologies. Chapter 5. USA: Nova Science Publishers, 93. ISBN: 978-1-53610-852-1

Branco, V. A. M., Mansoori, G. A., Xavier, L. C. D. A., Park, S. J., & Manafi, H. (2001). Asphaltene flocculation and collapse from petroleum fluids. Journal of Petroleum Science and Engineering, 32(2-4), 217-230. https://doi.org/10.1016/S0920-4105(01)00163-2

Chung, T. H. (1992, January). Thermodynamic modeling for organic solid precipitation. In SPE Annual Technical Conference and Exhibition. Society of Petroleum Engineers. https://doi.org/10.2118/24851-MS

Chandio, Z. A., Ramasamy, M., & Mukhtar, H. B. (2015). Temperature effects on solubility of asphaltenes in crude oils. Chemical Engineering Research and Design, 94, 573-583. https://doi.org/10.1016/j.cherd.2014.09.018

Elturki, M., and Imqam, A. (2020a, September). Application of Enhanced Oil Recovery Methods in Unconventional Reservoirs: A Review and Data Analysis. In 54th US Rock Mechanics/Geomechanics Symposium. American Rock Mechanics Association.

Elturki, M., and Imqam, A. (2020b, December). High Pressure-High Temperature Nitrogen Interaction with Crude Oil and Its Impact on Asphaltene Deposition in Nano Shale Pore Structure: An Experimental Study. In Unconventional Resources Technology Conference, 20–22 July 2020 (pp. 2830-2845). https://doi.org/10.15530/urtec-2020-3241

Elturki, M., McElroy, P. D., Li, D., Kablan, A., and Shaglouf, H. (2021, June). Simulation Study Investigating the Impact of Carbon Dioxide Foam Fracturing Fluids on Proppant Transport. In SPE Trinidad and Tobago Section Energy Resources Conference. https://doi.org/10.2118/200950-MS

Elturki, M. and Imqam, M. (2021a). Analysis of Nitrogen Minimum Miscibility Pressure (MMP) and Its Impact on Instability of Asphaltene Aggregates: An Experimental Study. Paper presented at the SPE Trinidad and Tobago Section Energy Resources Conference Virtual, 28–30 June. SPE-200900-MS. https://doi.org/10.2118/200900-MS.

Elturki, M., and Imqam, A. (2021b). Asphaltene Thermodynamic Flocculation during Immiscible Nitrogen Gas Injection. SPE Journal, 1-17. https://doi.org/10.2118/206709-PA

Elwegaa, K., and Emadi, H. (2019). Improving oil recovery from shale oil reservoirs using cyclic cold nitrogen injection–An experimental study. Fuel, 254, 115716. https://doi.org/10.1016/j.fuel.2019.115716

Goual, L. (2012) Petroleum asphaltenes, crude oil emulsions-composition stability and characterization; Abdul-Raouf, M., El-Sayed, Eds.; InTech. https://doi.org/10.5772/35875

Hassanpouryouzband, A., Joonaki, E., Taghikhani, V., Bozorgmehry Boozarjomehry, R., Chapoy, A., & Tohidi, B. (2017). New two-dimensional particle-scale model to simulate asphaltene deposition in wellbores and pipelines. Energy & Fuels, 32(3), 2661-2672. https://doi.org/10.1021/acs.energyfuels.7b02714

Hassanpouryouzband, A., Yang, J., Tohidi, B., Chuvilin, E., Istomin, V., Bukhanov, B., & Cheremisin, A. (2018). CO_2 capture by injection of flue gas or CO_2–N_2 mixtures into hydrate reservoirs: Dependence of CO_2 capture efficiency on gas hydrate reservoir conditions. Environmental science & technology, 52(7), 4324-4330. https://doi.org/10.1021/acs.est.7b05784

Hassanpouryouzband, A., Yang, J., Tohidi, B., Chuvilin, E., Istomin, V., & Bukhanov, B. (2019). Geological CO_2 capture and storage with flue gas hydrate formation in frozen and unfrozen sediments: method development, real time-scale kinetic characteristics, efficiency, and clathrate structural transition. ACS Sustainable Chemistry & Engineering, 7(5), 5338-5345. https://doi.org/10.1021/acssuschemeng.8b06374

Hassanpouryouzband, A. et al (2020). Gas hydrates in sustainable chemistry. Chemical Society Reviews, 49(15), 5225-5309. https://doi.org/10.1039/C8CS00989A

Hoepfner, M. P., Limsakoune, V., Chuenmeechao, V., Maqbool, T., & Fogler, H. S. (2013). A fundamental study of asphaltene deposition. Energy & fuels, 27(2), 725-735. https://doi.org/10.1021/ef3017392

Jamaluddin, A. K. M., Joshi, N., Iwere, F., & Gurpinar, O. (2002, January 1). An Investigation of Asphaltene Instability Under Nitrogen Injection. Society of Petroleum Engineers. https://doi.org/10.2118/74393-MS

Kar, T., Naderi, K., & Firoozabadi, A. (2020). Asphaltene Deposition and Removal in Flowlines and Mitigation by Effective Functional Molecules. SPE Journal. https://doi.org/10.2118/199878-PA

Mahdaviara, M., Amar, M. N., Hemmati-Sarapardeh, A., Dai, Z., Zhang, C., Xiao, T., & Zhang, X. (2021). Toward smart schemes for modeling CO_2 solubility in crude oil: Application to carbon dioxide enhanced oil recovery. Fuel, 285, 119147. https://doi.org/10.1016/j.fuel.2020.119147

Moradi, S., Dabir, B., Rashtchian, D., & Mahmoudi, B. (2012a). Effect of miscible nitrogen injection on instability, particle size distribution, and fractal structure of asphaltene aggregates. Journal of dispersion science and technology, 33(5), 763-770. https://doi.org/10.1080/01932691.2011.567878

Mozaffari, S., Tchoukov, P., Atias, J., Czarnecki, J., & Nazemifard, N. (2015). Effect of asphaltene aggregation on rheological properties of diluted athabasca bitumen. Energy & Fuels, 29(9), 5595-5599. https://doi.org/10.1021/acs.energyfuels.5b00918

Moradi, S., Dabiri, M., Dabir, B., Rashtchian, D., & Emadi, M. A. (2012b). Investigation of asphaltene precipitation in miscible gas injection processes: experimental study and modeling. Brazilian Journal of Chemical Engineering, 29(3), 665-676. https://doi.org/10.1590/S0104-66322012000300022

Nguyen, T. A., & Ali, S. M. (1998). Effect of nitrogen on the solubility and diffusivity of carbon dioxide into oil and oil recovery by the immiscible WAG process. Journal of Canadian Petroleum Technology, 37(02). https://doi.org/10.2118/98-02-02

Pereira, J. C., López, I., Salas, R., Silva, F., Fernández, C., Urbina, C., & López, J. C. (2007). Resins: The molecules responsible for the stability/instability phenomena of asphaltenes. Energy & fuels, 21(3), 1317-1321. https://doi.org/10.1021/ef0603333

Rostami, A., Arabloo, M., Kamari, A., & Mohammadi, A. H. (2017). Modeling of CO_2 solubility in crude oil during carbon dioxide enhanced oil recovery using gene expression programming. Fuel, 210, 768-782. https://doi.org/10.1016/j.fuel.2017.08.110

Rashid, Z., Wilfred, C. D., Gnanasundaram, N., Arunagiri, A., & Murugesan, T. (2019). A comprehensive review on the recent advances on the petroleum asphaltene aggregation. Journal of Petroleum Science and Engineering, 176, 249-268. https://doi.org/10.1016/j.petrol.2019.01.004

Sebastian, H. M., & Lawrence, D. D. (1992, January 1). Nitrogen Minimum Miscibility Pressures. Society of Petroleum Engineers. https://doi.org/10.2118/24134-MS

Shen, Z., & Sheng, J. J. (2017). Experimental study of permeability reduction and pore size distribution change due to asphaltene deposition during CO_2 huff and puff injection in Eagle Ford shale. Asia-Pacific Journal of Chemical Engineering, 12(3), 381-390. https://doi.org/10.1002/apj.2080

Shen and Sheng, 2018, Experimental and numerical study of permeability reduction caused by asphaltene precipitation and deposition during CO_2 huff and puff injection in Eagle Ford shale, Fuel, 211, 432-445, https://doi.org/10.1016/j.fuel.2017.09.047.

Shi, B. et al (2021). Status of Natural Gas Hydrate Flow Assurance Research in China: A Review. Energy & Fuels, 35(5), 3611-3658. https://doi.org/10.1021/acs.energyfuels.0c04209

Soroush, S., Pourafshary, P., & Vafaie-Sefti, M. (2014, March 31). A Comparison of Asphaltene Deposition in Miscible and Immiscible Carbon Dioxide Flooding in Porous Media. Society of Petroleum Engineers. https://doi.org/10.2118/169657-MS

Srivastava, R. K., & Huang, S. S. (1997, January). Asphaltene deposition during CO_2 flooding: a laboratory assessment. In SPE Production Operations Symposium. Society of Petroleum Engineers. https://doi.org/10.2118/37468-MS

Su, X., Moghanloo, R. G., Qi, M., & Yue, X. A. (2021). An Integrated Simulation Approach to Predict Permeability Impairment under Simultaneous Aggregation and Deposition of Asphaltene Particles. SPE Journal, 1-14. https://doi.org/10.2118/205028-PA

Vahidi, A., & Zargar, G. (2007, January 1). Sensitivity Analysis of Important Parameters Affecting Minimum Miscibility Pressure (MMP) of Nitrogen Injection into Conventional Oil Reservoirs. Society of Petroleum Engineers. https://doi.org/10.2118/111411-MS

Wang, P., Zhao, F., Hou, J., Lu, G., Zhang, M., & Wang, Z. (2018). Comparative analysis of CO_2, N_2, and gas mixture injection on asphaltene deposition pressure in reservoir conditions. Energies, 11(9), 2483. https://doi.org/10.3390/en11092483

IV. ASPHALTENE PRECIPITATION AND DEPOSITION UNDER MISCIBLE AND IMMISCIBLE CARBON DIOXIDE GAS INJECTION IN NANO SHALE PORE STRUCTURE

Mukhtar Elturki and Abdulmohsin Imqam

Missouri University of Science and Technology

ABSTRACT

Asphaltene precipitation and deposition is considered one of the prevailing issues during carbon dioxide (CO_2) gas injection in gas enhanced oil recovery techniques, which leads to pore plugging, oil recovery reduction, and damage surface and subsurface equipment. This research provides a comprehensive investigation of the effect of immiscible and miscible CO_2 gas injection in nanopore shale structures on asphaltene instability in crude oil. A slim tube was used to determine the minimum miscibility pressure (MMP) of the CO_2. This step is important to ensure that the immiscible and miscible conditions will be achieved during the filtration experiments. For the filtration experiments, nanocomposite filter paper membranes were used to mimic the unconventional shale pore structure, and a specially designed filtration apparatus was used to accommodate the filter paper membranes. The uniform distribution (i.e., same pore size filters) was used to illustrate the influence of the ideal shale reservoir structure and to provide an idea on how asphaltene will deposit when utilizing the heterogeneous distribution (i.e., various pore size filters) that depicts the real shale structure. The factors investigated include immiscible and miscible CO_2 injection pressures, temperature, CO_2 soaking time, and pore size structure heterogeneity. Visualization tests were undertaken after the filtration experiments to

provide a clear picture of the asphaltene precipitation and deposition process over time. The results showed an increase in asphaltene weight percent in all experiments of the filtration tests. The severity of asphaltene aggregations were observed at a higher rate under miscible CO_2 injection. It was observed that the miscible conditions have a higher impact on asphaltene instability compared to immiscible conditions. The results revealed that the asphaltene deposition was almost equal across all the paper membranes for each pressure used when using a uniform distribution. Higher asphaltene weight percentages were determined on smaller pore structures of the membranes when using heterogeneous distribution. Soaking time results revealed that increasing the soaking time resulted in an increase in asphaltene wight precent especially for 60- and 120-min. Visualization tests showed that after 1 h, the asphaltene clusters started to precipitate and can be seen in the uppermost section of the test tubes and were fully deposited after 12 h with less clusters found in the supernatant. Also, smaller pore size of filter membranes showed higher asphaltene weight percent after the visualization test. Chromatography analysis provided further evaluation on how asphaltene was reduced though the filtration experiments. Microscopy and scanning electron microscopy (SEM) imaging of the filter paper membranes showed the severity of pore plugging in the structure of the membranes.

This research highlights the impact of CO_2 injection on asphaltene instability in crude oil in nanopore structures under immiscible and miscible conditions. The findings in this research can be used for further research of asphaltene deposition under gas injection and scale the results up for better understanding the main factors that may influence asphaltene aggregation in real shale unconventional reservoirs.

1. INTRODUCTION

Gas injection has become a promising technique to enhance the oil recovery from unconventional resources, and the results revealed a positive impact on increasing the oil recovery (Elwegaa et al. 2019; Altawati et al. 2016; Zheng et al. 2021; Elturki et al. 2021). Even though hydraulic fracturing in horizontal wells was utilized to extract the remaining oil from unconventional reservoirs, only a very small percentage can be recovered and the production declines after few months due to the ultra-small permeability (Sheng 2015; Zoback and Kohli 2019; Liu et al. 2021). During multiphase flow production, many problems with multiphase fluids (i.e., gas, oil, condensate, and water) with scale are possible, which could lead to wax and asphaltene deposition, formation hydrates, emulsions, and slugging (Shi et al. 2021). Deposition of organic hydrocarbon solids in oil and gas reservoirs could cause many flow assurance problems during the oil and gas production process. These materials could increase the flow resistance and production disrupt or even plug the pipelines (Hassanpouryouzband et al. 2020; Ali et al. 2021). One of the major problems during gas injection in unconventional resources is asphaltene instability in crude oil. Normally, three main components in crude oil can be found in different percentages which are liquids, dissolved gases, and solids; however, the most common solid in crude oil is asphaltene (Elturki and Imqam 2020a). SARA (saturates, aromatics, resins, and asphaltene) analysis is used to characterize the crude oil elements. Asphaltene can be defined as "the heaviest component of petroleum fluids that is insoluble in light n-alkanes such as n-pentane or n-heptane, but soluble in aromatics such as toluene" (Goual 2012). Heavier n-alkanes precipitate less asphaltene than lighter n-alkanes

(Behbahani et al. 2011). Asphaltene can be found in colloidal suspensions stabilized by the presence of resins or in solution under reservoir pressure and temperature conditions (Punase et al. 2016; Ali et al. 2021). Changes in reservoir conditions, such as pressure or temperature, lead to asphaltene instability and thus asphaltene deposition and precipitation on solid surface during oil production process (Kar et al. 2020; Mohammed et al. 2021). This phenomenon would cause porosity and permeability reduction, wettability alteration in the reservoir, and subsurface and surface equipment blockages (Madhi et al. 2018; Alimohammadi et al. 2019) and is costly to treat (Melendez-Alvarez et al. 2016; Abutaqiya et al. 2019). CO_2 and N_2 may produce asphaltene flocculation in the reservoir to varying degrees. CO_2 has a high solubility in crude oil and may quickly reach supercritical levels in reservoirs (Wang et al. 2018). Thus, the mass transfer ability of supercritical CO_2 is strong. In the CO_2 injection process, the CO_2-crude oil system could easily reach a miscible or near-miscible state that enhances and extracts the light hydrocarbon components from crude oil into the gas phase. N_2 has weaker solubility in crude oil than CO_2 in the same thermodynamic conditions. Consequently, N_2 has a weak mass transfer capacity which could lead to the poor extraction of light hydrocarbons and probably less asphaltene flocculation compared to CO_2 (Chung 1992; Wang et al. 2018). Under gas injection, asphaltene aggregations can form clusters that may cause critical issues during oil production and thus impact the oil recovery negatively. Understanding the main factors that may affect the asphaltene instability in crude oil during gas injection is extremely important in order to determine how gas injection flow assurance problems can be avoided in future unconventional EOR applications.

CO_2 gas injection has been widely used to increase oil recovery from both conventional and unconventional resources (Luo et al. 2017; Elturki and Imqam 2020b; Milad et al. 2021). Asphaltene instability during CO_2 and N_2 injection have been studied by many researchers using experimental studies (Jamaluddin et al. 2002; Negahban et al. 2005; Alizadeh et al. 2011; Moradi et al. 2012; Jafari et al. 2012; Soroush et al. 2014; Shen and Sheng 2018; Zanganeh et al. ; 2012; 2018; Guzmán et al. 2020; Elturki and Imqam 2021a; 2021b; 2022a; 2022b; Afra et al. 2020; Nascimento et al. 2021; Espinoza et al. 2022), and numerical/modeling techniques (Tavakkoli et al. 2014; Alimohammadi et al. 2017; Hajizadeh et al. 2020; Syed et al. 2020; Su et al. 2021; Carvalhal et al. 2020). Negahban et al. (2005) evaluated the asphaltene instability in the reservoir fluids during CO_2 and hydrocarbon gas injection. Results showed an increase in asphaltene precipitation when more hydrocarbon gas was injected. Asphaltene instability was observed during CO_2 injection when increasing the temperature. Using a cubic-plus-association equation of state (CPA-EOS), Li and Firoozabadi (2010) investigated the effects of pressure, temperature, and composition on asphaltene precipitation in several live oils. They mainly studied the effect of pressure decrease and mixing with CO_2 at high temperature and pressure. The tests on the quantity and onset pressures of asphaltene precipitation in different living oils over a wide variety of composition, temperature, and pressure conditions were reproduced. They successfully reproduced the asphaltene precipitation envelop as the temperature is less than 400 K, the temperature shift has a significant effect on the upper onset pressure, according to their findings. The upper onset pressure decreases by 1300 bar as the temperature rises from 300 to 400 K. Once the temperature exceeds 400 K, the temperature's influence on the upper onset pressure becomes low. In comparison to the upper onset pressure, the bubble point pressure and lower onset pressure are very poorly temperature dependent. Espinoza et al. (2022) investigated the phase behavior of asphaltenes instability experimentally. They revealed that when CO_2 concentration increased, the lower asphaltene onset pressure (LAOP) increased in all situations. They also suggested that higher temperatures are advantageous conditions for minimizing asphaltene deposition for the CO_2 injection fraction of 25 to 35 % and temperature and CO_2 fraction are the main controlling factors. In the other hand, the main factor controlling the asphaltene deposition is the CO_2 injection proportion when the fraction ranged from 35 to 45%. To investigate the influence of temperature on asphaltene precipitation and aggregation in light-live oils, Mohammadi et al. (2016) conducted several high pressure-high temperature depressurization tests. They revealed that depressurization at higher temperatures resulted in higher asphaltene onset pressures or early asphaltene formation. Alves et al. (2019) investigated the influence of temperature on different Brazilian crude oils and observed that as temperature increased, asphaltene precipitation decreased but asphaltene onset increased. Moradi et al. (2012) conduced laboratory experiments to evaluate the asphaltene particle precipitation and aggregation under natural depletion and nitrogen (N_2) injection using high pressure filtration. The results highlighted that an extreme asphaltene destabilization was observed under N_2 injection. Also, the asphaltene fluctuation masses grew and became more organized when the aggregation of cluster increased. Jafari et al. (2012) proposed and conducted a set of experiments using bottom hole live oil sample during CO_2 flooding to study the effect of CO_2 injection on oil recovery and permeability reduction. The cyclohexane and toluene reverse flooding was conducted, and the asphaltene deposition amount was measured by spectrophotometer. Their findings demonstrate that increasing the CO_2 injection pressure led to a significant increase in pressure drop which resulted in more asphaltene deposition and permeability reduction. Soroush et al. 2014 investigated experimentally, using a core flooding method, the effect of miscible and immiscible CO_2 injection on asphaltene deposition in porous media. Their observations highlighted that the asphaltene content in the produced oil decreased when increasing the pressure. The results showed that the damage during immiscible injection was due to gas trapping in the pores while during the miscible conditions the asphaltene was responsible for the damage along the cores. Elturki and Imqam (2021a) conducted experiments using the filtration technique to highlight the effect of immiscible N_2 injection on asphaltene instability. They used various filter membrane papers (i.e., 450, 100, and 50 nm) to mimic the structure of unconventional reservoir structure. First, the slim tube technique was used to determine the N_2 MMP. Based on their results, increasing the pressure led to an increase in asphaltene weight percent, and decreasing the filter membrane pore size increased the asphaltene weight percent significantly. Pore size distribution of the filter paper membrane after the filtration experiments showed a decrease in the pore size due to asphaltene particles. Guzmán et al. (2020) evaluated the asphaltene stability of various Mexican crude oils (API 10 to 52) using spot test, S-value, and static stability test column. Their results showed no uniform results of the stability using different methodologies. Four crude oil samples were used by Afra et al. (2020) to study the effect of CO_2 injection on the structure and stability of asphaltene. Their results showed that, using infrared spectroscopy and acid/base identification, asphaltene stability was disturbed when the amine group of one of the tested asphaltene samples formed an amide functional group by reacting with CO_2. Their study suggested that asphaltene in oil matrix can be destabilized through both chemical reactions and physical interactions. Khalaf and Mansoori (2019) performed a simulation study to evaluate different asphaltenes in different concentrations under N_2 and air injection. The concentration of the injected gas affected the asphaltene aggregation process significantly. The results showed that the asphaltene architecture played an essential role in the process of asphaltene aggregation and significant differences between using N_2 and air on asphaltene aggregations during EOR. Carvalhal et al. (2021) modelled asphaltene precipitation and deposition by evaluating different factors and the results showed that the thermodynamic sources had more effect on the performance of the model compared to kinetics parameters which include asphaltene molar content, binary interaction parameters, reference pressure, asphaltene molar volume, surface deposition rate coefficient and flocculation parameters.

Although several researchers have studied the effect of CO_2 injection on asphaltene deposition and precipitation using multiple methods, few have evaluated both miscible and immiscible CO_2 gas injection and its effect on asphaltene stability in nano pore structures, mainly presents in unconventional reservoirs. This research aims to extend the previous work conducted by Elturki and Imqam (2021a; 2022a) which investigated the impact of immiscible and miscible N_2 injection on asphaltene deposition and precipitation. This research investigated the effect of immiscible and miscible CO_2 gas injection on asphaltene instability in crude oil using nano composite filter membranes. This research then quantifies the asphaltene content in all filter membranes under various factors and provides a holistic view on the impact of various factors. The studied factors include injection pressure, temperature, pore size heterogeneity, and soaking time. The process of asphaltene precipitation and deposition process was presented by visualization tests. Understating the behavior of asphaltene deposition under CO_2 gas injection is extremely important in unconventional EOR process to avoid any asphaltene problems in both surface and subsurface equipment during production operation.

2. EXPERIMENTAL SCOPE DESCRIPTION

The experiments were designed to be conducted in both miscible and immiscible CO_2 gas injection. **Figure** 1 shows the experiment flow chart design in this research which includes three main tests: (1) MMP determination, (2) filtration, and (3) asphaltene visualization. Further investigations were conducted such as chromatography analysis, microscopy imaging, and SEM analysis to highlight the effect of CO_2 gas injection on asphaltene instability in the crude oil, and to show the effect of asphaltene particles on pore plugging.

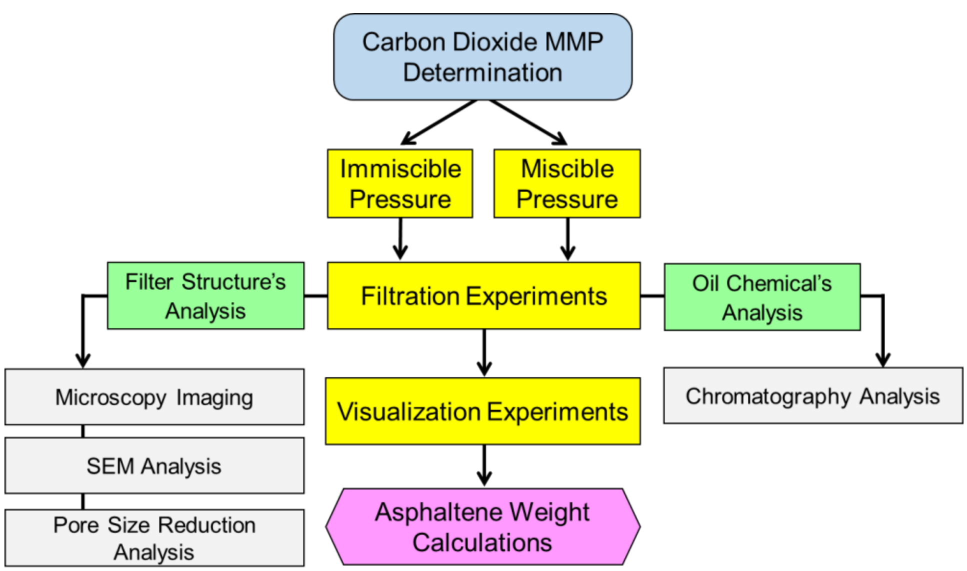

Figure 1. Experimental design flowchart.

2.1. EXPERIMENTAL MATERIALS

The materials used in this research include crude oil with a viscosity of 19 cp, density of 0.864 gm/cc, and ºAPI of 32. A rheometer was used to measure the viscosity of the crude oil. Gas chromatography-mass spectrometry determined the composition of the crude oil, as shown in Table 1. Filter paper membranes (i.e., 50, 100, and 450 nm) were used to mimic the unconventional reservoir pore structure and to investigate the effect of various pore sizes. The selection of filter membrane pore sizes was based on the pore size distribution of shale reservoirs, specifically Eagle Ford (Shen et al., 2017). The membranes were cut to the desired shape based on the 45-mm diameter of the filtration vessel. A High-pressure high-temperature (HPHT) stainless steel vessel was used to accommodate the filter paper membranes. The filtration vessel had a length of 15.24 centimeters with inside and outside diameters of 5 and 7.62 centimeters, respectively. To supply the CO_2 gas injection, a high-pressure CO_2 cylinder was used with a purity of 99.99% and connected to the vessel. A pressure regulator was installed on the cylinder to control the injected pressure. To investigate various temperatures, an oven was used to adjust the temperature during the gas injection. The oven manufactured by Despatch (Model: LBB2-27-2, Chamber dimensions: 94(width) x 94(depth) x 89(height) centimeters). For the MMP determination, a slim tube made of stainless steel and packed with sand was used. The slim tube had a weight of 2,211 grams with a length of 13.1 meter (inside and outside diameters were 0.21 and 0.41 centimeters, respectively). The solvent of n-heptane was selected to be mixed with the crude oil samples after the filtration experiments in the test tubes to quantify the asphaltene weight percent which asphaltenes are insoluble in n-heptane.

Table 1. Grouped carbon number distributions of the original oil.

Component	Weight percentage (%)
C_8	64.55
C_9	0.28
C_{14}	0.31
C_{15}	0.35
C_{16}	0.43
C_{17}	3.92
C_{18}	0.20
C_{19}	1.17
C_{20}	3.60
C_{21}	0.93
C_{22}	2.66
C_{24}	1.97
C_{27}	5.94
C_{28}	7.22
C_{29}	1.32
C_{30}	1.07
C_{31}	0.53
C_{32}	0.76
C_{33}	0.57
C_{34}	0.59
C_{35}	0.64
C_{37}	0.31
C_{38}	0.38
C_{40}	0.32
Total	100

2.2. SLIM TUBE EXPERIMENTS

The slim tube technique was selected to determine the MMP of CO_2 which has been used for years to measure MMP because it simulates the one-dimension displacement of reservoir oil (Ekundayo et al. 2013; Amao et al. 2012; Elturki and Imqam 2021c). The MMP can be defined as the lowest pressure at which the miscibility of gas can be created with the reservoir oil at the reservoir temperature.

The miscibility can be achieved when the interfacial tension between the oil and gas vanishes after multiple contacts. The main components of the MMP experiment included a syringe pump, three accumulators, gas cylinders, a stainless-steel slim tube packed with sand, and a back pressure regulator. The first step was a pretest to calculate the pore volume. In the second step, the slim tube was filled with the crude oil at a low rate of 0.5 PV to ensure that the slim tube was 100% saturated at the end of pumping. The final step involved experimental manipulation, whereby the temperature was adjusted to a predefined level, the gas cylinder was filled with CO_2, and gas was pumped at a rate of 0.25 ml/min. A back pressure regulator was installed at the outlet of the slim tube and used to adjust the pressure by using another water pump as a back pressure reservoir. Figure 2 shows a schematic diagram of the slim tube experimental setup.

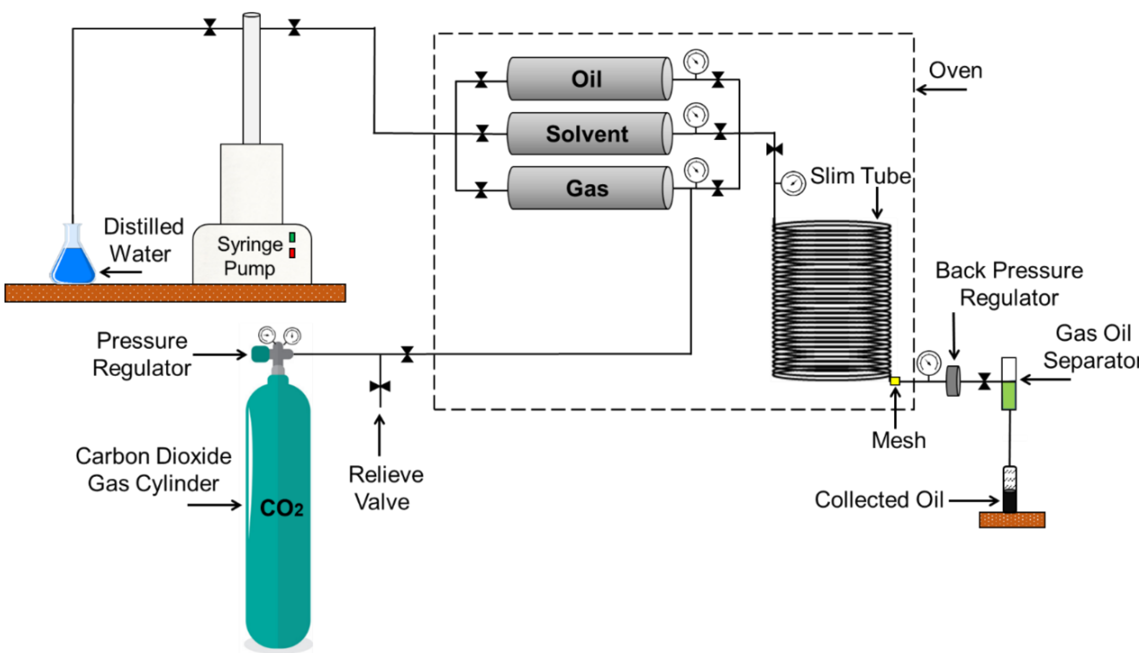

Figure 2. Schematic of the setup of the CO_2 MMP determination apparatus using the slim tube technique

The procedure of MMP determination was as follows. The slim tube was fully saturated with the distilled water, then the oil was injected into the slim tube unit fully saturated. This was observed at the outlet of the slim tube when the produced liquids are only oil and thus ensure the slim tube is fully saturated. During all the experiments, the back pressure regulator was placed at the outlet with the desired pressure. The gas accumulator was filled with CO_2. Then, CO_2 was injected at a rate of 0.25 ml/min. Each experiment was stopped when 1.2 PV of gas was injected or when the gas broke through. The effluent was used to collect the produced oil. The MMP was be determined by plotting CO_2 injection pressures versus cumulative oil recoveries. Finally, the solvent of Xylene was used after each experiment to clean the slim tube setup and to make sure there was no oil left in the slim tube that could affect the next experiment.

2.3. FILTRATION EXPERIMENTS

The components of the filtration setup are shown in Figure 3. The main components included a high-purity CO_2 cylinder with a pressure regulator to control the pressure from the cylinder. The gas accumulator was used to accumulate the CO_2 gas and inject it into the vessel using a syringe pump to reach higher pressures due to the limitation of outlet pressure in the CO_2 cylinder. The HPHT filtration vessel (Figure 4a) was designed to accommodate three mesh screens to support the filter membranes and prevent them from folding under high pressure. The mesh screens were designed with small holes that allowed the oil to pass through easily, as shown in Fig. 4b. Spacers between each mesh screen were added to support each mesh screen in its place, and rubber O-rings were used above and below each spacer to prevent leakage and to ensure that the oil and gas would pass through the filter paper membranes. A back pressure regulator was installed at the outlet of the filtration vessel and used to adjust the pressure using a syringe pump. The produced oil was collected using an effluent below the filtration vessel for further analysis. An oven controlled the temperature of the filtration vessel to study the effect of different temperatures. Finally, two transducers were installed at the inlet and outlet of the filtration vessel and were connected to a computer to monitor and record the pressure differences.

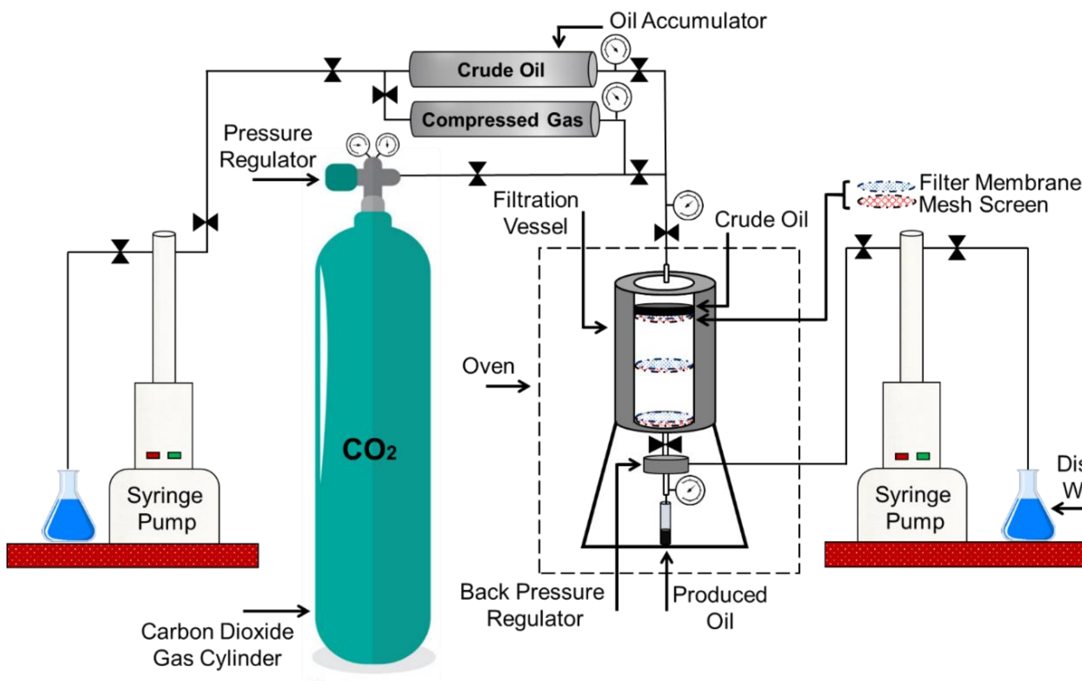

Figure 3. Filtration experiments setup.

The first set of mesh screens along with a filter membrane paper, rubber O-ring, and spacer were placed inside the filtration vessel, in that order. This step was repeated with the next two sets, after which the vessel was closed using a specially designed cap that ensured a tight connection between all of the sets and prevented leakage during the experiment. An oil accumulator injected 30 ml of crude oil into the vessel using a syringe pump. Next, the CO_2 cylinder injected gas into the vessel to the desired pressure level and exposed the crude oil to the gas for a specific soaking time. Then, the syringe pump at the outlet was turned to constant pressure but was adjusted to the required back pressure for each experiment to let the crude oil pass through the membranes. CO_2 was injected continuously into the vessel, and the produced oil was collected for further analysis (e.g., chromatography analysis). The experiment was stopped when no further oil production was observed. During the experiment, the inlet and outlet pressures were recorded using transducers connected to a computer. The difference between the two pressures did not exceed 50 psi. After the experiment, the vessel was opened, and the trapped crude oil was collected from each filter membrane for analysis. Finally, in preparation for the next experiment, the solvent n-heptane was used to clean the vessel, mesh screens, and spacers of precipitated and deposited oil.

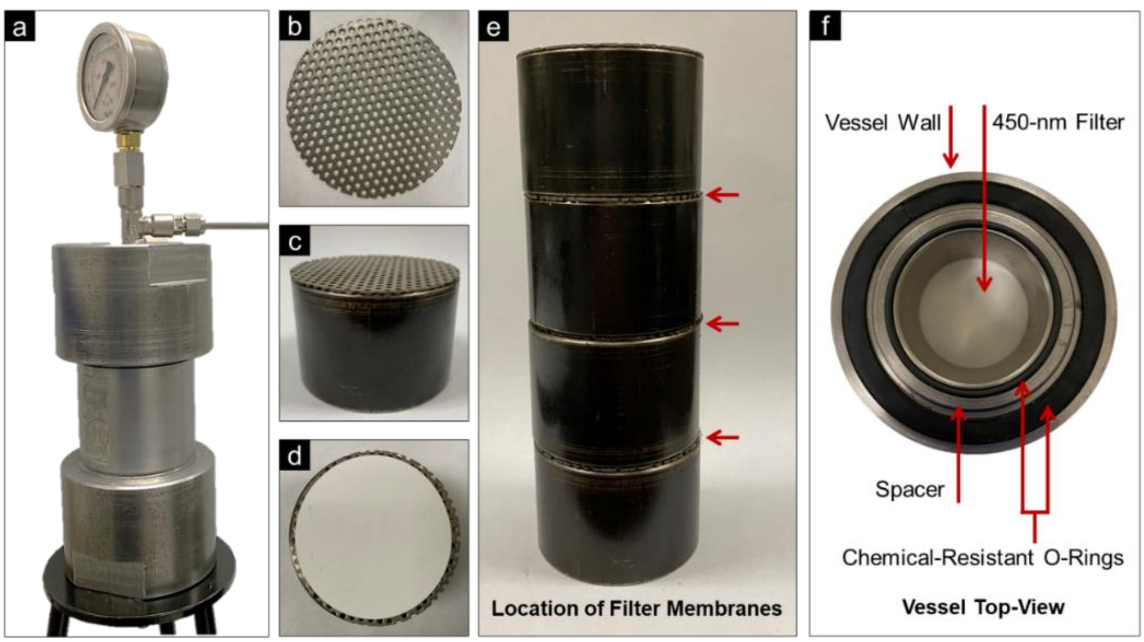

Figure 4. Filtration vessel equipment

- *Figure 4 details:* (a) real filtration vessel, (b) mech screen, (c) mech screen on top of spacer, (d) top-view of filter membrane on top of mech screen and spacer, respectively, (e) four Stainless steel spacers used inside the filtration vessel and the arrows indicates to the location of the filter paper membranes, (f) vessel top-view showing the 450-nm filter inside the vessel when using the heterogenous distribution.

2.4. ASPHALTENE VISUALIZATION AND DETECTION TESTS

The visualization tests were conducted to highlight the asphaltene precipitation and deposition process at various conditions. Then, the asphaltene percent was quantified using the standard test (IP 143) of the n-heptane insoluble asphaltene content determination in crude oil (Shahriar 2014). The visualization test was conducted by first placing in a test tube 1 ml of crude oil collected from all filter membranes, the produced oil, and the remaining oil from the filtration experiments. The oil was then collected using a pipette to ensure the accuracy of all samples. Second, 40 ml of n-heptane was added to each test tube. Tubes were closed tightly to prevent n-heptane evaporation. Each test tube was shaken well to ensure that the n-heptane was well dispersed within the crude oil. A special laboratory stand was used to handle the test tubes. The asphaltene then started to settle slowly. Photos were taken at specific time points (i.e., 0, 2, 4, and 12 h) to observe the change in asphaltene settling over time. A filter paper with 2.7 µm pore size was used to filter the precipitated asphaltenes in the test tube and then to quantify the asphaltene content. Asphaltene weight percent can be calculated by weighing the filter paper before and after the filtration process using a high-precision balance. The difference between these weights determines the asphaltene weight percent using the following equation:

$$\text{Asphaltene wt\%} = \frac{\text{wt}_{\text{asphaltene}}}{\text{wt}_{\text{oil}}} * 100 \tag{1}$$

Where asphaltene wt% is the asphaltene weight percent, wt asphaltene is the asphaltene weight on the filter paper, and wt oil is the oil sample weight. The asphaltene quantification test procedure is summarized in the flowchart shown in Figure 5.

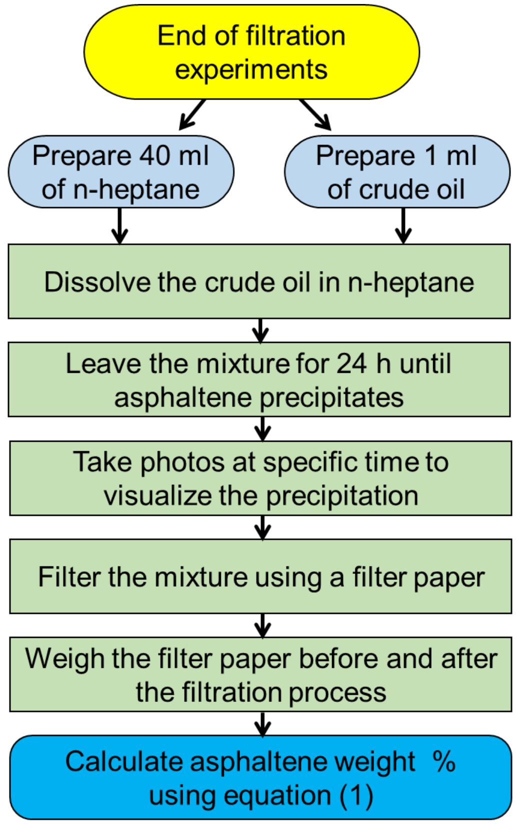

Figure 5. Flowchart highlighting the main steps of asphaltene visualization tests.

3. RESULTS AND DISCUSSION

3.1. MMP EXPERIMENTS RESULTS

The main mechanism by which CO_2 can achieve miscibility is the vaporizing mechanism. The MMP tests were conducted to ensure that we select the right miscible and immiscible pressure to conduct the filtration experiments. The impact of a high temperature on MMP was investigated to ensure that the filtration experiments were in the right condition of miscible or immiscible at higher temperatures. Oil recoveries were recorded at gas breakthrough or at 1.2 PV of the gas injected and were plotted with the tested injection pressures. When the cumulative oil recovery became higher than or equal to 90% of the initial oil in place (OOIP), the MMP could be determined, as shown in Figure 6. Table 2 shows the cumulative oil recoveries of slim tube tests at temperatures of 32 and 70ºC. The solid lines in Fig. 6 were utilized to establish the point where the observed oil recovery against injection pressure suddenly changed slope. Then, the MMP was determined using the intersection point. At 32°C, the MMP of CO_2 was determined to be 1450 psi. As a result, for examining asphaltene precipitation and stability under immiscible gas injection condition, pressures of 750, 1000, and 1250 psi were chosen, along with a temperature of 32ºC. On the other hand, a higher temperature of 70 ºC resulted in an MMP with 1650 psi. So, the pressure of 1500, 1750, and 2000 psi were selected to present the miscible condition in the filtration experiments. It was observed that the temperature has a direct relationship with MMP, as the temperature increases the MMP will increase (Zolghadr et al, 2013).

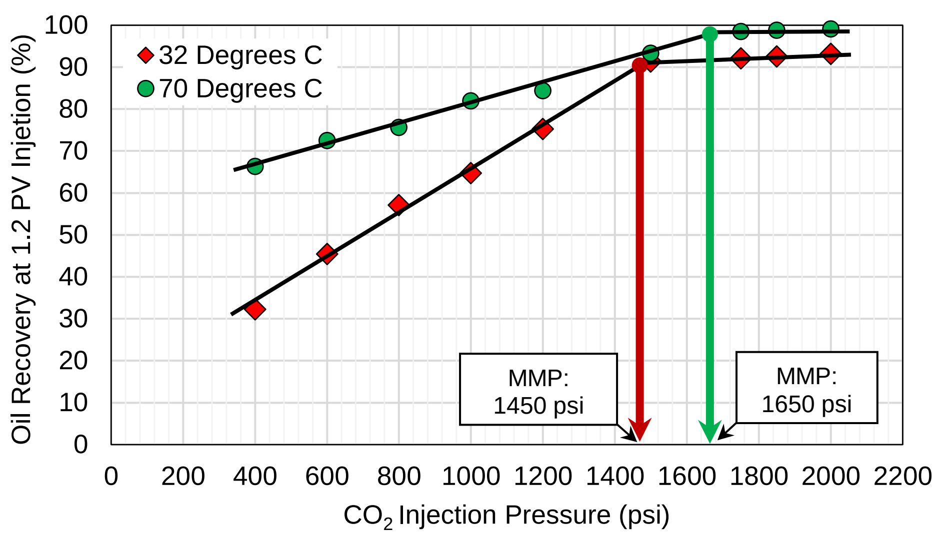

Figure 6. CO_2 MMP determination using an oil viscosity of 19 cp at 32ºC and 70ºC.

Table 2. CO_2 slim tube cumulative oil recoveries (%)

Tested injected pressure (psi)	400	600	800	1000	1200	1500	1750	1850	2000
Cumulative O.R at 32 ^oC	32.20	45.40	57.10	64.71	75.20	91.30	92.10	92.50	93.12
Cumulative O.R at 70 ^oC	66.30	72.50	75.60	81.90	84.40	93.30	98.50	98.80	99.10

3.2. FILTRATION AND VISUALIZATION RESULTS

3.2.1. Effect of Miscible and Immiscible Pressure Using Uniform Membrane Distribution. The term "uniform membrane distribution" refers to the use of the same pore size filter membrane in all the filtration experiments. The distribution of the paper membrane inside the vessel is shown in Figure 7 with a pore size of 100 nm for the entire membrane. The selection of filter membrane pore sizes was based on the pore size distribution of shale reservoirs, specifically Eagle Ford (Shen et al., 2017). The Impact of using a uniform pore size filter paper membrane on the asphaltene deposition during the filtration test is shown in Figure 8. The effect of applying the same pore size was investigated by placing three 100-nm filter membranes inside the vessel in each mesh screen, and the findings were compared to a heterogeneous distribution. A CO_2 immiscible pressure of 750, 1000, and 1250 psi and a miscible pressure of 1500, 1750, and 2000 psi were used to investigate the impact of miscibility on asphaltene disposition. All the experiments were conducted at a temperature of 32^oC. The results revealed that the asphaltene deposition was almost equal across all the paper membranes for each pressure used. Increasing the pressure increased the asphaltene weight percent in all the experiments. It was observed that the miscible conditions have a higher impact on asphaltene instability compared to immiscible conditions. For instance, the asphaltene weight percent ranged from 7.98% in the upper part of the 100-nm paper membrane to 7.95% in the lower part of the 100-nm paper membrane during the immiscible pressure of 750 psi gas injection. By comparing these findings to the miscible condition of 2000 psi, the asphaltene weight percent ranged from 19.95% in the upper part of the 100-nm paper membrane to 19.66% in the lower part of the 100-nm paper membrane. There is a slight difference between the asphaltene weight percent in all the filter membranes because some of asphaltene particles plugged some pores in the middle and the lower membranes during the injection process, thereby effecting the oil passage. These plugged pores resulted in a decrease in the asphaltene weight percent in the produced oil. Asphaltene particles larger than 100 nm precipitated on the upper section of the filter membrane, while particles less than 100 nm went through and were collected with the produced oil. A pressure of 1750 psi, for instance, created considerably more asphaltene clusters than a pressure of 750 psi, as well as more asphaltene deposited on the filter membranes. More clusters of 100 nm or larger were formed as a result of the increased pressure. Thus, more asphaltenes were quantified at higher pressure levels in all filter membranes. In summary, because of the uniform pore size of the filter paper membranes, the asphaltene clusters were forced and deposited into the filter membranes with almost the same concentrations in all the experiments.

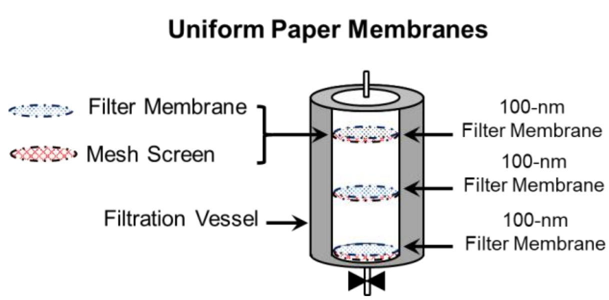

Figure 7. Illustration of the uniform paper membrane distribution inside the vessel.

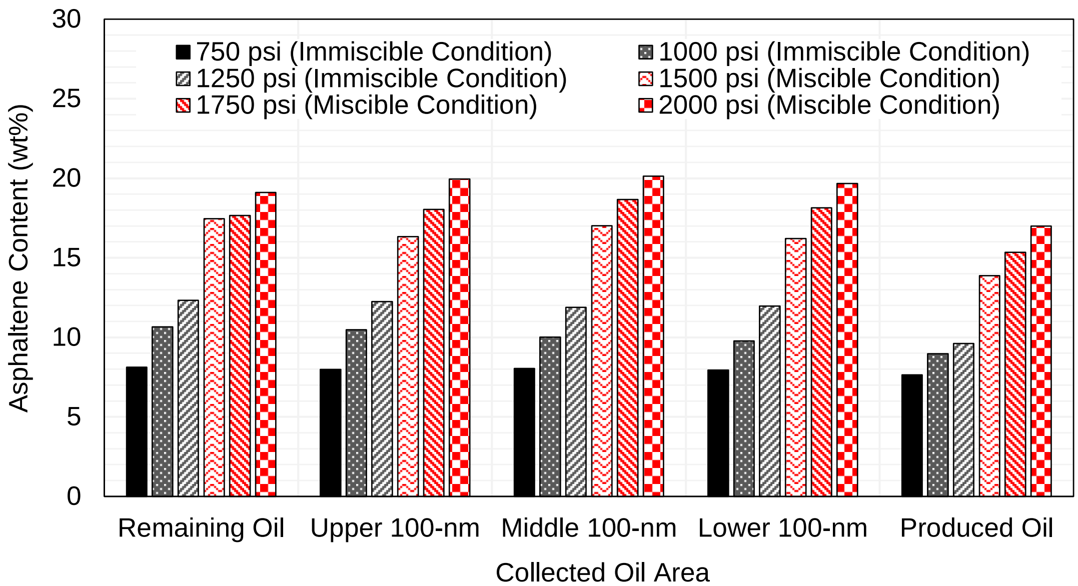

Figure 8. Asphaltene weight percent distribution using uniform paper membranes with immiscible and miscible CO_2 injections.

A miscible pressure of 1750 psi and immiscible pressure of 750 psi CO_2 injection were selected to investigate the asphaltene precipitation process over time. The remaining oil was collected after each experiment and dissolved in n-heptane at a ratio of 1:40. Various times were selected (i.e., 1, 4, and 12 h) to investigate and visualize the asphaltene deposition process. Figure 9a, and b shows the uniform asphaltene visualization tests at 750 and 1750 psi with 100-nm pore size membranes at 32ºC. There was no asphaltene present at zero elapsed time, and the crude oil sample was completely dissolved in n-heptane. The miscible pressure showed a slight dark color of the mixture at zero elapsed time compared to immiscible one. After 1 h, the asphaltene clusters started to appear and precipitate with a small amount of asphaltene particle in the bottom of the tube. Over time, the color of the top of the lab tubes started to be lighter with the present of some suspended particle of asphaltene. More asphaltene particles can be observed miscible conditions of

1750 psi indicating that miscibility impacts the instability of asphaltene at higher rate. Finally, after 12 h, almost all asphaltene particles and clusters were deposited in the bottom of the lab tube and the color of the solution was much lighter compared to the zero-time observation. The pictures reveal that miscibility had higher impact on asphaltene instability and same pore size distribution led to almost the same precipitation process for all filter paper membranes in both conditions.

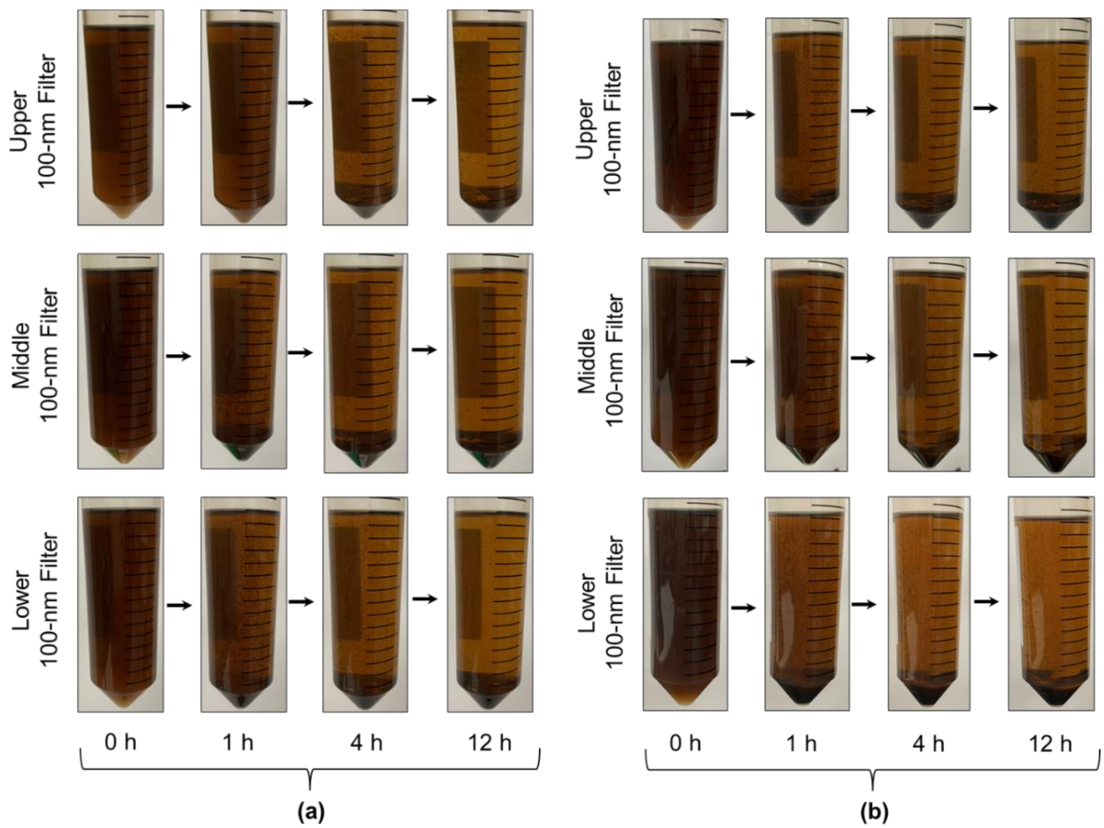

Figure 9. Visualization of asphaltene precipitation and deposition using a uniform membrane size distribution at: (a) immiscible pressure of 750 psi and (b) miscible pressure of 1750 psi.

3.2.2. Effect of Pore Size Heterogeneity. Figure 10 shows the heterogeneous distribution of the filter membranes, starting with a 450-nm filter in the upper mesh screen, a 100-nm filter in the middle, and a 50-nm filter in the lower mesh screen. As explained in the previous section, miscible pressures (i.e., 1500, 1750, and 2000 psi) and immiscible pressures (i.e., 750, 1000, and 1250 psi) were selected to investigate the heterogeneity of the filter paper membranes at 32ºC with a 2-h soaking time. The soaking time effect will be presented in the following sections. The asphaltene weight percent was increased when increasing the pressure and during the miscible conditions due to the resins that connect all the asphaltene particles and solid components in the crude oil broke down; thus, asphaltene weight percent will increase. Figure 11 presents the asphaltene weight percent using a heterogeneous paper membrane distribution during miscible and immiscible CO_2 injection pressures. When using low immiscible 750 psi gas injection, the asphaltene weight percent increased from 7.45% to 9.36% in the 450-nm and 50-nm filters, respectively. Increasing the pressure to 1000 and 1250 psi resulted in a significant increase in asphaltene weight percent in both pressures, especially at 1250 psi.

At 1250 psi injection pressure, the asphaltene weight percent increased up to 16.97% in 50-nm filter. This revealed that the injected pressure had an effect on the asphaltene particles and clusters, resulting in asphaltene deposition dependent on the asphaltene particle size. Filter membrane pores became almost blocked as a result, particularly in the 50-nm filter. The ability of asphaltene particles to pass through the filter membranes was affected by the size of their pores. The asphaltene aggregates continued to interact with one another because of Brownian motion, producing bigger particles. Smaller aggregates have a stronger tendency to deposit due to the significant radial diffusivity of the particles which describes the ability of a particle to be pushed by a collision with asphaltene aggregates (Hashmi and Firoozabadi, 2010; Hassanpouryouzband et al. 2017). More nanoaggregates combined together and resulted in more clusters which led to pore plugging in all filter membranes. Injecting higher pressures (i.e., 1500, 1750, and 2000 psi) with miscibility conditions increased the asphaltene weight percent sufficiently. For instance, the weight percent of asphaltene ranged from 13.01% to 20.20% in the 450-nm and 50-nm filters, respectively.

The highest weight percent was observed at miscible pressure of 2000 psi which was 25.47% in 50-nm filter membrane. These results confirm that the miscibility of gas impacts the asphaltene stability in oil at a higher rate compared to immiscible conditions of gas. Also, these findings clearly suggest that asphaltene particles changed the oil's capacity to flow through, which may happen in actual reservoirs and cause serious issues. Because the asphaltene clusters had plugged the pores in all of the filter membranes, the produced oil had a less asphaltene weight percent.

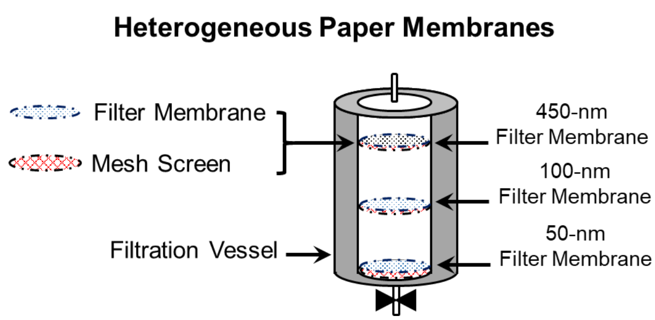

Figure 10. Illustration of the heterogeneous paper membrane distribution inside the vessel.

After each experiment was completed, the collected oil was analyzed to see the asphaltene deposition and precipitation process over time. The oil collected from 450-, 100-, and 50-nm filter membranes was analyzed under immiscible condition of 750 psi and miscible conditions of 1750 psi, as shown in Figure 12a and b. A ration of 1:40 was used to mix the oil samples with the solvent n-heptane in test tubes to observe the precipitation and deposition process over different times (i.e., 0, 1, 4, and 12 h). The captured photos show that at 0 h, all the oil samples collected from all filter paper membranes were fully dissolved in n-heptane, and no asphaltene clusters or particles were observed in both conditions of gas injection (i.e., immiscible and miscible). A slightly lighter color was observed in the test tube of 450-nm filter membranes in both conditions. After 1 hr, the asphaltene particles started to form in the mixture and started to form small clusters, especially in the sample collected from 100-nm and 50-nm filter membranes.

The miscible test tubes showed a slightly darker color due to higher pressure weakening the bonds between asphaltene and resins at a higher rate compared to immiscible conditions. It was interesting to observe that the asphaltene accumulations and deposition were clear in the bottom of the test tube after 4 hr of the oil samples collected from 450-nm filter membranes. Over time, the supernatant became lighter in color and the asphaltene clusters started to settle down and form higher amounts of asphaltenes. After 12 hr, most of the asphaltene particles were settled down and deposited for all oil samples collected from all paper membranes.

These findings showed that pressure (i.e., immiscible and miscible) has a substantial impact on the stability of asphaltene. As a result, it's critical to investigate the impact of pressure on asphaltene stability in order to predict and minimize any problems.

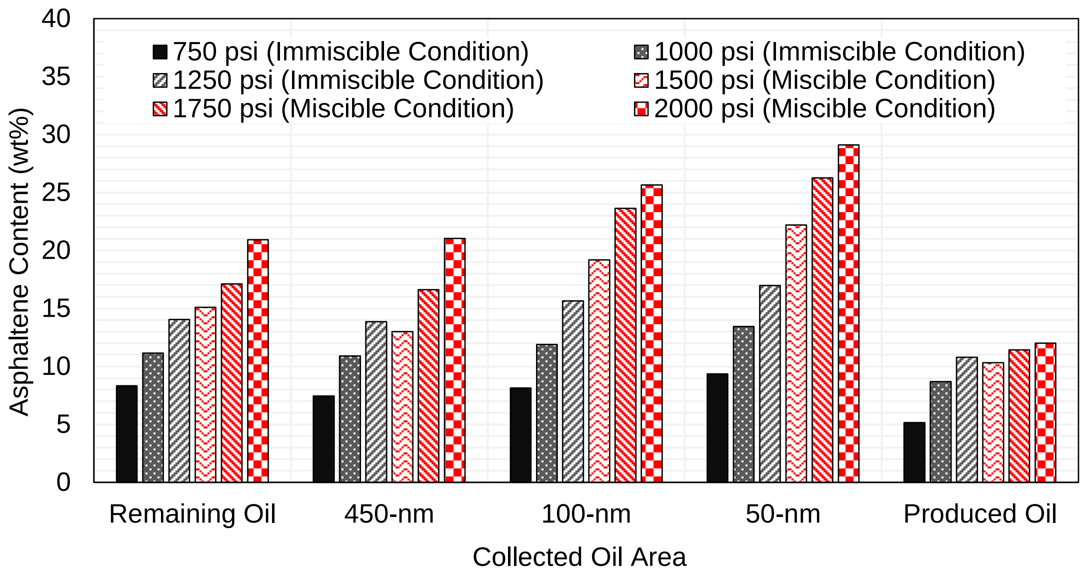

Figure 11. Asphaltene weight percent using a heterogeneous distribution using miscible and immiscible CO_2 injections.

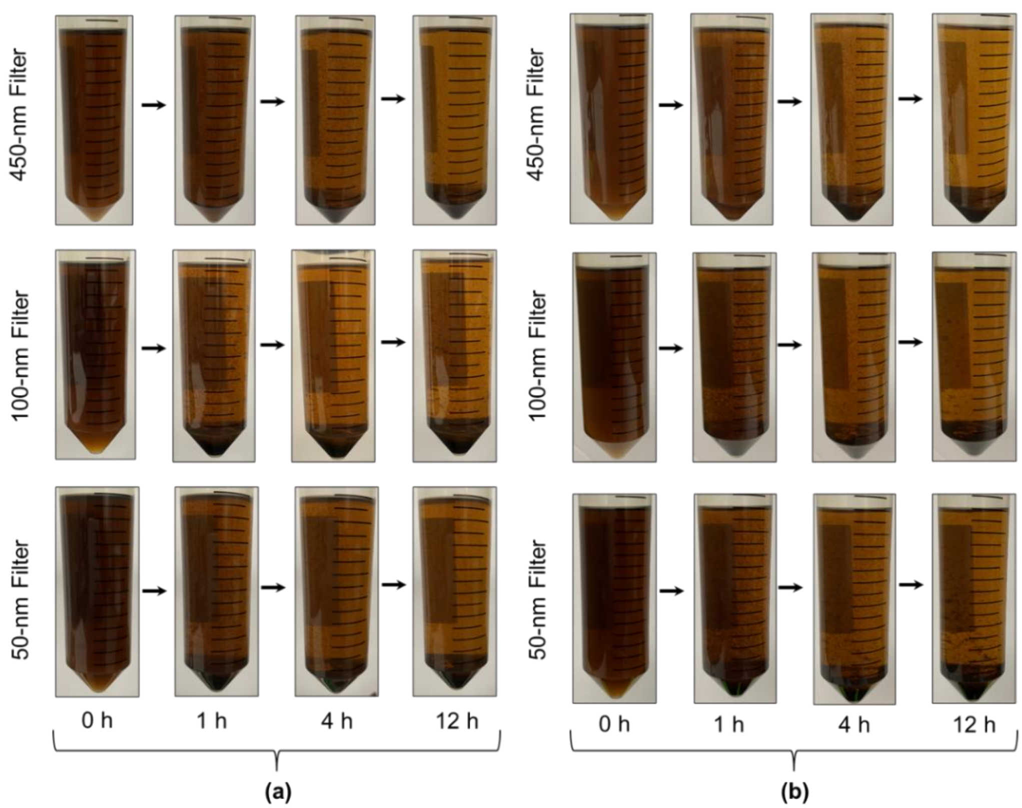

Figure 12. Visualization of asphaltene precipitation and deposition using a heterogenous membrane size distribution at: (a) immiscible pressure of 750 psi and (b) miscible pressure of 1750 psi.

3.2.3. Effect of Soaking Time. To understand the impact of soaking time on asphaltene precipitation and deposition, three separate experiments using 1000 psi injection pressure with durations of 10, 60, and 120 minutes were selected. The soaking time is when the gas was injected into the vessel at the desired pressure and at 32oC to allow the CO_2 to mix with the crude oil. Figure 13 shows the asphaltene weight percent in all filter membranes during various soaking times. The results demonstrated that increasing the soaking time led to an increase in asphaltene weight percent in all filter paper membranes. For example, the asphaltene weight percent in the 450-nm filter increased from 6.26% to up 10.14% for 10 and 120 min, respectively. The small pore size of the 50-nm filters resulted in an increase in asphaltene weight percent due to the asphaltene clusters plugging the small pores during the filtration process. The bonds between asphaltene and resins in the crude oil were weakened at a lower rate at 10-min soaking time which confirm that due to time limitation of soaking process, the asphaltene weight percent was lower compared to 120-min.

Given these observations, the soaking time had an impact on asphaltene instability in the crude oil, especially for a time longer than 10-min. The findings showed that the effect of 60-min had similar effect on asphaltene aggregation even though the weight percent was slightly higher at 120-min. The longer soaking time investigated was 120-min because the difference between the asphaltene weight percent in both 60-min and 120-min was not significant.

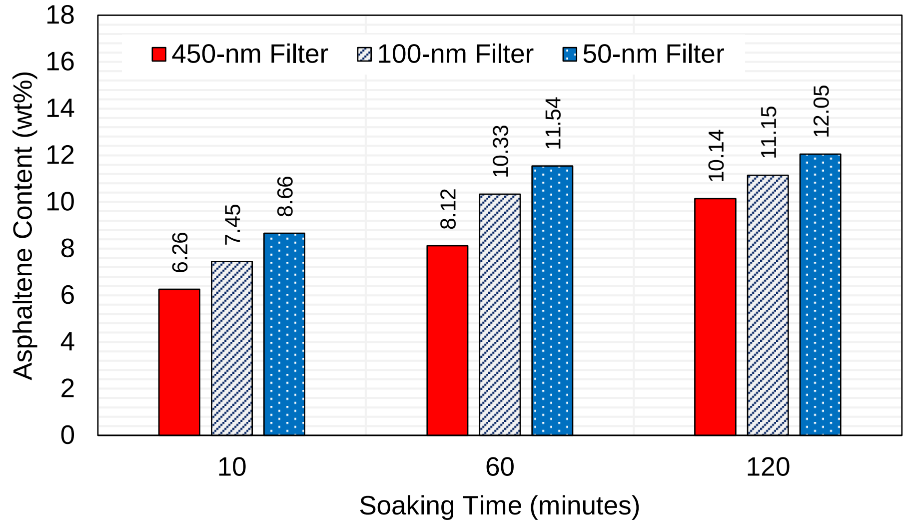

Figure 13. Asphaltene weight percent at soaking times of 10-, 60-, and 120-min using 450-, 100-, and 50-nm filter membranes.

3.2.4. Effect of Temperature on Asphaltene Deposition. Temperature has a great effect on asphaltene stability in crude oil. To study the influence of a higher temperature on asphaltene stability, two tests were performed at two temperatures (32°C and 70°C). The 32 °C represents normal temperature, and 70°C represents the average temperature of shale basins. A pressure of 1000 psi injection and a 2-h soaking time were used in both experiments to evaluate the temperature impact on asphaltene stability. A heterogenous filter paper distribution was used in both experiments. Increasing the pressure led to a decrease in asphaltene weight percent in all filter paper membranes, as shown in Figure 14. The higher percentage of asphaltene was found in the 50-nm filter paper membranes which changed from 18.90% to 16.23% for 32°C and 70°C, respectively. The suspension colloidal particles of asphaltene in stable oils are covered by resins that are strongly connected to the asphaltene. At higher temperatures, this connection between asphaltene and resins can be stronger and keeps the asphaltene dissolved in the crude oil (Hoepfner et al. 2013). Less asphaltene colloidal will be produced at higher temperatures and the associations are weaker due to resins dispersing strongly the collides of asphaltenes (Branco et al. 2001). At higher temperatures, the precipitated asphaltenes created from colloidal suspension particles tend to dissolve in the oil, resulting in more asphaltenes forming in soluble conditions but less in colloidal ones (Chandio et al. 2015). Moreover, resins tend to have a strong self-association like asphaltenes at lower temperatures; thus, the connection between resins and asphaltene is reduced (Pereira et al. 2007). As a result of these mechanisms, asphaltene aggregates can be formed because of strong polarity and self-association to form aggregates at lower temperatures. It can be concluded that the asphaltene precipitated out from the colloidal suspension was dissolved in the crude oil until reaching equilibrium. This resulted in more soluble asphaltenes in oil and less asphaltene in colloidal form (Chandio et al. 2015). Also, the same observation was noticed for the filter paper pore size in which smaller pore size had higher asphaltene weight percent in both temperatures. This was due to the asphaltene particles plugged the pores of 50-nm filter paper membrane much more compared to 450-nm and 100-nm; thus, higher asphaltene weight percent was determined.

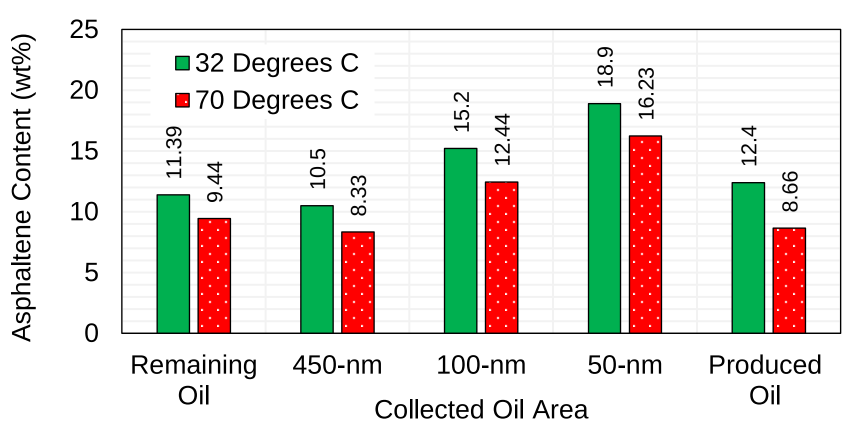

Figure 14. Asphaltene weight percent at different temperatures during CO_2 injection at 1000 psi.

4. FURTHER ANALYSIS AND DISCUSSION

4.1. CHROMATOGRAPHY ANALYSIS

Gas chromatography-mass spectrometry (GC6890-MS5973) was utilized to analysis the main chemical components of the crude oil used in the filtration experiments in order to highlight the chemical structure changes, including asphaltene, after the injection of CO_2. First, the original oil was analyzed before conducting the filtration experiments. Then, the produced oil after the filtration experiments was collected for further analysis. Four produced oils were selected after filtration experiments using pressures of 1000 and 1750 psi to investigate the impact of immiscibility and miscibility conditions on the chemical components of crude oil, and to show the influence of pore size of filter paper membranes on asphaltene deposition. Table 3 presents the grouped carbon number distributions before and after CO_2 gas injection filtration experiments at immiscible conditions (i.e., 750 and 1250 psi) and miscible conditions (i.e., 1750 and 2000 psi). The findings showed that the light components (C_8-C_{14}) were partially extracted when using 1250 psi which decreased from 52.72% to 47.32% when using 750 and 1250 psi, respectivley. When utilizing miscible gas injections of 1750 and 2000 psi, the light components substantially reduced to 40.66 % and 30.59 %, respectively. Miscible conditions had higher impact on the cude oil and this can be seen in the higher mole percentages of the intermediate and heavy components (C_{15}-C_{30+}). For instance, the heavy components of C_{30+} increased significanlty from 5.38% to 13.50 at immiscible pressure of 750 psi and miscible pressure of 2000 psi, sequentially. This confirms that asphaltene particles and clusters deposited on the filter paper membranes during the filtration experiment and reduced its content and the heavy components in the produced oil. Increasing the pressure above the MMP resulted in an increase in heavy components and asphaltene content compared to pressure below MMP (i.e., immiscible conditions). These results indicated that miscibility had impacted the crude oil and its chemical structure much more than immiscible gas injection conditions. The strong light-hydrocarbon extraction of miscible CO_2 leads to more percentage of the heavy hydrocarbons and less in light and intermediate hydrocarbons (Cao and Gu 2013). Higher pressure of miscibility will force the asphaltene particle and the heavy components to pass through the filter membranes at a higher rate and thus result in an increase in the asphaltene content in the produced oil.

Table 3: Grouped carbon number distributions of the original oil and the remaining oil after immiscible and miscible CO_2 injection.

Carbon Number Group	Original Oil Before Experiments	Pressure Condition			
		Immiscible Conditions		Miscible Conditions	
		750 psi	1250 psi	1750 psi	2000 psi
C_8 -C_{14}	65.14%	52.72%	47.32%	40.66%	30.59%
C_{15}-C_{19}	6.06%	3.85%	3.50%	8.45%	5.12%
C_{20}-C_{24}	9.16%	16.32%	20.11%	17.45%	20.10%
C_{25}-C_{29}	14.48%	21.74%	22.74%	25.28%	30.69%
C_{30+} (Including asphaltene)	5.17%	5.38%	6.33%	8.16%	13.50%
Total	100.00%	100.00%	100.00%	100.00%	100.00%

4.2. MICROSCOPY IMAGING ANALYSIS

Asphaltene clusters and aggregations can be formed after CO_2 injection, and these new forms of asphaltene particles can cause severe issues and plug the pores in a reservoir. A reduction in oil recovery, and wettability alteration can be encountered during asphaltene precipitation and deposition process. In this section, a solvent of n-heptane was used to clean the filter paper membranes after the filtration experiments to highlight the pore plugging due to asphaltene particle and clusters. Figure 15 shows the filter membranes (i.e., 450-nm, and 50-nm) before and after conducting the filtration experiment with 1500 psi gas injection as well as after cleaning the crude oil from the filter membrane. The photos reveal that the pores were plugged and the asphaltene particles were deposited causing a reduction in pore size and oil path in filter paper membranes, especially in the 50-nm filter paper membranes which has smaller pore size. To highlight the severity of pore plugging in all filter paper membranes, a HIROX digital microscope was used to show the plugging pores. The filter paper membranes of a heterogenous filter distribution of immiscible and miscible filtration experiments were selected for further analysis. Figure 16 shows the microscopic images of the filter membrane's pore structure of 450-, 100-, and 50-nm filters using immiscible conditions (i.e., 750, 1000, and 1250 psi) and miscible conditions (i.e., 1500, 1750, and 2000 psi) at 32 ^{o}C. All images were captured after cleaning the filter paper using n-heptane solvent for at least 24 h. It was observed that miscible conditions of CO_2 had higher pore plugging of the filter paper membranes compared to immiscible conditions. These observations confirm the results from the filtration experiments explained above. The asphaltene particles and clusters were deposited at a higher rate in smaller filter paper membranes such as 50-nm due to smaller pore size structure. The results showed darker colors for smaller pore size filter paper during miscible condition of gas injection. It can be concluded that miscibility impacts the asphaltene particle in crude oil significantly compared to immiscible gas injection conditions.

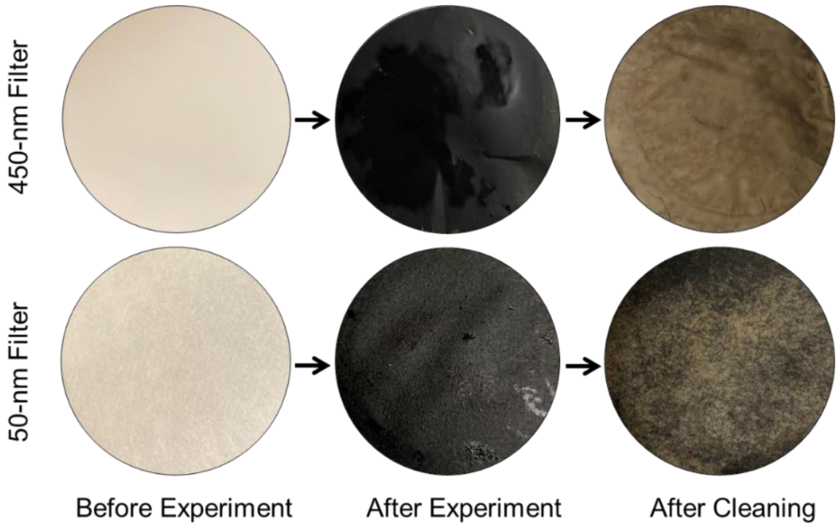

Figure 15. Illustration of the filter membranes (450- and 50-nm) at 1500 psi before and after the experiment, and after cleaning.

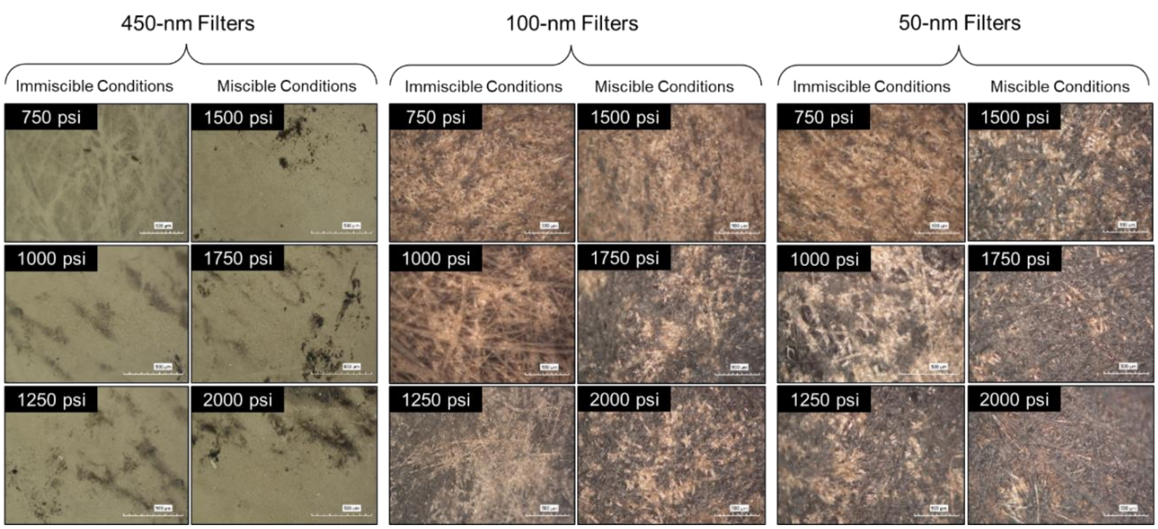

Figure 16. Digital microscopic images (500 µm) of 450-, 100-, and 50-nm filter membranes during immiscible and miscible CO_2 injection

4.3. SEM ANALYSIS

To provide an advance and clear imaging analysis of how asphaltene particles impact filter paper membranes, a scanning electron microscopy (SEM) was used to highlight the impact of pressure and asphaltene clusters on pore plugging. To illustrate this, heterogenous filter paper membranes (i.e., 450, 100, and 50 nm) during immiscible (i.e., 1000 psi) and miscible (i.e., 1750 psi) CO_2 injection were selected for further imaging analysis. Figure 17 shows SEM images (10 μm) of the filter membrane's pore structure for 450-, 100-, and 50-nm filters using miscible injection pressures of 1750 and 2250 psi, respectively at 32ºC. For 450-nm filter membrane, the structure of the filter showed some asphaltene particles which was colored black for both pressures. The structure of 450-nm filter was slightly clearer because it has large pore size compared to 100 and 50-nm filters. As the pore size decreased, the structure of the filters was darker and less details could be observed due to smaller pore size, especially in 50-nm filter papers. Large area of 100-nm filter paper was impacted by asphaltene clusters, and this can be observed on the darker color, especially for miscible pressure of 1750 psi. For the 50-nm filter membranes, most of the image area for both immiscible and miscible conditions was impacted by asphaltene deposition due to small pore size. These findings reveal that asphaltene particles plugged high percentage of the filter paper's area which was observed clearly in smaller pore size filters and high CO_2 pressure.

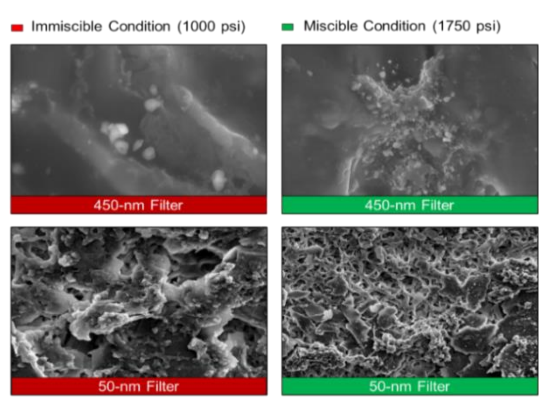

Figure 17. Scanning electron microscope (SEM) images (10 μm) of 450-, and 50-nm filter membranes at 1000 and 1750 psi injection pressures.

4.4. PORE SIZE REDUCTION DUE TO ASPHALTENE DEPOSITION

SEM images were processed using advanced computer software to determine the pore size distribution of all filter membranes and to highlight the impact of asphaltene clusters on pore plugging. All heterogenous filter membranes were selected for further analysis of immiscible pressure of 1000 psi and miscible pressure of 1750 psi experiments at 32°C. Figure 18a compares the pore size distribution in the 450-nm filter membrane after CO_2 injections at 1000 and 1750 psi. The major distribution of the pore size of filters ranged from 40 to 300-nm at immiscible pressure of 1000 psi, but 20 to 180 at miscible pressure of 1750 psi. The results showed that miscibility significantly impacted the pore size compared to immiscible conditions because higher pressure induced the asphaltene particles at higher rate, and thus plugged membrane's pores which led to reduce pore sizes.

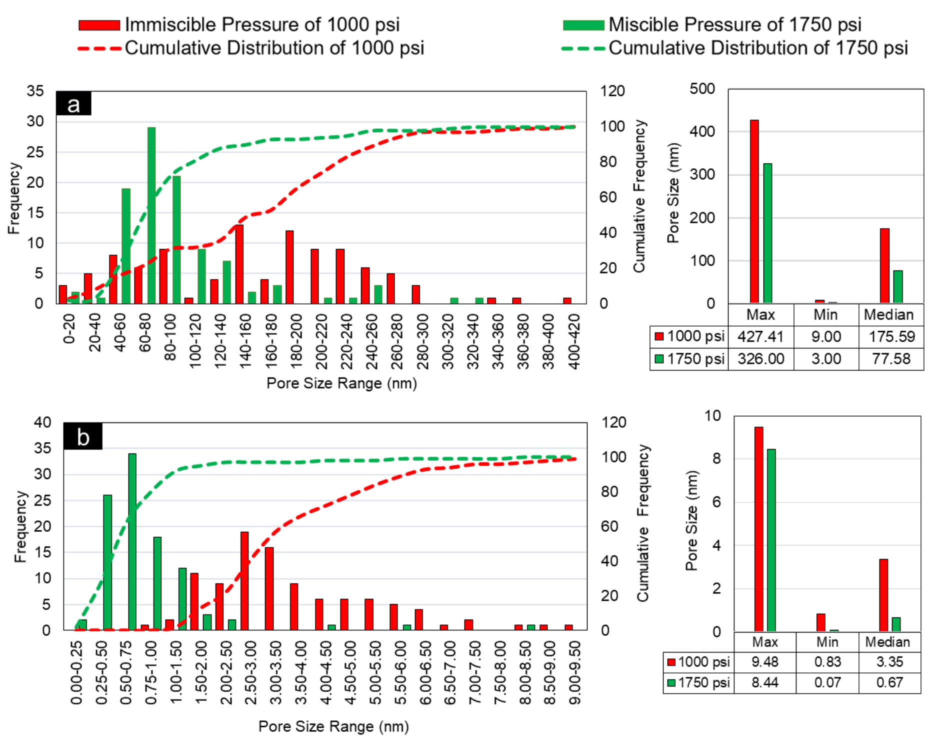

Figure 18. Comparison of the estimated pore size distribution in (a) 450-nm and (b) 50-nm filter membranes after CO_2 injections of 1000 and 1750 psi.

When the asphaltene was deposited inside the membranes, the oil was not able to pass through the filter easily due to pore plugging. These observations were found in 50-nm filter membranes. For the 50-nm filter membrane, the pore size distribution estimated to be between 1 to 7-nm for immiscible pressure (i.e.,1000 psi) and from 0.25 to 3-nm for miscible pressure (i.e.,1750 psi), as shown in Figure 18b. Due to the smaller pore size structure, a smaller pore size distribution was determined in the 50-nm filter membrane. The asphaltene clusters and particles deposited much more in 50-nm filter membranes for both immiscible and miscible pressure conditions due to smaller pore size which led to more plugging of the pores. Su et al (2021) developed an integrated simulation approach to predict permeability reduction under asphaltene particle aggregation and deposition. They concluded that longer aggregation time, higher flow velocity, and larger precipitation concentrations will lead to a faster reduction in permeability. These findings indicate that CO_2 injection can affect asphaltenes in crude oil during both immiscible and miscible conditions, causing significant pore blockage, especially in reservoirs with small pores, such as those found in unconventional reservoirs.

4.5. CARBON DIOXIDE VS. NITROGEN DISCUSSION

In this section, a holistic comparison discussion on how asphaltene deposition process differs under CO_2 and N_2 gas injections. The results in this research will be compared to the previous work using miscible and immiscible N_2 injection (Elturki and Imqam 2021a; 2022a). The MMP of N_2 was determined to be 1600 psi. CO_2 and N_2 could impact the asphaltene particles in crude oil at various degrees of fluctuations. Figure 19 shows the asphaltene weight precent during immiscible CO_2 and N_2 injection. The results show that CO_2 impacted the asphaltene particles significantly compare to immiscible N_2 injection condition. For example, the asphaltene weight percent during 1000 psi N_2 injection pressure on 450-nm filter was 2.52%, but for 1000 psi CO_2 injection was 10.90% indicating that CO_2 had influenced the asphaltene much more than N_2. For 50-nm filter, more asphaltene particles were trapped due to small pore size resulting in asphaltene weight percent up to 8.14% and 13.44% for N_2 and CO_2 during 1000 psi injection, respectively. This can be explained as the mass transfer of CO_2 is higher than N_2 due to the supercritical of CO_2 can be attained easily (Wang et al. 2018). Higher pressure led to more asphaltene precipitation and deposition in all filter membranes. In order to make a better comparison, Figure 20 shows the miscible condition results of CO_2 and N_2 on asphaltene stability. It is apparent from the figure that miscibility or near miscible conditions of both gases led to higher asphaltene rates. For example, during miscible pressure of 1750 psi, the asphaltene weight percent determinations were 17.33% and 26.26% on 50-nm filter for N_2 and CO_2, respectively. Higher pressure will break the bonds between the asphaltene and resins in the crude oil at higher degree and thus lead to more asphaltene fluctuations and deposition. Also, the solubility of CO_2 is higher than N_2 and thus N_2 has a weak mass transfer. This could lead to poor extraction process of light hydrocarbons of crude oil and thus less asphaltene flocculation compared to CO_2. Also, CO_2 and asphaltene both have polar molecules which lead to higher interaction rate and thus higher asphaltene deposition (Dashti et al. 2020). In terms of CO_2 and crude oil chemical interactions, the stability of asphaltenes in crude oil can be considerably impacted when they react with CO_2 and create amide functional group. The aggregation of asphaltenes during CO_2 injection would increase during the formation of the amide functional group due to the hydrogen bonding and metal coordination reaction that may occur through this group (Afra et al. 2020). These results illustrate both effects of miscible and immiscible conditions of CO_2 and N_2 which CO_2 is more advantageous in terms of reaching miscibility more easily. This could result in a high oil recovery but could lead to more asphaltene issues during gas injection process in real reservoirs.

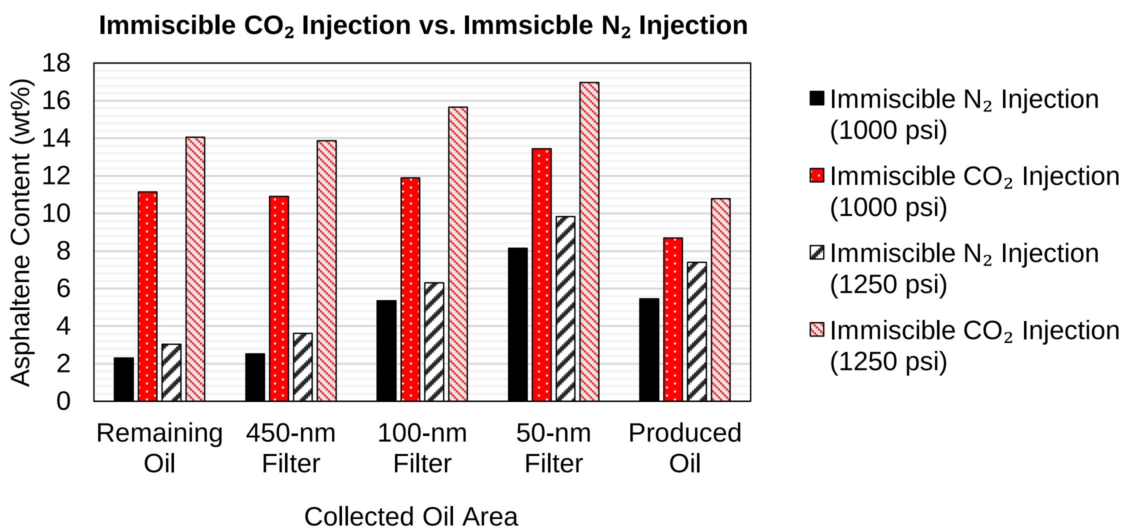

Figure 19. Comparison of asphaltene weight percentages during immiscible N_2 injection (Elturki and Imqam 2021a) and immiscible CO_2 injection pressure

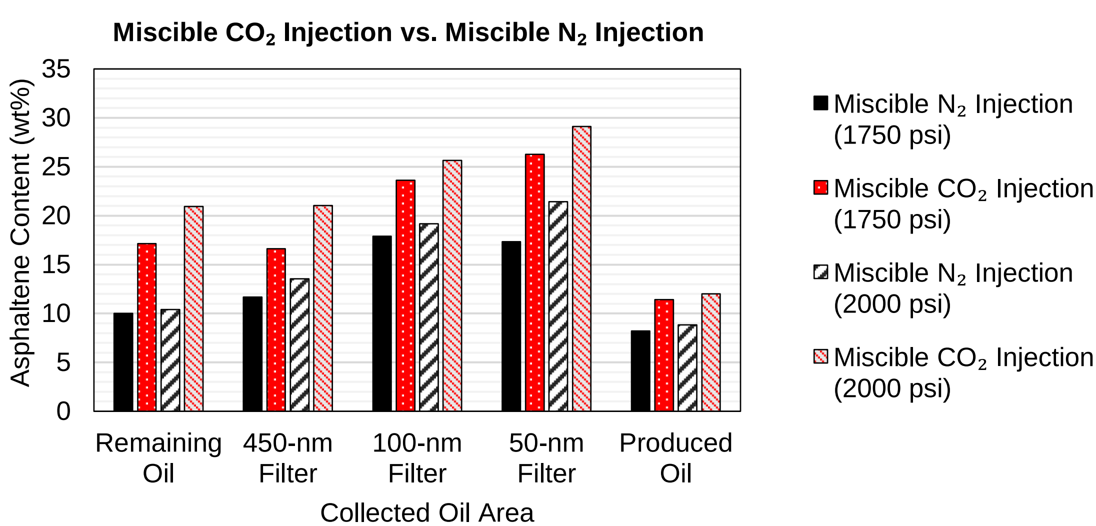

Figure 20. Comparison of asphaltene weight percentages during miscible N_2 injection (Elturki and Imqam 2022a) and miscible CO_2 injection pressure

5. CONCLUSIONS

This research provided a comprehensive experimental investigation of the impact of immiscible and miscible CO_2 injection on asphaltene stability in crude oil using nano pore structure which represents unconventional reservoirs. The filtration technique was used to conduct the experiments. A slim tube was used to determine the minimum miscibility pressure of CO_2. Various factors were studied including immiscible pressure, miscible pressure, temperature, filter membrane distribution, and pore size. The following conclusions can be drawn:

- The filtration experiments showed that the asphaltene weight percent increased as the CO_2 injection pressure increased because the greater pressure breaks the resins around the asphaltenes, resulting in asphaltene precipitation and deposition. These observations were significant during miscible injection pressures (i.e., 1500, 1750, and 2000 psi) due to miscible injections had higher solubility and strong extraction process of light components in the crude oil, resulting in more heavy oil components and asphaltenes. The severity of asphaltene deposition was higher in 50 nm filter paper membranes. Also, a soaking time of 120 min. had a higher impact on asphaltene instability compared to 60- and 10-min. soaking times.
- At higher temperature of 70^oC, the precipitated asphaltenes that formed from the colloidal suspension particles tended to dissolve in the oil; thus, more asphaltenes formed in a soluble condition but fewer formed under colloidal conditions.
- The advanced analysis of chromatography of the crude oil showed that miscible CO_2 injections (i.e., 1750 and 2000 psi) led to more intermediate and high components of crude oil compared to immiscible conditions (i.e., 750 psi and 1250

psi). Also, microscopy and SEM advanced imaging revealed the impact of asphaltene accumulation on pore clogging. The results showed that when the pressure increased, pore clogging increased along with a reduction in pore size, especially in 50-nm filter paper membranes.

REFERENCES

Abutaqiya, M. I., Sisco, C. J., & Vargas, F. M. (2019). A Linear Extrapolation of Normalized Cohesive Energy (LENCE) for fast and accurate prediction of the asphaltene onset pressure. Fluid Phase Equilibria, 483, 52-69. https://doi.org/10.1016/j.fluid.2018.10.025

Afra, S., Samouei, H., Golshahi, N., & Nasr-El-Din, H. (2020). Alterations of asphaltenes chemical structure due to carbon dioxide injection. Fuel, 272, 117708. https://doi.org/10.1016/j.fuel.2020.117708

Ali, S. I., Lalji, S. M., Haneef, J., Ahsan, U., Tariq, S. M., Tirmizi, S. T., & Shamim, R. (2021). Critical analysis of different techniques used to screen asphaltene stability in crude oils. Fuel, 299, 120874. https://doi.org/10.1016/j.fuel.2021.120874

Alimohammadi, S., Amin, J. S., & Nikooee, E. (2017). Estimation of asphaltene precipitation in light, medium and heavy oils: experimental study and neural network modeling. Neural Computing and Applications, 28(4), 679-694. https://doi.org/10.1007/s00521-015-2097-3

Alimohammadi, S., Zendehboudi, S., & James, L. (2019). A comprehensive review of asphaltene deposition in petroleum reservoirs: Theory, challenges, and tips. Fuel, 252, 753-791. https://doi.org/10.1016/j.fuel.2019.03.016

Alizadeh, A., Nakhli, H., Kharrat, R., & Ghazanfari, M. H. (2011). An experimental investigation of asphaltene precipitation during natural production of heavy and light oil reservoirs: The role of pressure and temperature. Petroleum science and technology, 29(10), 1054-1065. https://doi.org/10.1080/10916460903530531

Altawati, F. S. (2016). An experimental study of the effect of water saturation on cyclic N_2 and CO_2 injection in shale oil reservoir (Master thesis). http://hdl.handle.net/2346/68030

Alves, C. A., Romero Yanes, J. F., Feitosa, F. X., & de Sant'Ana, H. B. (2019). Effect of Temperature on Asphaltenes Precipitation: Direct and Indirect Analyses and Phase Equilibrium Study. Energy & Fuels, 33(8), 6921-6928. https://doi.org/10.1021/acs.energyfuels.9b00408

Amao, A. M., Siddiqui, S., & Menouar, H. (2012, January). A new look at the minimum miscibility pressure (MMP) determination from slimtube measurements. In SPE Improved Oil Recovery Symposium. Society of Petroleum Engineers. https://doi.org/10.2118/153383-MS

Behbahani TJ, Ghotbi C, Taghikhani V, Shahrabadi A. Experimental investigation and thermodynamic modeling of asphaltene precipitation. Scientia Iranica C 2011; 18(6):1384–90. https://doi.org/10.1016/j.scient.2011.11.006

Branco, V. A. M., Mansoori, G. A., Xavier, L. C. D. A., Park, S. J., & Manafi, H. (2001). Asphaltene flocculation and collapse from petroleum fluids. Journal of Petroleum Science and Engineering, 32(2-4), 217-230. https://doi.org/10.1016/S0920-4105(01)00163-2

Cao, M., & Gu, Y. (2013). Oil recovery mechanisms and asphaltene precipitation phenomenon in immiscible and miscible CO_2 flooding processes. Fuel, 109, 157-166. https://doi.org/10.1016/j.fuel.2013.01.018

Carvalhal, A. S., Costa, G. M., & de Melo, S. A. V. (2021). Full factorial sensitivity analysis of asphaltene precipitation and deposition in CO_2 and CH_4 coreflooding. Journal of Petroleum Science and Engineering, 197, 108098. https://doi.org/10.1016/j.petrol.2020.108098

Chandio, Z. A., Ramasamy, M., & Mukhtar, H. B. (2015). Temperature effects on solubility of asphaltenes in crude oils. Chemical Engineering Research and Design, 94, 573-583.

Chung, T. H. (1992, January). Thermodynamic modeling for organic solid precipitation. In SPE Annual Technical Conference and Exhibition. Society of Petroleum Engineers. https://doi.org/10.2118/24851-MS

Dashti, H., Zanganeh, P., Kord, S., Ayatollahi, S., & Amiri, A. (2020). Mechanistic study to investigate the effects of different gas injection scenarios on the rate of asphaltene deposition: An experimental approach. Fuel, 262, 116615. https://doi.org/10.1016/j.fuel.2019.116615

Ekundayo, J. M., & Ghedan, S. G. (2013, September). Minimum miscibility pressure measurement with slim tube apparatus-how unique is the value?. In SPE Reservoir Characterization and Simulation Conference and Exhibition. Society of Petroleum Engineers. https://doi.org/10.2118/165966-MS

Elwegaa, K., & Emadi, H. (2019). Improving oil recovery from shale oil reservoirs using cyclic cold nitrogen injection–An experimental study. Fuel, 254, 115716. https://doi.org/10.1016/j.fuel.2019.115716

Elturki, M., & Imqam, A. (2020a, July). High Pressure-High Temperature Nitrogen Interaction with Crude Oil and Its Impact on Asphaltene Deposition in Nano Shale Pore Structure: An Experimental Study. In SPE/AAPG/SEG Unconventional Resources Technology Conference. https://doi.org/10.15530/urtec-2020-3241

Elturki, M., & Imqam, A. (2020b, June). Application of Enhanced Oil Recovery Methods in Unconventional Reservoirs: A Review and Data Analysis. In 54th US Rock Mechanics/Geomechanics Symposium.

Elturki, M., McElroy, P. D., Li, D., Kablan, A., & Shaglouf, H. (2021, June). Simulation Study Investigating the Impact of Carbon Dioxide Foam Fracturing Fluids on Proppant Transport. In SPE Trinidad and Tobago Section Energy Resources Conference. https://doi.org/10.2118/200950-MS

Elturki, M., & Imqam, A. (2021a). Asphaltene Thermodynamic Flocculation during Immiscible Nitrogen Gas Injection. SPE Journal, 26(05), 3188-3204. https://doi.org/10.2118/206709-PA

Elturki, M., & Imqam, A. (2021b, November). An Experimental Study Investigating the Impact of Miscible and Immiscible Nitrogen Injection on Asphaltene Instability in Nano Shale Pore Structure. In SPE International Conference on Oilfield Chemistry. https://doi.org/10.2118/204294-MS

Elturki, M., & Imqam, A. (2021c, June). Analysis of Nitrogen Minimum Miscibility Pressure MMP and Its Impact on Instability of Asphaltene Aggregates-An Experimental Study. In SPE Trinidad and Tobago Section Energy Resources Conference. https://doi.org/10.2118/200900-MS

Elturki, M., & Imqam, A. (2022a). Asphaltene Thermodynamic Precipitation during Miscible Nitrogen Gas Injection. SPE journal, 27(01), 877-894. https://doi.org/10.2118/208588-PA

Elturki, M., & Imqam, A. (2022b, March). An Experimental Investigation of Asphaltene Aggregation Under Carbon Dioxide Injection Flow in Ultra-Low-Permeability Pore Structure. In SPE Canadian Energy Technology Conference. https://doi.org/10.2118/208950-MS

Espinoza Mejia, J. E., Li, X., & Zheng, R. (2022, February). Experimental Study of Asphaltene Precipitation and Deposition During Immiscible CO_2-EOR Process. In SPE International Conference and Exhibition on Formation Damage Control. https://doi.org/10.2118/208802-MS

Goual L (2012) Petroleum asphaltenes, crude oil emulsions composition stability and characterization. ISBN: 978-953-51-0220-5

Guzmán, R., Rodríguez, S., Torres-Mancera, P., & Ancheyta, J. (2020). Evaluation of Asphaltene Stability of a Wide Range of Mexican Crude Oils. Energy & Fuels. https://doi.org/10.1021/acs.energyfuels.0c03301

Hajizadeh, N., Moradi, G., & Ashoori, S. (2020). Experimental Investigation and Modelling of Asphaltene Precipitation during Gas Injection. Journal of Chemical and Petroleum Engineering, 54(2), 223-234. https://doi.org/10.22059/JCHPE.2020.291688.1299

Hassanpouryouzband, A. et al (2020). Gas hydrates in sustainable chemistry. Chemical Society Reviews, 49(15), 5225-5309. https://doi.org/10.1039/C8CS00989A

Hassanpouryouzband, A., Joonaki, E., Taghikhani, V., Bozorgmehry Boozarjomehry, R., Chapoy, A., & Tohidi, B. (2017). New two-dimensional particle-scale model to simulate asphaltene deposition in wellbores and pipelines. Energy & Fuels, 32(3), 2661-2672. https://doi.org/10.1021/acs.energyfuels.7b02714

Hashmi, S. M., & Firoozabadi, A. (2010, September). Effect of dispersant on asphaltene suspension dynamics: aggregation and sedimentation. In SPE Annual Technical Conference and Exhibition. https://doi.org/10.2118/135599-MS

Hoepfner, M. P., Limsakoune, V., Chuenmeechao, V., Maqbool, T., & Fogler, H. S. (2013). A fundamental study of asphaltene deposition. Energy & fuels, 27(2), 725-735. https://doi.org/10.1021/ef3017392

Jafari Behbahani, T., Ghotbi, C., Taghikhani, V., & Shahrabadi, A. (2012). Investigation on asphaltene deposition mechanisms during CO_2 flooding processes in porous media: a novel experimental study and a modified model based on multilayer theory for asphaltene adsorption. Energy & fuels, 26(8), 5080-5091. https://doi.org/10.1021/ef300647f

Jamaluddin, A. K. M., Joshi, N., Iwere, F., & Gurpinar, O. (2002, January 1). An Investigation of Asphaltene Instability Under Nitrogen Injection. Society of Petroleum Engineers. https://doi.org/10.2118/74393-MS

Kar, T., Naderi, K., & Firoozabadi, A. (2020). Asphaltene Deposition and Removal in Flowlines and Mitigation by Effective Functional Molecules. SPE Journal. https://doi.org/10.2118/199878-PA

Khalaf, M. H., & Mansoori, G. A. (2019). Asphaltenes aggregation during petroleum reservoir air and nitrogen flooding. Journal of Petroleum Science and Engineering, 173, 1121-1129. https://doi.org/10.1016/j.petrol.2018.10.037

Liu, J., Sheng, J. J., Emadibaladehi, H., & Tu, J. (2021). Experimental study of the stimulating mechanism of shut-in after hydraulic fracturing in unconventional oil reservoirs. Fuel, 300, 120982. https://doi.org/10.1016/j.fuel.2021.120982

Li, Z., & Firoozabadi, A. (2010). Cubic-plus-association equation of state for asphaltene precipitation in live oils. Energy & fuels, 24(5), 2956-2963. https://doi.org/10.1021/ef9014263

Luo, P., Luo, W., & Li, S. (2017). Effectiveness of miscible and immiscible gas flooding in recovering tight oil from Bakken reservoirs in Saskatchewan, Canada. Fuel, 208, 626-636. https://doi.org/10.1016/j.fuel.2017.07.044

Madhi, M., Kharrat, R., & Hamoule, T. (2018). Screening of inhibitors for remediation of asphaltene deposits: Experimental and modeling study. Petroleum, 4(2), 168-177. https://doi.org/10.1016/j.petlm.2017.08.001

Melendez-Alvarez, A. A., Garcia-Bermudes, M., Tavakkoli, M., Doherty, R. H., Meng, S., Abdallah, D. S., & Vargas, F. M. (2016). On the evaluation of the performance of asphaltene dispersants. Fuel, 179, 210-220. https://doi.org/10.1016/j.fuel.2016.03.056

Milad, M., Junin, R., Sidek, A., Imqam, A., & Tarhuni, M. (2021). Huff-n-puff technology for enhanced oil recovery in shale/tight oil reservoirs: Progress, gaps, and perspectives. Energy & Fuels, 35(21), 17279-17333.

Mohammed, I., Mahmoud, M., Al Shehri, D., El-Husseiny, A., & Alade, O. (2021). Asphaltene precipitation and deposition: A critical review. Journal of Petroleum Science and Engineering, 197, 107956. https://doi.org/10.1016/j.petrol.2020.107956

Mohammadi, S., Rashidi, F., Mousavi-Dehghani, S. A., & Ghazanfari, M. H. (2016). On the effect of temperature on precipitation and aggregation of asphaltenes in light live oils. The Canadian Journal of Chemical Engineering, 94(9), 1820-1829. https://doi.org/10.1002/cjce.22555

Moradi, S., Dabir, B., Rashtchian, D., & Mahmoudi, B. (2012). Effect of miscible nitrogen injection on instability, particle size distribution, and fractal structure of asphaltene aggregates. Journal of dispersion science and technology, 33(5), 763-770. https://doi.org/10.1080/01932691.2011.567878

Nascimento, F. P. et al. (2021). An experimental and theoretical investigation of asphaltene precipitation in a crude oil from the Brazilian pre-salt layer under CO_2 injection. Fuel, 284, 118968. https://doi.org/10.1016/j.fuel.2020.118968

Negahban, S., Bahamaish, J. N. M., Joshi, N., Nighswander, J., & Jamaluddin, A. K. M. (2005). An experimental study at an Abu Dhabi reservoir of asphaltene precipitation caused by gas injection. SPE Production & Facilities, 20(02), 115-125. https://doi.org/10.2118/80261-PA

Pereira, J. C., López, I., Salas, R., Silva, F., Fernández, C., Urbina, C., & López, J. C. (2007). Resins: The molecules responsible for the stability/instability phenomena of asphaltenes. Energy & fuels, 21(3), 1317-1321.

Punase, A., Prakoso, A., & Hascakir, B. (2016, May). The polarity of crude oil fractions affects the asphaltenes stability. In SPE Western Regional Meeting. https://doi.org/10.2118/180423-MS

Shahriar M (2014) The aggregation of asphaltene molecules as a function of carbon dioxide concentration (PhD Dissertation). Texas Tech University. https://hdl.handle.net/2346/87013

Shen, Z., & Sheng, J. J. (2017). Experimental study of permeability reduction and pore size distribution change due to asphaltene deposition during CO_2 huff and puff injection in Eagle Ford shale. Asia-Pacific Journal of Chemical Engineering, 12(3), 381-390. https://doi.org/10.1002/apj.2080

Shen, Z., & Sheng, J. J. (2018). Experimental and numerical study of permeability reduction caused by asphaltene precipitation and deposition during CO_2 huff and puff injection in Eagle Ford shale. Fuel, 211, 432-445. https://doi.org/10.1016/j.fuel.2017.09.047

Sheng, J. J. (2015). Enhanced oil recovery in shale reservoirs by gas injection. Journal of Natural Gas Science and Engineering, 22, 252-259. https://doi.org/10.1016/j.jngse.2014.12.002

Shi, B. et al (2021). Status of Natural Gas Hydrate Flow Assurance Research in China: A Review. Energy & Fuels, 35(5), 3611-3658. https://doi.org/10.1021/acs.energyfuels.0c04209

Soroush, S., Pourafshary, P., & Vafaie-Sefti, M. (2014, March 31). A Comparison of Asphaltene Deposition in Miscible and Immiscible Carbon Dioxide Flooding in Porous Media. Society of Petroleum Engineers. https://doi.org/10.2118/169657-MS

Su, X., Moghanloo, R. G., Qi, M., & Yue, X. A. (2021). An Integrated Simulation Approach To Predict Permeability Impairment under Simultaneous Aggregation and Deposition of Asphaltene Particles. SPE Journal, 26(02), 959-972. https://doi.org/10.2118/205028-PA

Su, X., Moghanloo, R. G., Qi, M., & Yue, X. A. (2021). An Integrated Simulation Approach to Predict Permeability Impairment under Simultaneous Aggregation and Deposition of Asphaltene Particles. SPE Journal, 1-14. https://doi.org/10.2118/205028-PA

Syed, F. I., Neghabhan, S., Zolfaghari, A., & Dahaghi, A. K. (2020). Numerical Validation of Asphaltene Precipitation and Deposition during CO_2 miscible flooding. Petroleum Research, 5(3), 235-243.

Tavakkoli, M., Panuganti, S. R., Taghikhani, V., Pishvaie, M. R., & Chapman, W. G. (2014). Precipitated asphaltene amount at high-pressure and high-temperature conditions. Energy & fuels, 28(3), 1596-1610. https://doi.org/10.1021/ef401074e

Wang, P., Zhao, F., Hou, J., Lu, G., Zhang, M., & Wang, Z. (2018). Comparative analysis of CO_2, N_2, and gas mixture injection on asphaltene deposition pressure in reservoir conditions. Energies, 11(9), 2483. https://doi.org/10.3390/en11092483

Zanganeh, P., Dashti, H., & Ayatollahi, S. (2018). Comparing the effects of CH_4, CO_2, and N_2 injection on asphaltene precipitation and deposition at reservoir condition: A visual and modeling study. Fuel, 217, 633-641. https://doi.org/10.1016/j.fuel.2018.01.005

Zanganeh, P., Ayatollahi, S., Alamdari, A., Zolghadr, A., Dashti, H., & Kord, S. (2012). Asphaltene deposition during CO_2 injection and pressure depletion: a visual study. Energy & fuels, 26(2), 1412-1419. https://doi.org/10.1021/ef2012744

Zheng, T. et al. Understanding Immiscible Natural Gas Huff-N-Puff Seepage Mechanism in Porous Media: A Case Study of CH_4 Huff-N-Puff by Laboratory Numerical Simulations in Chang-7 Tight Core. Nat Resour Res (2021). https://doi.org/10.1007/s11053-021-09836-2

Zoback, M. D., & Kohli, A. H. (2019). Unconventional reservoir geomechanics. Cambridge University Press.

Zolghadr, A., Escrochi, M., & Ayatollahi, S. (2013). Temperature and composition effect on CO_2 miscibility by interfacial tension measurement. Journal of Chemical & Engineering Data, 58(5), 1168-1175. https://doi.org/10.1021/je301283e

V. ASPHALTENE PRECIPITATION AND DEPOSITION DURING NITROGEN GAS CYCLIC MISCIBLE AND IMMISCIBLE INJECTION IN EAGLE FORD SHALE AND ITS IMPACT ON OIL RECOVERY

Mukhtar Elturki and Abdulmohsin Imqam

Missouri University of Science and Technology

ABSTRACT

Cyclic gas injection methods have been shown to improve oil recovery in conventional reservoirs. Even though similar technologies have been used in unconventional reservoirs with some success stories in shale resources, cyclic gas injection enhanced oil recovery (EOR) is still a little-understood subject in boosting oil recovery from unconventional reservoirs. During gas injection, asphaltenes starts to deposit and precipitate which causes pore plugging and reduces oil recovery. Studies of asphaltene deposition challenges during cyclic nitrogen (N_2) gas injection and oil production in unconventional reservoirs are yet relatively limited. Therefore, a comprehensive experimental study was conducted using 12 Eagle Ford shale cores (dynamic mode) and filter paper membranes (static mode) were used to evaluate whether miscible and immiscible huff-n-puff (cyclic) N_2 injection increases oil recovery and aggravates asphaltene precipitation. To ensuring that the miscibility can be examined in cycle experiments, the N_2 minimum miscibility pressure (MMP) was determined using the slim tube technique. The factors studied included the injection pressure, number of cycles, production time, and injection cyclic mode all conducted at 70°C. The findings showed that a high asphaltene weight percent was calculated during the static experiments (i.e.,

using filter membranes) and this increase was severe on smaller pore size structures. Dynamic tests (i.e., using shale cores) showed that miscibility increased the oil recovery, but a stronger intermediate wet system was observed when measuring the wettability of cores after N_2 cyclic tests. When starting with shorter soaking times, more oil recovery could be achieved. Oil recovery reduction and asphaltene depositions were observed at the later cycles. Microscopy and scanning electron microscopy (SEM) imaging of the Eagle Ford cores showed asphaltene clusters inside the cores after cyclic tests. A mercury porosimeter emphasized the degree of the pore plugging after the cyclic tests, and the findings revealed a smaller pore size distribution after N_2 tests due to the asphaltene deposition process when compared to cores that had not been pressured. This extensive study focuses on the effects of asphaltene deposition on oil recovery under cyclic N_2 miscible and immiscible conditions in shale resources.

1. INTRODUCTION

Gas injection has been a widely used technology for increasing oil production in unconventional shale plays in the United States, and it may be the most efficient approach for unlocking the remaining oil percentage. Unconventional resources, like shale reservoirs, are widely recognized for their extremely low permeability and porosity (Elturki and Imqam, 2020a). Despite multistage hydraulic fracturing and horizontal well drilling techniques are used to extract remaining oil from such reservoirs, only 4 to 6 percent of the trapped oil can be extracted, and oil production drops after a few months attributing to the ultra-low permeability (Warpinski et al., 2009; Sheng, 2015; Zoback and Kohli, 2019;

Ahmed et al., 2019; 2020; Ahmed S., 2020; Liu et al., 2021; Elturki et al., 2021). Water injection is also one of the suitable strategies for increasing oil recovery from conventional reservoirs; nevertheless, due to weak injectivity, insufficient sweep potency, and clay swelling concerns, this approach is not the ideal solution for tight reservoirs. (Yang et al., 2013; Ahmad et al., 2019). Cyclic gas injection outperforms gas flooding methods in terms of enhancing oil recovery, mainly in ultra-tight reservoirs (Milad et al., 2021; Tang and Sheng, 2022). The total organic carbon (TOC) is the most important influencing parameter on gas injection in tight reservoirs because kerogen makes the surface of the pore oil-wet, making the oil inside challenging to extract (Jia et al., 2019). Due to the combination of multiphase fluids (i.e., gas, oil, condensate, and water) and scales, multiphase flow production can create a number of challenges including wax and asphaltene deposition, hydrate formation, slugging, and emulsions (Shi et al., 2021). Organic hydrocarbon particles settling in oil and gas reservoirs might create many flow assurance problems throughout the extraction process. These materials may increase flow resistance, causing production reduction or even pipeline plugging (Hassanpouryouzband et al., 2020; Ali et al., 2021). Crude oil is a complicated composition of hydrocarbons with different molecular weights and organic components such as asphaltenes and wax. Asphaltene is a solid phase in crude oil that is soluble in toluene but insoluble in light n-alkanes like n-pentane or n-heptane. The injected gas reacts with the oil in the shale reservoir, causing the asphaltene inside the crude oil to become more unstable. Throughout most of the gas injection process, the gas alters the composition of crude oil, causing the oil's solubility to change. As a result of the instability of the colloidal suspension in crude oil, asphaltene tends to precipitate and flocculate (Zhou et al., 2018; Elturki and Imqam, 2020b). Asphaltene can negatively affect the permeability of formations by plugging or adsorption (Behbahani et al., 2013). One of the most challenging issues in the shale gas injection process is asphaltene precipitation and deposition, which causes shale pore plugging and wettability changes in the formation.

Because of the impact of asphaltene aggregation during gas injection, several studies have been conducted focusing on cyclic gas injection in conventional reservoir cores (Turta et al., 1997; Sim et al., 2005; Hamadou et al., 2008; Behbahani et al., 2014; Mehana et al., 2019; Lo et al., 2022). Others investigated the stability of asphaltene under carbon dioxide (CO_2) gas injection and different factors were studied (Afra et al., 2020; Elturki and Imqam, 2022a; 2022c; Espinoza et al., 2022). There have been very little studies employing N_2 gas injection to illustrate the severity of asphaltene deposition and precipitation, as well as the factors influencing its stability (Jamaluddin et al., 2002; Zadeh et al., 2011; Moradi et al., 2012; Khalaf and Mansoori, 2019; Elturki and Imqam, 2021a; 2021b). Jamaluddin et al. (2002) examined the asphaltene stability by contacting various molar concentrations of N_2 with the reservoir fluids and the findings revealed that increasing the concentration of N_2 negatively impacted the instability of asphaltene and increased the quantity of bulk precipitated asphaltene. Zadeh et al. (2011) designed an experimental study to evaluate the effect of N_2 and methane on asphaltene precipitation under high-pressure and high-temperature conditions. Their findings demonstrated that the asphaltene precipitation was higher under N_2 gas injection than methane, and temperature had less impact compared to pressure and gas concentrations. Moradi et al. (2012) used high-pressure filtration technique to study asphaltene particle precipitation, aggregation, and breakup using natural depletion and miscible N_2 injection processes. The results showed that N_2 severely destabilizes asphaltenes, and the issue was worsened in heavier crude samples. Khalaf and Mansoori (2019) conducted a simulation study to highlight the impact of using misciblized air and N_2 on asphaltene aggregation. They claimed that the aggregations of asphaltene influenced by the concentration of the injected gas, and the difference between asphaltene aggregations using air and N_2 was not significant. Elturki and Imqam (2021a) conducted an experimental study to investigate the effect of miscible and immiscible N_2 injections on asphaltene deposition using filter paper membranes. They found that miscibility of N_2 resulted in a high asphaltene weight percentage, especially in smaller pore structures.

Most of reported studies of cyclic injection EOR were implemented extensively using CO_2 in shale and tight reservoirs (Abedini et al., 2014; Yu W. et al., 2015; Li et al., 2019; Elwegaa et al., 2019; Zhu Z. et al., 2020; Badrouchi et al., 2022; Louk et al., 2017; Sheng et al., 2014; Sanchez-Rivera et al., 2015; Sun et al., 2016; Wang et al., 2019; Luo et al., 2022; Altawati et al., 2022; Wan et al., 2022) and others used lean gas, methane, rich gas, or gas mixture (Zheng et al., 2021; Baek et al., 2021; Mahzari et al., 2021; Sie et al., 2022; Shilov et al., 2022). Very little research was conducted using cyclic N_2 injection (Yu and Sheng 2015; Altawati, F.S., 2016; Yu et al., 2017; Elwegaa and Emadi 2019; Xiong et al., 2022). Yu and Sheng (2015) conducted an experimental study using N_2 and Eagle Ford shale cores. They soaked the cores in mineral oil before conducting the experiments. Their findings revealed that N_2 was efficient in improving oil recovery with the majority of oil produced within the first two hours of production time during the puff stage. Their study's weakness was that they employed mineral oil rather than crude oil, which ignores the influence of asphaltene precipitation on oil recovery. Altawati (2016) saturated several Eagle Ford cores with decane oil and 15% NaCl brine water to study the effect of water saturation on oil recovery utilizing the cyclic CO_2 and N_2 processes. The findings concluded that the partially saturated cores with water gave less recovery factor compared to cores with no water. The drawback of this study is also ignoring impact of asphaltene deposition. Li et al. (2017) investigated the effect of the minimum miscibility pressure (MMP) on oil recovery during the CO_2 cyclic process. They estimated the MMP for a Wolfcamp crude oil using the slim tube method. Wolfcamp cores were used in all the 15 experiments conducted, and the results showed an increase in oil recovery when injecting pressure higher than the MMP. Tovar et al. (2021) conducted several experiments using 11 Wolfcamp shale cores to investigate the effect of CO_2 and N_2 injection on oil recovery. They investigated various factors including MMP, soaking time, and injection-gas composition. The results showed that CO_2 injection led to more oil recovery compared to N_2 because the CO_2 had the ability to vaporize more hydrocarbon components. Higher pressure and longer soaking time led to higher oil recovery even beyond miscibility conditions for CO_2. Bougre et al. (2021) conducted an experimental investigation to study the effect of flooding with CO_2, N_2 and a CO_2-N_2 mixture on the oil recovery in tight formations. The same core sample was used in all experiments and saturated with live oil from the Eagle Ford formation. For each trial, the sample was cleaned and resaturated. Their results showed higher oil recovery during CO_2 gas injection, followed by the N_2–CO_2 mixture with longer breakthrough time. To sum up, a review of the literature shows that the impact of asphaltene due to N_2 miscible injection was not considered; hence, the oil recovery results due to the cyclic injection of N_2 is questionable. Lately, the asphaltene deposition process in tight reservoir has gained attention during CO_2 cyclic gas injection (Shen and Sheng, 2017a; 2017b; Mohammad R. S. et al., 2017; Lee et al., 2019; Shen et al., 2019; Li et al., 2020). To the best of our knowledge, no investigations or published work have focused on asphaltene aggregation and deposition under cyclic N_2 injection in tight and shale reservoirs.

Despite the fact that the aforementioned studies investigated various factors affecting the oil recovery from shale reservoirs during continuous and cyclic gas injection processes, there is a lack of a rigorous investigation on how asphaltene deposition impacts the oil recovery in shale reservoirs under miscible and immiscible N_2 cycle processes. This research extends the previous work conducted by Elturki and Imqam (2021b; 2022b), which investigated the impact of continuous immiscible and miscible N_2 injections on asphaltene precipitation. The research then studies the severity of asphaltene deposition in unconventional reservoirs due to cyclic miscible and immiscible N_2 gas injections. This extensive study provides a better knowledge of the parameters that influence asphaltene instability during N_2 miscible and immiscible injections in unconventional reservoirs.

2. MATERIALS AND METHODOLOGY

The laboratory work was divided into three sections:(1) MMP determination experiments, (2) cyclic gas injection experiments (using both filter paper membranes and shale cores), and (3) asphaltene pore plugging analysis. The first experiments established the MMP for N_2. Based on the MMP experiments, the miscible and immiscible pressures of the cyclic gas injection experiments were determined. This step was critical to ensuring that the miscibility and immiscibility of the injected gas would be studied in terms of oil recovery and asphaltene pore plugging. Further analysis of the shale cores after the cyclic gas injection experiments used scanning electron microscopy (SEM), wettability measurements, and pore size distribution measurements to highlight the severity of asphaltene deposition on pore plugging during N_2 miscible and immiscible gas injection. Figure 1 shows the experimental flowchart for the main experiments and analyses in this paper. The main materials and their supplier used in this study are summarized in Table 1. The details of materials used in each experiment will be discussed in the following sections.

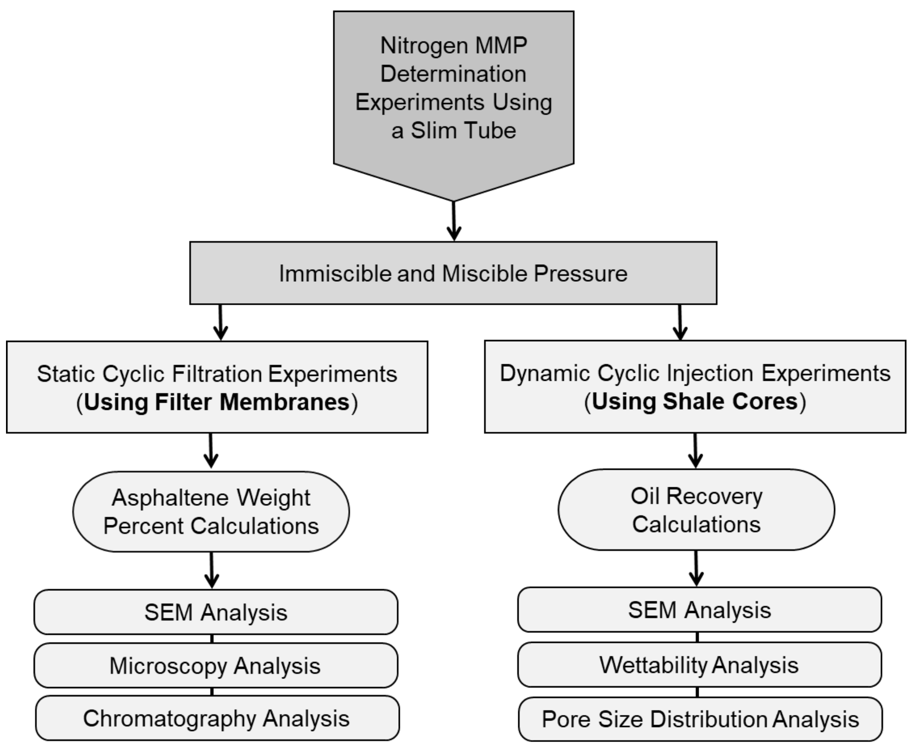

Figure 1. Experimental design flowchart.

Table 1. List of Suppliers of the Main Chemicals/Materials Used in This Study

Material	**Supplier**
n-heptane (chemical formula: C_7H_{16}, purity: ≥99%)	Lab Alley Powering
Crude oil	Western Missouri Oil Field
Whatman 2.7 μm filter paper	OFITE, Inc.
Filter paper membranes (size of 50, 100, and 450 nm)	Foxx Life Sciences, Fisher Scientific

The Eagle Ford shale outcrops were saturated with crude oil at 70^{o}C “158^{o}F” with a viscosity of 19 cp, density of 0.864 gm/cc, and ^{o}API of 32. The viscosity was measured using a rheometer, and gas chromatography-mass spectrometry (GC-MS) was utilized to determine the composition of the crude oil, as shown in Table 2. The crude oil was used in the slim tube experiments with N_2 to determine the MMP. For the cyclic filtration experiments, filter paper membranes of 450, 100, and 50 nm were used. N_2 gas cylinders of 99.9% purity were the source of gas injection to perform the slim tube and cyclic experiments. A specially designed high-pressure, high-temperature vessel (L: 15.24 cm “0.50 ft”, ID: 5 cm “0.164 ft”, OD: 7.62 cm “0.25 ft”) was employed to accommodate the cores during the cyclic experiments. An oven (model LBB2-27-2, Dispatch) was used to adjust the temperature during the MMP experiments. As shown in Figure 2, core samples from Eagle Ford shale outcrops were used in the gas cyclic experiments, with a diameter and length of 1 and 2 in., respectively. The average helium porosity was 5.7%, and the average permeability was 198 nD (0.000198 mD). The X-ray diffraction (XRD) analysis of the cores is presented in Table 3. The total organic carbon (TOC) of the cores was 5.5%, determined via Rock-Eval pyrolysis.

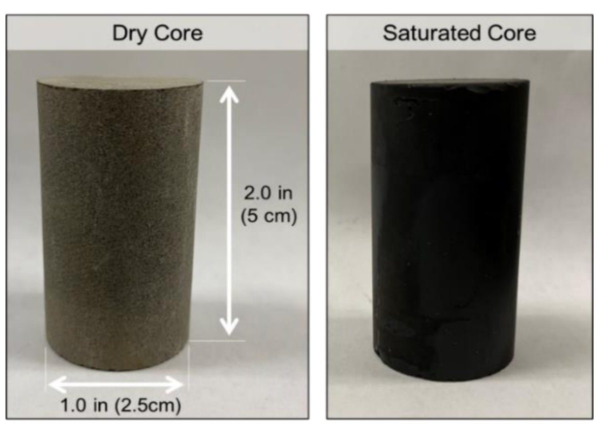

Figure 2. Sample of an Eagle Ford core plug before and after the oil saturation process.

Table 2. Crude oil composition

Composition	Mass %
C_1	0.000
C_2	0.000
C_3	0.000
C_4	0.003
C_5	0.063
C_6	0.430
C_7	0.540
C_8	64.484
C_9	0.278
C_{14}	0.309
C_{15}	0.349
C_{16}	0.425
C_{17}	3.490
C_{18}	0.196
C_{19}	1.166
C_{20}	3.596
C_{21}	0.926
C_{22}	2.662
C_{24}	1.973
C_{27}	5.395
C_{28}	7.225
C_{29}	1.322
C_{30+} (including asphaltene)	5.17
Total	100

Table 3. Eagle Ford XRD results

Mineral	Calcite	Quartz	Dolomite	Pyrite	Kaolinite
Composition (%)	70	18	2	1	9

Before the saturation process, 12 shale core samples were named and weighed with the same crude oil from the MMP experiments. An accumulator filled with crude oil was used to accommodate the shale cores, after which high pressure was injected along with high temperature from an oven being applied for 10 continuous months to ensure that the core samples are well saturated. The justification for discontinuing the experiment after 10 months was that the weight of the cores had not changed in the last two months of the saturation process, indicating that the cores had been saturated. Examples of the weight change during the saturation process are shown in Figure 3. Table 4 shows the saturated and dry weight of all cores used in this research.

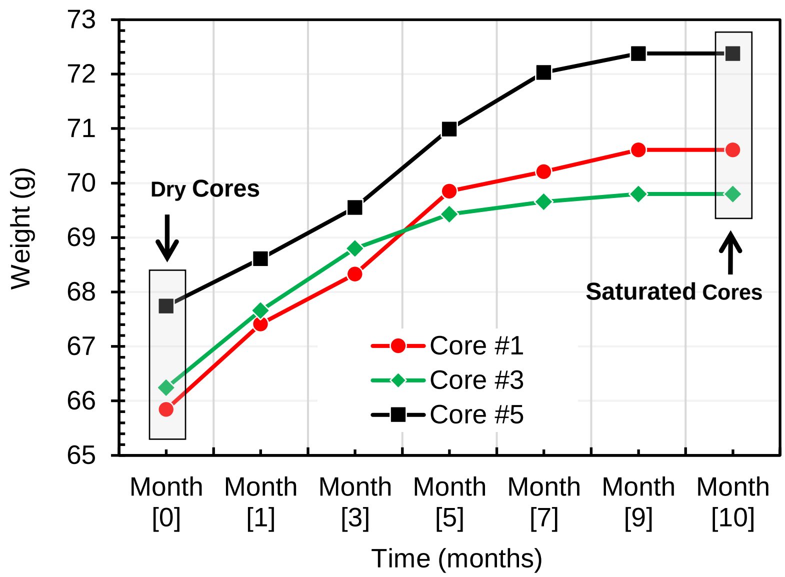

Figure 3. Three examples of core saturation process during a 10-month period.

Table 4. Dry and saturated weight of all cores.

Core No.	Dry Core (g)	Saturated Core (g)
1	65.84	70.61
2	65.54	69.33
3	66.24	69.8
4	64.25	68.64
5	67.74	72.38
6	63.05	68.47
7	57.15	61.58
8	64.16	67.97
9	60.76	64.44
10	60.44	65.12
11	64.92	67.86
12	64.21	69.02

2.1. SLIM TUBE EXPERIMENTS FOR MMP DETERMINATION.

A slim tube (L: 1310 m “42.97 ft”, ID: 0.21 cm “0.0068 ft”, OD: 0.41 cm “0.0134 ft”) packed with sand was used to perform the experiments, along with three accumulators. The permeability of the sand pack is 27.50 Darcy. Figure 4 shows the main components of the slim tube apparatus. The three main steps in slim tube experiments are (1) slim tube cleaning, (2) saturation of the slim tube with crude oil, and (3) gas injection. Therefore, accumulator 1 contained the crude oil to saturate the slim tube; accumulator 2 was filled with a solvent of n-heptane to clean the slim tube; and accumulator 3 was filled with gas to be injected into the slim tube during the experiments. The procedure to conduct the experiments started with the slim tube, which was fully saturated with distilled water. Next, oil was injected into the slim tube at a rate of 0.25 ml/min until fully saturated. This can be observed at the outlet of the slim tube when the produced liquids were only oil, thus ensuring that the slim tube was fully saturated. During all of the experiments, a back pressure regulator was placed at the outlet with the desired pressure. The gas accumulator was filled with N_2. Then, gas was injected at a predetermined pressure using the constant pressure mode of the syringe pump. Each experiment was stopped when 1.2 PV of gas had been injected or when the gas broke through. The produced oil was collected from the effluent. The MMP can be determined by plotting the gas injection pressure versus the cumulative oil recovery. Finally, after each experiment, the solvent xylene was used to clean the slim tube setup and guarantee that no oil remained in the slim tube to impact the following experiment.

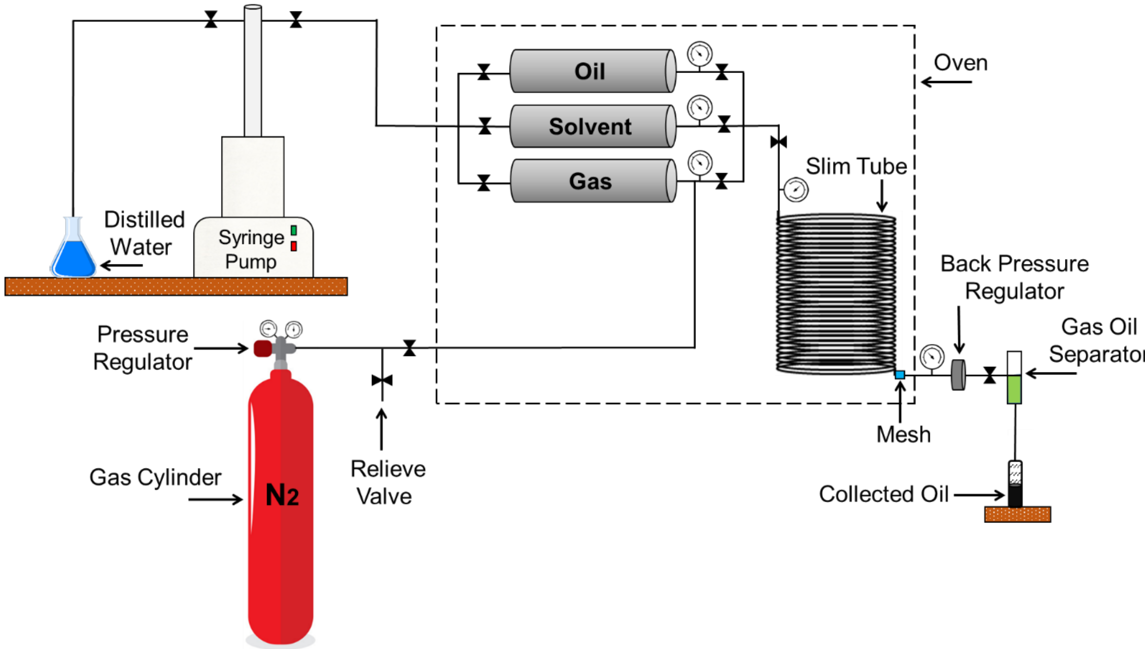

Figure 4. Schematic of the setup of the N_2 MMP determination apparatus using the slim tube technique.

2.2. GAS CYCLIC EXPERIMENTS USING FILTRATION TECHNIQUE

Figure 5 illustrates the main components of the cyclic gas process utilizing filter paper membranes. The main principle of filtration experiments is to understand the asphaltene deposition in a controlled pore size structure and the factors that may impact the process which then gives an idea about the process when using real shale cores. The primary component was a high-purity N_2 cylinder with pressure regulators to adjust the cylinder pressure. Because the outlet pressure of the N_2 cylinder was limited, a gas accumulator was utilized to collect the gas and inject it into the vessel using a syringe pump to achieve higher pressures if needed. Filter paper membranes (i.e., 50, 100, and 450 nm) were employed to mimic the shale reservoir structure and to investigate the effect of various pore sizes. A high-pressure high-temperature filtration vessel was designed to accommodate three mesh screens to support the filter membranes and prevent them from folding under high pressure. The mesh screens were designed with small holes that allowed the oil to pass through easily. Spacers between each mesh screen were added to support each screen in place, and rubber O-rings were placed above and below each spacer to prevent leakage and to ensure that the oil and gas would pass through the filter paper membranes. The injection and production lines were located on the top of the vessel for the cyclic technique. Finally, one transducer was installed on the top of the filtration vessel and connected to a computer to monitor and accurately record the injection pressure. The following procedure was followed to conduct the cyclic gas injection experiments using the filtration technique:

- The filter paper membranes were placed inside the vessel in the following order: 50 nm at the bottom, 100 nm in the center, and 450 nm at the top. Mesh screens and spacers were supported all filter paper membranes.
- The vessel was then sealed and connected to the system and the gas cylinder.
- The gas cylinder was opened to fill the gas accumulator. Then, the gas cylinder was closed using the pressure regulator.
- Crude oil (30 ml) was pumped into the vessel using a syringe pump linked to the oil accumulator, after which the gas was injected into the vessel at the predetermined pressure.
- The gas was allowed to interact with the crude oil inside the vessel for a predetermined soaking time (i.e., 6 h); this step is referred to as the “huff” stage.

- A heating jacket was turned on around the vessel to increase the temperature to the desired level (i.e., 70^{o}C).
- The vessel was depressurized after completing the soaking time. This step is referred to as the “puff” stage.
- The produced oil was collected from the effluent, after which, the vessel was opened, and a sample of the filtered crude oil was collected from each filter membrane for asphaltene analysis. Then, the collected filtered oil on each filter paper membrane was returned carefully for a new cycle.
- All of the above steps were repeated for a new cyclic process without changing the filter membranes.

The oil samples (1 ml) obtained from each filter membrane were mixed in test tubes after each cycle with the solvent n-heptane (40 ml) at a ratio of 1:40 for the asphaltene weight percent measurements. After the asphaltene was fully deposited in the test tube, the mixture was filtered using filter paper (2.7 µm). Weighing the filter paper before and after the filtration process quantified the asphaltene weight percent. Using the following equation, the difference between these weights determined the asphaltene weight percent.

$$\text{Asphaltene wt\%} = \frac{\text{wt}_{\text{asphaltene}}}{\text{wt}_{\text{oil}}} * 100 \tag{1}$$

Where asphaltene wt% is the asphaltene weight percent, wt asphaltene is the asphaltene weight on the filter paper, and wt oil is the oil sample weight.

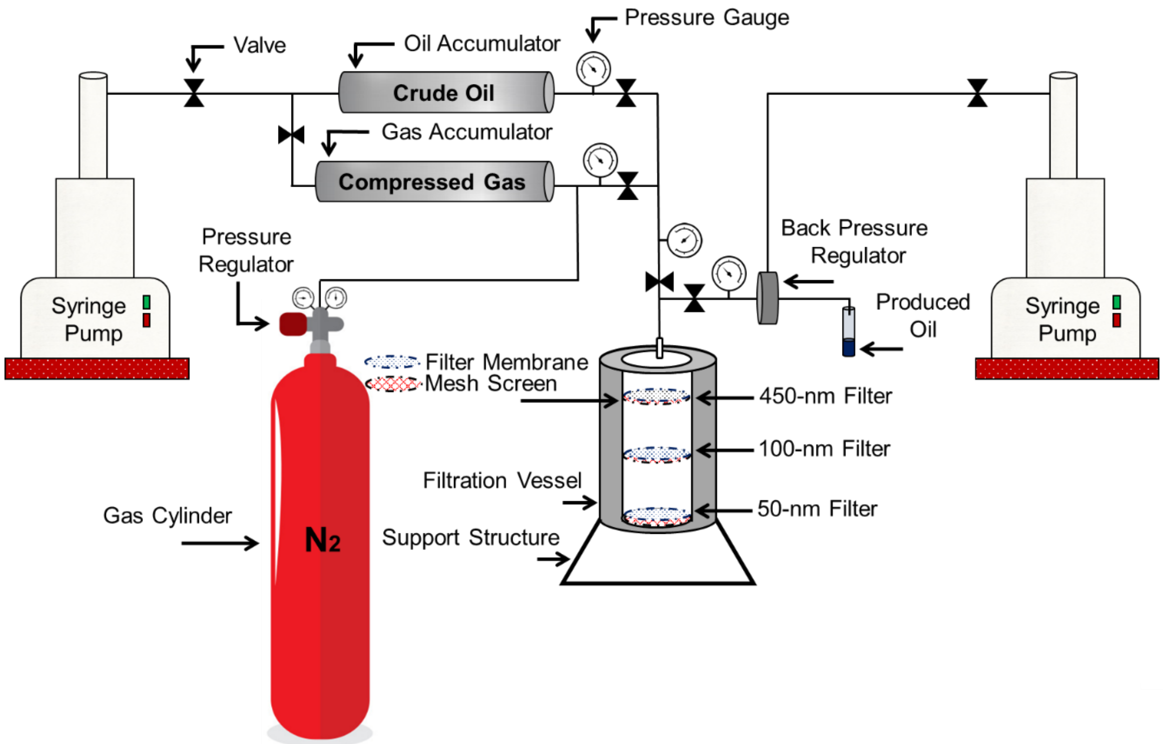

Figure 5. Illustration of the cyclic filtration tests setup.

2.2.1. Scope of Work for the Cyclic Filtration Technique. Four filtration experiments were designed to investigate the effect of gas injections on asphaltene in crude oil, including two experiments using two conditions (i.e., miscible and immiscible), with the pressures selected based on the previous MMP experiments. All of the experiments were conducted at 70°C to mimic the reservoir temperature, with a fixed soaking time of 6 h. These experiments were designed to provide a comprehensive evaluation of how each gas would impact the pore structure of the filter paper membranes (which represent shale unconventional reservoirs). The operating conditions are presented in Table 5.

Table 5. Operating conditions for the cyclic filtration tests at miscible and immiscible gas injections.

Test no.	**Pore size of Filter Membrane (nm)**	**Gas Injected**	**Soaking time (h)**	**Injection pressure (psi)**	**Pressure Condition**
1	450	Nitrogen (N_2)	6	1000	Immiscible
	100				
	50				
2	450		6	1750	Miscible
	100				
	50				

2.3. GAS CYCLIC EXPERIMENTS USING SHALE CORES

Based on the results of the MMP, eight experiments were conducted on eight Eagle Ford core samples at pressures above and below the N_2 MMP. The apparatus employed in the cyclic experiments is shown in Figure 6. A top view of the real vessel is shown in Figure 7.

After placing the core inside the vessel there were some spaces which were considered artificial fractures. The main components were a gas cylinder as the source of the gas injection, stainless steel high-pressure vessel to accommodate the core, syringe pump connected to the gas accumulator for storing the injected gas and increasing the pressure, and a heat jacket to mimic the temperature conditions in an actual tight reservoir.

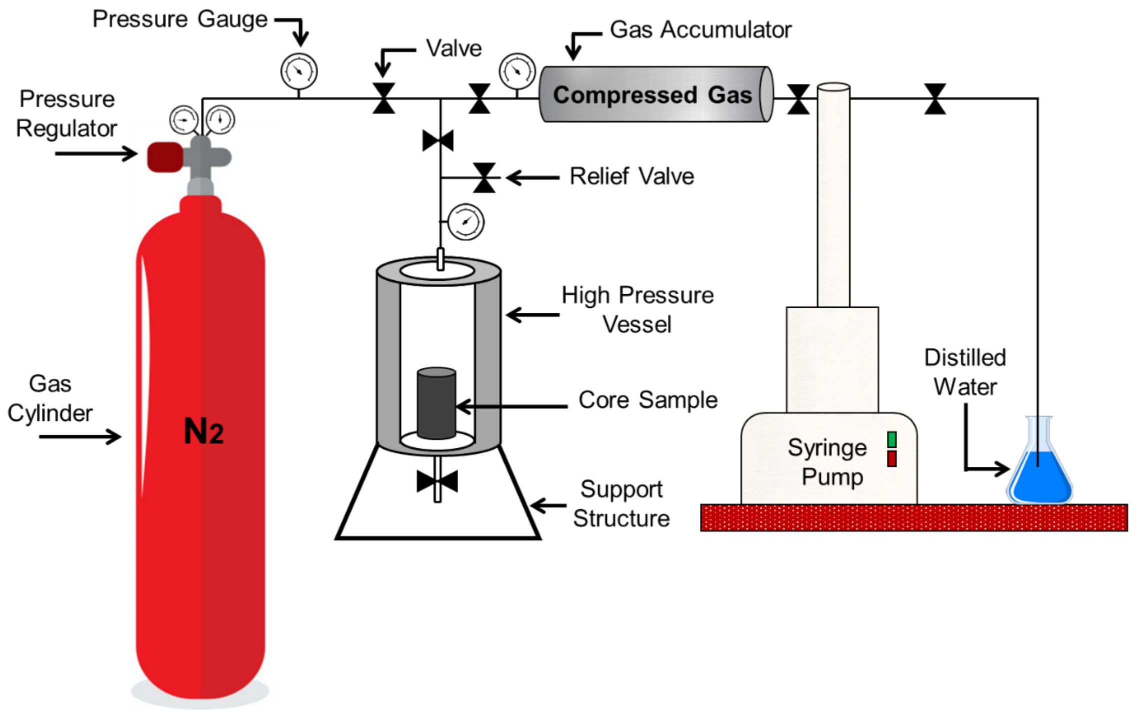

Figure 6. Cyclic experiments setup.

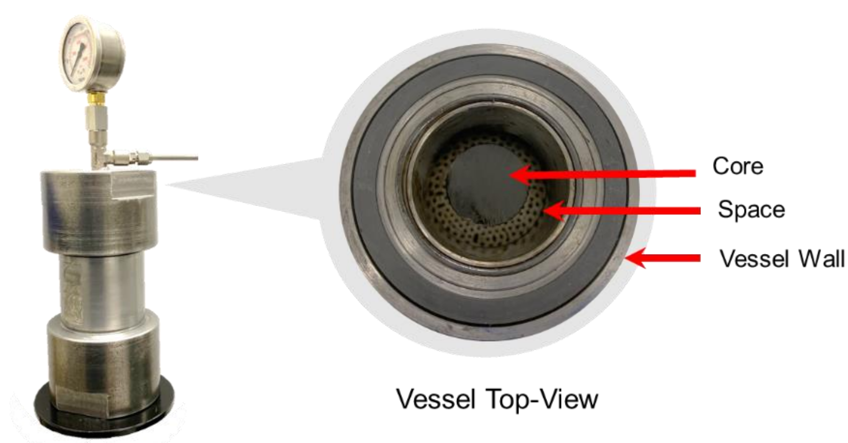

Figure 7. Top view of the real vessel.

After placing the core inside the vessel, there were some spaces, which acted as artificial fractures. The following procedure was followed to conduct the cyclic gas injection experiments:

- The saturated core was placed inside the vessel.
- The vessel was connected to the high-pressure gas cylinder and the gas accumulator; then, the vessel was secured.
- The gas was injected into the vessel at the designed pressure, and then, the gas was allowed to interact with the saturated core for a predetermined time (soaking period). This step is also called the huff stage.
- A heating jacket was turned on around the vessel to increase the temperature to the desired level.
- After the soaking time was completed, the vessel was depressurized (puff stage).
- The shale core was retrieved to calculate the oil recovery at specific production times using the change in weight method described in the following equation:

$$\text{Oil Recovery Factor} = \frac{wt_1 - wt_2}{wt_1 - wt_{dry}} \tag{2}$$

  Where wt_1 is the weight of the saturated core, wt_2 is the production time core weight, and wt_{dry} is the weight of the cores before the saturation process.

- A new gas cycle was conducted after measuring the oil recovery from the previous cycle, and the cycles were stopped when there was no oil recovery from the saturated core.
- After finishing the experiments, the shale cores were analyzed for asphaltene deposition, pore size distribution changes, and wettability alteration.

2.3.1. Scope of Work for the Gas Cyclic Process Using Shale Cores. Eight Eagle Ford shale cores were used to conduct cyclic gas injection experiments to investigate the effect of miscible and immiscible conditions for N_2 on oil recovery and asphaltene deposition. An additional four saturated cores were not exposed to gas injection and served as references (constants) to determine the wettability and pore size distribution before conducting the cyclic experiments. The effects of soaking time, production time, and injection pressure were analyzed. The operation conditions are presented in Table 6. To study the effect of the soaking time on the oil recovery, different cores underwent a gas cyclic pressure of 2000 psi and various soaking times (i.e., 1, 6, 12, and 24 h). The soaking time was investigated in two ways: using one core for all soaking times (test no. 5) and using different cores for each soaking time (tests no. 6-8) to highlight the effect of resoaking gas injections on oil recovery. (Note: this will be explained in the soaking time mode section in the results section.) All of the experiments were conducted at 70°C to mimic the reservoir temperature. In each experiment, the number of cycles was different, but the cycles were stopped when no more oil recovery occurred. The production times were selected to be 15, 60, and 90 min. for both miscible and immiscible conditions. The miscible and immiscible pressures were selected based on the slim tube experiments.

Table 6. Operating conditions for N_2 cyclic tests at miscible and immiscible gas injections.**

Test no.	Core no.	Gas Injected	Soaking time (h)	Injection pressure (psi)	Production time (min)
1	#1	Nitrogen (N_2)	6	1000	15, 60, and 90
2	#2		6	1300	
3	#3		6	1750*	
4	#4		6	2000*	
5	#5		1, 6, 12, and 24	2000*	15
6	#6		1	2000*	
7	#7		12	2000*	
8	#8		24	2000*	

* The injected gas in miscible condition

**Note: Four more cores served as references for the wettability measurement and pore size distribution determinations, with the cores numbered #9, #10, #11, and #12.

3. RESULTS AND DISCUSSION

3.1. MMP RESULTS

The minimum miscibility pressure (MMP) can be defined as the lowest pressure at which a gas can create miscibility with the reservoir oil at the reservoir temperature (Elturki and Imqam, 2021c). To investigate the effect of miscibility on the oil recovery and its impact on asphaltene deposition in shale cores during cyclic gas injection, seven experiments were conducted at pressures of 500, 750, 1000, 1250, 1500, 1750, and 2000 psi at 32 and 70°C, as shown in Figure 8. MMP experiment was conducted at 32 °C as a reference and to ensure the accuracy of the MMP results. Table 7 show the cumulative oil recovery at each injected pressure for N_2. The N_2 MMP pressures were determined to be 1600 and 1350 psi at 32 and 70°C, respectively. The results demonstrated that the MMP of N_2 was decreased when increasing the temperature due to the N_2 remaining in the gaseous phase at the same conditions and higher intermediate components of the oil (Sebastian et al., 1992; Vahidi et al., 2007; Belhaj et al., 2013; Zolghadr et al., 2013; Barati-Harooni et al., 2019). Based on the MMP results, miscible and immiscible pressures were selected to conduct the cyclic gas experiments and will be discussed in the next section.

Table 7. N_2 slim tube cumulative oil recoveries (%)

Tested injected pressure (psi)	**500**	**700**	**1000**	**1250**	**1500**	**1750**	**2000**
Cumulative OR at 32 °C	62.92	75.51	80.96	85.15	88.51	91.03	92.71
Cumulative OR at 70 °C	80.12	85.15	88.51	90.61	92.71	93.54	94.38

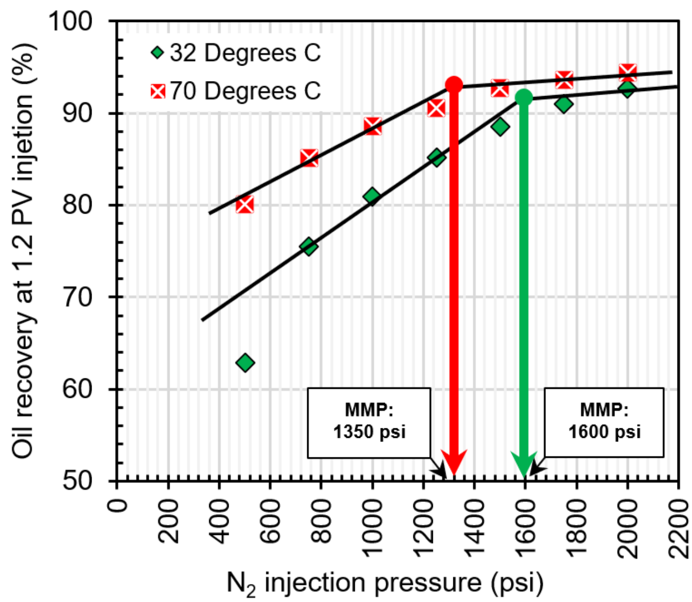

Figure 8. MMP determination using an oil viscosity of 19 cp at 32ºC and 70ºC.

3.2. RESULTS OF THE GAS CYCLIC EXPERIMENTS USING A FILTRATION TECHNIQUE

Two sets of cyclic experiments were conducted using the cyclic filtration technique. An immiscible pressure of 1000 psi and a miscible pressure of 1750 psi were used to evaluate asphaltene instability under immiscible and miscible scenarios. The soaking time was fixed at 6 h, and the temperature was 70ºC. Figure 9 shows the results of the N_2 cyclic filtration experiments, demonstrating that asphaltene in crude oil was altered at different degrees of aggregations by N_2 in the first two cycles in all the filter paper membranes. For the immiscible N_2 pressure of 1000 psi, the asphaltene weight percent increased slightly in 450-nm filter from 5.56 to 5.84% from the first to second cycles, respectively. The asphaltene weight percent increased slightly as the number of cycles increased until it started to stabilize in the fifth cycle which indicated that the asphaltene clusters and particles were impacted at a higher rate in the earlier cycles. A higher asphaltene weight percent was observed on the 50-nm filter due to its smaller pore size structure. In the 50-nm filter, the asphaltene weight precent increased from 9.16 to 11.88 % for the first and the fourth cycles, respectively. In the fifth cycle, the asphaltene weight precent increased slightly to 12.20% and then stabilized. On the other hand, the miscible N_2 pressure of 1750 psi increased the asphaltene weight percent much more in the all-filter paper membranes, which revealed that miscibility had significantly weakened the bonds between the asphaltene clusters and resins inside the crude oil. For instance, the asphaltene weight percent in the 50-nm filter in the first cycle was 20.19% and then increased significantly to 26.73% in the fourth cycle. Then, the asphaltene weight percent was almost stable at 27.46% in all of the next cycles.

In summary, for all cyclic tests, asphaltene weight percent increased as the pore size of the filter membranes decreased, and number of gas injection cycles increased. The results showed that the miscible N_2 pressure causes more asphaltene challenges, according to these findings, especially in smaller pores. The mass transfer ability (i.e., evaporation of light components) of the miscible conditions is stronger. The extraction of light components in crude oil was higher during the miscible N_2 injection and could result more heavy components (Chung, 1992; Tovar et al., 2021) and this explaining why the immiscible N_2 had less asphaltene deposition and fluctuations.

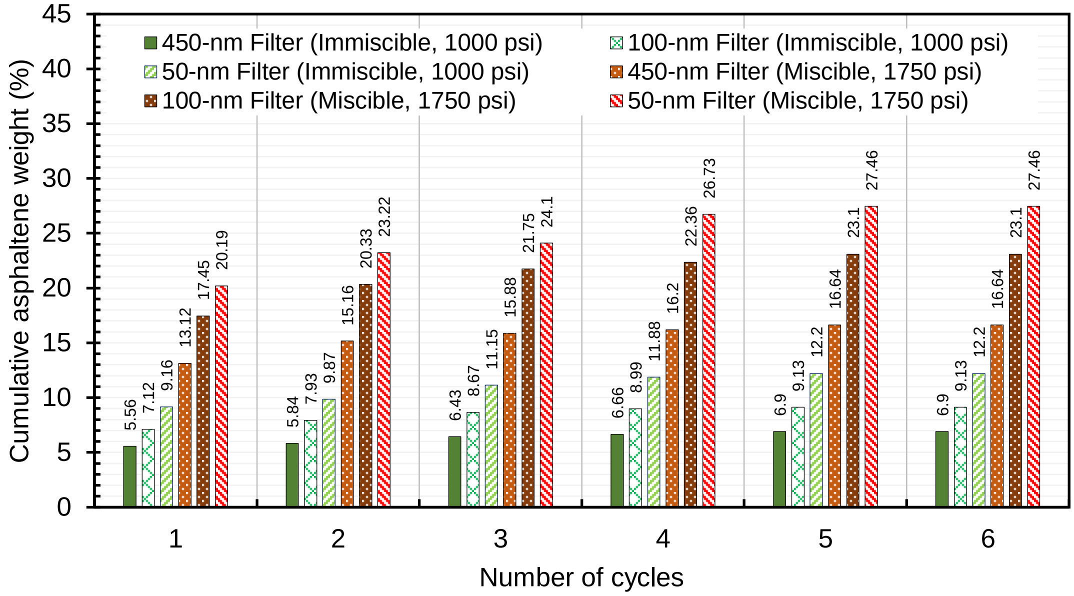

Figure 9. Asphaltene weight percent in all filter membranes after six immiscible (i.e., 1000 psi) and miscible (i.e., 1750 psi) cyclic N_2 gas injections at 70^{o}C.

3.2.1. Chromatography Analysis Results. After the last injection cycle of the filtration experiments, oil samples were collected from the produced oil to evaluate the influence of gas injection on the asphaltene stability in cude oil, and then gas chromatography-mass spectrometry (GC6890-MS5973) was used to determine the main chemical components, including asphaltenes. Figure 10 shows the grouped carbon number distribution of the produced oil following cyclic tests utilizing immiscible and miscible conditions for N_2.

The results showed that miscible N_2 injection had a higher impact on the crude oil which can be seen in the higher mole percentage of the intermediate and heavy components (C_{15}-C_{30}). The light components (C_8-C_{14}) were partially extracted from the original oil due to the high pressure and strong light hydrocarbons extraction of the N_2. Following miscible N_2 testing, higher amounts of C_{31+} including asphaltenes were found compared to the initial oil composition, but after immisicble N_2 tests, less heavy components were found because the mass transfer ability of the miscible N_2 is much strogner than immiscible N_2. Also, higher pressure during miscibility conditions will weaken the bonds between asphalten particles and resins inside the crude oil and thus more heavy compontnes and asphaltene deposition may occur. In the crude oil, immiscible N_2 has low solubility and thus immisicble N_2 has a low mass transfer capacity, which might result in less extraction of light hydrocarbons and likely less asphaltene flocculation compared to msicble N_2 injection pressure (Wang et al., 2018; Fu et al., 2021).

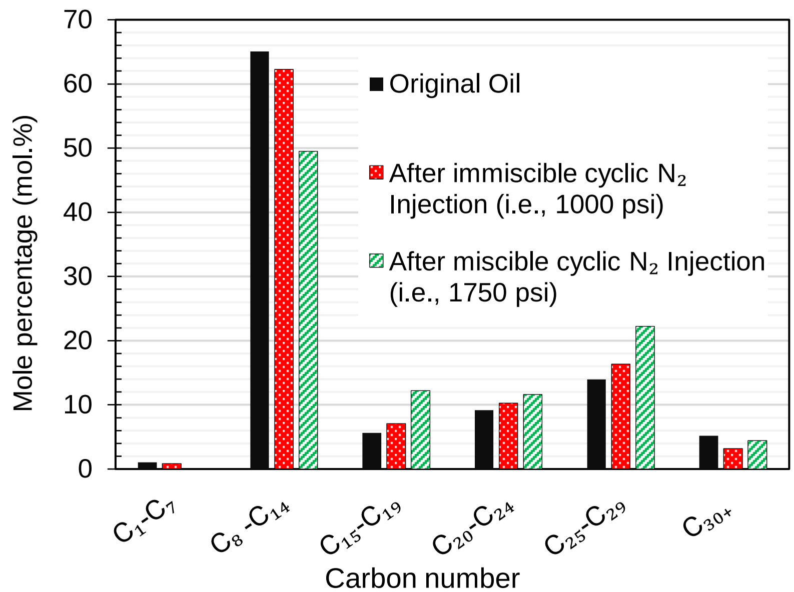

Figure 10. Distribution of oil components before and after N_2 cyclic filtration injections of 1000 and 1750 psi.

3.2.2. Microscope and SEM Analysis. After completing the filtration experiments, the impact of the gas injection and asphaltene clusters on the pore plugging on the filter paper membranes was determined using a Hirox digital microscope. Figure 11 shows the microscopic images (500 µm) of the filter paper membranes' pore structure for the 450-, 100-, and 50-nm filters using immiscible (i.e., 1000 psi) and miscible (i.e., 1750 psi) N_2 injection pressures. The photos were taken after the filter membranes had been cleaned and exposed to an n-heptane solvent for 24 h.

For miscible N_2 conditions, the asphaltene particles plugged more areas in the 50-nm due to its smaller pore size, which led to greater asphaltene deposition. On the other hand, the filter membranes of 450-nm showed a notable pore plugging and asphaltene clusters, as well as the 100-nm filter paper. Additionally, scanning electron microscopy (SEM) was utilized to obtain high-quality pictures of the pore structure of filter paper membranes for further imaging analysis. Various images (500 µm) were taken for the same size filter membranes (i.e., 450, 100, and 50-nm) during immiscible (i.e., 1000 psi) and miscible (i.e., 1750 psi) N_2 injection pressures at 70ºC, as shown in Figure 12. The photos of the 450-nm filter after N_2 injection showed that asphaltenes plugged the pores and accumulated inside the structure of the filter membranes. This was much more severe in the 50-nm filter due to its small pore size structure. Miscible N_2 injection led to more dark colors in the photos and more particles were noticed.

These findings confirm that miscible N_2 has a higher solubility and strong extraction of light hydrocarbons in crude oil compared to immiscible N_2 which could lead to less asphaltene issues.

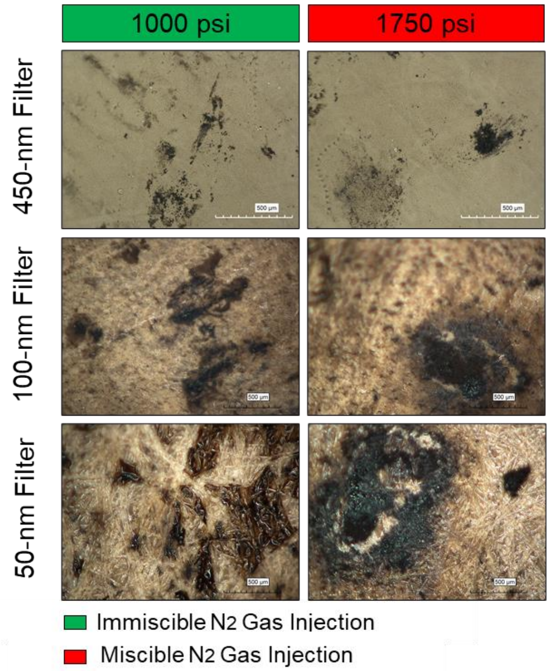

Figure 11. Digital microscopic images (500 µm) of 450-, 100-, and 50-nm filter membranes after the last cycle of 1000 and 1750 psi N_2 injection pressures.

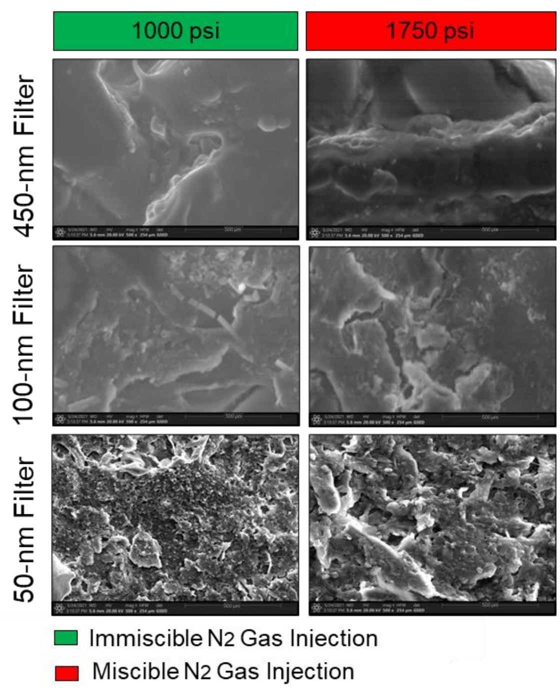

Figure 12. Scanning electron microscope (SEM) images (500 µm) of 450-, 100-, and 50-nm filter membranes after the last cycle of 1000 and 1750 psi N_2 injection pressures.

3.3. RESULTS OF CYCLIC GAS INJECTION USING SHALE CORES

3.3.1. Effect of Miscibility on Oil Recovery. In this section, the effect of the cyclic injection pressure on the oil recovery using eight Eagle Ford shale cores. To examine the miscibility influence on oil recovery, four sets of experiments (tests 1, 2, 3, and 4) were performed at pressures below and above the N_2 MMP. Table 8 presents the cumulative recovery factor (RF) data calculated after each cycle of cyclic N_2 tests. In all experiments, the soaking time was fixed at 6 h. The production time was investigated, and the oil recovery was measured at different production times (i.e., 15, 60, and 90 min). The cycles were stopped when no oil recovery was produced. The results (Figure 13) indicate that oil recovery was less under immiscible pressures than miscible pressures. As the pressure increased, the oil recovery increased, which can be observed in the first cycle. The findings also suggested that under both conditions, oil can be extracted effectively in the first four cycles, but no more oil can be extracted after the sixth cycle. For immiscible cyclic N_2 condition, the essential impact in oil recovery was after the second cycle. Immiscible pressure of 1000 psi had no significant effect in increasing the oil recovery, demonstrating that immiscibility is not the optimum choice when applying the cyclic N_2 techniques. These observations give the miscible pressure an advantage in increasing the oil recovery compared to the immiscible pressure. The key explanation for this is because miscible N_2 has a higher solubility, which reduces the oil's viscosity, thus increases the oil recovery as compared to immiscible N_2 pressures, which have a poor evaporation mechanism and oil swelling efficiency. In terms of asphaltene deposition, the figures suggested that it began to affect the oil recovery in the later cycles, as seen by the stable recovery in the last two cycles for all tests. Asphaltene particles began to precipitate mostly in the large pores at lower pressers (i.e., immiscible conditions) and then asphaltenes began to precipitate even in smaller pores (Huang et al., 2022) under miscible conditions and after multiple cycles. Consequently, the blockage rate increased. These findings imply that oil recovery occurred more during early cycles, when asphaltenes had not yet fully developed and plugged the pores of the cores.

During the cyclic experiments, we recognized that production time had an effect on oil recovery, thus; three different production times were considered to determine the oil recovery after each cycle. The production time was the time that had elapsed when the core sample was retrieved from the vessel and weighed. The oil recovery was determined at 15, 60, and 90 min of production time. The soaking time was fixed to be 6 h for each cycle and all the results are shown in Figure 13. The results revealed that the oil recovery was changed for all production times in all experiments of immiscible and miscible injection conditions. For example, the RF increased slightly during the second cycle from 2.86 to 3.12% during the immiscible pressure of 1000 psi for 15 and 90 min of production times, respectively. During the miscible pressure of 2000 psi, the oil recovery was observed in almost all cycles, but less change was determined in the last two cycles. This could be due to the fact that most of the retrievable oil was produced at the miscible pressure and first cycles. The results demonstrated that production time affected positively the RF during the cyclic N_2 tests.

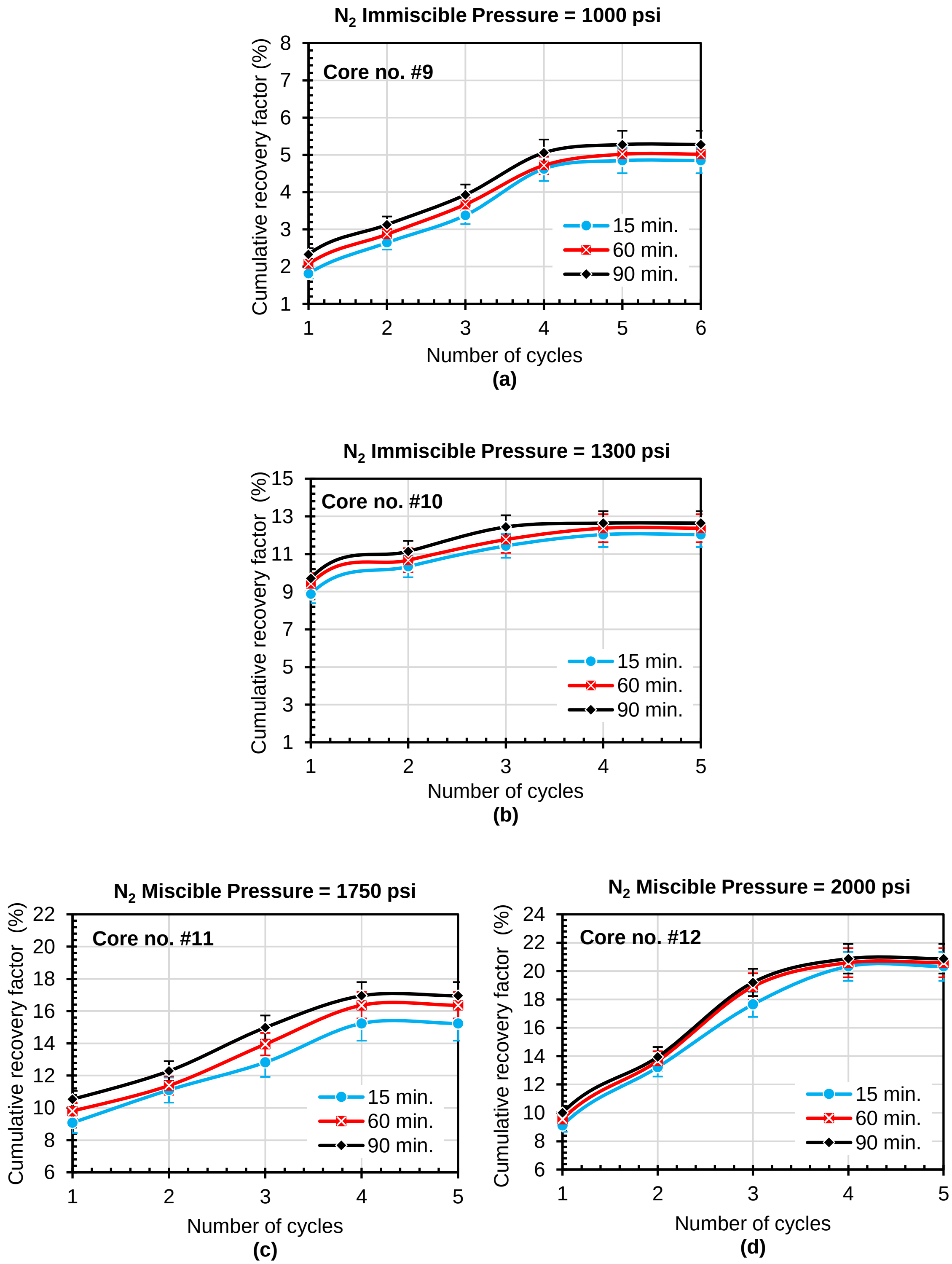

Figure 13. Comparison of recovery performance between the immiscible (a and b) and miscible (c and d) N_2 cycles under a 6-h soaking time.

Table 8. Summary of the cumulative RF (%) determined after N_2 cyclic tests.

Test no.	Soaking time (h)	Pressure (psi)	Production time (min)	Cycle 1	Cycle 2	Cycle 3	Cycle 4	Cycle 5	Cycle 6	Cycle 7
1	6	1000	15	1.81	2.64	3.38	4.63	4.85	4.85	-
			60	2.07	2.87	3.67	4.72	5.02	5.02	-
			90	2.33	3.13	3.93	5.06	5.28	5.28	-
2	6	1300	15	8.88	10.33	11.43	12.03	12.03	-	-
			60	9.42	10.67	11.77	12.37	12.37	-	-
			90	9.71	11.14	12.44	12.64	12.64	-	-
3	6	1750	15	9.08	11.10	12.82	15.24	15.24	-	-
			60	9.80	11.38	13.95	16.36	16.36	-	-
			90	10.53	12.28	14.98	16.95	16.95	-	-
4	6	2000	15	9.12	13.22	17.65	20.33	20.33	-	-
			60	9.55	13.66	18.90	20.59	20.59	-	-
			90	10.00	13.95	19.20	20.87	20.87	-	-
5	1	2000	15	7.61	11.07	12.68	13.14	13.56	14.02	14.00
	6	2000	15	14.10	15.20	16.00	16.19	17.33	18.50	18.50
	12	2000	15	17.20	18.66	21.00	23.65	24.67	26.48	26.48
	24	2000	15	28.32	30.16	32.55	35.84	37.39	40.22	40.22
6	1	2000	15	4.74	5.50	7.23	8.26	10.11	11.12	11.12
7	12	2000	15	9.14	14.80	19.87	22.19	23.50	23.60	23.60
8	24	2000	15	15.12	23.74	29.01	32.71	33.66	33.67	33.67

3.3.2. Soaking time mode. Two modes of soaking time were conducted at a constant pressure of 2000 psi and fixed production time of 15 min. Mode I refers to conducting several injection cycles at a constant injection pressure (i.e., 2000 psi) on the same core for varied soaking times (i.e., 1, 6, 12, and 24 h), while Mode II refers to using separate cores for a single constant soaking time for each core. One test was conducted for N_2, using the same core for each test (test no. 5). Soaking times of 1, 6, 12, and 24 h were selected and applied to the same core during the tests. Another three tests were conducted using Mode II (tests no. 6-8). Soaking times of 1, 12, and 24 were selected, and the 6-h soaking time results were discussed in the previous section. Figure 14 shows an illustration of the different soaking time modes.

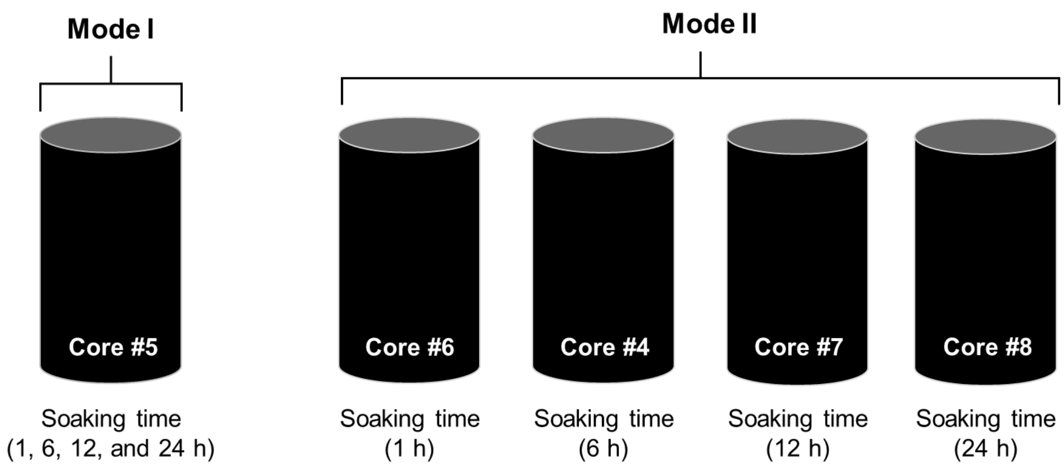

Figure 14. Illustration of the different soaking time modes.

The results showed that seven cycles were enough to produce more than 40% of the oil using Mode I, as shown in Figure 15. A soaking time of 24 h produced the highest oil recovery compared to other soaking times of 1, 6 and 12 h. Comparing the results with the oil recovery from Mode II, the highest oil recovery occurred when using a 24 h soaking time which the cumulative oil recovery was about 33.67% after seven cycles. The optimum number of cycles at which no more oil recovery was observed was six. These results demonstrated that longer soaking times lead to higher oil recovery and this process was observed clearly when using Mode I. More hydrocarbons evaporated using Mode I compared to Mode II. The results revealed that starting with shorter cycle time has more advantageous in increasing the oil recovery from shale cores due to the cyclic gas can condensate at higher concentration in crude oil giving the gas to evaporate more hydrocarbon from the shale cores, especially in miscible conditions. The asphaltene particles did not plug the pores completely and more oil recovered. Starting with longer soaking time impacted the asphaltene instability at higher rate inside the cores and thus more pore plugging could be exist resulting in oil recovery reduction, as shown in Mode II using 24 h soaking time. Figure 16 shows the core samples after N_2 cyclic tests after 24 h of soaking time and injection pressure of 2000 psi using Mode I and Mode II.

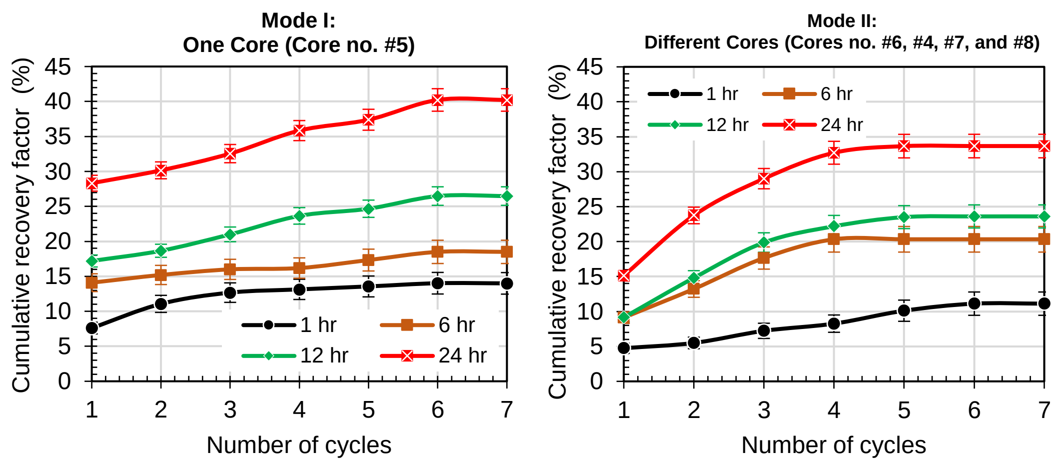

Figure 15. Results of cumulative recovery factor of cyclic N_2 injections using Mode I and Mode II at a 2000 psi cyclic injection pressure with different soaking times.

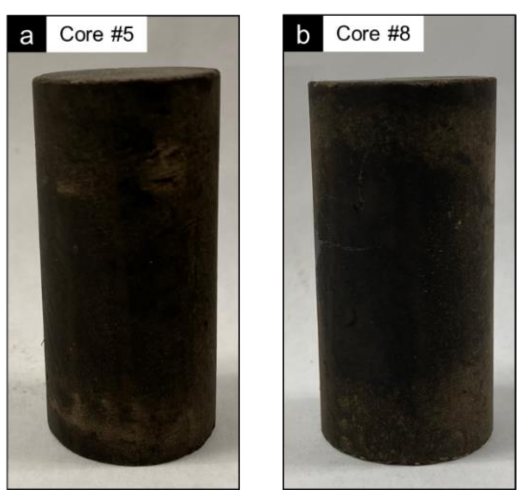

Figure 16. Photos of cores taken after cyclic gas injection experiments at a pressure of 2000 psi (a) after a N_2 test using Mode I, and (b) after a N_2 test (24-h soaking time) using Mode II.

3.3.3. Wettability Change Due to Asphaltene Deposition. In the literature, the contact angle and wettability of shales during N_2 cyclic gas injection are still poorly investigated. During gas injection, asphaltene deposition and precipitation may affect the wettability of shales; hence, the effectiveness of oil recovery. Due to the ultra-low permeability of the shale structure, capillary pressure in shale rocks is extremely high. The tendency of fluids to adhere to the surface is known as the wettability phenomenon (Abdallah et al., 1986). Wettability alterations during gas enhanced oil recovery, especially in unconventional reservoirs, are a significant factor in oil production. The wettability of shale rocks differs; it can be wet with water or oil, and it is not always oil wet as is usually assumed (Sheng, 2018). However, other investigations reported that shale rocks are more oil wet (Odusina et al., 2011; Akbarabadi et al., 2017). Wettability is influenced by the adsorption of asphaltenic components as well as total organic carbon (Kumar et al., 2008; Odusina et al., 2011; Pan et al., 2020; Mohammed et al., 2021). To investigate the wettability alteration after the cyclic gas injection process, an air-liquid-rock system was used to determine the wettability of the shale cores before and after the cyclic tests. The cores were not cleaned by a solvent because the solvent can wash away the asphaltene particles and impact the results. Figure 17 shows equilibrated droplets of brine and their contact angles (i.e., right and left contact angle) of the cores that no pressure applied on them, and cores after N_2 cyclic tests. In order to evaluate the asphaltene deposition and the effect of gas injection on pore plugging on Eagle Ford cores, four separate saturated cores (Figure 17b) were used to measure the contact angle which no pressure applied on them (i.e., core 9, 10, 11 and 12). These four cores are fully saturated with crude oil and the average contact angle measured was 82.95°. This indicates that weakly intermediate wettability existed before applying the gas pressure. For accuracy purpose, the contact angles from all of the shale cores (Table 9) were determined after N_2 cyclic tests in both conditions (i.e., miscible, and immiscible). The average contact angle following N_2 cycle testing was around 102.26^o, showing that N_2 changed the wettability to a strong intermediate-wet system. These results suggests that N_2 influenced the deposition of asphaltene in the shale cores. The contact angle rose when miscible gas was injected indicating that miscibility may generate a strongly intermediate-wet and close to oil-wet system during miscible N_2 cyclic gas injection. Our findings were quite similar with various experimental literature data, where the contact angle increased as the gas injection pressure increased (Sarmadivaleh et al., 2015; Iglauer et al., 2015; Arif et al., 2016; 2017; Roshan et al., 2016; Pan et al., 2018). This can be due to the shale surface structure had been altered by asphaltene deposition, making it rougher, resulting in a rise in contact angle readings (Amin et al., 2010; Hosseini, 2019). Furthermore, our findings indicate that oil reduction and asphaltene deposition occurred in the later cycles, since the decline in oil recovery was detected in the last two cycles in the majority of the cyclic experiments discussed earlier. As more cycles were applied, the asphaltene particles started to fill the big pores first at a higher rate (Huang et al., 2022) and more asphaltene was deposited in the cores along with an increase in the blockage rate, especially when using miscible N_2 which has a strong extraction of the hydrocarbon components. A reduction in the oil recovery factor followed the N_2 cyclic injections, and the influence of asphaltene deposition and precipitation on oil recovery was observed in subsequent cycles (Shen and Sheng, 2018).The results confirmed that cyclic gas injection, particularly at miscible pressures, affects the stability of the asphaltene clusters and reduced the strong bonds between the asphaltene particles and resins, resulting in increased asphaltene deposition and precipitation, specifically in later cycles.

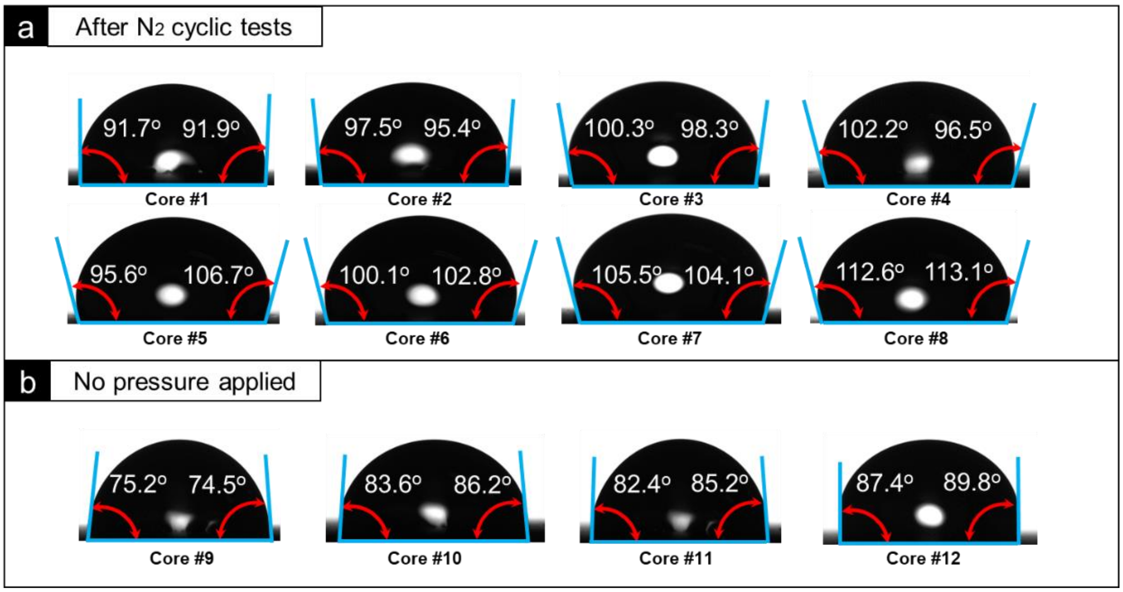

Figure 17. Equilibrated droplets of brine on different core samples and their contact angles (a) after N_2 cyclic tests, (b) no pressure applied on cores.

Table 9. Contact angle measurements for all cores in this study.

Stage	**Condition**	**Test No.**	**Pressure (psi)**	**Average Contact Angle (°)**	**Wettability Status ***	**Total Average**
Before Cyclic Tests		-	No Pressure Applied	83.80	Weakly intermediate-wet	82.95
				74.50	Weakly intermediate-wet	
				88.60	Weakly intermediate-wet	
				84.90	Weakly intermediate-wet	
After Nitrogen Cyclic Tests	Immiscible	1	1000	91.80	Strongly intermediate-wet	100.26
		2	1300	96.45	Strongly intermediate-wet	
	Miscible	3	1750	99.30	Strongly intermediate-wet	
		4	2000	99.35	Strongly intermediate-wet	
		5	2000	101.15	Strongly intermediate-wet	
		6	2000	101.45	Strongly intermediate-wet	
		7	2000	104.80	Strongly intermediate-wet	
		8	2000	107.85	Strongly intermediate-wet	

* Classification based on definitions adopted from Anderson, W. (1986) and Arif et al. (2017).
* Wettability is classified as follows: 0° = completely water wet; 0 to 50° = strongly water wet; 50 to 70° = weakly water wet; 70 to 90° = weakly intermediate-wet; 90 to 110° = strongly intermediate-wet; 110 to 130° = weakly oil wet; 130 to 180° = strongly oil wet.

3.3.4. Scanning Electron Microscope (SEM) Analysis. The primary goal of using the SEM was to reveal the impact of the asphaltene precipitation and deposition process in the shale formations after the cyclic tests. As presented in Figure 18, asphaltene deposition and pore plugging of shale cores were also investigated using a scanning electron microscope (SEM) at a magnification of 100 µm.

SEM examination can help to show the asphaltene deposition inside the cores and give a more detailed study of the small pores of shale formations. Gas injection can disrupt the connections between the resins and asphaltene particles in crude oil, causing asphaltene deposition to increase. Asphaltene clusters may form in reservoir pores as a result of this mechanism.

In this investigation, three samples were used for SEM examination following N_2 cyclic testing. Based on the SEM analysis, asphaltene clusters filled certain areas in the shale cores. For example, pictures (a) and (c) showed more asphaltene pore blockage than sample (b), perhaps because to the longer soaking times of 6 and 24 h, respectively.

Because of the different conditions of the injected pressure and the diverse structures of the samples, the severity of asphaltene deposition was clearer in samples (a) and (c) compared to sample (b). These photos confirms that cyclic N_2 injection changed the pore size structure inside the cores, and this led to lowering the oil recovery.

3.3.5. Pore Size Distribution Due to Asphaltene Deposition. The purpose of this section is to evaluate and see how the pore size distribution of the cores changed as a result of asphaltene deposition after N_2 cyclic tests. The mercury porosimeter technique is a practical method for determining the pore size distribution of rocks, and it is effective for comparing the findings of similar materials (Giesche H., 2006; Labani et al., 2016).

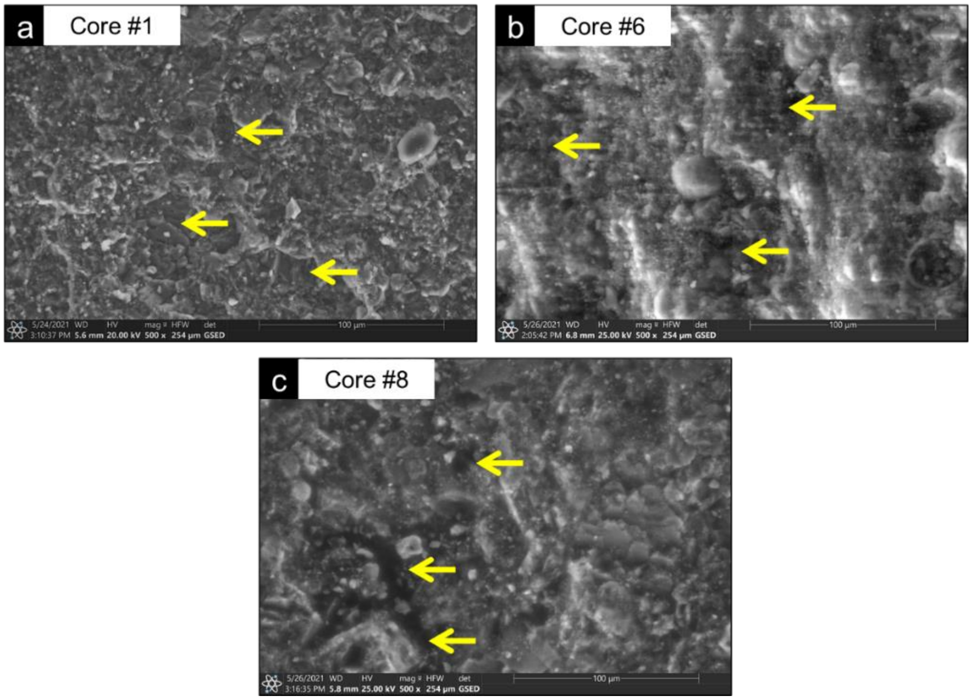

Figure 18. Scanning electron microscope (SEM) images (100 µm) of three cores after cyclic N_2 gas injection tests.

Two Eagle Ford cores were selected to measure the pore size distribution using PoreMaster mercury porosimeter. One sample (i.e., core #9) was selected from the samples that only saturated with crude oil and no pressure was applied. The results from this sample were compared to the other core (i.e., core #8) after applying cyclic N_2 pressure. Small pieces of each sample were needed, so before the measurements, each core was smashed into small pieces. During the test, a maximum pressure of 60,000 psi was applied to examine the small pores and the throat inside the cores. The volume of intruded mercury was calculated and recorded automatically by the PoreMaster at each intrusion pressure. The comparison of the pore size distribution of the Eagle Ford cores is shown in Figure 19 and 20. As a result of the gas injection, the composition of the oil in all cores changes resulting in the precipitation of asphaltene. The asphaltene aggregated and produced a solid phase that began to accumulate inside the cores and on the rock's surface, plugging the pores (Behbahani et al., 2015; Shen and Sheng, 2016; Wang et al., 2018).

By comparing the pore size distributions, lager pore size diameters were determined for the sample with no pressure applied compared to the other core. The figure demonstrates that the two samples' pore size peaks were in different ranges, indicating that the predominant pore diameter in the two samples was different. For instance, the peak of the pore size distribution of the sample before cyclic test was between 0.03 to 40 µm, but after N_2 cyclic test ranged between 0.01 and 20 µm. The intrusion of mercury into the sample selected after cyclic N_2 test was at a higher rate into the smaller pores.

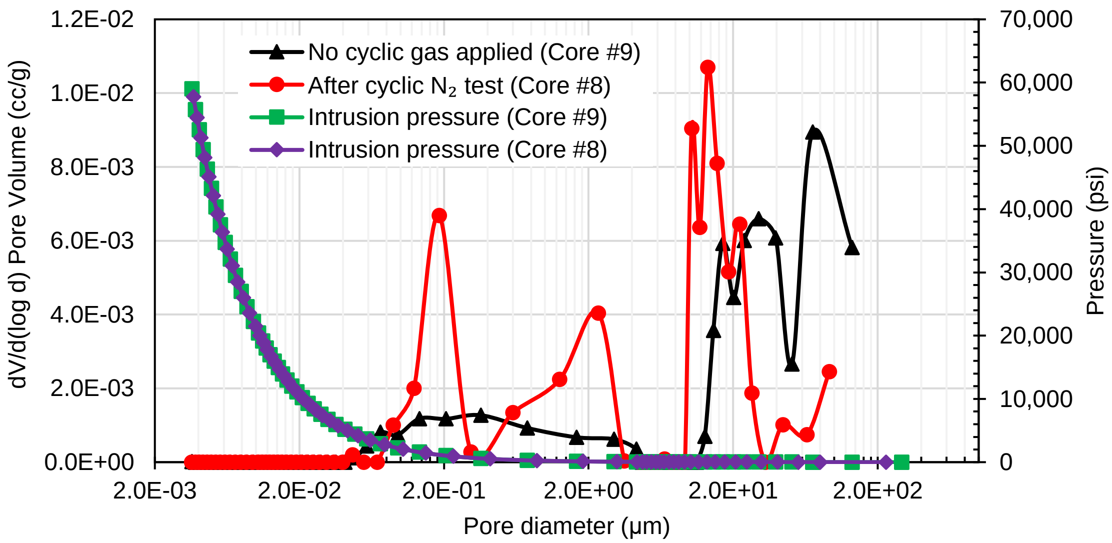

Figure 19. Pore size distribution of the tested cores before and after the N_2 cyclic gas injection mercury intrusion process.

These results reveal that the pore throat in the cores had been impacted by the asphaltene clusters and particles after the cyclic N_2 gas injection applied. Our findings are consistent with our early-explained results and explain why the oil recovery was reduced at later cycles and wettability changes after cycle N_2 tests.

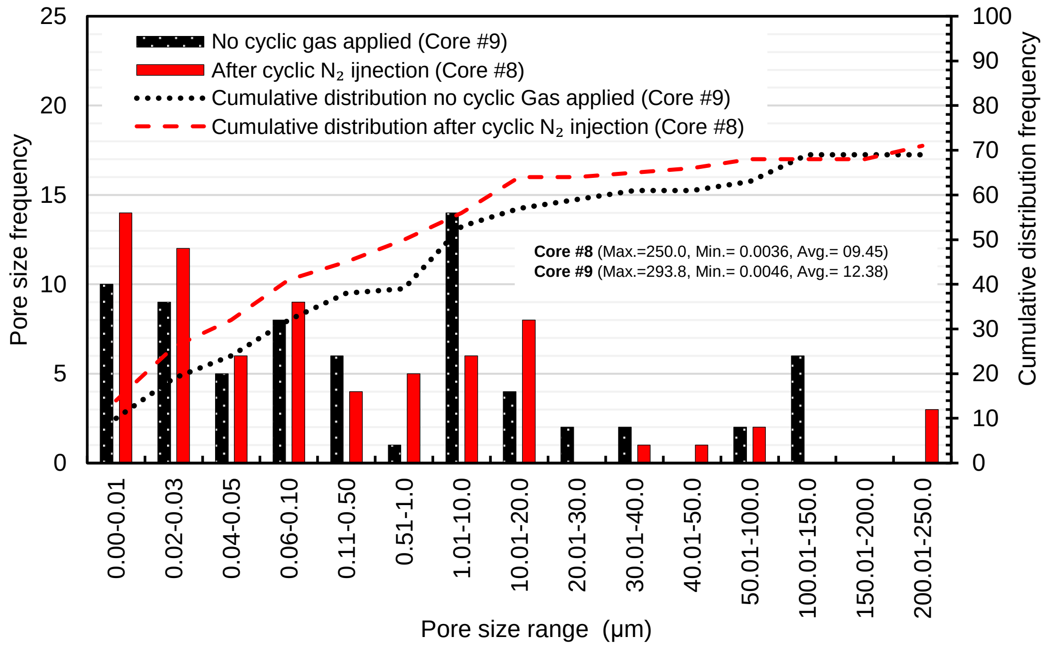

Figure 20. Comparison of the pore size distribution in Eagle Ford cores before and after the N_2 cyclic gas injection tests.

4. CONCLUSIONS

A comprehensive experimental study was conducted to investigate asphaltene deposition and precipitation under cyclic N_2 injections using Eagle Ford shale cores (dynamic mode) and ultra-small mesh filter paper membranes (static mode). The effect of pressure, miscibility, and soaking time was evaluated. To provide a holistic assessment of the influence of asphaltene deposition in such gas injection techniques, wettability analysis and pore size distribution evaluation of the cores were undertaken. The results support the following conclusions:

a. During the cyclic filtration experiments (i.e., static mode), the results showed that the asphaltene weight percent increased when increasing the pressure, and miscible pressure had the highest rate of asphaltene weight percent. Also, the impact of N_2 injection on asphaltene instability was found mainly in the first four cycles. Due to the lower pore size structure, the 50-nm filter membranes had a higher asphaltene weight percentage.

b. After the cyclic filtration experiments, the chromatography analysis of the produced oil revealed that N_2 injection produced more heavy hydrocarbon components after the final cycle, especially under miscible conditions. The miscibility of N_2 gas extracted more light hydrocarbon components from the crude oil than immiscible conditions.

c. Using Eagle Ford cores under cyclic N_2 gas injection (i.e., dynamic mode) showed an increase in the oil recovery when increasing the pressure, and more cycles resulted in more oil recovery, especially during the early cycles. During miscible conditions, these observations were substantially more effective.

d. In the dynamic mode, the soaking time modes results demonstrated that starting with a shorter soaking period improved oil recovery. Longer soaking periods affected the deposition of asphaltene inside the cores, increasing the drop speed in oil recovery. In all experiments, longer soaking time led to higher oil recovery.

e. Our findings imply that oil reduction and asphaltene deposition occurred in the later cycles because the majority of cyclic tests revealed a reduction in oil recovery in the last two cycles. The asphaltene particles began to fill the bigger pores at a faster rate as the number of cycles increased, converting the wettability of the shale cores to a strongly intermediate wet system.

f. A smaller pore size distribution was determined using a PoreMaster mercury porosimeter of the cores after the cyclic experiments indicating that the asphaltene particles reduced the size of the pores.

REFERENCES

Abdallah, W. et al. (1986). Fundamentals of wettability. Technology, 38(1125-1144), 268.

Abedini, A., & Torabi, F. (2014). Oil recovery performance of immiscible and miscible CO_2 huff-and-puff processes. Energy & Fuels, 28(2), 774-784. https://doi.org/10.1021/ef401363b

Afra, S., Samouei, H., Golshahi, N., & Nasr-El-Din, H. (2020). Alterations of asphaltenes chemical structure due to carbon dioxide injection. Fuel, 272, 117708. https://doi.org/10.1016/j.fuel.2020.117708

Ahmad, H. M., Kamal, M. S., Mahmoud, M., Shakil Hussain, S. M., Abouelresh, M., & Al-Harthi, M. A. (2019). Organophilic clay-based drilling fluids for mitigation of unconventional shale reservoirs instability and formation damage. Journal of Energy Resources Technology, 141(9). https://doi.org/10.1115/1.4043248

Ahmed, S., Elldakli, F., Heinze, L., Elwegaa, K., & Emadi, E. (2019). Investigating Effects of the Ball Size on the Gas Throughput Using Partially Curved and Wholly Curved Seats. Int J Pet Petrochem Eng, 5(3), 1-9. http://dx.doi.org/10.20431/2454-7980.0503001

Ahmed, S., Emadi, H., Heinze, L., Elwegaa, K., & Elldakli, F. (2020). An experimental comparison between actual valve and benchmark valve using modified design and optimized design. SSRG International Journal of Engineering Trends and Technology, 68(2), 64-73. http://dx.doi.org/10.14445/22315381/IJETT-V68I2P212

Ahmed, S. (2020). Investigating effects of the ball configuration on the gas throughput using partially curved and wholly curved seats (Doctoral dissertation). https://hdl.handle.net/2346/85869

Akbarabadi, M., Saraji, S., Piri, M., Georgi, D., & Delshad, M. (2017). Nano-scale experimental investigation of in-situ wettability and spontaneous imbibition in ultra-tight reservoir rocks. Advances in Water Resources, 107, 160-179. https://doi.org/10.1016/j.advwatres.2017.06.004

Ali, S. I., Lalji, S. M., Haneef, J., Ahsan, U., Tariq, S. M., Tirmizi, S. T., & Shamim, R. (2021). Critical analysis of different techniques used to screen asphaltene stability in crude oils. Fuel, 299, 120874. https://doi.org/10.1016/j.fuel.2021.120874

Altawati, F. S. (2016). An experimental study of the effect of water saturation on cyclic N_2 and CO_2 injection in shale oil reservoir (Master thesis). http://hdl.handle.net/2346/68030

Altawati, F., Emadi, H., Khalil, R., Heinze, L., & Menouar, H. (2022). An experimental investigation of improving Wolfcamp Shale-Oil recovery using Liquid-N_2-assisted N_2 and/or CO_2 Huff-n-Puff injection technique. Fuel, 324, 124450. https://doi.org/10.1016/j.fuel.2022.124450

Amin, J. S., Nikooee, E., Ayatollahi, S., & Alamdari, A. (2010). Investigating wettability alteration due to asphaltene precipitation: Imprints in surface multifractal characteristics. Applied Surface Science, 256(21), 6466-6472. https://doi.org/10.1016/j.apsusc.2010.04.036

Arif, M., Al-Yaseri, A. Z., Barifcani, A., Lebedev, M., & Iglauer, S. (2016). Impact of pressure and temperature on CO_2–brine–mica contact angles and CO_2–brine interfacial tension: Implications for carbon geo-sequestration. Journal of colloid and interface science, 462, 208-215. https://doi.org/10.1016/j.jcis.2015.09.076

Arif, M., Lebedev, M., Barifcani, A., & Iglauer, S. (2017). Influence of shale-total organic content on CO_2 geo-storage potential. Geophysical Research Letters, 44(17), 8769-8775. https://doi.org/10.1002/2017GL073532

Anderson, W. (1986). Wettability literature survey-part 2: Wettability measurement. Journal of petroleum technology, 38(11), 1246-1262. https://doi.org/10.2118/13933-PA

Badrouchi, N., Pu, H., Smith, S., & Badrouchi, F. (2022). Evaluation of CO_2 enhanced oil recovery in unconventional reservoirs: Experimental parametric study in the Bakken. Fuel, 312, 122941. https://doi.org/10.1016/j.fuel.2021.122941

Baek, S., & Akkutlu, I. Y. (2021). Enhanced Recovery of Nanoconfined Oil in Tight Rocks Using Lean Gas (C2H6 and CO_2) Injection. SPE Journal, 1-20. https://doi.org/10.2118/195272-PA

Barati-Harooni, A., Najafi-Marghmaleki, A., Hoseinpour, S. A., Tatar, A., Karkevandi-Talkhooncheh, A., Hemmati-Sarapardeh, A., & Mohammadi, A. H. (2019). Estimation of minimum miscibility pressure (MMP) in enhanced oil recovery (EOR) process by N_2 flooding using different computational schemes. Fuel, 235, 1455-1474. https://doi.org/10.1016/j.fuel.2018.08.066

Behbahani, T. J., Ghotbi, C., Taghikhani, V., & Shahrabadi, A. (2013). A modified scaling equation based on properties of bottom hole live oil for asphaltene precipitation estimation under pressure depletion and gas injection conditions. Fluid Phase Equilibria, 358, 212-219. https://doi.org/10.1016/j.fluid.2013.08.027

Behbahani, T. J., Ghotbi, C., Taghikhani, V., & Shahrabadi, A. (2014). Investigation of asphaltene adsorption in sandstone core sample during CO_2 injection: Experimental and modified modeling. Fuel, 133, 63-72. https://doi.org/10.1016/j.fuel.2014.04.079

Behbahani, T. J., Ghotbi, C., Taghikhani, V., & Shahrabadi, A. (2015). Experimental study and mathematical modeling of asphaltene deposition mechanism in core samples. Oil & Gas Science and Technology–Revue d'IFP Energies nouvelles, 70(6), 1051-1074. https://doi.org/10.2516/ogst/2013128

Belhaj, H., Abu Khalifeh, H. A., & Javid, K. (2013, April 15). Potential of Nitrogen Gas Miscible Injection in South East Assets, Abu Dhabi. Society of Petroleum Engineers. https://doi.org/10.2118/164774-MS

Bougre, E.S., Gamadi, T.D. Enhanced oil recovery application in low permeability formations by the injections of CO_2, N_2 and CO_2/N_2 mixture gases. J Petrol Explor Prod Technol 11, 1963–1971 (2021).https://doi.org/10.1007/s13202-021-01113-5

Chung, T. H. (1992, January). Thermodynamic modeling for organic solid precipitation. In SPE Annual Technical Conference and Exhibition. Society of Petroleum Engineers. https://doi.org/10.2118/24851-MS

Elturki, M., Imqam, A. (2020a, June 28). Application of Enhanced Oil Recovery Methods in Unconventional Reservoirs: A Review and Data Analysis. American Rock Mechanics Association.

Elturki, M., & Imqam, A. (2020b, July). High Pressure-High Temperature Nitrogen Interaction with Crude Oil and Its Impact on Asphaltene Deposition in Nano Shale Pore Structure: An Experimental Study. In SPE/AAPG/SEG Unconventional Resources Technology Conference. https://doi.org/10.15530/urtec-2020-3241

Elturki, M., & Imqam, A. (2021a, November). An Experimental Study Investigating the Impact of Miscible and Immiscible Nitrogen Injection on Asphaltene Instability in Nano Shale Pore Structure. In SPE International Conference on Oilfield Chemistry. https://doi.org/10.2118/204294-MS

Elturki, M., & Imqam, A. (2021b). Asphaltene Thermodynamic Flocculation during Immiscible Nitrogen Gas Injection. SPE Journal, 26(05), 3188-3204. https://doi.org/10.2118/206709-PA

Elturki, M., & Imqam, A. (2021c, June). Analysis of Nitrogen Minimum Miscibility Pressure MMP and Its Impact on Instability of Asphaltene Aggregates-An Experimental Study. In SPE Trinidad and Tobago Section Energy Resources Conference. https://doi.org/10.2118/200900-MS

Elturki, M., & Imqam, A. (2022a, March). An Experimental Investigation of Asphaltene Aggregation Under Carbon Dioxide Injection Flow in Ultra-Low-Permeability Pore Structure. In SPE Canadian Energy Technology Conference. https://doi.org/10.2118/208950-MS

Elturki, M., & Imqam, A. (2022b). Asphaltene Thermodynamic Precipitation during Miscible Nitrogen Gas Injection. SPE journal, 27(01), 877-894. https://doi.org/10.2118/208588-PA

Elturki, M., & Imqam, A. (2022c). Asphaltene Precipitation and Deposition under Miscible and Immiscible Carbon Dioxide Gas Injection in Nanoshale Pore Structure. SPE Journal, 1-17. https://doi.org/10.2118/210592-PA

Elturki, M., McElroy, P. D., Li, D., Kablan, A., & Shaglouf, H. (2021, June). Simulation Study Investigating the Impact of Carbon Dioxide Foam Fracturing Fluids on Proppant Transport. In SPE Trinidad and Tobago Section Energy Resources Conference. https://doi.org/10.2118/200950-MS

Elwegaa, K., & Emadi, H. (2019). Improving oil recovery from shale oil reservoirs using cyclic cold nitrogen injection–An experimental study. Fuel, 254, 115716. https://doi.org/10.1016/j.fuel.2019.115716

Elwegaa, K., Emadi, H., Soliman, M., Gamadi, T., & Elsharafi, M. (2019). Improving oil recovery from shale oil reservoirs using cyclic cold carbon dioxide injection–An experimental study. Fuel, 254, 115586. https://doi.org/10.1016/j.fuel.2019.05.169

Espinoza Mejia, J. E., Li, X., & Zheng, R. (2022, February). Experimental Study of Asphaltene Precipitation and Deposition During Immiscible CO_2-EOR Process. In SPE International Conference and Exhibition on Formation Damage Control. https://doi.org/10.2118/208802-MS

Fu, Q. et al (2021). Investigating the role of diffusion in hydrocarbon gas huff-n-puff injection-an Eagle Ford study. Journal of Petroleum Science and Engineering, 198, 108146. https://doi.org/10.1016/j.petrol.2020.108146

Hamadou, R., Khodja, M., Kartout, M., & Jada, A. (2008). Permeability reduction by asphaltenes and resins deposition in porous media. Fuel, 87(10-11), 2178-2185. https://doi.org/10.1016/j.fuel.2007.12.009

Hassanpouryouzband, A. et al (2020). Gas hydrates in sustainable chemistry. Chemical Society Reviews, 49(15), 5225-5309. https://doi.org/10.1039/C8CS00989A

Hosseini, E. (2019). Experimental investigation of effect of asphaltene deposition on oil relative permeability, rock wettability alteration, and recovery in WAG process. Petroleum Science and Technology, 37(20), 2150-2159. https://doi.org/10.1080/10916466.2018.1482335

Huang, X., Zhang, Y., He, M., Li, X., Yang, W., & Lu, J. (2022). Asphaltene precipitation and reservoir damage characteristics of CO_2 flooding in different microscopic structure types in tight light oil reservoirs. Fuel, 312, 122943. https://doi.org/10.1016/j.fuel.2021.122943

Iglauer, S., Al-Yaseri, A. Z., Rezaee, R., & Lebedev, M. (2015). CO_2 wettability of caprocks: Implications for structural storage capacity and containment security. Geophysical Research Letters, 42(21), 9279-9284. https://doi.org/10.1002/2015GL065787

Jamaluddin, A. K. M., Joshi, N., Iwere, F., & Gurpinar, O. (2002, January 1). An Investigation of Asphaltene Instability Under Nitrogen Injection. Society of Petroleum Engineers. https://doi.org/10.2118/74393-MS

Jia, B., Tsau, J. S., & Barati, R. (2019). A review of the current progress of CO_2 injection EOR and carbon storage in shale oil reservoirs. Fuel, 236, 404-427. https://doi.org/10.1016/j.fuel.2018.08.103

Khalaf, M. H., & Mansoori, G. A. (2019). Asphaltenes aggregation during petroleum reservoir air and nitrogen flooding. Journal of Petroleum Science and Engineering, 173, 1121-1129. https://doi.org/10.1016/j.petrol.2018.10.037

Kumar, K., Dao, E. K., & Mohanty, K. K. (2008). Atomic force microscopy study of wettability alteration by surfactants. SPE Journal, 13(02), 137-145. https://doi.org/10.2118/93009-PA

Lee, J. H., & Lee, K. S. (2019). Investigation of asphaltene-derived formation damage and nano-confinement on the performance of CO_2 huff-n-puff in shale oil reservoirs. Journal of Petroleum Science and Engineering, 182, 106304. https://doi.org/10.1016/j.petrol.2019.106304

Li, L., Su, Y., Lv, Y., & Tu, J. (2020). Asphaltene deposition and permeability impairment in shale reservoirs during CO_2 huff-n-puff EOR process. Petroleum Science and Technology, 38(4), 384-390. https://doi.org/10.1080/10916466.2019.1705855

Li, L. et al., (2019). Experimental and numerical study on CO_2 sweep volume during CO_2 huff-n-puff enhanced oil recovery process in shale oil reservoirs. Energy & Fuels, 33(5), 4017-4032. https://doi.org/10.1021/acs.energyfuels.9b00164

Li, L., Zhang, Y., & Sheng, J. J. (2017). Effect of the injection pressure on enhancing oil recovery in shale cores during the CO_2 huff-n-puff process when it is above and below the minimum miscibility pressure. Energy & Fuels, 31(4), 3856-3867. https://doi.org/10.1021/acs.energyfuels.7b00031

Liu, J., Sheng, J. J., Emadibaladehi, H., & Tu, J. (2021). Experimental study of the stimulating mechanism of shut-in after hydraulic fracturing in unconventional oil reservoirs. Fuel, 300, 120982. https://doi.org/10.1016/j.fuel.2021.120982

Luo, Y., Zheng, T., Xiao, H., Liu, X., Zhang, H., Wu, Z., ... & Xia, D. (2022). Identification of distinctions of immiscible CO_2 huff and puff performance in Chang-7 tight sandstone oil reservoir by applying NMR, microscope and reservoir simulation. Journal of Petroleum Science and Engineering, 209, 109719. https://doi.org/10.1016/j.petrol.2021.109719

Lo, P. A., Tinni, A. O., & Milad, B. (2022). Experimental study on the influences of pressure and flow rates in the deposition of asphaltenes in a sandstone core sample. Fuel, 310, 122420. https://doi.org/10.1016/j.fuel.2021.122420

Louk, K. et al., (2017). Monitoring CO_2 storage and enhanced gas recovery in unconventional shale reservoirs: Results from the Morgan County, Tennessee injection test. Journal of Natural Gas Science and Engineering, 45, 11-25. https://doi.org/10.1016/j.jngse.2017.03.025

Mahzari, P. et al. (2021). Novel laboratory investigation of huff-n-puff gas injection for shale oils under realistic reservoir conditions. Fuel, 284, 118950. https://doi.org/10.1016/j.fuel.2020.118950

Mehana, M., Abraham, J., & Fahes, M. (2019). The impact of asphaltene deposition on fluid flow in sandstone. Journal of Petroleum Science and Engineering, 174, 676-681. https://doi.org/10.1016/j.petrol.2018.11.056

Mohammad, R. S., Zhang, S., Lu, S., Jamal-Ud-Din, S., & Zhao, X. (2017). Simulation study of asphaltene deposition and solubility of CO_2 in the brine during cyclic CO_2 injection process in unconventional tight reservoirs. International Journal of Geological and Environmental Engineering, 11(6), 495-510. https://doi.org/10.5281/zenodo.1340202

Mohammed, I., Mahmoud, M., El-Husseiny, A., Al Shehri, D., Al-Garadi, K., Kamal, M. S., & Alade, O. S. (2021). Impact of Asphaltene Precipitation and Deposition on Wettability and Permeability. ACS omega, 6(31), 20091-20102. https://doi.org/10.1021/acsomega.1c03198

Moradi, S., Dabir, B., Rashtchian, D., & Mahmoudi, B. (2012). Effect of miscible nitrogen injection on instability, particle size distribution, and fractal structure of asphaltene aggregates. Journal of dispersion science and technology, 33(5), 763-770. https://doi.org/10.1080/01932691.2011.567878

Milad, M., Junin, R., Sidek, A., Imqam, A., & Tarhuni, M. (2021). Huff-n-Puff Technology for Enhanced Oil Recovery in Shale/Tight Oil Reservoirs: Progress, Gaps, and Perspectives. Energy & Fuels, 35(21), 17279-17333. https://doi.org/10.1021/acs.energyfuels.1c02561

Nuttal, B. C., Eble, C., Bustin, R. M., & Drahovzal, J. A. (2005). Analysis of Devonian black shales in Kentucky for potential carbon dioxide sequestration and enhanced natural gas production. In Greenhouse Gas Control Technologies 7 (pp. 2225-2228). Elsevier Science Ltd. https://doi.org/10.1016/B978-008044704-9/50306-2

Odusina, E., Sondergeld, C., & Rai, C. (2011, November). An NMR study on shale wettability. In Canadian unconventional resources conference. https://doi.org/10.2118/147371-MS

Pan, B., Li, Y., Wang, H., Jones, F., & Iglauer, S. (2018). CO_2 and CH_4 wettabilities of organic-rich shale. Energy & Fuels, 32(2), 1914-1922. https://doi.org/10.1021/acs.energyfuels.7b01147

Pan, B., Li, Y., Zhang, M., Wang, X., & Iglauer, S. (2020). Effect of total organic carbon (TOC) content on shale wettability at high pressure and high temperature conditions. Journal of Petroleum Science and Engineering, 193, 107374. https://doi.org/10.1016/j.petrol.2020.107374

Roshan, H., Al-Yaseri, A. Z., Sarmadivaleh, M., & Iglauer, S. (2016). On wettability of shale rocks. Journal of colloid and interface science, 475, 104-111. https://doi.org/10.1016/j.jcis.2016.04.041

Sanchez-Rivera, D., Mohanty, K., & Balhoff, M. (2015). Reservoir simulation and optimization of Huff-and-Puff operations in the Bakken Shale. Fuel, 147, 82-94. https://doi.org/10.1016/j.fuel.2014.12.062

Sarmadivaleh, M., Al-Yaseri, A. Z., & Iglauer, S. (2015). Influence of temperature and pressure on quartz–water–CO_2 contact angle and CO_2–water interfacial tension. Journal of colloid and interface science, 441, 59-64. https://doi.org/10.1016/j.jcis.2014.11.010

Sebastian, H. M., & Lawrence, D. D. (1992, January). Nitrogen minimum miscibility pressures. In SPE/DOE enhanced oil recovery symposium. Society of Petroleum Engineers. https://doi.org/10.2118/24134-MS

Shen, Z., & Sheng, J. J. (2017a). Experimental study of permeability reduction and pore size distribution change due to asphaltene deposition during CO_2 huff and puff injection in Eagle Ford shale. Asia-Pacific Journal of Chemical Engineering, 12(3), 381-390. https://doi.org/10.1002/apj.2080

Shen, Z., & Sheng, J. J. (2017b). Investigation of asphaltene deposition mechanisms during CO_2 huff-n-puff injection in Eagle Ford shale. Petroleum Science and Technology, 35(20), 1960-1966. https://doi.org/10.1080/10916466.2017.1374403

Shen, Z., & Sheng, J. J. (2018). Experimental and numerical study of permeability reduction caused by asphaltene precipitation and deposition during CO_2 huff and puff injection in Eagle Ford shale. Fuel, 211, 432-445. https://doi.org/10.1016/j.fuel.2017.09.047

Shen, Z., & Sheng, J. J. (2019). Optimization Strategy to Reduce Asphaltene Deposition-Associated Damage During CO 2 Huff-n-Puff Injection in Shale. Arabian Journal for Science and Engineering, 44(6), 6179-6193. https://doi.org/10.1007/s13369-018-03701-w

Shen, Z., & Sheng, J. J. (2016, April). Experimental study of asphaltene aggregation during CO_2 and CH_4 injection in shale oil reservoirs. In SPE improved oil recovery conference. https://doi.org/10.2118/179675-MS

Sheng, J. J. (2015). Enhanced oil recovery in shale reservoirs by gas injection. Journal of Natural Gas Science and Engineering, 22, 252-259. https://doi.org/10.1016/j.jngse.2014.12.002

Sheng, J. J. (2018). Discussion of shale rock wettability and the methods to determine it. Asia-Pacific Journal of Chemical Engineering, 13(6), e2263. https://doi.org/10.1002/apj.2263

Sheng, J. J., & Chen, K. (2014). Evaluation of the EOR potential of gas and water injection in shale oil reservoirs. Journal of Unconventional Oil and Gas Resources, 5, 1-9. https://doi.org/10.1016/j.juogr.2013.12.001

Shi, B. et al (2021). Status of Natural Gas Hydrate Flow Assurance Research in China: A Review. Energy & Fuels, 35(5), 3611-3658. https://doi.org/10.1021/acs.energyfuels.0c04209

Shilov, E., Dorhjie, D. B., Mukhina, E., Zvada, M., Kasyanenko, A., & Cheremisin, A. (2022). Experimental and numerical studies of rich gas Huff-n-Puff injection in tight formation. Journal of Petroleum Science and Engineering, 208, 109420. https://doi.org/10.1016/j.petrol.2021.109420

Sie, C. Y., & Nguyen, Q. P. (2022). Field gas huff-n-puff for enhancing oil recovery in Eagle Ford shales–Effect of reservoir rock and crude properties. Fuel, 328, 125127. https://doi.org/10.1016/j.fuel.2022.125127

Sim, S. S. K., Okatsu, K., Takabayashi, K., & Fisher, D. B. (2005, January). Asphaltene-induced formation damage: Effect of asphaltene particle size and core permeability. In SPE Annual Technical Conference and Exhibition. Society of Petroleum Engineers. https://doi.org/10.2118/95515-MS

Sun, J., Zou, A., Sotelo, E., & Schechter, D. (2016). Numerical simulation of CO_2 huff-n-puff in complex fracture networks of unconventional liquid reservoirs. Journal of Natural Gas Science and Engineering, 31, 481-492. https://doi.org/10.1016/j.jngse.2016.03.032

Tang, W., & Sheng, J. J. (2022). Huff-n-puff gas injection or gas flooding in tight oil reservoirs?. Journal of Petroleum Science and Engineering, 109725. https://doi.org/10.1016/j.petrol.2021.109725

Tovar, F. D., Barrufet, M. A., & Schechter, D. S. (2021). Enhanced Oil Recovery in the Wolfcamp Shale by Carbon Dioxide or Nitrogen Injection: An Experimental Investigation. SPE Journal, 26(01), 515-537. https://doi.org/10.2118/204230-PA

Turta, A. T., Najman, J., Singhal, A. K., Leggitt, S., & Fisher, D. (1997, January). Permeability impairment due to asphaltenes during gas miscible flooding and its mitigation. In International Symposium on Oilfield Chemistry. Society of Petroleum Engineers. https://doi.org/10.2118/37287-MS

Vahidi, A., & Zargar, G. (2007, January). Sensitivity analysis of important parameters affecting minimum miscibility pressure (MMP) of nitrogen injection into conventional oil reservoirs. In SPE/EAGE reservoir characterization and simulation conference. Society of Petroleum Engineers. https://doi.org/10.2118/111411-MS

Wan, T., Zhang, J., & Jing, Z. (2022). Experimental evaluation of enhanced shale oil recovery in pore scale by CO_2 in Jimusar reservoir. Journal of Petroleum Science and Engineering, 208, 109730. https://doi.org/10.1016/j.petrol.2021.109730

Wang, L., & Yu, W. (2019). Mechanistic simulation study of gas Puff and Huff process for Bakken tight oil fractured reservoir. Fuel, 239, 1179-1193. https://doi.org/10.1016/j.fuel.2018.11.119

Wang, P., Zhao, F., Hou, J., Lu, G., Zhang, M., & Wang, Z. (2018). Comparative analysis of CO_2, N_2, and gas mixture injection on asphaltene deposition pressure in reservoir conditions. Energies, 11(9), 2483. https://doi.org/10.3390/en11092483

Warpinski, N. R., Mayerhofer, M. J., Vincent, M. C., Cipolla, C. L., & Lolon, E. P. (2009). Stimulating unconventional reservoirs: maximizing network growth while optimizing fracture conductivity. Journal of Canadian Petroleum Technology, 48(10), 39-51. https://doi.org/10.2118/114173-PA

Xiong, X., Sheng, J. J., Wu, X., & Qin, J. (2022). Experimental investigation of foam-assisted N_2 huff-n-puff enhanced oil recovery in fractured shale cores. Fuel, 311, 122597. https://doi.org/10.1016/j.fuel.2021.122597

Yang, P., Guo, H., & Yang, D. (2013). Determination of residual oil distribution during waterflooding in tight oil formations with NMR relaxometry measurements. Energy & Fuels, 27(10), 5750-5756. https://doi.org/10.1021/ef400631h

Yu, W., Lashgari, H. R., Wu, K., & Sepehrnoori, K. (2015). CO_2 injection for enhanced oil recovery in Bakken tight oil reservoirs. Fuel, 159, 354-363. https://doi.org/10.1016/j.fuel.2015.06.092

Yu, Y., & Sheng, J. J. (2015, July 20). An Experimental Investigation of the Effect of Pressure Depletion Rate on Oil Recovery from Shale Cores by Cyclic N_2 Injection. Unconventional Resources Technology Conference. https://doi.org/10.15530/URTEC-2015-2144010

Yu, Y., Li, L., & Sheng, J. J. (2017). A comparative experimental study of gas injection in shale plugs by flooding and huff-n-puff processes. Journal of Natural Gas Science and Engineering, 38, 195-202. https://doi.org/10.1016/j.jngse.2016.12.040

Zheng, T., Yang, Z., Liu, X., Luo, Y., Xiao, Q., Zhang, Y., & Zhao, X. (2021). Understanding Immiscible Natural Gas Huff-N-Puff Seepage Mechanism in Porous Media: A Case Study of CH 4 Huff-N-Puff by Laboratory Numerical Simulations in Chang-7 Tight Core. Natural Resources Research, 30(3), 2397-2411. https://doi.org/10.1007/s11053-021-09836-2

Zhou, X., Yuan, Q., Peng, X., Zeng, F., & Zhang, L. (2018). A critical review of the CO_2 huff 'n'puff process for enhanced heavy oil recovery. Fuel, 215, 813-824. https://doi.org/10.1016/j.fuel.2017.11.092

Zhu, Z., Fang, C., Qiao, R., Yin, X., & Ozkan, E. (2020). Experimental and Molecular Insights on Mitigation of Hydrocarbon Sieving in Niobrara Shale by CO_2 Huff 'N'Puff. SPE Journal, 25(04), 1803-1811. https://doi.org/10.2118/196136-PA

Zoback, M.D., Kohli, A.H., 2019. Unconventional Reservoir Geomechanics. Cambridge University Press.

Zuloaga, P., Yu, W., Miao, J., & Sepehrnoori, K. (2017). Performance evaluation of CO_2 Huff-n-Puff and continuous CO_2 injection in tight oil reservoirs. Energy, 134, 181-192. https://doi.org/10.1016/j.energy.2017.06.028

Zadeh, G. A., Moradi, S., Dabir, B., Emadi, M. A., & Rashtchian, D. (2011, July). Comprehensive study of asphaltene precipitation due to gas injection: experimental investigation and modeling. In SPE Enhanced Oil Recovery Conference. https://doi.org/10.2118/143454-MS

Zolghadr, A., Riazi, M., Escrochi, M., & Ayatollahi, S. (2013). Investigating the effects of temperature, pressure, and paraffin groups on the N_2 miscibility in hydrocarbon liquids using the interfacial tension measurement method. Industrial & Engineering Chemistry Research, 52(29), 9851-9857. https://doi.org/10.1021/ie401283q

Labani, M. M., Rezaee, R., Saeedi, A., & Al Hinai, A. (2013). Evaluation of pore size spectrum of gas shale reservoirs using low pressure nitrogen adsorption, gas expansion and mercury porosimetry: A case study from the Perth and Canning Basins, Western Australia. Journal of Petroleum Science and Engineering, 112, 7-16. https://doi.org/10.1016/j.petrol.2013.11.022

Giesche, H. (2006). Mercury porosimetry: a general (practical) overview. Particle & particle systems characterization, 23(1), 9-19. https://doi.org/10.1002/ppsc.200601009

VI. AN EXPERIMENTAL INVESTIGATION OF ASPHALTENE DEPOSITION AND ITS IMPACT ON OIL RECOVERY IN EAGLE FORD SHALE DURING MISCIBLE AND IMMISCIBLE CO_2 HUFF-N-PUFF GAS INJECTION

Mukhtar Elturki and Abdulmohsin Imqam

Missouri University of Science and Technology

ABSTRACT

One of the challenges in extracting oil from unconventional resources using hydraulic fracturing and horizontal drilling techniques is the low primary recovery rate, which is caused by the ultra-small permeability of these resources. Consequently, it is essential to investigate gas injection methods to produce the trapped oil in shale formations. However, the injection process can cause asphaltene depositions inside the reservoir, leading to plugging of pores and oil recovery reduction. There has been limited research on using gas injection techniques to improve oil production in tight/unconventional resources, although Carbon Dioxide (CO_2) and gas enhanced oil recovery (GEOR) methods have been used in conventional resources. In order to determine whether or not cyclic (huff-n-puff) CO_2 process improves oil recovery and aggravate asphaltene precipitation, a rigorous experimental investigation was undertaken utilizing filter membranes and Eagle Ford shale cores. After the minimum miscibility pressure (MMP) was calculated for CO_2, various injection pressures were selected to perform CO_2 huff-n-puff experiments. Investigations were carried out at 70^{o}C on injection pressure, cycle number, production time, and huff-and-puff mode injection. The results demonstrated that when pore size structure of the membranes used smaller and gas injection cycles increased, a higher

asphaltene weight percent (wt. %) was determined during the static experiments (i.e., employing filter paper membranes). Miscibility improved oil recovery in dynamic testing (i.e., using shale cores), but a more oil-wet system was detected in wettability measurements taken following CO_2 huff-and-puff tests. The plugging impact of asphaltene particles on the pore structure was studied using optical microscopy and scanning electron microscopy (SEM) imaging. Following the huff-and-puff tests, a mercury porosimeter revealed how severely the pores were plugged, and after the CO_2 tests, the pore size distribution reduced as a consequence of asphaltene deposition. This study examines the significance of CO_2 injection in oil recovery under miscible/immiscible conditions to identify the critical parameters that could impact the effectiveness of CO_2 huff-n-puff operation in unconventional formations.

1. INTRODUCTION

Tight oil and gas have come into the forefront in the United States in recent years as conventional oil reserves have been depleted. Unconventional resources, such as shale reservoirs, are well-known to have ultra-small permeability and very low porosity (Elturki and Imqam, 2020). Only 4-6% of the trapped oil may be retrieved using multi-stage hydraulic fracturing and horizontal well drilling methods (Warpinski et al., 2009; Sheng, 2015; Zoback et al., 2019; Liu et al., 2021), and oil production decreases after months attributable to the ultra-small permeability of such reservoirs (Elturki et al., 2021a). The water flooding technique is one applicable method that can increase oil recovery from conventional reservoirs; however, this technique is not the optimal choice for tight reservoirs due to their poor injectivity, poor sweep potency, and clay swelling issues (Yang et al., 2013; Ahmad et al., 2019). Gas injection has become a widespread technology that improves oil production in unconventional reservoirs in the U.S. and could be the best reliable method to unlock the remaining oil percentage (Zhou et al., 2018). Huff-n-puff gas injection has a more advantageous impact in increasing oil recovery compared to gas flooding techniques, especially in ultra-tight reservoirs with the matrix permeability under 0.001 mD (Tang et al., 2021; Milad et al., 2021). Because kerogen renders the surface of the pores oil-wet, extracting the oil from inside tight reservoirs is restricted by the presence of a high total organic carbon (TOC) (Jia et al., 2019). In multiphase-flow operations, the mixture of scales and multiphase fluids, such as gas and oil, may result in several challenges, such as the deposition of wax and asphaltene, the creation of hydrates, slugging, and the generation of emulsions (Shi et al., 2021). Particles made mostly of organic hydrocarbons that settle in oil and gas reservoirs might cause a number of flow-assurance concerns during oil extraction. Increased resistance to flow caused by these materials might decrease productivity or possibly plug pipelines (Hassanpouryouzband et al., 2020; Ali et al., 2021). Asphaltene precipitation and deposition is a difficult aspect of huff-and-puff gas injection into shale formations because it causes pore plugging in the shale and changes the wettability of the formation, which in turn reduces oil recovery. In crude oil, asphaltene is a solid-phase material that dissolves in aromatics like toluene but not in light n-alkanes such as n-pentane (Ahmed et al., 2022). The stability of asphaltenes in the crude oil decreases due to the interaction between the gas injected into the shale reservoir and the oil (Mohammed et al., 2021). Injecting gas into crude oil causes changes that affect the oil's solubility. Therefore, asphaltene starts to precipitate and flocculate because of the unstable condition of the colloidal suspension in the crude oil (Elturki and Imqam, 2020; Behbahani et al., 2013). Various studies have investigated the effect of a number of factors on asphaltene deposition in conventional reservoir cores on permeability reduction (Turta et al., 1997; Sim et al., 2005; Hamadou et al., 2008; Behbahani et al., 2014; Mehana et al., 2019; Lo et al., 2020). Many investigations have been conducted to highlight the impact of gas injection on asphaltene deposition using nitrogen (N_2) and CO_2 (Jamaluddin et al., 2002; Moradi et al., 2012; Zadeh et al., 2011; Khalaf et al., 2019; Takahashi et al., 2003; Afra et al., 2020; Elturki and Imqam, 2021; 2022; Espinoza Mejia et al., 2022; Zanganeh et al., 2018; Nascimento et al., 2021). The asphaltene instability in shale/unconventional resources during the miscible/immiscible CO_2 huff-n-puff operation is still not fully understood. To do so requires investigating the conditions under which the asphaltene may deposit and precipitate in tight shale resources during the CO_2 huff-n-puff injection process.

Recently, gas huff-n-puff and flooding process have been studied extensively in shale resources by various approaches, including experimental studies (Abedini et al., 2014; Yu et al., 2015; Yu and Sheng, 20115; Altawati, 2016; Song et al., 2022; Li et al., 2019; Sie et al., 2021; 2022; Zhu et al., 2020; Elwegaa et al., 2020; Badrouchi et al., 2022; Shilov et al., 2022; Mahzari et al., 2021; Sennaoui et al., 2022; Ma et al., 2019; Min et la., 2020), field pilots (Nuttal et al., 2005; Louk et al., 2017), and through simulation work (Sheng and Chen, 2014; Sanchez-Rivera et al., 2015; Sun et al., 2016; Wan et al., 2018; Wang et al., 2019; Zheng et al., 2021; Baek et al., 2021; Luo et al., 2022; Wang et al., 2022; Zhang et al., 2022). Using N_2 and Eagle Ford shale cores, Yu and Sheng (2015) carried out an experimental investigation. They used mineral oil to saturate the cores and to perform the study. The majority of the oil was extracted in the first two hours of production, during the "puff" phase, proving that N_2 was successful in enhancing oil recovery. There was a weakness in their research, however, since they didn't utilize crude oil but mineral oil instead, so avoiding the impact of asphaltene precipitation on the performance of oil recovery. To examine how water saturation influences oil recovery using CO_2 and N_2 huff-n-puff processes, Altawati (2016) saturated Eagle Ford outcrops with oil of decane and brine with a percentage of 15%. Altawati (2016) discovered that cores that were slightly wet with water had a lower recovery factor than those that were not saturated with water. Oil recovery during the CO_2 huff-and-puff process was studied by Li et al. (2017), who looked at the impact of the MMP. All fifteen tests utilized Wolfcamp cores, and the findings revealed an improvement in oil recovery at injection pressures higher than the MMP. Tovar et al. (2021) used 11 Wolfcamp shale cores in a number of tests to study the impact of CO_2 and N_2 injections on the performance of oil recovery. MMP, soaking length, and injection-gas mixtures were all variables investigated. Injecting CO_2 instead of N_2 was shown to increase oil recovery because CO_2 can evaporate a wider range of hydrocarbons. Oil recovery increased with increasing pressure and soaking duration beyond the miscibility limits for CO_2. Evaluating the oil recovery in tight resources was the focus of experiments done by Bougre et al. (2021), who compared the results of flooding with CO_2, N_2, and a CO_2-N_2 mixture. All of the tests utilized the same oil-soaked core sample from the Eagle Ford shale. Each experiment included washing and resaturating the sample. The CO_2 gas injection produced the best oil recovery, followed by the CO_2-N_2 mixture with a relatively slow breakthrough. The findings of oil recovery from the huff-and-puff injection of CO_2 are controversial, since a literature study reveals the influence of asphaltene attributable to CO_2 miscible injection was not evaluated.

Recent years have seen a few studies looking at the effects of asphaltene precipitation during huff-and-puff gas injection (Shen and Sheng, 2017a; 2017b; 2019; Mohammad et al., 2017; Li et al., 2020). Shen and Sheng (2017a) researched the impact of CO_2 huff-n-puff injection on the permeability and pore plugging due to asphaltene plugging in Eagle Ford shale. Results demonstrated that after six CO_2 cycles, pore diameters in the 100–800 nm range decreased as well as pore sizes below 100 nm. Also, a decrement of 47.5 nD of permeability was determined after six cycles of the CO_2 huff-n-puff process compared to the original permeability of 126 nD. Based on their results, pore plugging and asphaltene adsorption in shale cores were significant during the CO_2 huff-n-puff injection process. Mohammad et al. (2017) used computer simulations to estimate the formation of asphaltene in low-permeability reservoirs after huff-and-puff CO_2 injection. They aimed to optimize CO_2 injection by including brine into the huff-and-puff CO_2 injection in order to decrease asphaltene issues. Shen et al. (2019) conducted a simulation study to provide a better idea of the main factors that might affect asphaltene deposition and precipitation in hydraulically fractured shale reservoirs under the CO_2 huff-n-puff injection process. They found that asphaltene deposition can be different in the rock matrix and fractured network, and thus, the permeability reduction will also differ. Li et al. (2020) performed experimental research to highlight the impact of CO_2 huff-n-puff process on a shale outcrop using four cycles and two oil samples. Their findings revealed that the greatest amount of asphaltene was deposited in the first cycle. Despite the aforementioned studies' emphasis on a variety of variables that influence oil production from shale formations using the gas huff-and-puff technique, there is a lack of comprehensive studies on how to evaluate asphaltene precipitation issues and how to determine its impact on oil production performance in shale resources using gas huff-n-puff technique (especially below and above MMP). The novelty of the work lies in presenting a comprehensive experimental evaluation of asphaltene instability in tight shale reservoirs during miscible and immiscible conditions using shale cores and filter paper membranes. This study further expands the work of Elturki and Imqam (2021; 2022a; 2022b; 2022c) who evaluated the effect of continuous and huff-n-puff immiscible/miscible N_2 injections on the deposition of asphaltenes.

The ultimate goal of this research is to highlight the process of asphaltene damage during miscible and immiscible CO_2 huff-n-puff process, especially in ultra-small-permeability reservoirs (mainly unconventional reservoirs). A better understanding of the factors impacting asphaltene instability during miscible and immiscible CO_2 huff-n-puff injections in tight-shale resources must therefore contribute from the completion of this extensive comparative study.

2. MATERIALS AND METHODOLOGY

There were three primary parts to the laboratory work. First, MMP determination experiments. Second, CO_2 huff-n-puff gas injection tests. Third, asphaltene deposition and pore plugging analysis. Initial investigations determined the MMP for CO_2 huff-n-puff tests. The miscible and immiscible pressures of the huff-n-puff gas injection tests were selected based on the findings of MMP. Figure 1 illustrates the experimental design for the primary tests and analysis presented in this research. Table 1 provides a summary of the study's primary materials and their suppliers.

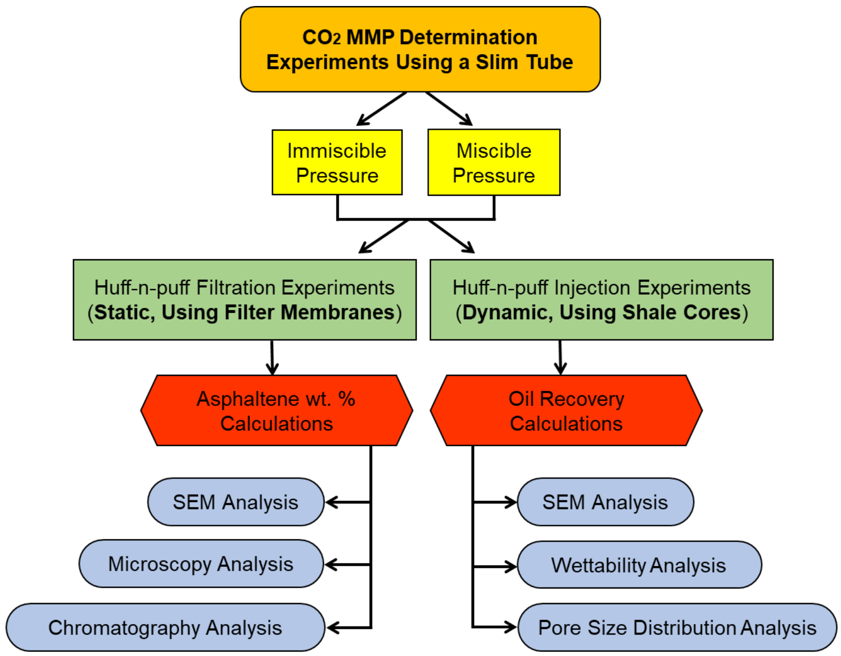

Figure 1. Flowchart of experimental design.

Table 1. List of Chemical/Material Suppliers Used in This Research

Material/Equipment	**Type/Size**	**Supplier/Company**
Crude oil	-	Western Missouri Oil Field
Solvent of n-heptane	Chemical formula: C_7H_{16}, purity: ≥99%)	Lab Alley Powering
Whatman filter paper	Size: 2.7 μm	OFITE
Filter paper membranes	Pore size structure: 50, 100, and 450-nm	Foxx Life Sciences
Oven	LBB2-27-2	Despatch

2.1. EXPERIMENTAL MATERIALS

Shale outcrops from the Eagle Ford formation were completely saturated with Western Missouri Oil (viscosity: 19 cP, density: 0.864 g/cc, ^{o}API: 32). The crude oil's composition was analyzed utilizing gas chromatography and mass spectrometry (GC-MS), and the findings are presented in Table 2. For the MMP tests, the western Missouri oil was used to saturate the slim tube and then the gas (i.e., CO_2) was injection to determine the MMP, more details will be discussion in the following section. For the huff-and-puff filtration studies, 450, 100, and 50 nm filter papers were used. The gas injection for the slim tube and huff-and-puff trials supplied from CO_2 gas cylinders with a 99.9% purity level. During the huff-and-puff tests, the cores were placed in a specially made vessel (Length: 15.25 cm, Inside Diameter: 5.0 cm, Outside Diameter: 7.63 cm). During the MMP tests, the temperature was controlled through an oven. Figure 2 shows a core sample dimensions and after the saturation process. Their diameter and length, respectively, were 2.5-cm and 5-cm. The average permeability and porosity were 0.000198 mD and 5.7% (helium porosity), respectively. Figure 3 shows the cores' XRD (X-ray diffraction) results. Finlay, the TOC (total organic carbon) of the Eagle Ford samples was 5.5% (measure by Rock Eval pyrolysis).

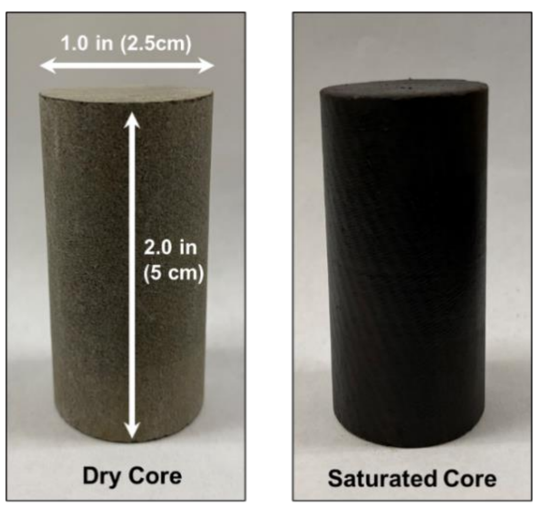

Figure 2. A core taken before and after the saturation phase.

Table 2. The elemental composition of crude oil

Carbon Number	**Mass %**
C_1	0.000
C_2	0.000
C_3	0.000
C_4	0.003
C_5	0.063
C_6	0.430
C_7	0.540
C_8	64.48
C_9	0.278
C_{14}	0.309
C_{15}	0.349
C_{16}	0.425
C_{17}	3.490
C_{18}	0.196
C_{19}	1.166
C_{20}	3.596
C_{21}	0.926
C_{22}	2.662
C_{24}	1.973
C_{27}	5.395
C_{28}	7.225
C_{29}	1.322
C_{30+} (including asphaltene)	5.170
Total	100.0

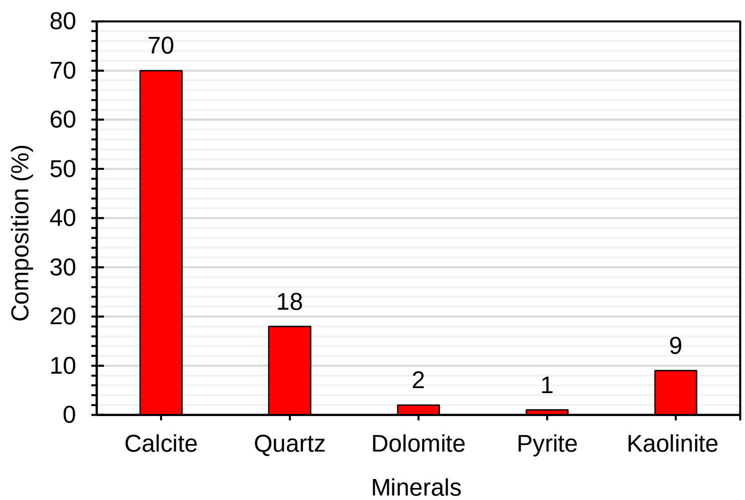

Figure 3. Eagle Ford XRD results.

2.2. SLIM TUBE EXPERIMENTS

In order to carry out the MMP tests, we used a slim tube that was filled with sand as well as three accumulators. The slim tube has the following dimensions: length: 13.10 m, inside diameter: 0.21 cm, and outside diameter: 0.41 cm. Figure 4 highlights the primary parts of the setup. The first phase was cleaning the slim tube, the second step was saturating the slim tube with the oil, and the third step was injecting gas into the slim tube. Therefore, the first accumulator stored the crude oil that was going to saturate the slim tube, the second accumulator contained the n-heptane solvent that was utilized to wash the slim tube, and the third accumulator contained the gas that was pumped into the slim tube throughout the tests. The methodology for carrying out the tests began with the preparation of the slim tube, which included completely filling it with distilled water. Constant injections of crude oil at a rate of 0.25 ml/min were conducted until the tube was saturated with oil. This can be confirmed at the outflow of the slim tube, which only received oil as a fluid. This insured that the whole slim tube was completely filled with oil. The gas accumulator was loaded with CO_2, and after that, the syringe pump's constant pressure mode was used to inject gas at a pressure that had been previously determined. When the gas breaks through or 1.2 pore volume of gas was injected, the test was stopped. The MMP may be calculated by generating a graph that compares the pressure of the gas injection to the total amount of oil recovered. After each experiment, the slim tube setup was given a thorough cleaning using the solvent xylene. This was done to guarantee that there was no oil residue left in the slim tube, which may have had an impact on the following experiment.

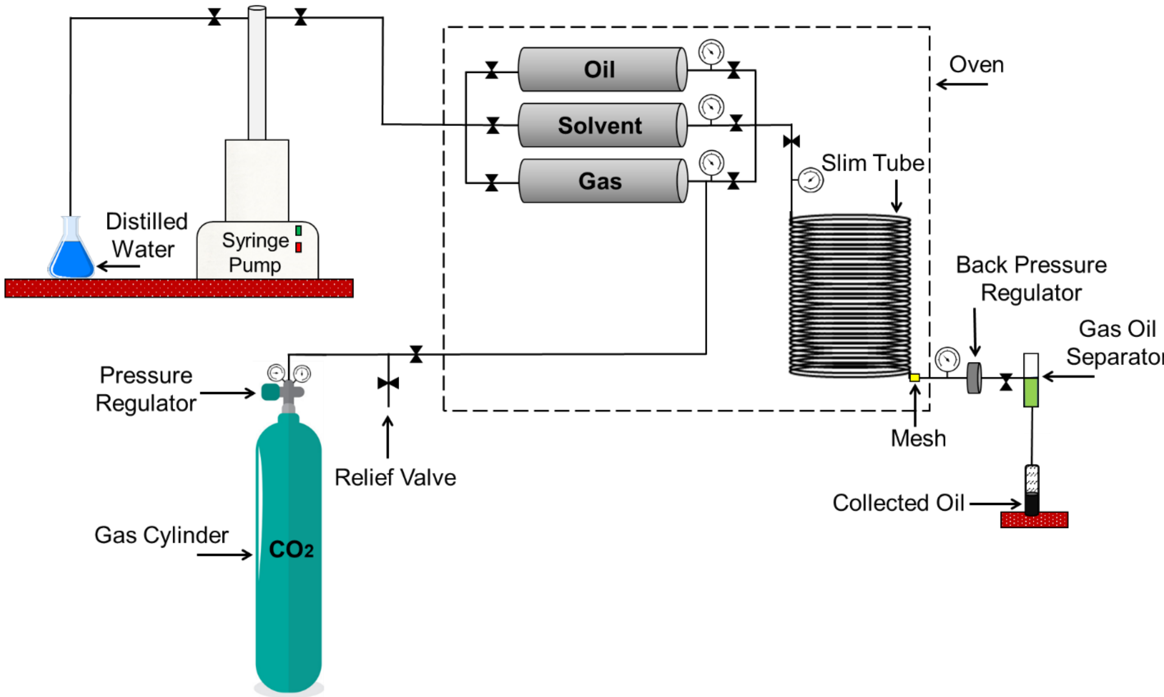

Figure 4. Slim tube apparatus for CO_2 MMP.

2.3. HUFF-N-PUFF FILTRATION TECHNIQUE (STATIC MODE)

The primary parts of the huff-n-puff tests using the static mode are shown in Figure 5. Due to the low outlet pressure of CO_2 cylinder, an accumulator was used to store the CO_2 and pump it directly into the vessel utilizing a syringe pump to accomplish high-pressure levels. Various filter-paper membranes with pore sizes of 50, 100, and 450-nm were used to represent the structure of shale reservoirs and to examine the influence of variable sizes. Utilizing a filtration vessel with three mesh screens as a means of protecting the filter papers and avoiding the possibility of the sheets breaking at higher pressures. The mesh screens were built with porous structure to allow the oil to flow across them freely. One transducer was used to record and monitor the pressure during the experiments. The following steps were taken to perform the static mode experiments:

- The vessel was loaded with 50 nm, 100 nm, and 450 nm filter membranes and then was closed and attached to the gas source/cylinder in order to fill the accumulator of gas. Next, the pressure regulator was used to secure the gas cylinder.
- The gas cylinder was opened using the pressure regulator at the desired pressure after 30 ml of crude oil was injected into it by utilizing a syringe pump attached to the accumulator of oil.
- During the "huff" stage, the gas was able to mix with the crude oil for a set period of time (in this case, 6 h).
- The temperature within the vessel was adjusted to 70^oC by operating a heating jack.
- When the soaking time was over, the pressure inside the vessel was released. This is known as the "puff" phase.
- After taking the oil from the effluent and opening the vessel, a sample of the crude oil that had been filtered through the membranes was taken for asphaltene examination. Next, the oil that had been filtered through the paper membranes was carefully returned for yet another new cycle.
- Without changing the filter membranes, the aforementioned procedures were carried out once again to create a new huff-and-puff process.

Figure 6 shows a simple sketch of test tube and the process of asphaltene deposition to quantify the weight of asphaltenes after mixing 1 ml of crude oil with 40 ml of n-heptane (ratio of 1:40). Before measuring the asphaltene wt. %, 1 ml of oil from each filter paper was mixed with 40 ml of n-heptane in a test tube (ratio of 1:40).

Filter paper (2.7 μm) was used to filter the mixture. The asphaltene wt. % determined using the following equation:

$$\text{Asphaltene wt. \%} = \frac{\text{wt.}_{\text{asphaltene}}}{\text{wt.}_{\text{oil}}} * 100 \tag{1}$$

Where asphaltene wt. % is the asphaltene weight percentage, wt. $_{\text{asphaltene}}$ is the asphaltene particles' weight on the filter paper, and wt. $_{\text{oil}}$ is the weight of oil sample.

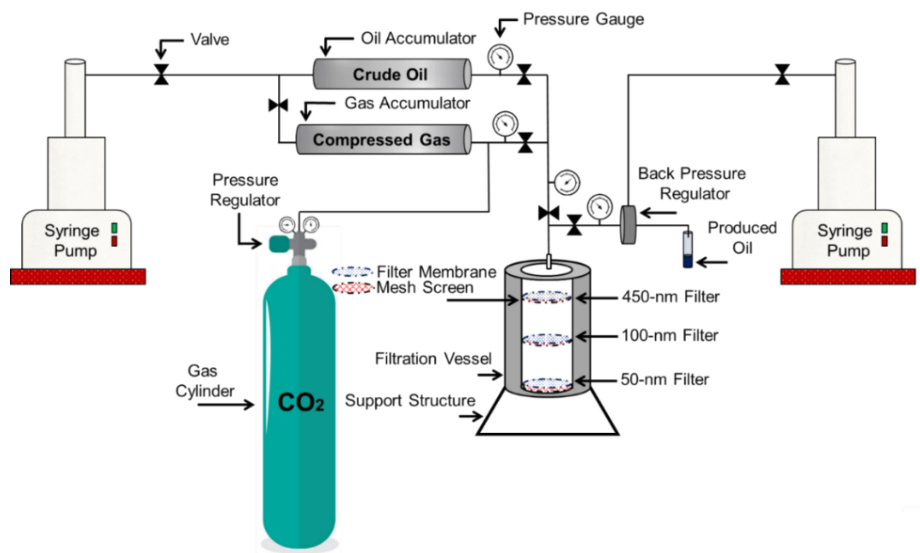

Figure 5. Huff-n-puff filtration test setup.

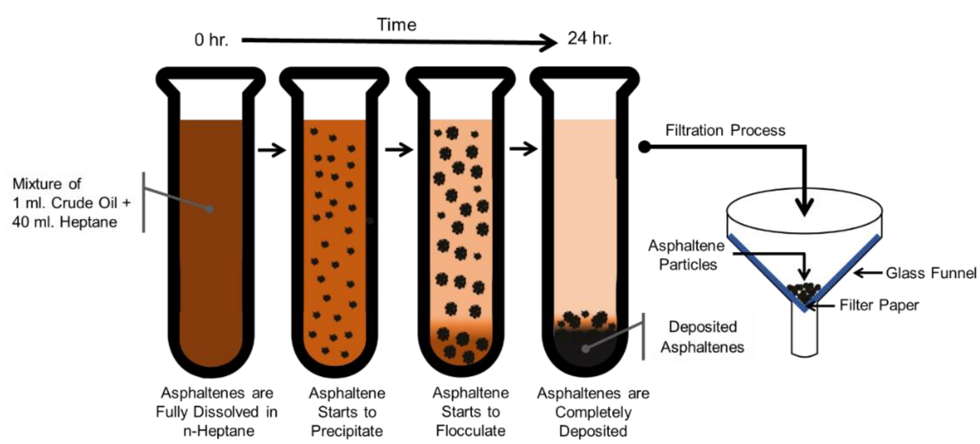

Figure 6. Simple sketch of test tube showing the process of asphaltene precipitation, flocculation, and deposition.

2.3.1. Huff-n-puff Filtration Technique Scope of Work. Two filtration huff-n-puff experiments were conducted utilizing one miscible pressure (i.e., 1750 psi) and one immiscible pressure (i.e., 1000 psi). Various filter paper membranes were used in each test as shown in the table below. All experiments were carried out at 70^{o}C and for 6 h soaking time. The purpose of these tests was to examine how gas condition influences the asphaltene stability and the structure of filter membranes. These tests were implemented to highlight and evaluate of how CO_2 condition can influence the asphaltene stability and the membranes' pore structure. These tests will provide an understanding of how asphaltene affects ultra-pore structures which represent real tight shale structures. Table 3 summarizes the operating conditions used in this section.

Table 3. CO_2 huff-n-puff filtration experiments' operating parameters.

Test No.	Filter Membrane's Pore size (nm)	Gas Used	Soaking time (h)	Injected pressure (psi)	CO_2 Condition
1	450	Carbon Dioxide (CO_2)	6	1000	Immiscible
	100				
	50				
2	450		6	1750	Miscible
	100				
	50				

2.4. HUFF-N-PUFF PROCESS USING EAGLE FORD CORES

Eagle Ford outcrops (8 cores) were used to conduct immiscible/miscible CO_2 huff-n-puff tests based on the findings of MMP tests. Figure 7 illustrates the setup used in the dynamic mode tests. A high-pressure vessel was utilized for accommodating the cores. A syringe pump attached directly to the accumulator of gas for holding and boosting the pressure of CO_2 gas. Finally, to mimic the real shale temperature during the experiments, a heat jacket was used.

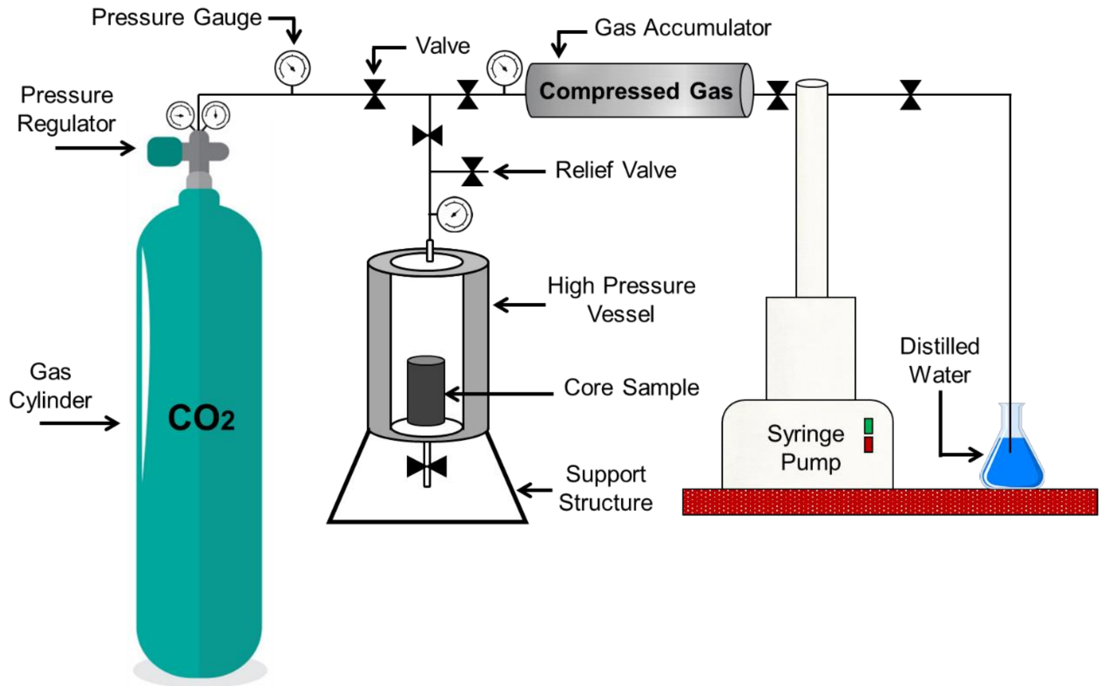

Figure 7. CO_2 Huff-n-puff experiments setup.

Prior to the saturation step, twelve Eagle Ford cores were labelled and saturated with the same properties of crude oil used in the MMP tests. An accumulator was used to accommodate the core, and then they were subjected to high pressure and high temperature for a period of ten months to guarantee that the cores would be saturated. The saturation process was discontinued after ten months since the cores' weight did not change during the last two months of the saturation time, demonstrating that the outcrops were completely saturated. Figure 8 illustrates the weight change of three selected cores throughout the saturation step.

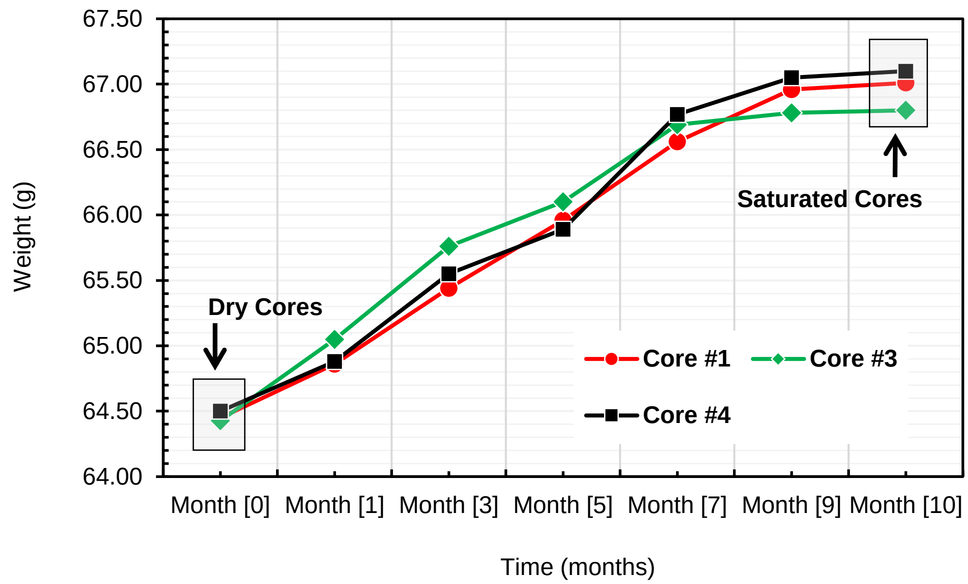

Figure 8. Core saturation examples during a 10-month period.

Spaces surrounding the core improved gas flow during the tests after inserting it in the vessel. Figure 9 displays a top view of the actual vessel. The experiments were conducted using the following steps:

- Following the placement of the core inside the vessel, the vessel was then closed after being attached to the CO_2 cylinder and the gas accumulator.
- The CO_2 was pumped into the vessel at the specified pressure during the huff stage, and then the CO_2 was allowed to soak the saturate core for the amount of time that was set for the soaking process.
- For the temperature, a heating jacket was used to boost the temperature to mimic the reservoir temperature (i.e., 70^{o}C).
- Depressurizing the vessel after the end of soaking time is called the “puff” stage.

- The core was collected in order to determine the recovery factor at certain production durations by applying the following formula:

$$\text{Oil Recovery Factor (RF)} = \frac{wt_1 - wt_2}{wt_1 - wt_{dry}} \quad (2)$$

Where:

- wt_1 is the saturated core weight.
- wt_2 is the core weight after production time.
- wt_{dry} is the core weight when its dry

- After calculating the RF from the previous gas cycle, a new cycle was started, and the cycles were terminated when no cumulative oil recovery was calculated/determined.
- Once all the required cycles were completed, the Eagle Ford cores were tested for asphaltene precipitation, alteration in pore size distribution and wettability phase.

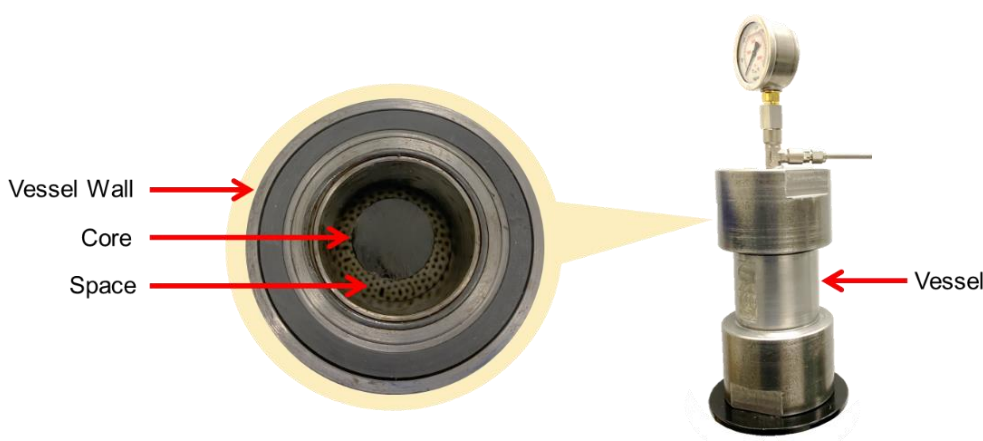

Figure 9. Real vessel top-view.

2.4.1. Huff-n-puff Tests Using Shale Cores Scope of Work. Eight Eagle Ford outcrops were utilized to study the effect of CO_2 miscibility on oil recovery performance and asphaltene precipitation using huff-n-puff injection technique. Extra four-reference cores that were only saturated (no CO_2 gas exposure) used to measure their wettability phase and pore size structure range. Various factors were examined such as soaking time, injection pressure, and production time. Table 4 summarizes the operation conditions.

In order to investigate how the soaking period influences the amount of oil that can be extracted, many cores were exposed to a gas huff-n-puff pressure of 2,000 psi and a range of soaking durations (i.e., 1, 6, 12, and 24 h). Two techniques were used to investigate the influence of soaking time: one core for all soaking durations (test no. 5) and utilizing various cores for each soaking time (tests no. 6-8) to evaluate the influence of re-soaking procedure on the performance of oil recovery (more details in the following sections). The temperature for all the tests was maintained at 70^{o}C.

For each test, the cycle number ranged, but the cycles were stopped when there was no observation of oil (i.e., no oil recovery recorded/calculated). For both miscible and immiscible scenarios, the production times (i.e., the time when the core was weighed after finishing the huff-n-puff cycle) were defined as 15, 60, and 90 min. Finally, slim tube results were the reference for selecting the CO_2 miscible and immiscible pressures.

Table 4. CO_2 huff-n-puff experiments' operating parameters

Test no.	Core no. **	Gas Used	Soaking time (h)	Injected pressure (psi)	Production time (min)
1	#1	Carbon Dioxide (CO_2)	6	1000	15, 60, and 90
2	#2		6	1300	
3	#3		6	1750 *	
4	#4		6	2000 *	
5	#5		1, 6, 12, and 24	2000 *	15
6	#6		1	2000 *	
7	#7		12	2000 *	
8	#8		24	2000 *	

** Miscible pressure condition*

*** Note: Four additional cores, numbered #9, #10, #11, and #12, were used as references for the wettability assessment and pore size distribution measurements.*

3. FINDINGS AND DISCUSSION

3.1. MINIMUM MISCIBILITY PRESSURE (MMP) RESULTS

The gas injection process can occur in either condition–miscible or immiscible; however, miscibility had a significant influence on the performance of oil recovery. The MMP is the pressure at which a gas becomes miscible with the crude oil at the conditions of the reservoir such as temperature (Sebastian et al., 1992; Vahidi et al., 2007; Belhaj et al., 2013; Elturki and Imqam, 2021c). Nine tests were performed to estimate the CO_2 MMP at pressures of 400, 600, 800, 1000, 1200. 1500, 1750, 1850, and 2000 psi at 32 and 70^oC, as shown in Figure 10. As a point of reference of the MMP findings, the first MMP tests were carried out at 32^oC. The cumulative oil recovery (OR) at each of the CO_2 pressures is shown in Table 5. The MMP of CO_2 was estimated to be 1450 and 1650 psi at 32 and 70^oC, respectively. The MMP findings were utilized to determine which miscible and immiscible pressures of CO_2 that could be selected for the static and dynamic CO_2 huff-n-puff tests.

Table 5. CO_2 slim tube cumulative oil recoveries (%).

Pressure Injected (psi)	**400**	**600**	**800**	**1000**	**1200**	**1500**	**1750**	**1850**	**2000**
Cumulative OR at 32ºC	32.20	45.40	57.10	64.71	75.20	91.30	92.10	92.50	93.12
Cumulative OR at 70ºC	66.30	72.50	75.60	81.90	84.40	93.30	98.50	98.80	99.10

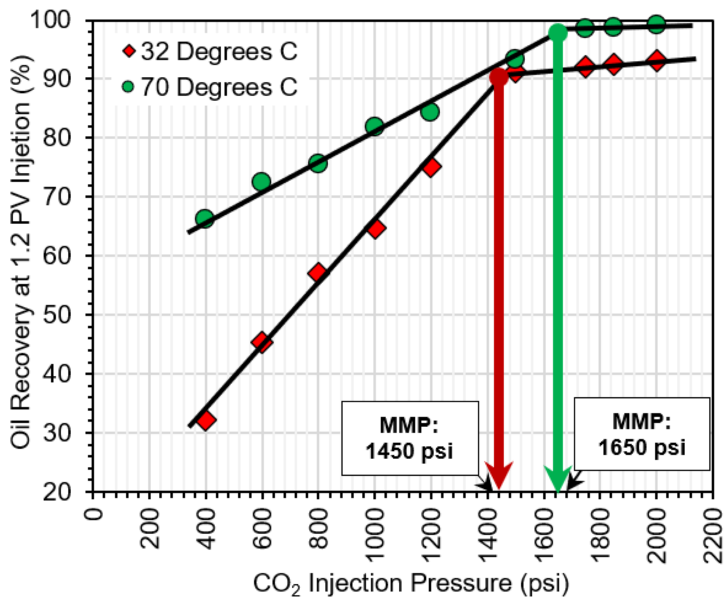

Figure 10. Results of CO_2 MMP experiments at 32ºC and 70ºC.

3.2. RESULTS OF HUFF-N-PUFF FILTRATION TESTS

The huff-and-puff filtration methodology was used to perform two sets of huff-and-puff tests (i.e., static mode). In order to examine the influence of CO_2 pressures (i.e., above and below MMP) on asphaltene deposition, two scenarios were designed. Pressures of 1000 psi and 1750 psi were considered for immiscible and miscible circumstances, respectively. For both tests, the temperature and soaking time were fixed to be 70ºC and 6 h, respectively. The findings of the CO_2 huff-n-puff filtration tests are presented in Figure 11. These findings suggest that asphaltenes in crude oil were impacted by varying degrees of aggregation during the first-two cycles. The figure reveals that the asphaltene wt.% in the 450-nm filter upsurged considerably from 8.89% to 10.23% when comparing the first cycle to the second cycle, respectively, with an immiscible CO_2 pressure of 1000 psi. The asphaltene wt. % increased considerably as the number of cycles increased until the fifth cycle, demonstrating that asphaltene particles were affected at a higher pace in the early cycles. Because of the ultra-small pore structure, the 50-nm filter was identified to have a more asphaltene wt. % than the other filters. For example, a significant increase was observed in the fifth cycle in which the asphaltene wt.% climbed to 18.21% compared to 14.22% in the first cycle. The asphaltene wt. % started growing slowly to 19.68% in the sixth cycle, then stabilized after the seventh cycle. However, the miscible CO_2 pressure of 1750 psi dramatically increased the asphaltene wt. % in all filter membranes, indicating that the miscibility notably disrupted the connections between asphaltene particles and resins in the crude oil. For example, the asphaltene wt. % in the 50-nm filter was 24.98% during the first cycle, however by the fifth cycle, it had dramatically jumped to 35.5%. The asphaltene wt. % remained nearly constant at 35.98% during the subsequent cycles. To sum up, the asphaltene wt. % went up in all huff-and-puff experiments as the pore size structure of the membranes became smaller and in the first cycles of the huff-and-puff process. According to these findings, CO_2 causes more rates of asphaltene deposition and flocculation, especially at miscible gas conditions which has strong light component extraction (Chung, 1992). That could occur because CO_2 has high solubility, thus, the mass transfer potential of CO_2 is very strong.

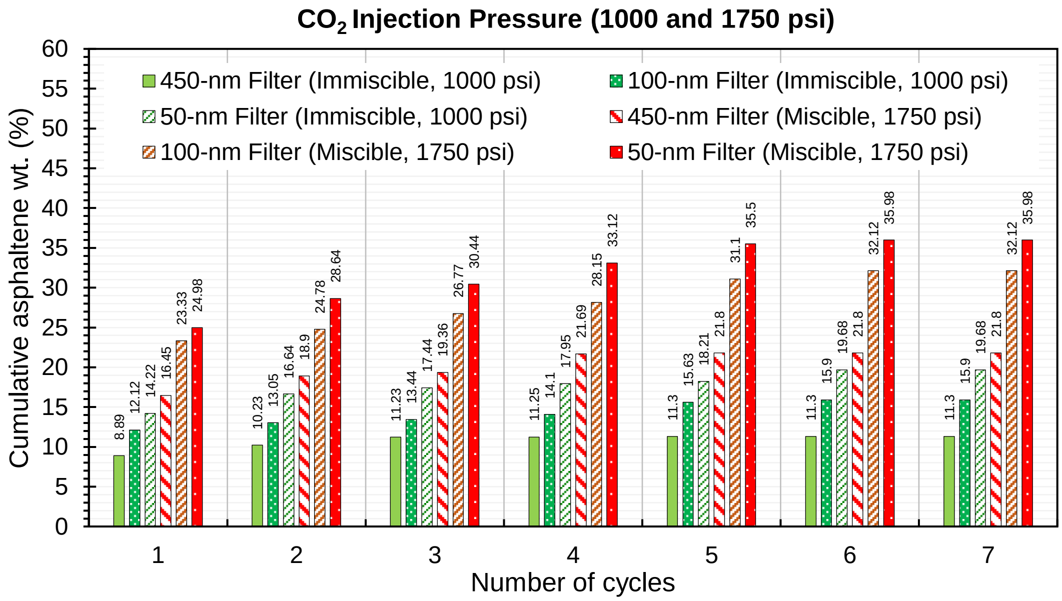

Figure 11. Asphaltene wt. % in all filter membranes after seven CO_2 cycles at 70°C.

3.2.1. Results of Chromatography Analysis. Following the completion of the last cycle of the filtration tests, samples of crude oil were taken from the oil that was produced in order to analyze the alteration in its elemental composition using gas chromatography-mass spectrometry (GC6890-MS5973). This step will ensure that the structure of filter membranes and gas cycles have an influence on heavy components in crude oil, such as asphaltenes. Figure 12 reveals the oil composition of the produced oil after miscible and immiscible CO_2 huff-and-puff tests. The findings demonstrated that CO_2 injection at miscible scenarios had a substantial influence on crude oil, as shown by the increased mole fraction of both the intermediate and heavy components (C_{15}-C_{30}). Partial extraction was observed for the light components (C_8-C_{14}) as CO_2 had a considerable light extraction mechanism. More heavy components (i.e., C_{31+}) were detected after CO_2 tests, including asphaltenes, due to the high mass transfer mechanism of high CO_2 pressure. Moreover, miscible pressure had weakened the connections between asphaltene particles and resins in the crude oil, resulting in an increase in asphaltene deposition and heavy components (Pereira et al., 2006; Wang et al., 2018).

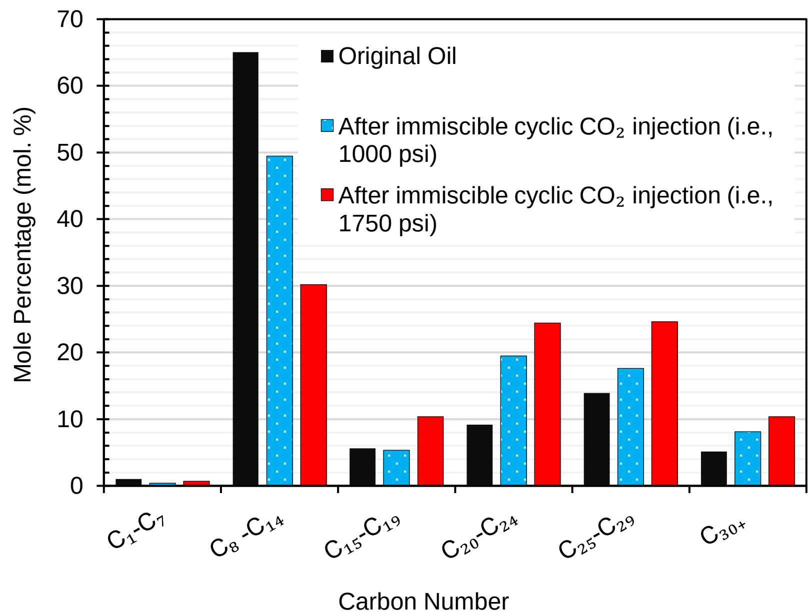

Figure 12. Crude oil carbon number before and after CO_2 huff-n-puff filtration tests.

3.2.2. Microscope and SEM Analysis. A Hirox digital microscope was used in order to investigate the pore structure plugging that resulted in the filter membranes as an outcome of the buildup of asphaltenes. After completing immiscible and miscible CO_2 tests (static mode), microscopic photos showing the filter membranes's pore structure (i.e., 450, 100, and 50nm) were taken at a magnification of 500 µm, as shown in Figure 13. Before the photos were captured, the filter paper membranes were cleaned and exposed to the solvent of heptane for 24 h. The figure reveals that asphaltene clusters plugged more spots in the 50-nm filter during miscible CO_2 pressure, resulting in more asphaltene depositions. This is due to the smaller pore structure of the 50-nm filter paper. This observation confirms the above results in previous sections. To provide a clear picture of filter membranes, scanning electron microscopy (SEM) was used for high-resolution photos of the membrane's structure. As shown in Figure 14, different photos of the membranes were captured to highlight the asphaltene deposition and its severity in pore plugging. The same sizes of the filter membranes were selected (i.e., 450, 100, and 50 nm) in both conditions of miscible and immiscible gas injections. Similar observations of the digital microscope were noticed in all filter membranes. For example, more asphaltene particles were found in the filter paper of 50-nm compared to 450-nm filter due to 50-nm has smaller pore structure. Moreover, the photos shows that darker colors were found during miscible CO_2 pressure. These results provide support to the observations above that CO_2 has a high solubility and high extraction of light-hydrocarbon compounds in oil, both of which have the potential to cause asphaltenes' related issues.

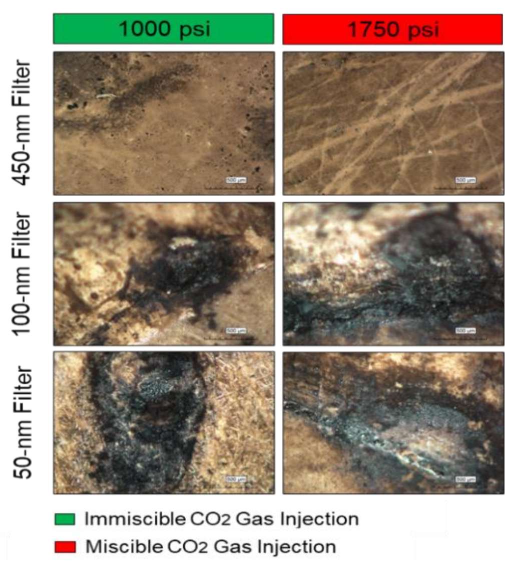

Figure 13. Microscopic photos at a magnification of 500 µm showing the structure of 450, 100, and 50 nanometer membranes following the last cycle of immiscible and miscible CO_2 injections.

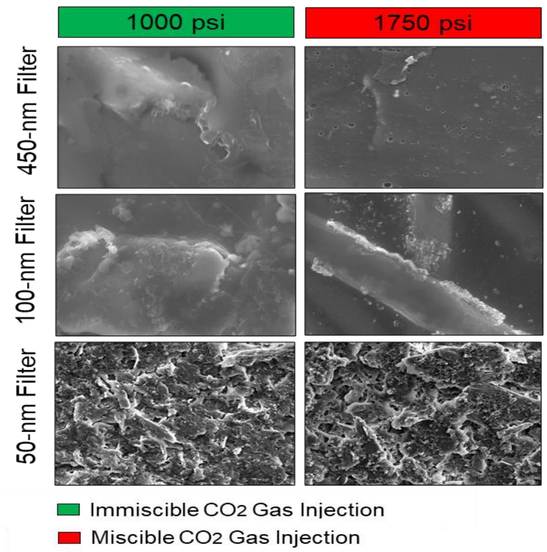

Figure 14. SEM photos at a magnification of 500 µm showing the structure of 450, 100, and 50 nanometer membranes structure following the last cycle of immiscible and miscible CO_2 injections.

3.3. RESULTS OF HUFF-N-PUFF GAS INJECTION USING SHALE CORES

3.3.1. Effect of Injected Pressure. The influence of CO_2 huff-n-puff injection pressure on the performance of oil recovery using eight Eagle Ford shale cores will be discussed. Table 6 presents the cumulative recovery factor (RF) results that were determined after each cycle for each test for CO_2.

Four sets of tests (test 1 to 4) were designed to evaluate the impact of CO_2 miscible conditions on the performance of oil recovery. The tests were carried out utilizing pressures both below and above the CO_2 MMP with a fixing soaking time of 6 h. At different production intervals of 15, 60, and 90 min, the oil recovery performance was measured, and the production time was evaluated. When there was no oil recovery recorded, the cycles were ended, and a new experiment was started.

Figure 15 demonstrates that at immiscible huff-n-puff conditions, oil recovery was significantly lower than under miscible conditions. The oil recovery performance significantly improved as the pressure continued to increase, as seen in the first cycle. According to the findings, oil can be recovered during the first five cycles in both scenarios, but after the sixth cycle, no more oil can be collected. These findings therefore confirms that miscible pressures were more effectiveness and advantageous over the immiscible pressure in terms of improving oil recovery. Similar results were obtained for the miscibility conditions, where miscibility positively impacted the oil recovery more than immiscible conditions. The possible explanation is that miscible CO_2 has a good solubility, which decreases the viscosity of oil and resulting in more oil extraction and recovery. Under miscible CO_2 pressure, hydrocarbon contents can be evaporated at a quicker pace, resulting in an increased oil recovery factor at higher pressures. The steady cumulative oil recovery in the last cycles indicates that asphaltene precipitation started to impact oil recovery performance in later cycles.

During conditions of immiscibility (i.e., low pressure), asphaltene clusters started to deposit mostly in the larger pores (Huang et al., 2022). During miscible conditions, asphaltenes started to fill both large and small pores especially after several cycles of huff-n-puff pressures; thus, the pore plugging rate in shale structure increased. These findings suggest that oil recovery existed primarily in early cycles, when asphaltenes were not yet fully deposited and blocked all pore spaces in the cores.

In terms of production time shown in the figures which is the time when the cores were collected from the vessel after the cycle phase and then leave it for a certain period of time to weight it. At 15, 60, and 90 min of production time, the oil recovery was calculated, and every cycle's soaking period was set at 6 h.

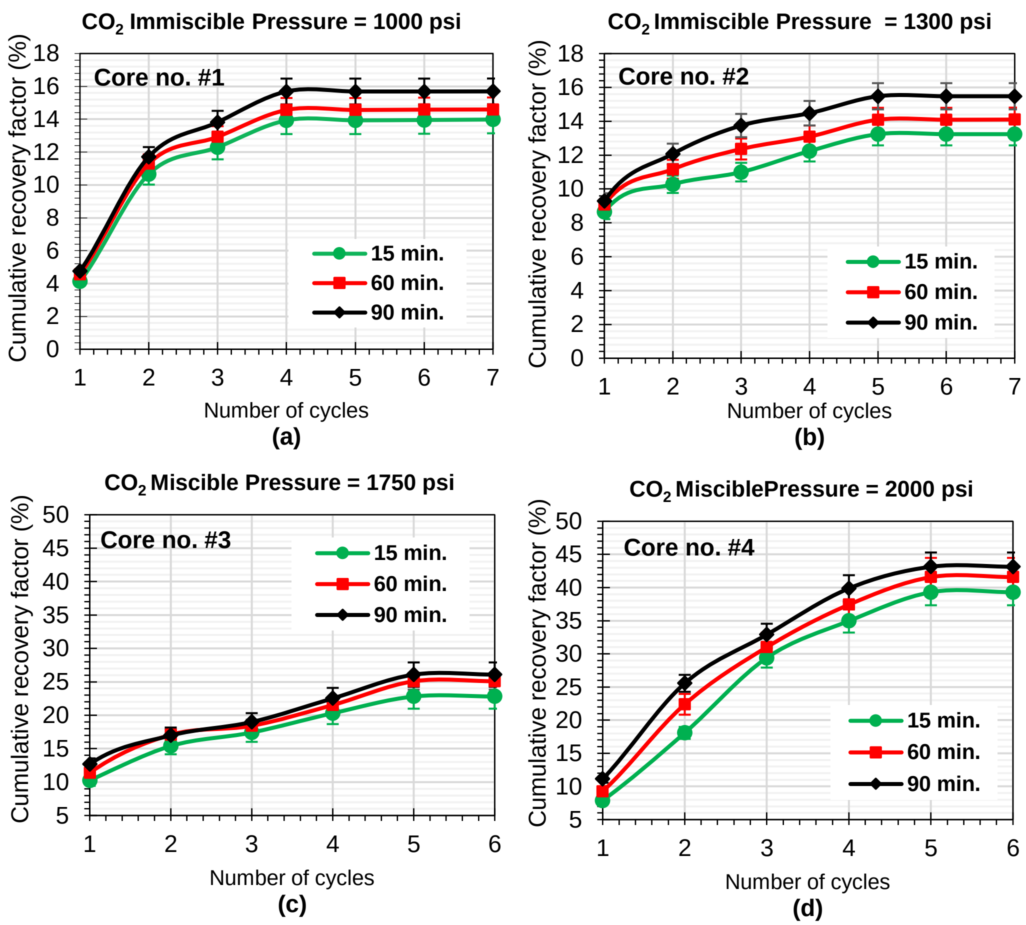

Figure 15. Cumulative oil recovery factor of CO_2 huff-n-puff pressures (6-h soaking time).

Figure 15 presents the findings of the CO_2 huff-and-puff experiments with different production periods. The figure reveals that for all CO_2 huff-n-puff cycles the recovery slightly increased in all production periods. After the second immiscible CO_2 cycle, the influence on oil recovery was most considerable. This was because more soaking time led to more interactions between the crude oil and the CO_2; thus, a higher solubility occurred, which led to a higher performance of oil recovery. A slight increase in oil recovery was determined during the second cycle which increased from 10.66% to 11.71% during the 1000 psi CO_2 gas injection for 15 and 90 min of production time, respectively. The oil recovery increased from 13.95% to 15.69% in the fifth cycle (conditions: 1000 psi, 15- and 90-min production time).

Table 6. Cumulative recovery factor (%) summary determined after CO_2 huff-n-puff tests.

Test no.	Soaking time (h)	Pressure (psi)	Production time (min)	Cycle 1	Cycle 2	Cycle 3	Cycle 4	Cycle 5	Cycle 6	Cycle 7	Cycle 8	Cycle 9
1	6	1000	15	4.14	10.66	12.30	13.93	13.93	13.95	13.98	-	-
			60	4.55	11.29	12.93	14.57	14.57	14.59	14.60	-	-
			90	4.76	11.72	13.82	15.69	15.69	15.69	15.70	-	-
2	6	1300	15	9.10	10.72	11.66	12.24	13.24	13.24	13.24	-	-
			60	9.07	11.16	12.36	13.09	14.09	14.09	14.10	-	-
			90	9.28	12.07	13.75	14.48	15.48	15.48	15.48	-	-
3	6	1750	15	10.26	15.40	17.42	20.30	22.81	22.81	-	-	-
			60	11.38	17.08	18.42	21.53	25.08	25.08	-	-	-
			90	12.67	16.97	18.99	22.52	26.08	26.08	-	-	-
4	6	2000	15	7.87	18.08	29.40	34.96	39.30	39.30	-	-	-
			60	9.26	22.39	31.01	37.42	41.57	41.57	-	-	-
			90	11.11	25.56	32.90	39.87	43.14	43.14	-	-	-
5	1	2000	15	11.16	13.25	18.68	21.74	24.30	25.20	26.40	26.20	26.19
	6	2000	15	27.46	31.46	40.03	44.03	45.61	47.36	47.10	47.41	47.41
	12	2000	15	47.50	61.79	68.93	71.30	73.22	75.46	75.60	75.61	75.61
	24	2000	15	76.06	81.66	85.47	90.12	91.54	92.33	93.11	93.12	93.12
6	1	2000	15	2.26	8.94	12.61	15.13	16.33	18.01	19.25	20.33	20.35
7	12	2000	15	17.93	25.43	32.48	41.13	45.12	46.32	47.10	47.11	47.11
8	24	2000	15	31.01	37.39	47.69	53.44	59.12	61.31	61.32	61.32	61.32

For miscible conditions (i.e., higher pressures), the change in oil recovery performance was seen from the second cycle, especially for the 2000 psi injection pressure. The previously discussed findings indicated that production time had a slightly positive influence on the performance of recovery factor during the process of CO_2 huff-n-puff.

3.3.2. Soaking Time Mode. The impact of the soaking step will be discussed in this section using different techniques at a pressure of 2,000 psi. The first technique is referred to as Mode-I, and it involved using many cycles on the same core with changing soaking times of 1, 6, 12, and 24 h. The second technique, known as Mode-II, is defined by the use of a separate core for each soaking time, as well as multiple cycles. Figure 16 illustrates the difference between these two modes. Test no. 5 was conducted using the Mode-I technique and one core was used for all soaking time and cycles parameters. To implement Mode-II, three more tests were designed (tests no. 6 to 8) in which each soaking time had its separate core. The results for the fourth test (soaking time of 6-h) were addressed in an earlier section. All experiments used a constant production period of 15 min and a miscible injection pressure of 2000 psi. As demonstrated in Figure 17a, nine CO_2 cycles using Mode-I were sufficient to extract more than 90 % of the crude oil (soaking time of 24 h). On the other hand, using Mode-II resulted in a maximum oil recovery of 61% after seven cycles, as shown in Figure 17b.

The optimal number of cycles was found to be eight, beyond which there was no more recovery recorded. According to these findings, increasing the soaking duration resulted in a larger amount of recovery, especially in Mode-I. This could be because of the high rate of hydrocarbon evaporation that was encountered while employing Mode-I with a range of soaking times.

The findings showed that carbon dioxide (CO_2) is effective for increasing oil recovery from shale cores for two main reasons: (1) because CO_2 can condense at a higher concentration in crude oil, and (2) because CO_2 can vaporize more hydrocarbon from the shale cores, mainly in miscible conditions. Both of these advantages were demonstrated by the findings of this study. Based on the findings, it appears that a higher proportion of oil recovery could be achieved by beginning with a short soaking time, during which asphaltene would not have time to completely precipitate in the core. Figure 18 shows the core samples (for Mode-I and Mode-II) following CO_2 huff-n-puff experiments with a 24 h soaking period and a 2000 psi injection pressure.

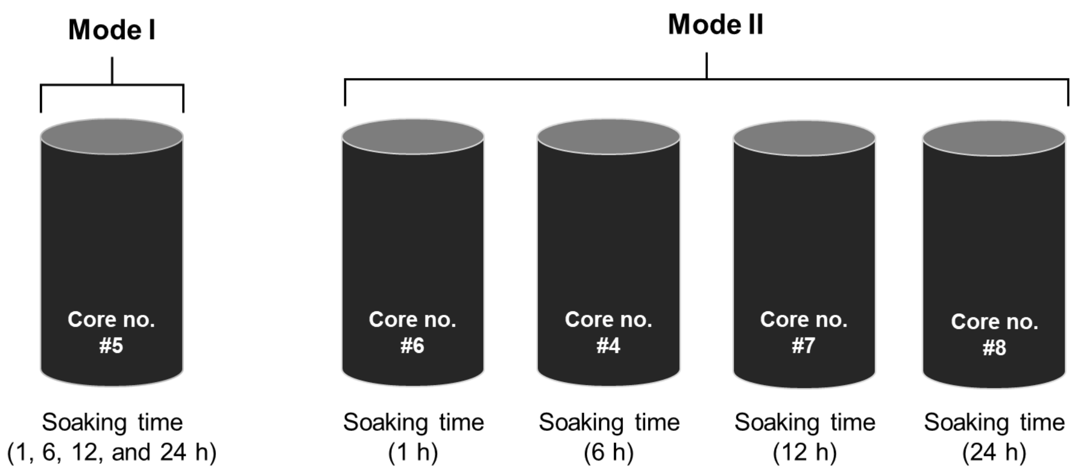

Figure 16. Soaking time modes Illustration.

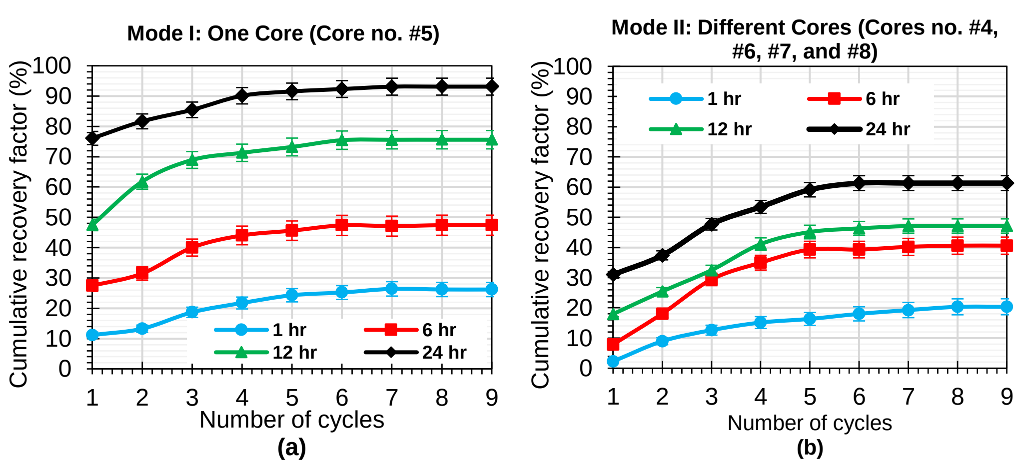

Figure 17. Cumulative recovery factor of CO_2 (a and b) huff-n-puff injections using Mode I and II at a 2000 psi CO_2 huff-n-puff pressure.

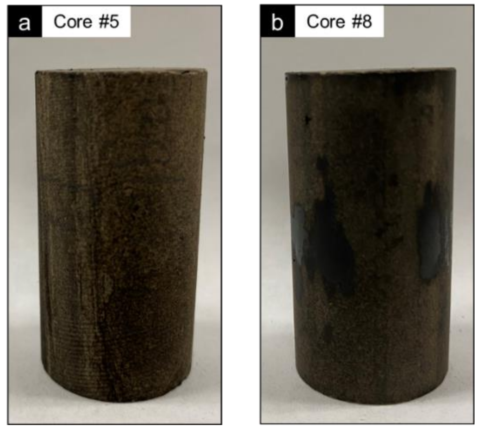

Figure 18. Photos of cores following huff-n-puff gas injection tests at 2000 psi (a) after a Mode-I CO_2 test and (b) after a Mode-II CO_2 test (24-h soaking period).

3.3.3. Wettability Analysis Due to Asphaltene Precipitation. Wettability can be defined as “the tendency of fluids to adhere to the surface” (Sheng, 2018). Wettability changes during enhanced oil recovery are a critical characteristic for oil production, specifically in unconventional reservoirs. During gas injection processes, asphaltene may be deposited and precipitated, which has the possibility of changing the wettability of shales and, as a result, the efficiency of oil recovery. Capillary pressure in shale rocks is relatively high because of the small permeability of the shale structure. The wettability of shale rocks is variable; it is not necessarily oil-wet as has been commonly believed but can be water- or oil-wet (Sheng, 2018). However, some studies have indicated that shale rocks tend to have more oil-wet phase wettability (Odusina et al., 2011; Akbarabadi et al., 2017). The asphaltenic components and the total organic carbon (TOC) content both have an impact of wettability phase of shale rocks (Kumar et al., 2008; Pan et al., 2020; Mohammed et al., 2021). This study implemented an air-liquid-rock system to examine the Eagle Ford cores’ wettability before and after CO_2 huff-and-puff experiments. Figure 19 displays equilibrated droplets of brine on all shale samples before and after the CO_2 huff-and-puff experiments. Before CO_2 huff-n-puff gas injection experiments, the contact angle was measured using four separate saturated cores which used as a reference (Figure 19b). The four cores were saturated with crude oil and the average contact angle was determined to be 82.95o (neutral wettability phase). After completing CO_2 huff-and-puff tests in both scenarios, the contact angles of all shale cores were measured as presented in Table 7. After the CO_2 huff-n-puff testing, the cores were found to have an average wettability of 114.17o (i.e., weakly oil-wet). These findings show that CO_2 had a greater influence on the asphaltene precipitation in Eagle Ford cores. When CO_2 gas was injected at miscible injection pressures, the contact angle increased, suggesting that miscibility may promote a weak oil-wet to moderate oil-wet system during CO_2 huff-n-puff tests. Asphaltene deposition has affected the surface structure of the shale, making it harder, leading to an increase in contact angle measurements (Amin et al., 2010; Hosseini et al., 2019). Our results were consistent with the results of other researchers, who reported that an increase in gas injection pressure led to an increase in the contact angle (Sarmadivaleh et al., 2015; Iglauer et al., 2015; Roshan et al., 2016; Arif et al., 2016; 2017; Pan et al., 2018). When injecting miscible CO_2 gas into shale basins, more oil-wet systems may be observed. Moreover, our results indicate that reduction of oil recovery and asphaltene precipitations was mostly found and accumulated during the later cycles. This is due to the fact that a decrease in oil recovery was observed in the last two cycles of the majority of CO_2 huff-and-puff tests. More cycles increased the pace at which asphaltene clusters begun to fill the larger spaces in core’s structure (Chung, 1992), and more asphaltenes were precipitated in the cores with an increase in the plugging rate. Following CO_2 huff-and-puff tests, the oil recovery factor decreased, and more cycles revealed that asphaltene deposition and precipitation had a negative influence on the oil recovery's performance (Shen and Sheng, 2018). To sum up, our results suggested that CO_2 huff-and-puff method, particularly at miscible conditions, affected the asphaltene's stability and severely damaged the strong connection between asphaltenes and resins, leading to an increase in asphaltene plugging rate.

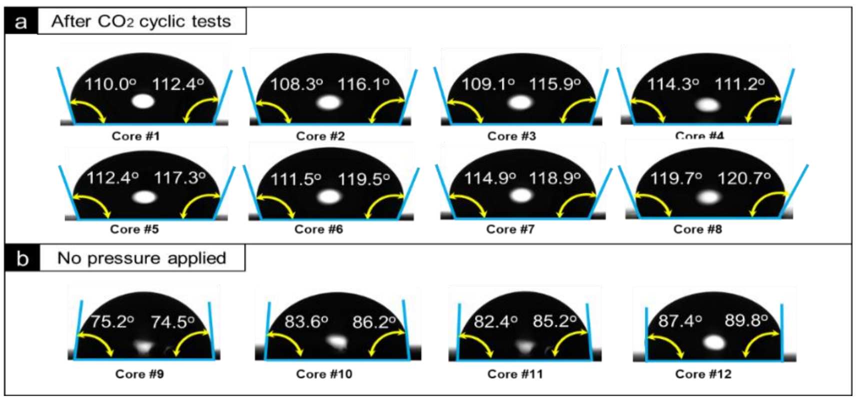

Figure 19. Contact angle determination using brine droplets (a) after CO_2 huff-n-puff tests, and (b) no pressure exposure.

Table 7. Contact angle determination.

Stage	CO_2 Condition	Test No.	Pressure Used (psi)	Average Contact Angle (°)	Status of Wettability *	Total Average
Four Separate Cores		-	No Pressure Exposure	83.80	Neutrally-Wet	82.95
				74.50	Neutrally-Wet	
				88.60	Neutrally-Wet	
				84.90	Neutrally-Wet	
After CO_2 Huff-n-puff Tests	Immiscible	1	1000	111.20	Weakly Oil-Wet	114.51
		2	1300	112.20	Weakly Oil-Wet	
	Miscible	3	1750	112.50	Weakly Oil-Wet	
		4	2000	112.75	Weakly Oil-Wet	
		5	2000	114.85	Weakly Oil-Wet	
		6	2000	115.50	Weakly Oil-Wet	
		7	2000	116.90	Weakly Oil-Wet	
		8	2000	120.20	Weakly Oil-Wet	

* Based on definitions from Arif et al. (2016) and Anderson (1986). ** Wettability was classified as: 0°= completely water-wet; 0 to 50°= strongly water-wet; 50 to 70°= weakly water-wet; 70 to 110°= neutrally wet; 110 to 130°= weakly oil-wet; 130 to 180°= strongly oil-wet.

3.3.4. Scanning Electron Microscope (SEM) Examination. The main objective of utilizing SEM was to detect alterations in the structure of shale formations caused by asphaltenes The SEM examinations may provide further details on asphaltene particles inside the shale core and also give a precise image of the ultra-small pores that were plugged with asphaltenes. Gas injection may break the bonds between the resins and asphaltene molecules in crude oil, resulting in an increased in asphaltene instability and an increase in pore plugging. A scanning electron microscope (SEM) was utilized (100 µm) to show the severity of asphaltene's pore plugging of the cores used, as shown in Figure 20. After the CO_2 huff-and-puff tests, three cores were selected for SEM evaluation in this study, with the findings presented in Figure 20. (a, b, and c).

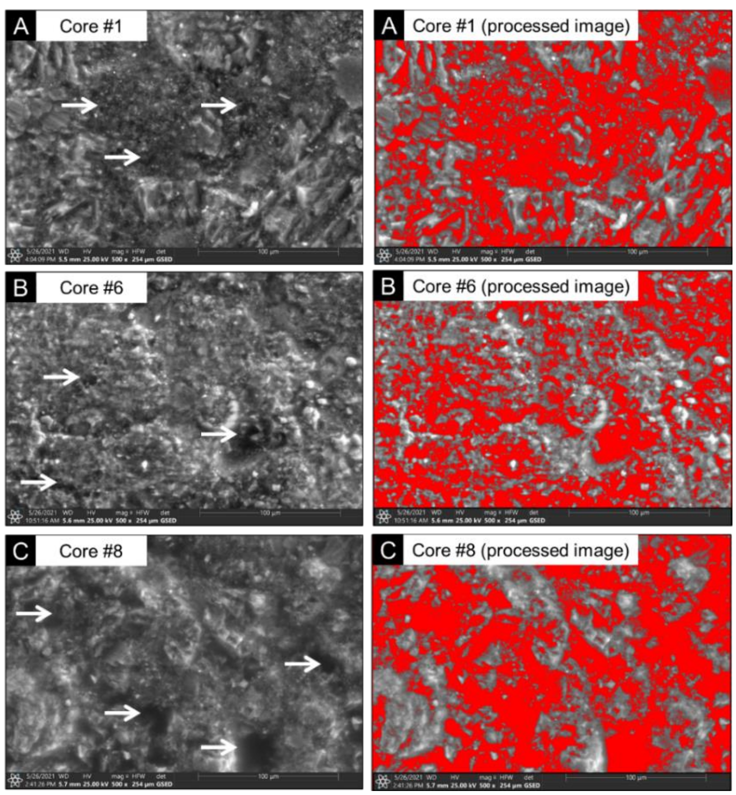

Figure 20. Scanning electron microscope (SEM) pictures (100 µm) of three cores after CO_2 huff-n-puff gas injection tests.

Asphaltene particles appeared to fill some spots in the shale cores, as demonstrated by the SEM pictures. For instance, pictures (a) and (c) demonstrated a higher level of asphaltene pore blockage in comparison to sample (b). This might be because pictures (a) and (c) were exposed to longer soaking periods of 6 and 24 h, respectively. Furthermore, the degree and distribution of the blocked pores in all samples was never identical. Finally, image-processing software was utilized to show the asphaltene areas from SEM photos, as shown in red color in Figure 20.

3.3.5. Change of Pore Size Distribution Due to Asphaltenes. Permeability reduction is one of the crucial challenges produced by asphaltene plugging in shale resources during huff-n-puff gas process. This test was designed to determine how the pore size distribution altered as a result of increasing of asphaltene deposition after CO_2 huff-and-puff process. Using a PoreMaster mercury porosimeter, the pore size distribution of two Eagle Ford cores was measured. A sample was picked among those that were fully saturated with oil, but no pressure was exposed to them. Another sample after the huff-n-puff CO_2 test (i.e., test no. 8) of the Eagle Ford outcrops sample was selected to compare the results. Because it was necessary to have very little pieces of each sample, each outcrop was broken into smaller pieces prior to the tests were performed.

During the measurement, a high pressure of 60,000 psi was applied to evaluate the cores' microstructure pores and throats. At each intrusion pressure, the PoreMaster determined and recorded precisely the volume of mercury intruded. Pore size distribution results are shown in Figure 21 and Figure 22. Huff-n-puff gas injection altered the oil's composition and resulted in asphaltene deposition. Asphaltene aggregated and generated a solid material that started to settle and fill the pores within the cores and on the surface of the cores

(Behbahani et al., 2015; Shen et al., 2016; Lee et al., 2019; 2020; Huang et al., 2023). Compared to after huff-n-puff test, the samples before the test showed larger pore size diameters.

Figure 21 indicates that the pore size peaks of two samples occur in completely separate ranges, showing that the major pore diameter in the samples significantly vary. The pore size distribution's peak was determined to be between 0.03 to 40-µm before CO_2 huff-n-puff tests, while the peak was changed to be between 0.01 and 10-µm after CO_2 huff-n-puff tests. Based on these findings, it can be concluded that the asphaltene particles that were injected into the cores had an influence on the pore throats. Due to the presence of asphaltenes, more pore plugging was found after using CO_2 huff-n-puff gas technique during the EOR process.

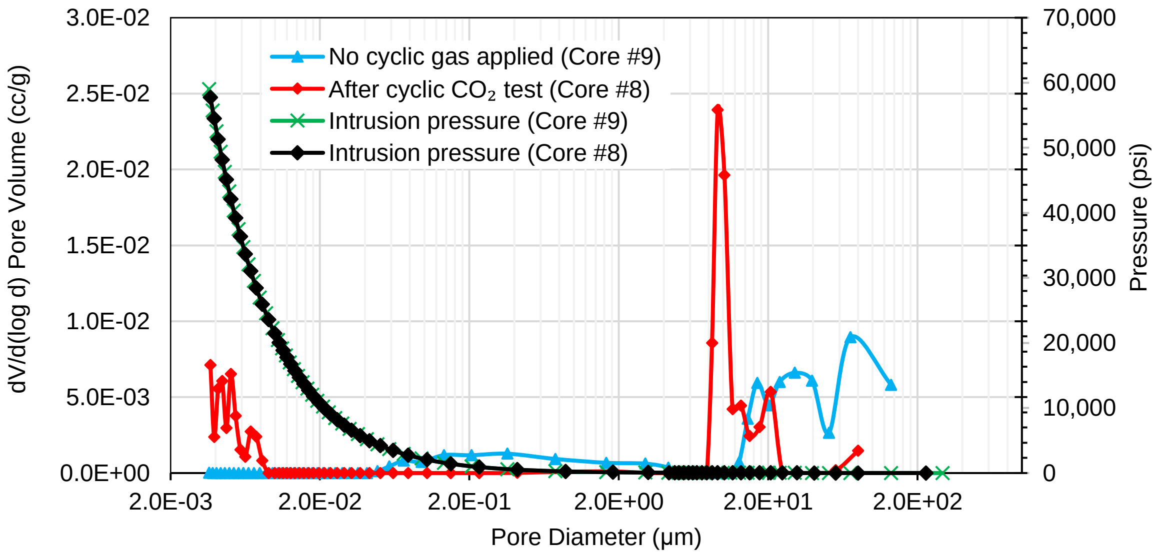

Figure 21. Pore size distribution results.

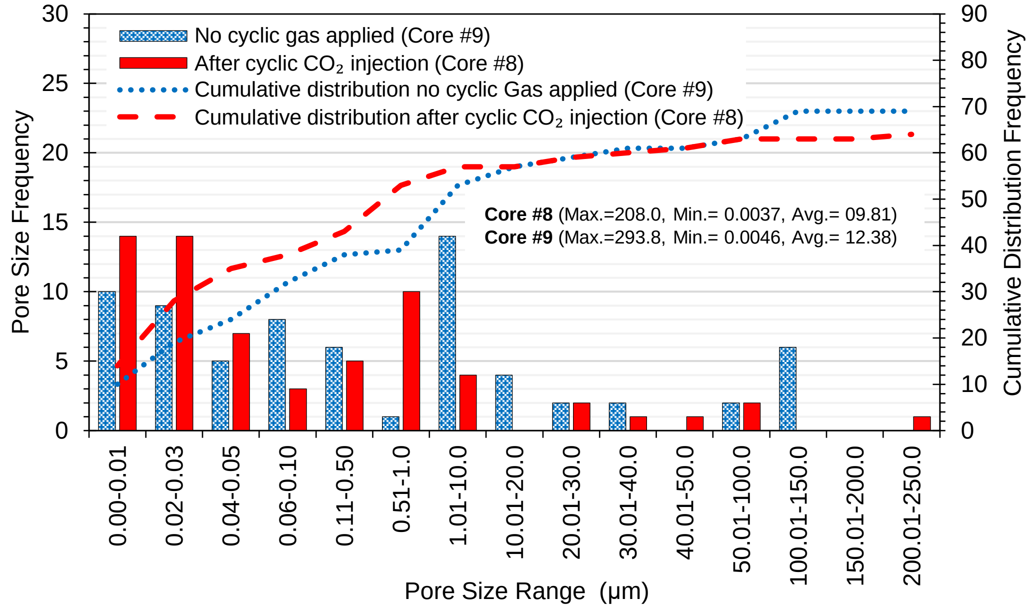

Figure 22. Pore size distribution comparison.

3.4. FURTHER DISCUSSION (CO_2 VS. N_2 HUFF-N-PUFF PROCESS)

The performance of oil recovery under CO_2 and N_2 gas injections, as well as the effect of asphaltene deposition, are comprehensively compared in this section. The results of oil recovery results under N_2 gas injection are from our previous work (Elturki and Imqam, 2022b). For the comparison, two immiscible pressures (i.e., 1000 and 1300 psi) and two miscible pressures (i.e., 1750 and 2000 psi) for the two gases were selected with a production time of 15 min. and 6 h soaking time, as summarized in Table 8.

Figure 23 shows the performance of oil recovery during immiscible and miscible CO_2 and N_2 injections. The difference between the cumulative oil recovery for both gases started from the first cycle in all pressures. The huff-n-puff process was more effective to extract more oil from shale cores under CO_2 gas compared to lower performance using N_2 due to CO_2 can reduce the interfacial tension at a higher rate than N_2. For both gases, more recovery was seen in the first three cycles before it started to stabilize or slightly increase.

For instance, using CO_2 immiscible pressure of 1000 psi resulted in cumulative oil recovery of about 4.14%, which increased to 12.30% in the third cycle. After that, it began to rise gradually, reaching 13.93% and reaching 13.98% in the latest cycle. Under N_2 gas injection, the same observation was obtained, but the cumulative oil recovery was much lower.

Interestingly, the cumulative oil recovery for both gases was close to each other under immiscible pressure of 1300 psi gas injection, but CO_2 gas still had a higher cumulative recovery. This might be a result of the oil being trapped in the deep core's pores during test #2 of CO_2, which prevented the gas from evaporating more of the crude oil's light hydrocarbons and lowering cumulative recovery. Miscible huff-n-puff pressure had better oil recovery performance in both gases. For example, using miscible 2000 psi CO_2 pressure led to up 39.30% cumulative oil recovery compared to 16.01% when using N_2 gas at the same pressure.

The oil recovery factor in all of the experiments decreased in the later cycles, which is clear from the earlier results and suggests that asphaltene deposition had an immediate impact after the first cycle but accumulated over the subsequent cycles. Our finding suggests that the CO_2 huff-and-puff process in shale reservoirs can extract more oil than the N_2 process, but additional cycles may lead to accumulated issues with asphaltene deposition. More research must be done in order to scale up these laboratory-scale findings to actual shale resources.

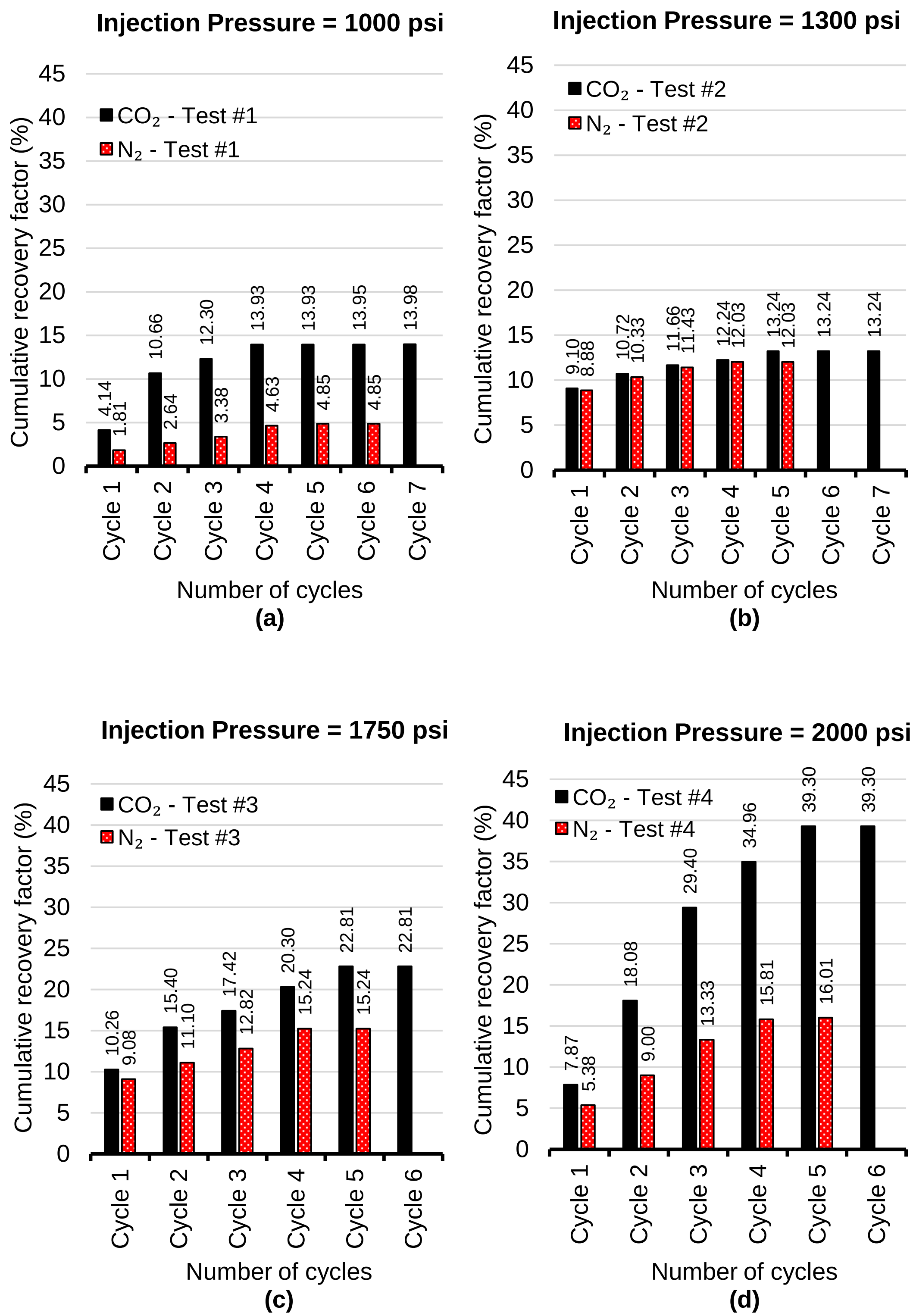

Figure 23. Comparison of oil recovery performance during immiscible and miscible CO_2 and N_2 huff-n-puff injection pressures.

Table 8. Results of cumulative oil recovery factor (%) after (CO_2) and (N_2) huff-n-puff tests.

Test no.	**Test #1**		**Test #2**		**Test #3**		**Test #4**	
Pressure (psi)	1000		1300		1750		2000	
Condition	Immiscible				Miscible			
Gas	N_2	CO_2	N_2	CO_2	N_2	CO_2	N_2	CO_2
Cycle 1	1.81	4.14	8.88	9.10	9.08	10.26	5.38	7.87
Cycle 2	2.64	10.66	10.33	10.72	11.10	15.40	9.00	18.08
Cycle 3	3.38	12.30	11.43	11.66	12.82	17.42	13.33	29.40
Cycle 4	4.63	13.93	12.03	12.24	15.24	20.30	15.81	34.96
Cycle 5	4.85	13.93	12.03	13.24	15.24	22.81	16.01	39.30
Cycle 6	4.85	13.95	-	13.24	-	22.81	-	39.30
Cycle 7	-	13.98	-	13.24	-	-	-	-

4. CONCLUSIONS

In this research, asphaltene instability under CO_2 huff-and-puff process were investigated experimentally using Eagle Ford shale cores and ultra-small membranes. Examinations were conducted on the effects of pressure, miscibility, and soaking duration. The wettability study and pore size distribution examination of the cores provided a comprehensive picture of the impact of asphaltene's related pore plugging during CO_2 huff-and-puff operations. When using the static mode (i.e., filter paper membranes), the asphaltene wt. % climbed as the pressure increased and the influence of the huff-n-puff gas process on the instability of asphaltene particles was found in the first five cycles and accumulated in later cycles. The results showed that more asphaltene wt. % resulted in the 50-nm filter paper due to the ultra-small pore structure. During the static mode experiments, chromatography analysis revealed the influence of the CO_2 on the asphaltene wt. %, with the findings revealing that CO_2 generated more accumulated heavy hydrocarbon components after the last CO_2 huff-n-puff injection, especially under miscible conditions. The results of the dynamic mode (i.e., using Eagle Ford shales) indicated that the oil recovery improved when both the miscible-high pressure and more cycles achieved. The findings of the dynamic mode suggested that starting with a shorter soaking time led to more oil recovery. Longer soaking durations induced asphaltenes to accumulate within the cores, which accelerated the decline in oil recovery. Our results show that oil reduction and asphaltene deposition accumulated mostly in the later cycles as a result of the fact that the final two cycles in the majority of CO_2 huff-and-puff experiments revealed a decrease in the volume of oil recovered during those cycles. As the number of cycles increased, asphaltene clusters started to fill the bigger pores at a higher pace, altering the wettability of the shale cores to be oil-wet phase. After CO_2 huff-and-puff experiments on Eagle Ford cores, a PoreMaster mercury porosimeter revealed a reduction in pore size distribution related to asphaltene deposition. Our finding suggests that the CO_2 huff-and-puff process in shale reservoirs can extract more oil than the N_2 process, but additional cycles may lead to issues with asphaltene deposition. More research must be done in order to scale up these laboratory-scale findings to real shale resources and to highlight other variable/factors that may influence the effectiveness of such operations in tight-shale resources.

REFERENCES

Elturki, M., Imqam, A. (2020a, June 28). Application of Enhanced Oil Recovery Methods in Unconventional Reservoirs: A Review and Data Analysis. American Rock Mechanics Association.

Warpinski, N. R., Mayerhofer, M. J., Vincent, M. C., Cipolla, C. L., & Lolon, E. P. (2009). Stimulating unconventional reservoirs: maximizing network growth while optimizing fracture conductivity. Journal of Canadian Petroleum Technology, 48(10), 39-51. https://doi.org/10.2118/114173-PA

Sheng, J. J. (2015). Enhanced oil recovery in shale reservoirs by gas injection. Journal of Natural Gas Science and Engineering, 22, 252-259. https://doi.org/10.1016/j.jngse.2014.12.002

Zoback, M.D., Kohli, A.H., 2019. Unconventional Reservoir Geomechanics. Cambridge University Press.

Liu, J., Sheng, J. J., Emadibaladehi, H., & Tu, J. (2021). Experimental study of the stimulating mechanism of shut-in after hydraulic fracturing in unconventional oil reservoirs. Fuel, 300, 120982. https://doi.org/10.1016/j.fuel.2021.120982

Elturki, M., McElroy, P. D., Li, D., Kablan, A., & Shaglouf, H. (2021, June). Simulation Study Investigating the Impact of Carbon Dioxide Foam Fracturing Fluids on Proppant Transport. In SPE Trinidad and Tobago Section Energy Resources Conference. https://doi.org/10.2118/200950-MS

Ahmed, S.; Emadi, H.; Heinze, L.; Elwegaa, K.; Elldakli, F. An experimental comparison between actual valve and benchmark valve using modified design and optimized design. SSRG Int. J. Eng. Trends Technol. 2020, 68, 64−73.

Saleh, A., Fathi, E., & Phillip, M. Simulation techniques used for modeling horizontal wells and the role of grid refinement. The International Journal of Engineering and Science (IJES). 2019, 8(3), 80-84.

Ahmed, S.; Elldakli, F.; Heinze, L.; Elwegaa, K.; Emadi, E. Investigating Effects of the Ball Size on the Gas Throughput Using Partially Curved and Wholly Curved Seats. Int. J. Pet. Petrochem. Eng. 2019, 5, 1−9.

Ahmed, S. Investigating effects of the ball configuration on the gas throughput using partially curved and wholly curved seats. Doctoral Dissertation, Texas Tech University, 2020.

Elwegaa, K., Kolawole, O., Ahmed, S., & Tomomewo, O. S. (2022, October). A Non-Conventional Well Technology Approach to Improve Hydrocarbon Recovery from a Mature Field: Brown Field Case Study. In SPE Eastern Regional Meeting.

Ahmed, S., Elwegaa, K., Htawish, M., & Alhaj, H. Safsaf D Oil Reservoir–Oil in Place, Reserves, and Production Performance Estimations. The International Journal of Engineering and Science (IJES). 2021, 10(5), 48-58.

Ahmed, S., Emadi, H., Heinze, L., Khalil, R., Elldakli, F., & Elwegaa, K. Optimizing Gas Throughput of Actual Valve Using Different Seat Designs, Seat Sizes, and Ball Sizes–An Experimental Study. The International Journal of Engineering and Science (IJES). 2019, 10(4), 36-47.

Yang, P., Guo, H., & Yang, D. (2013). Determination of residual oil distribution during waterflooding in tight oil formations with NMR relaxometry measurements. Energy & Fuels, 27(10), 5750-5756. https://doi.org/10.1021/ef400631h

Ahmad, H. M., Kamal, M. S., Mahmoud, M., Shakil Hussain, S. M., Abouelresh, M., & Al-Harthi, M. A. (2019). Organophilic clay-based drilling fluids for mitigation of unconventional shale reservoirs instability and formation damage. Journal of Energy Resources Technology, 141(9).

Zhou, X., Yuan, Q., Peng, X., Zeng, F., & Zhang, L. (2018). A critical review of the CO_2 huff 'n'puff process for enhanced heavy oil recovery. Fuel, 215, 813-824.

Tang, W., & Sheng, J. J. (2021). Huff-n-puff gas injection or gas flooding in tight oil reservoirs?. Journal of Petroleum Science and Engineering, 109725. https://doi.org/10.1016/j.petrol.2021.109725

Milad, M., Junin, R., Sidek, A., Imqam, A., & Tarhuni, M. (2021). Huff-n-Puff Technology for Enhanced Oil Recovery in Shale/Tight Oil Reservoirs: Progress, Gaps, and Perspectives. Energy & Fuels, 35(21), 17279-17333. https://doi.org/10.1021/acs.energyfuels.1c02561

Jia, B., Tsau, J. S., & Barati, R. (2019). A review of the current progress of CO_2 injection EOR and carbon storage in shale oil reservoirs. Fuel, 236, 404-427. https://doi.org/10.1016/j.fuel.2018.08.103

Shi, B. et al (2021). Status of Natural Gas Hydrate Flow Assurance Research in China: A Review. Energy & Fuels, 35(5), 3611-3658. https://doi.org/10.1021/acs.energyfuels.0c04209

Hassanpouryouzband, A. et al (2020). Gas hydrates in sustainable chemistry. Chemical Society Reviews, 49(15), 5225-5309. https://doi.org/10.1039/C8CS00989A

Ali, S. I., Lalji, S. M., Haneef, J., Ahsan, U., Tariq, S. M., Tirmizi, S. T., & Shamim, R. (2021). Critical analysis of different techniques used to screen asphaltene stability in crude oils. Fuel, 299, 120874. https://doi.org/10.1016/j.fuel.2021.120874

Ahmed, M. A., Abdul-Majeed, G. H., & Alhuraishawy, A. K. (2022). An Integrated Review on Asphaltene: Definition, Chemical Composition, Properties, and Methods for Determining Onset Precipitation. SPE Production & Operations, 1-28.

Mohammed, I., Mahmoud, M., Al Shehri, D., El-Husseiny, A., & Alade, O. (2021). Asphaltene precipitation and deposition: A critical review. Journal of Petroleum Science and Engineering, 197, 107956.

Elturki, M., & Imqam, A. (2020b, July). High Pressure-High Temperature Nitrogen Interaction with Crude Oil and Its Impact on Asphaltene Deposition in Nano Shale Pore Structure: An Experimental Study. In SPE/AAPG/SEG Unconventional Resources Technology Conference. https://doi.org/10.15530/urtec-2020-3241

Behbahani, T. J., Ghotbi, C., Taghikhani, V., & Shahrabadi, A. (2013). A modified scaling equation based on properties of bottom hole live oil for asphaltene precipitation estimation under pressure depletion and gas injection conditions. Fluid Phase Equilibria, 358, 212-219. https://doi.org/10.1016/j.fluid.2013.08.027

Turta, A. T., Najman, J., Singhal, A. K., Leggitt, S., & Fisher, D. (1997, January). Permeability impairment due to asphaltenes during gas miscible flooding and its mitigation. In International Symposium on Oilfield Chemistry. Society of Petroleum Engineers. https://doi.org/10.2118/37287-MS

Sim, S. S. K., Okatsu, K., Takabayashi, K., & Fisher, D. B. (2005, January). Asphaltene-induced formation damage: Effect of asphaltene particle size and core permeability. In SPE Annual Technical Conference and Exhibition. Society of Petroleum Engineers. https://doi.org/10.2118/95515-MS

Hamadou, R., Khodja, M., Kartout, M., & Jada, A. (2008). Permeability reduction by asphaltenes and resins deposition in porous media. Fuel, 87(10-11), 2178-2185. https://doi.org/10.1016/j.fuel.2007.12.009

Behbahani, T. J., Ghotbi, C., Taghikhani, V., & Shahrabadi, A. (2014). Investigation of asphaltene adsorption in sandstone core sample during CO_2 injection: Experimental and modified modeling. Fuel, 133, 63-72. https://doi.org/10.1016/j.fuel.2014.04.079

Mehana, M., Abraham, J., & Fahes, M. (2019). The impact of asphaltene deposition on fluid flow in sandstone. Journal of Petroleum Science and Engineering, 174, 676-681. https://doi.org/10.1016/j.petrol.2018.11.056

Lo, P. A., Tinni, A. O., & Milad, B. (2022). Experimental study on the influences of pressure and flow rates in the deposition of asphaltenes in a sandstone core sample. Fuel, 310, 122420. https://doi.org/10.1016/j.fuel.2021.122420

Jamaluddin, A. K. M., Joshi, N., Iwere, F., & Gurpinar, O. (2002, January 1). An Investigation of Asphaltene Instability Under Nitrogen Injection. Society of Petroleum Engineers. https://doi.org/10.2118/74393-MS

Moradi, S., Dabir, B., Rashtchian, D., & Mahmoudi, B. (2012). Effect of miscible nitrogen injection on instability, particle size distribution, and fractal structure of asphaltene aggregates. Journal of dispersion science and technology, 33(5), 763-770. https://doi.org/10.1080/01932691.2011.567878

Zadeh, G. A., Moradi, S., Dabir, B., Emadi, M. A., & Rashtchian, D. (2011, July). Comprehensive study of asphaltene precipitation due to gas injection: experimental investigation and modeling. In SPE Enhanced Oil Recovery Conference. https://doi.org/10.2118/143454-MS

Khalaf, M. H., & Mansoori, G. A. (2019). Asphaltenes aggregation during petroleum reservoir air and nitrogen flooding. Journal of Petroleum Science and Engineering, 173, 1121-1129. https://doi.org/10.1016/j.petrol.2018.10.037

Takahashi, S., Hayashi, Y., Takahashi, S., Yazawa, N., & Sarma, H. (2003, October). Characteristics and impact of asphaltene precipitation during CO_2 injection in sandstone and carbonate cores: an investigative analysis through laboratory tests and compositional simulation. In SPE International Improved Oil Recovery Conference in Asia Pacific.

Afra, S., Samouei, H., Golshahi, N., & Nasr-El-Din, H. (2020). Alterations of asphaltenes chemical structure due to carbon dioxide injection. Fuel, 272, 117708. https://doi.org/10.1016/j.fuel.2020.117708

Elturki, M., & Imqam, A. (2021a, November). An Experimental Study Investigating the Impact of Miscible and Immiscible Nitrogen Injection on Asphaltene Instability in Nano Shale Pore Structure. In SPE International Conference on Oilfield Chemistry. https://doi.org/10.2118/204294-MS

Elturki, M., & Imqam, A. (2022, March). An Experimental Investigation of Asphaltene Aggregation Under Carbon Dioxide Injection Flow in Ultra-Low-Permeability Pore Structure. In SPE Canadian Energy Technology Conference. https://doi.org/10.2118/208950-MS

Espinoza Mejia, J. E., Li, X., & Zheng, R. (2022, February). Experimental Study of Asphaltene Precipitation and Deposition During Immiscible CO_2-EOR Process. In SPE International Conference and Exhibition on Formation Damage Control. https://doi.org/10.2118/208802-MS

Zanganeh, P., Dashti, H., & Ayatollahi, S. (2018). Comparing the effects of CH_4, CO_2, and N_2 injection on asphaltene precipitation and deposition at reservoir condition: A visual and modeling study. Fuel, 217, 633-641.

Nascimento, F. P. et al. (2021). An experimental and theoretical investigation of asphaltene precipitation in a crude oil from the Brazilian pre-salt layer under CO_2 injection. Fuel, 284, 118968.

Abedini, A., & Torabi, F. (2014). Oil recovery performance of immiscible and miscible CO_2 huff-and-puff processes. Energy & Fuels, 28(2), 774-784. https://doi.org/10.1021/ef401363b

Yu, W., Lashgari, H. R., Wu, K., & Sepehrnoori, K. (2015). CO_2 injection for enhanced oil recovery in Bakken tight oil reservoirs. Fuel, 159, 354-363. https://doi.org/10.1016/j.fuel.2015.06.092

Yu, Y., & Sheng, J. J. (2015, July 20). An Experimental Investigation of the Effect of Pressure Depletion Rate on Oil Recovery from Shale Cores by Cyclic N_2 Injection. Unconventional Resources Technology Conference. https://doi.org/10.15530/URTEC-2015-2144010

Altawati, F. S. (2016). An experimental study of the effect of water saturation on cyclic N_2 and CO_2 injection in shale oil reservoir (Master thesis). http://hdl.handle.net/2346/68030

Yu, Y., Li, L., & Sheng, J. J. (2017). A comparative experimental study of gas injection in shale plugs by flooding and huff-n-puff processes. Journal of Natural Gas Science and Engineering, 38, 195-202. https://doi.org/10.1016/j.jngse.2016.12.040

Song, Y. L., Song, Z. J., Zhang, Y. F., Xie, Z. H., Zhang, L. C., Wang, D. G., & Hui, G. (2022). Pore scale performance evaluation and impact factors in nitrogen huff-n-puff EOR for tight oil. Petroleum Science.

Li, L. et al., (2019). Experimental and numerical study on CO_2 sweep volume during CO_2 huff-n-puff enhanced oil recovery process in shale oil reservoirs. Energy & Fuels, 33(5), 4017-4032.

Li, L., Su, Y., Hao, Y., Zhan, S., Lv, Y., Zhao, Q., & Wang, H. (2019). A comparative study of CO_2 and N_2 huff-n-puff EOR performance in shale oil production. Journal of Petroleum Science and Engineering, 181, 106174.

Sie, C. Y., & Nguyen, Q. P. (2021). Laboratory Investigations on Field Gas Huff-n-Puff for Improving Oil Recovery in Eagle Ford Shale─ Effect of Operating Conditions. Energy & Fuels, 36(1), 195-209.

Sie, C. Y., & Nguyen, Q. P. (2022). Field gas huff-n-puff for enhancing oil recovery in Eagle Ford shales–Effect of reservoir rock and crude properties. Fuel, 328, 125127.

Zhu, Z., Fang, C., Qiao, R., Yin, X., & Ozkan, E. (2020). Experimental and Molecular Insights on Mitigation of Hydrocarbon Sieving in Niobrara Shale by CO_2 Huff 'N'Puff. SPE Journal, 25(04), 1803-1811. https://doi.org/10.2118/196136-PA

Elwegaa, K., Emadi, H., Soliman, M., Gamadi, T., & Elsharafi, M. (2019). Improving oil recovery from shale oil reservoirs using cyclic cold carbon dioxide injection–An experimental study. Fuel, 254, 115586.

Badrouchi, N., Pu, H., Smith, S., & Badrouchi, F. (2022). Evaluation of CO_2 enhanced oil recovery in unconventional reservoirs: Experimental parametric study in the Bakken. Fuel, 312, 122941. https://doi.org/10.1016/j.fuel.2021.122941

Shilov, E., Dorhjie, D. B., Mukhina, E., Zvada, M., Kasyanenko, A., & Cheremisin, A. (2022). Experimental and numerical studies of rich gas Huff-n-Puff injection in tight formation. Journal of Petroleum Science and Engineering, 208, 109420. https://doi.org/10.1016/j.petrol.2021.109420

Mahzari, P. et al. (2021). Novel laboratory investigation of huff-n-puff gas injection for shale oils under realistic reservoir conditions. Fuel, 284, 118950. https://doi.org/10.1016/j.fuel.2020.118950

Sennaoui, B., Pu, H., Rylander, E., Afari, S., & Malki, M. L. (2022, June). An Experimental Study of CO_2 Huff-N-Puff Enhanced Oil Recovery in Three Forks Formation, Williston Basin. In 56th US Rock Mechanics/Geomechanics Symposium.

Ma, Q., Yang, S., Lv, D., Wang, M., Chen, J., Kou, G., & Yang, L. (2019). Experimental investigation on the influence factors and oil production distribution in different pore sizes during CO_2 huff-n-puff in an ultra-high-pressure tight oil reservoir. Journal of Petroleum Science and Engineering, 178, 1155-1163.

Min, B., Mamoudou, S., Dang, S., Tinni, A., Sondergeld, C., & Rai, C. (2020, August). Comprehensive experimental study of huff-n-puff enhanced oil recovey in eagle ford: Key parameters and recovery mechanism. In SPE Improved Oil Recovery Conference.

Nuttal, B. C., Eble, C., Bustin, R. M., & Drahovzal, J. A. (2005). Analysis of Devonian black shales in Kentucky for potential carbon dioxide sequestration and enhanced natural gas production. In Greenhouse Gas Control Technologies 7 (pp. 2225-2228). Elsevier Science Ltd. https://doi.org/10.1016/B978-008044704-9/50306-2

Louk, K. et al., (2017). Monitoring CO_2 storage and enhanced gas recovery in unconventional shale reservoirs: Results from the Morgan County, Tennessee injection test. Journal of Natural Gas Science and Engineering, 45, 11-25. https://doi.org/10.1016/j.jngse.2017.03.025

Sheng, J. J., & Chen, K. (2014). Evaluation of the EOR potential of gas and water injection in shale oil reservoirs. Journal of Unconventional Oil and Gas Resources, 5, 1-9. https://doi.org/10.1016/j.juogr.2013.12.001

Sanchez-Rivera, D., Mohanty, K., & Balhoff, M. (2015). Reservoir simulation and optimization of Huff-and-Puff operations in the Bakken Shale. Fuel, 147, 82-94. https://doi.org/10.1016/j.fuel.2014.12.062

Sun, J., Zou, A., Sotelo, E., & Schechter, D. (2016). Numerical simulation of CO_2 huff-n-puff in complex fracture networks of unconventional liquid reservoirs. Journal of Natural Gas Science and Engineering, 31, 481-492. https://doi.org/10.1016/j.jngse.2016.03.032

Wan, T., & Mu, Z. (2018). The use of numerical simulation to investigate the enhanced Eagle Ford shale gas condensate well recovery using cyclic CO_2 injection method with nano-pore effect. Fuel, 233, 123-132. https://doi.org/10.1016/j.fuel.2018.06.037

Wang, L., & Yu, W. (2019). Mechanistic simulation study of gas Puff and Huff process for Bakken tight oil fractured reservoir. Fuel, 239, 1179-1193. https://doi.org/10.1016/j.fuel.2018.11.119

Zheng, T., Yang, Z., Liu, X., Luo, Y., Xiao, Q., Zhang, Y., & Zhao, X. (2021). Understanding Immiscible Natural Gas Huff-N-Puff Seepage Mechanism in Porous Media: A Case Study of CH 4 Huff-N-Puff by Laboratory Numerical Simulations in Chang-7 Tight Core. Natural Resources Research, 30(3), 2397-2411. https://doi.org/10.1007/s11053-021-09836-2

Baek, S., & Akkutlu, I. Y. (2021). Enhanced Recovery of Nanoconfined Oil in Tight Rocks Using Lean Gas (C2H6 and CO_2) Injection. SPE Journal, 1-20. https://doi.org/10.2118/195272-PA

Luo, Y. et al. (2022). Identification of distinctions of immiscible CO_2 huff and puff performance in Chang-7 tight sandstone oil reservoir by applying NMR, microscope and reservoir simulation. Journal of Petroleum Science and Engineering, 209, 109719. https://doi.org/10.1016/j.petrol.2021.109719

Wang, L., Wei, B., You, J., Pu, W., Tang, J., & Lu, J. (2022). Performance of a tight reservoir horizontal well induced by gas huff–n–puff integrating fracture geometry, rock stress-sensitivity and molecular diffusion: A case study using CO_2, N_2 and produced gas. Energy, 125696.

Zhang, H., Wang, S., Yin, X., & Qiao, R. (2022). Soaking in CO_2 huff-n-puff: A single-nanopore scale study. Fuel, 308, 122026.

Li, L., Zhang, Y., & Sheng, J. J. (2017). Effect of the injection pressure on enhancing oil recovery in shale cores during the CO_2 huff-n-puff process when it is above and below the minimum miscibility pressure. Energy & Fuels, 31(4), 3856-3867. https://doi.org/10.1021/acs.energyfuels.7b00031

Tovar, F. D., Barrufet, M. A., & Schechter, D. S. (2021). Enhanced Oil Recovery in the Wolfcamp Shale by Carbon Dioxide or Nitrogen Injection: An Experimental Investigation. SPE Journal, 26(01), 515-537. https://doi.org/10.2118/204230-PA

Bougre, E.S., Gamadi, T.D. Enhanced oil recovery application in low permeability formations by the injections of CO_2, N_2 and CO_2/N_2 mixture gases. J Petrol Explor Prod Technol 11, 1963–1971 (2021).

Shen, Z., & Sheng, J. J. (2017). Experimental study of permeability reduction and pore size distribution change due to asphaltene deposition during CO_2 huff and puff injection in Eagle Ford shale. Asia-Pacific Journal of Chemical Engineering, 12(3), 381-390.

Shen, Z., & Sheng, J. J. (2017). Investigation of asphaltene deposition mechanisms during CO_2 huff-n-puff injection in Eagle Ford shale. Petroleum Science and Technology, 35(20), 1960-1966.

Mohammad, R. S., Zhang, S., Lu, S., Jamal-Ud-Din, S., & Zhao, X. (2017). Simulation study of asphaltene deposition and solubility of CO_2 in the brine during cyclic CO_2 injection process in unconventional tight reservoirs. International Journal of Geological and Environmental Engineering, 11(6), 495-510.

Shen, Z., & Sheng, J. J. (2019). Optimization Strategy to Reduce Asphaltene Deposition-Associated Damage During CO 2 Huff-n-Puff Injection in Shale. Arabian Journal for Science and Engineering, 44(6), 6179-6193. https://doi.org/10.1007/s13369-018-03701-w

Li, L., Su, Y., Lv, Y., & Tu, J. (2020). Asphaltene deposition and permeability impairment in shale reservoirs during CO_2 huff-n-puff EOR process. Petroleum Science and Technology, 38(4), 384-390. https://doi.org/10.1080/10916466.2019.1705855

Elturki, M., & Imqam, A. (2021b). Asphaltene Thermodynamic Flocculation during Immiscible Nitrogen Gas Injection. SPE Journal, 26(05), 3188-3204. https://doi.org/10.2118/206709-PA

Elturki, M., & Imqam, A. (2022a). Asphaltene Thermodynamic Precipitation During Miscible Nitrogen Gas Injection. SPE journal, 27(01), 877-894.

Elturki, M., & Imqam, A. (2022b). Asphaltene Precipitation and Deposition during Nitrogen Gas Cyclic Miscible and Immiscible Injection in Eagle Ford Shale and Its Impact on Oil Recovery. Energy & Fuels, 36(20), 12677-12694.

Elturki, M., & Imqam, A. (2022c). Asphaltene Precipitation and Deposition under Miscible and Immiscible Carbon Dioxide Gas Injection in Nanoshale Pore Structure. SPE Journal, 27(06), 3643-3659.

Sebastian, H. M., & Lawrence, D. D. (1992, January). Nitrogen minimum miscibility pressures. In SPE/DOE enhanced oil recovery symposium. Society of Petroleum Engineers. https://doi.org/10.2118/24134-MS

Vahidi, A., & Zargar, G. (2007, January). Sensitivity analysis of important parameters affecting minimum miscibility pressure (MMP) of nitrogen injection into conventional oil reservoirs. In SPE/EAGE reservoir characterization and simulation conference. Society of Petroleum Engineers. https://doi.org/10.2118/111411-MS

Belhaj, H., Abu Khalifeh, H. A., & Javid, K. (2013, April 15). Potential of Nitrogen Gas Miscible Injection in South East Assets, Abu Dhabi. Society of Petroleum Engineers. https://doi.org/10.2118/164774-MS

Elturki, M., & Imqam, A. (2021c, June). Analysis of Nitrogen Minimum Miscibility Pressure MMP and Its Impact on Instability of Asphaltene Aggregates-An Experimental Study. In SPE Trinidad and Tobago Section Energy Resources Conference.

Chung, T. H. (1992, January). Thermodynamic modeling for organic solid precipitation. In SPE Annual Technical Conference and Exhibition. Society of Petroleum Engineers. https://doi.org/10.2118/24851-MS

Pereira, J. C., López, I., Salas, R., Silva, F., Fernández, C., Urbina, C., & López, J. C. (2007). Resins: The molecules responsible for the stability/instability phenomena of asphaltenes. Energy & fuels, 21(3), 1317-1321.

Wang, P., Zhao, F., Hou, J., Lu, G., Zhang, M., & Wang, Z. (2018). Comparative analysis of CO_2, N_2, and gas mixture injection on asphaltene deposition pressure in reservoir conditions. Energies, 11(9), 2483. https://doi.org/10.3390/en11092483

Huang, X., Zhang, Y., He, M., Li, X., Yang, W., & Lu, J. (2022). Asphaltene precipitation and reservoir damage characteristics of CO_2 flooding in different microscopic structure types in tight light oil reservoirs. Fuel, 312, 122943.

Sheng, J. J. (2018). Discussion of shale rock wettability and the methods to determine it. Asia-Pacific Journal of Chemical Engineering, 13(6), e2263.

Odusina, E., Sondergeld, C., & Rai, C. (2011, November). An NMR study on shale wettability. In Canadian unconventional resources conference. https://doi.org/10.2118/147371-MS

Akbarabadi, M., Saraji, S., Piri, M., Georgi, D., & Delshad, M. (2017). Nano-scale experimental investigation of in-situ wettability and spontaneous imbibition in ultra-tight reservoir rocks. Advances in Water Resources, 107, 160-179. https://doi.org/10.1016/j.advwatres.2017.06.004

Kumar, K., Dao, E. K., & Mohanty, K. K. (2008). Atomic force microscopy study of wettability alteration by surfactants. SPE Journal, 13(02), 137-145. https://doi.org/10.2118/93009-PA

Pan, B., Li, Y., Zhang, M., Wang, X., & Iglauer, S. (2020). Effect of total organic carbon (TOC) content on shale wettability at high pressure and high temperature conditions. Journal of Petroleum Science and Engineering, 193, 107374. https://doi.org/10.1016/j.petrol.2020.107374

Mohammed, I., Mahmoud, M., El-Husseiny, A., Al Shehri, D., Al-Garadi, K., Kamal, M. S., & Alade, O. S. (2021). Impact of Asphaltene Precipitation and Deposition on Wettability and Permeability. ACS omega, 6(31), 20091-20102. https://doi.org/10.1021/acsomega.1c03198

Amin, J. S., Nikooee, E., Ayatollahi, S., & Alamdari, A. (2010). Investigating wettability alteration due to asphaltene precipitation: Imprints in surface multifractal characteristics. Applied Surface Science, 256(21), 6466-6472. https://doi.org/10.1016/j.apsusc.2010.04.036

Hosseini, E. (2019). Experimental investigation of effect of asphaltene deposition on oil relative permeability, rock wettability alteration, and recovery in WAG process. Petroleum Science and Technology, 37(20), 2150-2159. https://doi.org/10.1080/10916466.2018.1482335

Sarmadivaleh, M., Al-Yaseri, A. Z., & Iglauer, S. (2015). Influence of temperature and pressure on quartz–water–CO_2 contact angle and CO_2–water interfacial tension. Journal of colloid and interface science, 441, 59-64. https://doi.org/10.1016/j.jcis.2014.11.010

Iglauer, S., Al-Yaseri, A. Z., Rezaee, R., & Lebedev, M. (2015). CO_2 wettability of caprocks: Implications for structural storage capacity and containment security. Geophysical Research Letters, 42(21), 9279-9284. https://doi.org/10.1002/2015GL065787

Roshan, H., Al-Yaseri, A. Z., Sarmadivaleh, M., & Iglauer, S. (2016). On wettability of shale rocks. Journal of colloid and interface science, 475, 104-111. https://doi.org/10.1016/j.jcis.2016.04.041

Arif, M., Al-Yaseri, A. Z., Barifcani, A., Lebedev, M., & Iglauer, S. (2016). Impact of pressure and temperature on CO_2–brine–mica contact angles and CO_2–brine interfacial tension: Implications for carbon geo-sequestration. Journal of colloid and interface science, 462, 208-215. https://doi.org/10.1016/j.jcis.2015.09.076

Arif, M., Lebedev, M., Barifcani, A., & Iglauer, S. (2017). Influence of shale-total organic content on CO_2 geo-storage potential. Geophysical Research Letters, 44(17), 8769-8775. https://doi.org/10.1002/2017GL073532

Pan, B., Li, Y., Wang, H., Jones, F., & Iglauer, S. (2018). CO_2 and CH_4 wettabilities of organic-rich shale. Energy & Fuels, 32(2), 1914-1922. https://doi.org/10.1021/acs.energyfuels.7b01147

Shen, Z., & Sheng, J. J. (2018). Experimental and numerical study of permeability reduction caused by asphaltene precipitation and deposition during CO_2 huff and puff injection in Eagle Ford shale. Fuel, 211, 432-445. https://doi.org/10.1016/j.fuel.2017.09.047

Anderson, W. (1986). Wettability literature survey-part 2: Wettability measurement. Journal of petroleum technology, 38(11), 1246-1262. https://doi.org/10.2118/13933-PA

Behbahani, T. J., Ghotbi, C., Taghikhani, V., & Shahrabadi, A. (2015). Experimental study and mathematical modeling of asphaltene deposition mechanism in core samples. Oil & Gas Science and Technology–Revue d'IFP Energies nouvelles, 70(6), 1051-1074. https://doi.org/10.2516/ogst/2013128

Shen, Z., & Sheng, J. J. (2016, April). Experimental study of asphaltene aggregation during CO_2 and CH_4 injection in shale oil reservoirs. In SPE improved oil recovery conference. https://doi.org/10.2118/179675-MS

Lee, J. H., & Lee, K. S. (2019). Investigation of asphaltene-derived formation damage and nano-confinement on the performance of CO_2 huff-n-puff in shale oil reservoirs. Journal of Petroleum Science and Engineering, 182, 106304.

Lee, J. H., Jeong, M. S., & Lee, K. S. (2020). Comprehensive modeling of CO_2 Huff-n-Puff in asphaltene-damaged shale reservoir with aqueous solubility and nano-confinement. Journal of Industrial and Engineering Chemistry, 90, 232-243.

Huang, X. et al. (2023). The influence of CO_2 huff and puff in tight oil reservoirs on pore structure characteristics and oil production from the microscopic scale. Fuel, 335, 127000.

SECTION

2. CONCLUSIONS AND RECOMMENDATIONS

2.1. CONCLUSIONS

This research provides a comprehensive experimental investigation of the impact of immiscible and miscible carbon dioxide (CO_2) and nitrogen (N_2) gas injections on asphaltene instability in crude oil and its impact on oil recovery in unconventional reservoirs. Continuous and huff-n-puff (cyclic) gas injection EOR techniques were implemented to highlight the severity of asphaltene deposition and precipitation in nano pore shale structures and Eagle Ford cores. The following are the key findings in this research:

- The analysis of gas EOR data revealed a number of parameters that might affect the miscibility of the injected gas during gas EOR methods, including permeability, porosity, reservoir temperature, oil viscosity, reservoir depth, MMP, and reservoir pressure.
- Based on the slim tube experiments, the minimum miscibility pressure (MMP) of CO_2 was lower than N_2 MMP, and the MMP for both gases decreased with the decrease in oil viscosity due to the reduction in interfacial tension between the fluids when the oil viscosity was decreased. Also, higher pressures are required to determine the MMP for high oil viscosities.
- When using the filtration technique, asphaltenes were determined quantitively using the weight percent method during continuous gas injection modes on various

ultra-small filter paper membrane structures mimicking the unconventional reservoirs, and the results showed severe asphaltene deposition after CO_2 gas injection compared to lower asphaltene weight percent after N_2 gas injection. Moreover, the smaller pore structure of filter paper membranes during filtration technique showed higher asphaltene percent because the asphaltene particle could not pass easily through the small pores.

- Injection pressure was found to be the most significant factor impacting asphaltene instability during filtration experiments, compared to other factors such as temperature and mixing time. The severity of asphaltene deposition and precipitation was observed under miscibility pressures, which may weaken the bonds between asphaltenes and resins in crude oil at a faster pace, resulting in a higher percentage of asphaltene deposition.
- The huff-n-puff process was found to be more effective to extract more oil from Eagle Ford shale cores under CO_2 gas injection compared to lower performance using N_2. This is due to CO_2 reducing the interfacial tension at a higher rate than N_2. For both gases, higher recovery was observed in the first three cycles, after which it stabilized or slightly increased, especially during miscible conditions. Miscible huff-n-puff pressure had better oil recovery performance in both gases. Asphaltene deposition had an immediate impact after the first cycle but accumulated over subsequent cycles.
- Findings suggest that the CO_2 huff-and-puff process outperforms N_2 huff-n-puff in shale reservoirs, but additional cycles may lead to accumulated issues with asphaltene deposition.

2.2. FUTURE WORK RECOMMENDATIONS

This study investigated only the thermodynamic factors that may impact asphaltene instability under gas injection. Although this work was comprehensive, several parameters still need to be investigated. Below are some recommendations to extend the study of this research:

- Examine other gases, such as methane (CH_4), and gas mixtures, such as N_2-CO_2, to understand the instability of asphaltene under different scenarios.
- Investigate the chemical interaction of crude oil and gas, particularly under miscible gas injection conditions and use various crude oils to compare the results.
- Study the effect of formation brine on asphaltene deposition and precipitation to expand the knowledge to the field scale.
- Study the flocculation kinetics of asphaltene colloidal particles using confocal microscopy imaging techniques and the size distribution of flocculated asphaltene, as a function of time.
- Generate mathematical correlations and models that can be used to minimize asphaltene deposition upon miscible and immiscible gas injection in the field, compensating for variations in oil composition, pressure, temperature, time, and gas injection composition.

BIBLIOGRAPHY

Ahmed, M. A., Abdul-Majeed, G. H., & Alhuraishawy, A. K. (2022). An Integrated Review on Asphaltene: Definition, Chemical Composition, Properties, and Methods for Determining Onset Precipitation. SPE Production & Operations, 1-28.

Alagorni, A. H., Yaacob, Z. B., & Nour, A. H. (2015). An overview of oil production stages: enhanced oil recovery techniques and nitrogen injection. International Journal of Environmental Science and Development, 6(9), 693.

Bahman J, et al. (2017). An Introduction to Asphaltene Chemistry. Heavy Oil: Nova Science Publishers, New York, USA.

Elturki, M., & Imqam, A. (2020, June). Application of Enhanced Oil Recovery Methods in Unconventional Reservoirs: A Review and Data Analysis. In 54th US rock mechanics/geomechanics symposium.

Elturki, M., & Imqam, A. (2021). Asphaltene Thermodynamic Flocculation during Immiscible Nitrogen Gas Injection. SPE Journal, 26(05), 3188-3204.

Elturki, M., et al. (2023, June). Oil Recovery Performance and Asphaltene Deposition Evaluation of Miscible and Immiscible Carbon Dioxide or Nitrogen Huff-N-Puff Processes in Shale Reservoirs. In SPE/AAPG/SEG Unconventional Resources Technology Conference (p. D031S074R010). URTEC.

Elwegaa, K., & Emadi, H. (2019). Improving oil recovery from shale oil reservoirs using cyclic cold nitrogen injection–An experimental study. Fuel, 254, 115716.

Goual, L. (2012). Petroleum asphaltenes. Crude oil emulsions—composition stability and characterization, ed. ME Abdul-Raouf, 27-42.

Okwen, R. T. (2006, February). Formation damage by CO_2 asphaltene precipitation. In SPE International Symposium and Exhibition on Formation damage control.

Sim, S. S. K., Okatsu, K., Takabayashi, K., & Fisher, D. B. (2005, October). Asphaltene-induced formation damage: effect of asphaltene particle size and core permeability. In SPE Annual Technical Conference and Exhibition.

Soulgani, B. S., Tohidi, B., Jamialahmadi, M., & Rashtchian, D. (2011). Modeling formation damage due to asphaltene deposition in the porous media. Energy & Fuels, 25(2), 753-761.

Srivastava, R. K., & Huang, S. S. (1997, March). Asphaltene deposition during CO_2 flooding: a laboratory assessment. In SPE production operations symposium.

Srivastava, R. K., Huang, S. S., & Dong, M. (1999). Asphaltene deposition during CO_2 flooding. SPE production & facilities, 14(04), 235-245.

Tang, W., & Sheng, J. J. (2022). Huff-n-puff gas injection or gas flooding in tight oil reservoirs?. Journal of Petroleum Science and Engineering, 208, 109725.

Tovar, F. D., Barrufet, M. A., & Schechter, D. S. (2021). Enhanced Oil Recovery in the Wolfcamp Shale by Carbon Dioxide or Nitrogen Injection: An Experimental Investigation. SPE Journal, 26(01), 515-537.

Yu, W., Lashgari, H. R., Wu, K., & Sepehrnoori, K. (2015). CO_2 injection for enhanced oil recovery in Bakken tight oil reservoirs. Fuel, 159, 354-363.

Zhou, X., Yuan, Q., Peng, X., Zeng, F., & Zhang, L. (2018). A critical review of the CO_2 huff 'n'puff process for enhanced heavy oil recovery. Fuel, 215, 813-824.

VITA

Mukhtar Elturki was born in Misrata, Libya. He received his bachelor's degree in Petroleum Engineering from Misurata University, Misrata, Libya, in 2011. He received his Master of Science degree in Petroleum Engineering from Texas Tech University, Lubbock, Texas, USA, in 2016. He was admitted as a PhD student at Missouri University of Science and Technology, in the department of Geosciences and Geological and Petroleum Engineering, in January 2019. His research interest included Gas Enhanced Oil Recovery (GEOR), hydraulic fracturing, and flow assurance with a focus on asphaltene deposition and precipitation in unconventional reservoirs. He published many journal and research papers with Society of Petroleum Engineers (SPE), American Chemical Society (ACS), and American Rock Mechanics Association (ARMA). He received his PhD in Petroleum Engineering from Missouri University of Science and Technology in December 2023.